Functional Impact of CD161 on T cells

Kira Smith

Keble College, University of Oxford

and Nuffield Department of Medicine

Peter Medawar Building for Pathogen Research, Oxford

Thesis submitted for degree of Doctor of Philosophy

University of Oxford, Trinity 2013

Supervisors: Paul Klenerman and Chris O'Callaghan

In Memory of

my beloved Grandaddy

Acknowledgements

I would like to first thank my primary supervisor Paul Klenerman who has been such a constant support through all of the ups and downs and has made this thesis possible. You were always interested and excited to see what my experiments revealed and your incredible knowledge helped guide me through the many turns the project took. I would also like to thank my secondary supervisor Chris O'Callaghan for his support in making my proteins.

Second I would like to thank the Post-docs who have helped supervise my project. Yu-hoi Kang, thank you for helping me set up the original functional experiment. Chris Willberg, your input and guidance have been immeasurable over the last few years. A special thanks goes to you as well for reading my whole thesis and giving feedback!

I would also like to thank the rest of the Klenerman lab for the technical help, the space to bounce ideas off of and ask questions, for the tea/cake breaks, and for the support when everything went wrong. Past and present this includes: Ruth, Ayako, Jo, Alba, James U, Chris, Matt, Narayan, Annette, Rachel H, Rachel T, Leo, Lucy, Isla, Vicki, Cormac, and Abby. I also have to thank all of the lab members who have selflessly donated blood over the years!

Thank you to the Clarendon Foundation and Nuffield Department of Medicine Prize Studentship for my Dphil funding, which has made it possible for me to live and study at Oxford. I want to thank the Keble Association for helping fund my attendance at an international conference.

My life in Oxford has been greatly enriched by the many dear friends I have made over the years here: Ruth Simmons, Calique Martinez Hague, Christian, Helen, Hannah and Sam Hofreiter, Jamila Headley, Ayako Kurioka, Joannah Fergusson, Alba Llibre, Annette von Delft, Leo Swadling, Matt Bilton, Rachel Richardson, Isla Humphreys, Suzanne English, Chris Smith, Nathan Rose, Ilse GVP, Jessica Whittle, Miriam Kline Flugge, Melissa Huitt and Addie Yandell. You have helped me get through the ups and downs of life and the Dphil for which I am eternally grateful!

I also must thank teachers from throughout my life because without them I never would have made it here. They encouraged me and believed in me even when I didn't believe in myself. Mrs. Reeves – thank you for giving a love for Biology! Mrs. Andes- you may have taught me history, but you also taught me how to study, take notes, and write! Without those things I never would have made it this far! Dr. Johnston- you saw something in me that I couldn't see in myself. You taught me to love research and encouraged me to go to Oxford!

Last but not least I have to thank my wonderful Mom and Dad and my beloved Grandmomma. Your love and belief in me has kept me going through thick and thin. Thank for all of your prayers and support from across the pond!!!

Table of Contents

Table of Contents ..... **iv**
Abstract **1**

Chapter 1 Introduction **2**
1.1 Introduction – Part I **2**
1.1.1 Immune System 2
1.1.2 Innate Immune System 2
1.1.3 Adaptive Immune System 6
1.1.4 Innate-like T cells that bridge the gap between adaptive and innate immunity 11
1.2 Introduction – Part II **18**
1.2.1 Relationship between CD161 and disease states 18
1.2.2 CD161 Protein 21
1.2.3 Ligands of Human CD161 25
1.2.4 Functional Effects of Human CD161 Ligation 31
1.3 Aims of this Thesis **32**

Chapter 2 Material and Methods **33**
2.1 Subjects **33**
2.1.1 Subjects 33
2.2 Materials **33**
2.2.1 Media 33
2.2.2 Soluble Protein 33
2.2.3 Cell Lines 34
2.3 Methods **35**
2.3.1 PBMC Separation 35
2.3.2 PBMC Freezing and Thawing 35
2.3.3 Cell Selection 35
2.3.4 Surface Stain, Intracellular Stain, and Flow Cytometry 36
2.3.5 Truncated Extracellular Protein Vector Production 37
2.3.6 Transient Transfection 38
2.3.7 PCR 39
2.3.8 Sequencing 39
2.3.9 Protein Purification 39
2.3.10 SDS PAGE 40
2.3.11 Coomassie 40
2.3.12 PNGase F 40
2.3.13 Western Blot 40
2.3.14 Binding Protein and mAb to Plates 41
2.3.15 Gene Microarray Processing 41
2.3.16 Real-time qPCR 42
2.3.17 Irradiation 44
2.3.18 T Cell Activation 44
2.3.19 *E. coli* activation of B cell line 45
2.3.20 Proliferation Assay 45
2.3.21 FATAL Assay 45

Chapter 3 Protein Production and Purification **47**
3.1 Introduction **47**
3.2 Aims **48**
3.3 Material and Methods **49**

3.3.1 Truncated Extracellular PILAR Vector Production 49
3.3.2 Transient Transfection 50
3.3.3 PCR 50
3.3.4 Sequencing 50
3.3.5 Protein Purification 51
3.3.6 SDS PAGE 51
3.3.7 Coomassie 52
3.3.8 PNGase F 52
3.3.9 Western Blot 52
3.3.10 PILAR protein provided by Gordon Freeman 52
3.4 Results 54
3.4.1 Predicted Extracellular Domains 54
3.4.2 PHL-sec Plasmid 57
3.4.3 Transient Transfection 58
3.4.4 PILAR protein purification 59
3.4.5 PILAR protein characteristics 60
3.4.6 Binding pattern of conjugated PILAR protien 62
3.4.7 Functional Impact of PILAR ligation on $CD8^+$ T cells 64
3.5 Discussion 67
3.5.1 Why soluble protein instead of stable transfection? 67
3.5.2 Unable to produce LLT1 protein 67
3.5.3 Expression of PILAR protein 68
3.5.4 Differential glycosylation of PILAR 68
3.5.5 Fluorescently labeled LLT1 protein did not bind $CD3^+$ cells 68
3.5.6 Fluorescently labeled PILAR protein binds $CD19^+$ cells 69
3.5.7 Maturation state of $CD19^+PILAR^+$ cells 70
3.5.8 PILAR protein decreases IFNγ expression non-specifically 70
3.5.9 PILAR is not a ligand of CD161 71
3.6 Summary 71

Chapter 4 CD161 Expression Patterns on T cells 72
4.1 Introduction 72
4.2 Aims 73
4.3 Materials and Methods 74
4.3.1 αCD161 74
4.3.2 Subjects 74
4.3.3 LLT1 Transfected cell line 74
4.3.4 $CD8^+$ T cell Selection 75
4.3.5 Surface Stain, Intracellular Stain, and Flow Cytometry 75
4.3.6 FACS Gating Strategy 76
4.4 Results 78
4.4.1 CD161 expression patterns on T cells 78
4.4.2 Surface vs Internal expression of CD161 79
4.4.3 CD161 staining decreases after cross-linking with plate bound CD161 mAb 80
4.4.4 Unconjugated αCD161 mAb detached from plate could block binding 82
4.4.5 Do other αCD161 mAb clones have non-overlapping epitopes? 83
4.4.6 αCD161 mAbs have different binding kinetics 84
4.4.7 CD161 expression is downregulated by CD161 mAb cross-linking 85
4.4.8 CD26 is a poor marker for selection of $CD161^{+/++}$ cells. 86
4.4.9 IL-18R is a good marker for selection of $CD161^{++}$ $CD8^+$ T cells 87
4.4.10 Vα7.2 highly co-stains $CD8^+$ $CD161^{++}$ cells 88
4.4.11 Vα7.2 expression is not significantly affected by CD161 cross-linking 90
4.4.12 CD161 downregulation is time dependent 91

4.4.13 αCD161 clones have different effects on time dependent downregulation 93
4.4.14 CD161 downregulation is dose dependent ... 95
4.4.15 CD161 expression improves after LLT1 ligation is removed in a time dependent manner ... 97
4.4.16 CD161 downregulation is not regulated from the mRNA level ... 97
4.5 Discussion ... 101
4.5.1 CD161 expression patterns on T cells ... 101
4.5.2 Surface and intracellular staining of CD161 ... 101
4.5.3 CD161 staining decreased by αCD161 mAb cross-linking with unconjugated plate bound αCD161 mAb ... 101
4.5.4 Staining CD161 with multiple clones of αCD161 mAb ... 102
4.5.5 αCD161 mAb cross-linking downregulated CD161 expression ... 103
4.5.6 CD26 is a poor marker for $CD161^{+}/^{++}$ T cells ... 104
4.5.7 CD8+ CD161++ T cells is significantly co-expressed IL-18R ... 104
4.5.8 $CD8^{+}$ $CD161^{++}$ T cells significantly co-express $V\alpha7.2^{+}$ ... 104
4.5.9 Expression of Vα7.2 is not affected by αCD161 mAb cross-linking ... 105
4.5.10 αCD161 mAb induced downregulation of CD161 is time dependent ... 105
4.5.11 The αCD161 mAb clone used affects the time frame of CD161 downregulation ... 106
4.5.12 CD161 downregulation induced by CD161 ligation is dose dependent ... 107
4.5.13 CD161 expression recovers after removal of CD161 ligation ... 107
4.5.14 CD161 downregulation is not regulated at the mRNA level ... 108
4.5.15 Model of CD161 downregulation ... 108
4.6 Summary ... 111

Chapter 5 Gene Microarray ... 112
5.1 Introduction ... 112
5.2 Aims ... 113
5.3 Material and Methods ... 114
5.3.1 Type of Microarray ... 114
5.3.2 Gene Microarray Processing ... 116
5.3.3 Gene microarray P-value calculations ... 116
5.4 Results ... 117
5.4.1 Experiment Design ... 117
5.4.2 Microarray cells downregulated CD161 expression ... 118
5.4.3 Top Hit Gene lists ... 119
5.4.4 Ingenuity Pathway Analysis ... 125
5.4.5 Gene confirmation with Real-Time qPCR ... 127
5.4.6 Low Intensity Microarray Probe Signals ... 132
5.5 Discussion ... 135
5.6 Summary ... 139

Chapter 6 CD161 Functional Effects ... 140
6.1 Introduction ... 140
6.2 Aims ... 141
6.3 Material and Methods ... 142
6.3.1 αCD161 mAb staining ... 142
6.3.2 Subjects ... 142
6.3.3 Binding mAb to Plates ... 142
6.3.4 $CD8^{+}$ T cell Selection ... 143
6.3.5 Irradiation ... 143
6.3.6 αCD3/28 Dynabeads ... 143
6.3.7 αBiotin Activation Beads Design ... 143

6.3.8 B cell line 144
6.3.9 *E. coli* activation of B cell line 145
6.3.10 FACS Gating Strategy 145
6.3.11 Proliferation Assay 146
6.3.12 FATAL Assay 146
6.3.13 Statistics 148
6.4 Results 149
6.4.1 $CD8^+$ T cells cross-linked with plate bound αCD161 mAb decreased IFNγ expression at some concentrations 149
6.4.2 CD161 ligation of MAIT cells did not affect IFNγ or TNFα expression regardless of ligation or activation methods used 151
6.4.3 CD161 ligation of $CD4^+$ T cells decreased IFNγ expression with plate bound stimulation but not other forms of stimulation 152
6.4.4 Cross-linking of CD161 on MAIT cells stimulated with a biotin activation beads increased expression of IFNγ and TNFα 152
6.4.5 Bead bound CD161 cross-linking of $CD8^+$ T cells stimulated with IL-12 + IL-18 does not affect IFNγ expression 155
6.4.6 CD161 cross-linking did not induce changes in IL-22 expression 157
6.4.7 CD161 cross-linking did not induce changes in IL-17a expression 159
6.4.8 CD161 ligation increased specific killing by activated MAIT cells 161
6.4.9 CD161 cross-linking increased degranulation (CD107a) and activation (CD69) of $CD8^+$ T cells 162
6.4.10 CD161 ligation increased Granzyme B expression 164
6.4.11 CD161 ligation had no effect on perforin expression 165
6.4.12 CD161 ligation decreased Granzyme A expression 165
6.4.13 CD161 ligation decreased Granzyme K expression with αBiotin bead activation but not with FATAL assay 166
6.4.14 CD161 ligation reduced MAIT cell proliferation 170
6.4.15 CD161 cross-linking increased MAIT cell apoptosis 172
6.5 Discussion 176
6.5.1 The effects of CD161 ligation on IFNγ and TNFα expression 176
6.5.2 IL-22 and IL-17a expression was low and not clearly affected by CD161 cross-linking 178
6.5.3 CD161 cross-linking increased specific cell killing in the FATAL Assay 179
6.5.4 Degranulation and Activation were increased by CD161 ligation 179
6.5.5 The effects of CD161 ligation on Granzymes and Perforin Expression 180
6.5.6 Proliferation of MAIT cells was inhibited by CD161 ligation 181
6.5.7 CD161 ligation increased apoptosis on MAIT cells 182
6.5.8 Summary of Functional effects of CD161 ligation on activated $CD8^+$ T cells 182
6.5.9 Potential Mechanism for functional effects CD161 ligation on T cells 184
6.6 Summary 186

Chapter 7 Conclusions 188
7.1 Summary of Experimental Results 188
7.1.1 Production of Soluble CD161 ligands 188
7.1.2 CD161 expression patterns on T cells 189
7.1.3 Gene microarray analysis of the effects of CD161 ligation on $CD8^+$ $Vα7.2^+$ T cells 189
7.1.4 Functional effects of CD161 ligation on activated $CD8^+$ $Vα7.2^+$ T cells 191
7.1.5 Summary of all results 192
7.2 Caveats of this study 192
7.2.1 Non-physiological levels of activation were used 192
7.2.2 LLT1 may not be the only ligand of CD161 193

7.2.3 In-vitro experiments do not always accurately reflect in-vivo effects 194
7.3 Model of CD161 ligation on activated MAIT ($CD8^+$ $V\alpha7.2^+$) T cells 194
7.4 Future directions.....198
References 200
Appendix 213

Abbreviations

α	anti (when used before an antibody name)
AICD	Activation induced cell death
APC	Antigen presenting cell
BCL	B cell line
CCR6	Chemokine receptor 6
CFSE	Carboxyfluorescein succinimidyl ester
CLAX	C-type Lectin, Activation Expressed
CLEC	C-type lectin-like receptor
CTV	CellTrace violet
CXCL10	C-X-C motif chemokine 10
CXCR6	C-X-C chemokine receptor type 6
DMEM	Dulbecco's modified Eagle's medium
E. coli	*Escherichia coli*
EDTA	Ethylenediaminetetraacetic acid
FACS	Fluorescence Activated Cell Sorter
FCS	Fetal calf serum
gMFI	geo mean fluorescence intensity
HCV	Hepatitis C Virus
HIV	Human immunodeficiency virus
IFN	Interferon
Ig	Immunoglobulin
IL	Interleukin
ITAM	Immunoreceptor tyrosine-based activating motif
ITIM	Immunoreceptor tyrosine-based inhibitory motif
KACL	Keratinocyte-associated C-type lectin
kDa	kilaDalton
LB	Lysogeny Broth
LLT1	Lectin-Like Transcript 1
mAb	Monoclonal antibody
MAIT	Mucosa-associated invariant T (cells)
mRNA	Messenger Ribonucleic acid
mw	Molecular weight
NK	Natural Killer
NKR-P1	Natural Killer Receptor - Protein 1
NKT cell	Natural Killer T cell
OCIL	Osteoclast inhibitory lectin
PAMP	Pathogen-associated molecular patterns
PBMCs	Peripheral blood mononuclear cells
PBS	Phosphate buffered saline
PCR	Polymerase chain reaction

PEI	Polyethyleneimine
PFA	Paraformaldehyde
PILAR	Proliferation-induced lymphocyte-associated receptor
PMA/I	Phorbol-Myristate-Acetate and Ionomycin
PRR	Pattern recognition receptor
qPCR	quantitative polymerase chain reaction
R10	RPMI 1640 supplemented with 10% FCS, 50,000 U penicillin, 50mg streptomycin and 1 mmol L-glutamine
RH10	RPMI 1640 supplemented with 10% human serum, 50,000 U penicillin, 50mg streptomycin and 1 mmol L-glutamine
RORyt	RAR-related orphan receptor gamma t
TCR	T cell receptor
TNFa	Tumor necrosis factor-*alpha*
FES	Feature Extraction Software

Abstract

The Functional Impact of CD161 ligation on T cells

Kira Smith, Keble College

Submitted for D.Phil Clinical Medicine at the University of Oxford, Trinity term 2013

Human CD161 is protein that is expressed by most Natural Killer (NK) cells, of T cells (including both $CD4^+$ and $CD8^+$ subsets), Natural Killer T (NKT) cells and immature thymocytes. CD161 is expressed on many of the T cell receptor (TCR) expressing cell types that "bridge" both the innate and the adaptive immune systems, including mucosal associated invariant T (MAIT) cells. Changes in expression levels of CD161 in peripheral blood or tissue have been seen in multiple disease states such as: HIV, tuberculosis, multiple sclerosis, rheumatoid arthritis and psoriasis. However, the functional role of CD161 on T cells was unclear.

Therefore, this thesis explores the impact of CD161 ligation on $CD8^+$ T cells. CD161 surface expression was seen to be significantly downregulated upon ligation with its receptor (LLT1) or cross-linked by anti-CD161 antibodies. Despite this, no clear functional impact of CD161 ligation was seen on resting $CD8^+$ $V\alpha7.2^+$ cells. In contrast, ligation of CD161 on TCR stimulated $CD8^+$ $V\alpha7.2^+$ cells resulted in increased IFNγ and TNFα expression, cell activation and cytotoxicity. The increased cytotoxicity was potentially due to both an increase in the ability of the cells to degranulate and the expression of Granzyme B. Furthermore, ligation of CD161 induced an increase in activated Caspase 3 expression, indicating increased apoptosis. CD161 ligation over a prolonged period resulted in a decrease in proliferation. In total these results suggest that CD161 acts as a co-stimulatory molecule for T cells in the context of TCR activation.

Chapter 1 Introduction

1.1 Introduction – Part I

1.1.1 Immune System

The immune system is a complex arrangement of cells that must recognize and address foreign invasion or dangerous changes within the organism's cells. The destruction of infected or transformed cells must be balanced with preserving healthy cells. In addition, the immune system must not react unnecessarily to commensal flora.

The immune response can be broken broadly into two branches: the innate and the adaptive immune systems. The innate system produces an immediate but non-specific first line of defence against pathogens. The adaptive system, however, is much more precise, targeting specific epitopes and developing "memory" populations to provide long-term protection against that epitope (Sallusto et al. 1995).

However, the distinctions between the innate and adaptive branches get somewhat blurry where the two branches interact and overlap. Several cell types bear characteristics that bridge the both systems. In this first section of the introduction, the characteristics of both innate and adaptive systems will be discussed in detail along with the cell types that bridge both systems.

1.1.2 Innate Immune System

An innate type immune system is ancient in origin and is found in both invertebrates and vertebrates (Rinkevich 1999). The innate immune system responds rapidly and without prior activation signals to a broad range of infectious agents

detected by innate cells. Cells of the innate immune system include natural killer (NK) cells, dendritic cells (DCs), macrophages, neutrophils, eosinophils, basophils and mast cells.

Innate immune system cells express pattern recognition receptors (PRRs) that specifically recognize structures known as pattern-associated molecular patterns (PAMPs), such as mannose-rich oligosaccharides, peptidoglycans, and lipopolysaccharides found in bacterial cell walls, and unmethylated CpG DNA. PRRs on innate immune cells include toll-like receptors (TLRs), RIG-I-like receptors (RLR), NOD-like receptors (NLR), or DNA receptors. Some of the PRRs recognize the PAMPs located at the surface of cells and others recognize intracellular patterns (Medzhitov and Janeway 1997; Ozinsky et al. 2000).

PRR triggering by PAMPs can induce production of multiple proteins including interferon regulatory factors (IRFs). The IRFs activate type I interferons, which include interferon alpha (IFNα) and interferon beta (IFNβ) (reviewed Tailor 2006).

1.1.2.1 Type 1 interferons

The expression of IRFs leads to the upregulation of type 1 interferons IFNα and IFNβ, aid innate immune responses in multiple ways. For example, both IFNα and IFNβ induce increased MHC on surface of cells, which leads to greater levels of antigens presentation to the adaptive response, in the form of T cells. Increased MHC on the surface of cells also inhibits NK cell activation (Ljunggren and Kärre 1990; Moretta et al. 1993; Ciccone et al. 1992). IFNα and IFNβ can also induce the release of cytotoxic granules that kill infected cells (Jewett and Bonavida 1995; Liang et al. 2003). Furthermore, type I IFNs induce the

maturation of DCs, macrophages and their expression of co-stimulatory molecules that promote a strong adaptive response, thus linking both arms of the immune system (Murphy 2012).

1.1.2.2 NK cells

Natural Killer (NK) cells play a significant role in the innate immune system because they are capable of detecting and killing non-self or infected cells without prior specific activation. Activation of NK cells is determined by a balance of the activation and inhibition signals received by the cell (Sallusto et al. 1999; Wallace and Smyth 2005) NK cells are activated by sensing decreased levels of major histocompatibility complex (MHC) on a cell (Rinkevich 1999; Ljunggren and Kärre 1990; Moretta et al. 1993; Ciccone et al. 1992).

The killer cell immunoglobulin-like receptor (KIR) or the killer lectin-like receptors (KLR) families (Medzhitov and Janeway 1997; Vilches and Parham 2002; Ozinsky et al. 2000; Parham 2005) also interact with NK cells to induce signals that activate (Ljunggren and Kärre 1990; Diefenbach et al. 2002; Moretta et al. 1993; Bauer et al. 1999; Ciccone et al. 1992) or inhibit activation (Jewett and Bonavida 1995; López-Botet et al. 2000; Liang et al. 2003). The balance of activating and inhibitory signals regulates the activity if NK cells.

When NK cells are activated sufficiently, they secrete granzymes and perforin, which induce apoptosis of nearby cells (Trapani and Smyth 2002).

Interactions with cytokines can also induce NK cell activation. When NK cells encountered type 1 interferons it induced an upregulation of cytolytic effectors such as Fas-L and perforin which increased cell cytotoxic potential and increased expression of IFNγ (Jewett and Bonavida 1995; Liang et al. 2003). NK cells can

also be activated by interleukin 12 (IL-12) and interleukin 18 (IL-18) to produce large quantities of IFNγ (Chaix et al. 2008).

1.1.2.3 Dendritic Cells

DCs express a variety of TLR receptors, PRRs, Fc receptors, complement receptors, or c-type lectins that recognize mannose receptors to sense pathogenic molecules (Savina and Amigorena 2007). DCs also regularly macropinocytose the environment around them, engulfing molecules from the extracellular environment (Sallusto, Cella, and Danieli 1995).

Dendritic cells (DCs) are considered antigen-presenting cells (APCs) because they are capable of degrading through proteolysis the molecules that are taken up by the cell. Then antigen peptides from the molecule are loaded onto MHC molecules to be presented to other cells. Although other phagocytes can also present antigen on MCH molecules DCs are much more efficient and DCs are the only type capable of activating naïve T cells (Savina and Amigorena 2007). When activated through TLRs, DCs secrete cytokines that affect both the innate and adaptive immune systems (Kadowaki et al. 2001).

1.1.2.4 Macrophages

Macrophages are mature monocytes whose main function is to engulf (phagocytosis) and destroy invading organisms. Macrophages are activated by IFNγ, microbal stimuli binding PAMPS, TLRs and other receptors such as CD14, Fc or complement receptors, or by cytokines such as IL-4 and IL-13. The activation of macrophages can induce an increase production of co-stimulatory molecules and cytokines, phagocytosis of molecules and an upregulation of MHC molecules. The

phagocytised molecules can then be destroyed and then the processed antigens from these molecules can be loaded onto MHC molecules (Gordon 2003).

1.1.2.5 Neutrophils, Eosinophils and Basophils

Neutrophils make up the largest proportion of innate immune cells. These cells are granulocytes that migrate to infection or inflammation sites and take up many microorganisms by phagocytosis. Neutrophils then degrade the ingested microorganisms using antimicrobial molecules and enzymes that help break down the organism. Eosinophils and basophils perform a similar role with parasites that are too large for neutrophils to phagocytose (Murphy 2012).

1.1.3 Adaptive Immune System

The adaptive immune system is of a more recent origin than the innate immune system and it is found only in vertebrates (Rinkevich 1999) reviewed by(Cooper and Alder 2006). The adaptive immune system response is another level of protection in the body against infectious agents. The adaptive immune system cells are mostly comprised of B cells and T cells. These cells use antigen-specific receptors to respond to pathogen-specific epitopes and, thus, develop a highly targeted response.

More time is necessary to produce the targeted adaptive response than is needed for the innate immune response. However, the targeted response can persist after the elimination of a pathogen, preventing sort-term re-infection and can provide a long-lasting immunity against specific pathogens. This long lasting immunity is known as immunological memory (Zinkernagel and Bachmann 1996).

The activation of the adaptive immune system requires the innate immune system the innate immune system to produce cytokines, co-stimulatory molecules or

present MHC loaded with antigen to the cells of the adaptive immune system for efficient activation to occur (Medzhitov and Janeway 1997).

1.1.3.1 B cells

B cells are adaptive immune system cells that have a B cell receptor (BCR) to detect antigens. Properly activated and differentiated B cells produce antibodies that can help directly control infection or mark infectious molecules for destruction by the innate immune system.

The diversity of the BCR comes from the arrangement of variable copies of the V and J genes of the heavy and light chains using somatic recombination along with the diversity of the D genes in the heavy chain of the BCR (Tonegawa 1983). Mature B cells can be activated by APCs, antigen or CD4 helper T cells presenting antigen on the MHC that the B cell BCR recognizes. Additional co-stimulatory molecules such as CD40 ligand (CD40L) also aid in B cell activation (Murphy 2012).

After the B cell has been activated it migrates to germinal centres, where it proliferates and undergoes hypermutation of the BCR (Rajewsky et al. 1987). Cells can also undergo immunoglobulin class switching. These proliferated and hypermutated B cells, now called centroblasts, then undergo affinity selection in the germinal centers. Only the centroblasts that still recognize the antigen presented by the CD4 T cells or APCs survive and the other centroblasts undergo apoptosis(Thorbecke et al. 1994).

Differentiated centrocyte cells become the plasma cells or long-lived memory B cells. Plasma cells produce antibodies that upon binding with antigen can neutralize the antigen, activate the complement cascade, or induce phagocytosis by innate immune cells. Long-lived memory B cells persist in the organism for long

periods of time proving protection against re-infection from that specific antigen (Fairfax et al. 2008).

1.1.3.2 T cells

The T cell is the other main cell of the adaptive immune system. Naïve T cells must be activated by antigen, appropriate co-receptors and appropriate cytokine signals. When all of the appropriate activation signals occur, T cells proliferate and differentiate into specific types of T cells with different effector functions. These functions generally divided into three classes: activating (Helper T cells), killing (Cytotoxic T cells) and regulation (Regulatory T cells). Some activated T cells also differentiate into memory cells, which can provide long-lasting immune responses against an antigen (Murphy 2012).

1.1.3.2.1 CD8 T cells

Naïve T cells that express the CD8 co-receptor will become cytotoxic T cells, which are capable of killing other cells, after appropriate activation. CD8 T cells have TCRs that recognize antigens presented by APCs on MHCs. The CD8 co-receptor specifically binds MHC class I. The MHC class I pathway loads antigen from digested intracellular pathogens. Thus, cytotoxic CD8 T cells are important in protection against intracellular pathogens, most notably viruses (Hewitt 2003).

Activation of naïve CD8 T cells is highly regulated due to the high destructive capacity of the cells, and therefore, requires very strong signals for activation (Piccirillo and Shevach 2001). With some viral infections, DCs can be activated enough to directly activate CD8 T cells, however, CD4 T cells are often needed to aid activation of CD8 T cells(Ekkens et al. 2007).

Once $CD8^+$ T cells are activated to become effector cytotoxic CD8 T cells, further activation of the TCR by APCs presenting the specific antigen/MHC class I by can induce cytotoxic and other effector functions of the cell. Activated CD8 T cells can produce various cytokines such as IFNγ, TNFα, and IL-17. These cytokines can be anti-viral or pro-inflammatory and further activate the immune system. Activated CD8 T cells can also secrete granules with granzymes, perforin, and express Fas ligand on the cell membrane, which can induce apoptosis of other cells (Harty et al. 2000).

1.1.3.2.2 CD4 T cells

CD4 T cells express the co-receptor CD4 that binds to the MHC class II receptor (Doyle and Strominger 1987). The MHC class II molecules present antigen from intracellular vesicles. These intracellular vesicles often contain molecules that have been phagocytosed by macrophages, dendritic cells, or other phagocytotic cells. Therefore, the CD4 T cells are often presented with antigen from extracellular infections. The CD4 T cell is also capable of producing cytokines that help activate other cell types in both the innate and adaptive immune systems.

Naïve T cells that express CD4 can differentiate into cells with many different effector subsets with different functions upon activation. The cytokines present during the early stages of naïve T cell activation helps to determine the type of effector function the CD4 T cell will develop. These subsets of activated $CD4^+$ T cells include T_H1, T_H2, T_H17, T follicular helper cell (T_{FH}), and regulatory T cells.

- T_H1 cells are distinguished by the production of IFNγ and IL-2. T_H1 cells help control intracellular bacteria such as tuberculosis and leprosy along with viruses. T_H1 cells also aid in tumour immune rejection.

- T_H2 cells are distinguished by the production of IL-4, IL-5, IL-9 IL-10 and IL-13. The T_H2 response is often associated with humoral immune response and associated with extracellular pathogens like helminthes. T_H2 cells are also attributed to some allergen-specific responses.
- T_H17 are distinguished by the production of IL-17 and they help neutrophils respond to extracellular bacteria and fungi.
- T_{FH} cells help B- cells produce high affinity antibodies and are identified by expression of markers such as CXCR5 and ICOS.
- Regulatory T cells help suppress T cell responses, which limits the immune response and helps prevent autoimmunity. These cells express CD25 and FoxP3 (Wan and Flavell 2009).

1.1.3.2.3 T Cell Maturation

T cells recognize antigen presented by APCs on MHCs using a T cell receptor (TCR). The diversity of the TCR, and thus the antigens the TCR is able to recognize, comes from gene rearrangement similar to the rearrangement found in the BCR. T cell development occurs in the thymus. During this process the T cell precursors thymocytes, differentiate, express various co-receptors and proliferate. In the proliferated T cells, the genes in the variable amino-terminal region are rearranged to increase diversity in the TCR. There are two types of TCR based on the type of glycoprotein chains they are composed of: αβ and γδ. The αβ TCR is the most common type of TCR.

For αβ TCRs, the α and β chains have V and J domains are recombined and the β chain also has a D domain that is recombined. This is added to a constant region that makes up the rest of the chain (Tonegawa 1983). Further diversity is

added with the addition of N and P nucleotides to the joint regions between the V, J and D domains. For γδ TCRs, the V, J, and D domain are rearranged in the same way; however, γδ cells have substantially fewer V gene segments to rearrange on both γ and δ chains. The decreased diversity in arrangement of V genes may be compensated for by increased variability in the joint regions between the domains than is seen in αβ TCRs (Alt et al. 1992).

For a T cell to survive the maturation and selection processes within the thymus, the final rearrangement of the TCR must not bind self-antigens presented on MHCs strongly, but if the signal also cannot be too weak. If a T cell does not fall into the acceptable middle range of TCR signalling towards self-antigens, the cell undergoes apoptosis. Around 98% of T cells produced in the thymus undergo apoptosis within the thymus. The mature T cells which emerges from the thymus express an appropriately specific TCR, CD3 complex, and either CD4 or CD8 co-receptor molecules(Starr and Jameson 2003; Murphy 2012).

1.1.4 Innate-like T cells that bridge the gap between adaptive and innate immunity

Although cells and functions of the immune system are often classified into either adaptive or innate immunity, the distinction between these two groups becomes increasingly unclear. One area where the lack of distinction is seen is in the classification of specific cell subsets. As more specific cell subsets are studied in depth, cells have been found that would normally be classified as adaptive based on cell type but the cell functions in a manner that more closely resembles innate immunity. These cell types are often considered cells that bridge the innate and

adaptive immune systems. Many of these "bridge" cells are types of T cells and include γδ T cells, CD8αα T cells, iNKT cells, and MAIT cell (Figure 1.1).

Figure 1.1

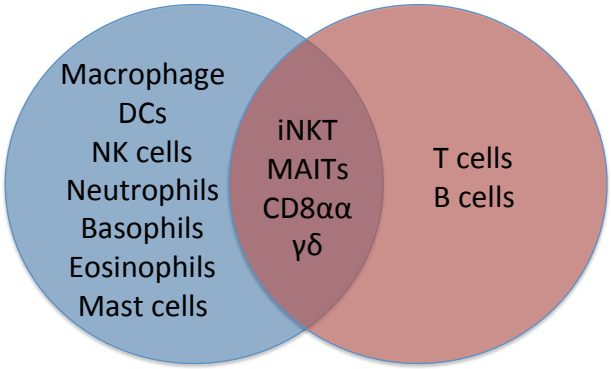

Cells of the adaptive and innate immune systems
Diagram of the cells considered to be in the innate and adaptive immune systems and the cells that share characteristics of both systems.

1.1.4.1 γδ T cells

γδ T cells are a small subset of T cells that express TCRs composed of γ and δ glycoprotein chains. Intraepithelial γδ T cells TCRs display much less diversity than αβ TCRs. The ligands of these γδ TCRs have been suggested to be heat-shock proteins, MHC class Ib molecules, and unorthodox nucleotides and phospholipids (Witherden and Havran 2012; Murphy 2012) (Figure 6.1 on page 144). The γδ T cells do not appear to require antigen processing and presentation by classical MHCs, but recognize the target antigen directly (Sciammas et al. 1994; Cavallari et al. 2013). The direct recognition of target antigen allows for a quicker cytokine production response. γδ T cells were shown to be important in the antiviral immune response (Maccario et al. 1993) (Sciammas and Bluestone 1999).

1.1.4.2 Invariant Natural Killer T (iNKT) cells

Invariant Natural Killer T (iNKT) cells functionally resemble innate cells by rapidly eliciting effector functions after activation, and they do not develop immunological memory. iNKT cells express many of the markers of NK cells but also express a TCR like T cells.

The TCR on iNKT cells is semi-invariant and in humans expresses Vα24 Jα18. This TCR recognizes the MHC class Ib molecule CD1d. The CD1d molecule binds and presents lipids or glycolipids, most commonly α-galactosyl ceramide (α-GalCer) (Van Kaer et al. 2011) (Figure 6.1 on page 144).

After activation of the TCR, iNKT cells can rapidly secrete cytokines (IFNγ, TNFα, GMCSF, IL-2, IL-3, IL-4, IL-5, IL-6, IL-9, IL-10, IL-13, IL-17, and IL-21), chemokines (RANTES, MIP-1α), or induce cytotoxic activity (Coquet and Chakravarti 2008; Matsuda et al. 2008). iNKT cell activation is regulated by the balance of activating and inhibitory signals, such as IL-2, PD-1, PD-L1, PD-L2, and cell anergy (W.-S. Chang et al. 2008; Parekh et al. 2009). iNKT cells also tend to constitutively express molecules such as CD25 and CD69 (Van Kaer et al. 2011).

The activation of iNKT cells and consequent expression of cytokines has been shown to induce both pro-inflammatory and anti-inflammatory effect depending on the specific activation (Godfrey and Kronenberg 2004). iNKT cells have also been shown to exhibit different effector functions depending on the tissue/organ they are located in (Crowe et al. 2005).

1.1.4.2.1 iNKT cells and Disease

iNKT cells have been shown to play a protective role against infection of microrganisms that contain α-GalCer or other known iNKT antigens but may also

protect against other infectious organisms (Joyee et al. 2007). iNKT cells have also been shown to be protective against graft vs. host disease (Pillai et al. 2007). Experiments showed proinflammatory activities of iNKT cells were critical in some anti-tumor responses (Terabe and Berzofsky 2008).

However, iNKT cells have also been shown to be pathogenic in some infections such as *Chlamydia muridarum* (Joyee et al. 2007). In other experiments, iNKT cells contributed to the occurrence of sepsis syndrome (Mattner et al. 2005). iNKT cells have also been shown to play a pathogenic role in models of arthritis (Coppieters et al. 2007), primary billiary cirrhosis (Joyce and Van Kaer 2008), and airway hyper-responsiveness, a main feature of asthma (Van Kaer 2007).

1.1.4.3 Mucosal Associated Invariant T (MAIT) cells

Mucosal Associated Invariant T (MAIT) cells are an evolutionarily conserved innate-like T cell population that can detect certain bacterially infected cells and respond by the upregulation of activation markers and cytokine production (Le Bourhis et al. 2010; Goldfinch et al. 2010).

MAIT cells are a phenotypically homologus population of T cells. This T cell subset expresses a semi-invariant TCR Vα7.2 Jα33)(Porcelli et al. 1993) that is restricted by the non-classical MHC class Ib molecule MR1 (Huang et al. 2008; Chua et al. 2011). The canonical Vα7.2 Jα33 TCR along with surface expression of either CD161 or IL-18R defines the MAIT population (Martin et al. 2009; Le Bourhis et al. 2010; Dusseaux et al. 2011) (Figure 1.2 on page 18).

The MR1 molecule has been shown to bind to riboflavin metabolites (Kjer-Nielsen et al. 2012). Similar vitamin derivatives are produced as part of the bacterial riboflavin biosynthetic pathway in many bacteria. The origin of the MR1 antigen

being found in the riboflavin biosynthetic pathway was further confirmed by presence of the pathway in bacterial strains that MAIT cells are activated by, and missing in the strains that do not activate MAIT cells (Kjer-Nielsen et al. 2012).

MAIT cells have been suggested to be preferentially located in mucosal associated tissues, but substantial populations are also found in peripheral blood, the liver, and other tissues (Treiner et al. 2003; Martin et al. 2009; Le Bourhis et al. 2010; Goldfinch et al. 2010; Billerbeck et al. 2010; Walker et al. 2012).

1.1.4.3.1 MAIT Cell Development

MAIT cells are absent in mice raised in a germ free environment, but MAIT cells can be recovered if the mice are reconstituted with even a single strain of bacteria containing the riboflavin synthetic pathway (Treiner et al. 2003; Le Bourhis et al. 2010; Kjer-Nielsen et al. 2012). In humans, umbilical cord blood contains low numbers of MAIT cells. However, after birth, the numbers of MAIT cells dramatically expand. The numbers of naïve MAIT cells in the thymus are also low, but they can constitute up to 4% of the T cells in the periphery. The MAIT cells in the periphery express a memory phenotype.

The naïve MAIT cells are thought to leave the thymus, migrate to mucosal tissues where the naïve MAIT cells encounter riboflavin metabolite derivatives from the riboflavin synthetic pathway positive bacteria. The riboflavin metabolites are presented to the MAIT cells, activating the MAIT cells and inducing proliferation.

MAIT cell development is also different from iNKT cell development, since active SLAM adaptor protein (SAP) is necessary for $CD4^{-}CD8^{-}$ thymocytes to develop into iNKT cells, but not MAIT cells (Martin et al. 2009).

1.1.4.3.2 MAIT Cells and Disease

Multiple groups, who used different phenotypic markers to define the subset, have studied the MAIT cell population. However, many of the studies used phenotypic markers that did not select the MAIT population exclusively, but would identify a subset that was largely populated by MAIT cells. The results of these studies will also be included in this section.

MAIT cells respond to APCs expressing antigens from bacteria such as *Escherichia coli* and *Mycobacterium abscessus* (Le Bourhis et al. 2010), but also to *Mycobacterium tuberculosis* infected epithelial cells (Goldfinch et al. 2010). Originally it was thought that MAIT cells were unresponsive towards viral infections, but a recent study indicates that MAIT cells can respond to viral and inflammatory stimuli due to specific responses to IL-12 and IL-18 stimulation (Ussher et al. 2013).

Changes in levels of MAITs found in the blood can be seen during viral infections. In HIV infection, MAIT cells decrease in a non-reversible manner even with highly active antiretroviral treatment (HAART) (Cosgrove et al. 2013). In chronic HCV infection, MAIT cells in the blood decrease and high numbers are found in the liver (Billerbeck et al. 2010).

Changes in the levels of MAIT cells present can also be seen in autoimmune diseases. One study of a mouse model for arthritis showed MAIT cells to promote inflammation and exacerbate arthritis (Chiba et al. 2012). However, another study in humans indicated that MAIT cells (determined by $CCR6^{+}$ IL-$18R\alpha^{hi}$ $CD161^{++}$ $CD8^{+}$ $CD3^{+}$ expression) were decreased in the peripheral blood of arthritis patients compared with healthy controls (Annibali et al. 2011).

A study looking at multiple sclerosis (MS) showed reduced numbers of MAIT cells in blood of active MS patients and correlated the levels of disease activity. The study suggested MAIT cells had a suppressive role against pathogenic TH1 cells (Miyazaki et al. 2011). In contrast, a second study showed increased numbers of MAIT cells (determined by $CCR6^{+}$ IL-$18R\alpha^{hi}$ $CD161^{++}$ $CD8^{+}$ $CD3^{+}$ expression) were increased in MS patients compared to controls (Annibali et al. 2011). A study of experimental autoimmune encephalomyelitis (EAE), a mouse mode for MS, showed MAIT cells to have a protective role against EAE (Croxford et al. 2006).

MAIT cells have also been found in inflammatory tissues including tumours of the brain and kidney (Peterfalvi et al. 2008).

One caveat, however, to any correlations seen in levels of MAIT cells within the blood or a specific tissue location is that a correlation does not equal causation of actually being involved in the pathogenesis of the disease. The presence or absence of MAIT cells in tissues could simply be a consequence of the disease setting.

1.1.4.4 CD8αα T cells

CD8αα T cells are cells that express an αβ TCR; however, the CD8 molecule is formed by an α chain homodimer instead of an αβ heterodimer. The CD8αα T cells were believed to have a regulatory role with the CDαα acting as a co-repressor (Tang et al. 2006; Tang et al. 2007). CD8αα have also been suggested to play a role in memory cell formation during influenza A infections (Zhong and Reinherz 2005).

A study comparing CD8αα with MAIT cells found that all CD8αα cells express high levels of CD161 and 87% contain the Vα7.2 restricted TCR, indicating that most CD8αα cells are MAIT cells (Walker et al. 2012) Figure 1.2 on page 18.

Figure 1.2

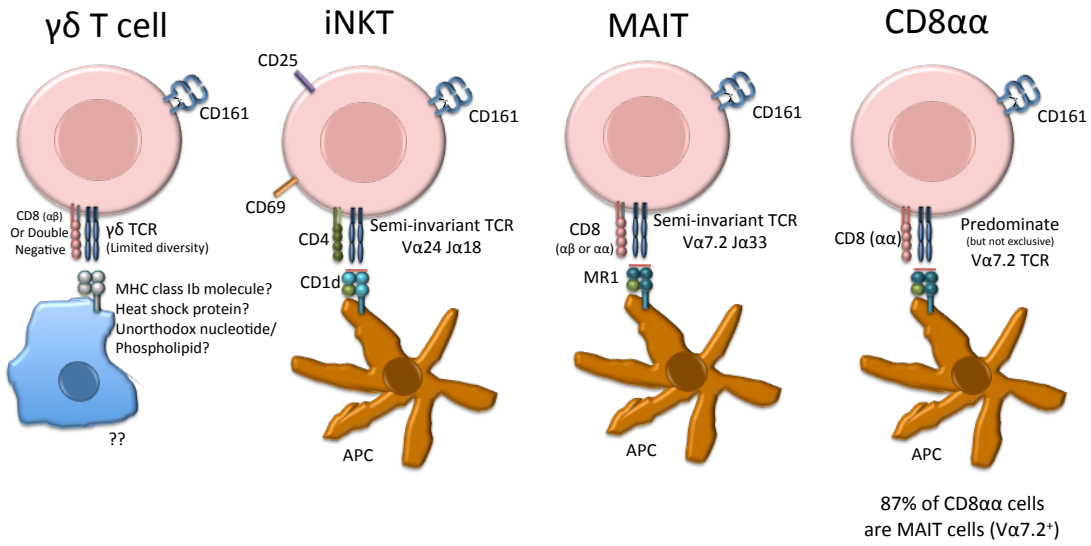

Cells that Bridge the Adaptive and Innate immune systems
Diagram comparing some of the different cells that are considered bridges between the adaptive and innate immune systems, along with the cells and antigens capable of act.

1.2 Introduction – Part II

When looking at T cells that bridge both the adaptive and innate immune systems, one protein stands out as being expressed highly by all of these cell types: CD161. This commonality of CD161 expression on the "bridge" cells led to further examination of CD161.

1.2.1 Relationship between CD161 and disease states

The CD161 protein is not only present on "bridge" types of cells that have been implicated in regulation of disease states, but changes in expression or location of cells expressing CD161 have been shown in multiple disease states including viral infections, bacterial infections, and immune related diseases.

1.2.1.1 CD161 and viral infection

Changes in the levels of cells expressing CD161 have been seen in viral infections. In patients with human immunodeficiency virus (HIV) $CD161^{++}$ MAIT cell levels decreased in peripheral blood compared to healthy controls, and the levels did not recover after HAART (Cosgrove et al. 2013). In patients with chronic hepatitis C (HCV) $CD161^{++}$ $CD8^{+}$ T cells were reduced in the peripheral blood and enriched in the liver. However, increases of $CD161^{++}$ $CD8^{+}$ T cells in the liver were also seen in patients with autoimmune hepatitis, alcoholic liver disease, primary biliary cirrhosis, and non-alcoholic steatohepatitis (Billerbeck et al. 2010; Oo et al. 2012). This suggested that the increased levels of $CD161^{++}$ $CD8^{+}$ T cells could be related more to the inflammation process rather than the viral activity (Billerbeck et al. 2010).

1.2.1.2 CD161 and bacterial infection

Associations have also been found linking the presence of cells expressing high levels of CD161 protein and the presence or outcome of bacterial infections. $CD161^{++}$ MAIT cells have been observed to decrease in the blood and increase in the lungs of tuberculosis patients (Gold and Lewinsohn 2013). In mouse models, the $CD161^{++}$ MAIT cell population has been associated with protection against *Klebsiella pneumoniae* (Georgel et al. 2011), *Escherichia coli*, *Mycobacterium abscessus* (Le Bourhis et al. 2010), and *Mycobacterium bovis* from the BCG vaccine strain (Chua et al. 2012).

1.2.1.3 CD161 and immune related diseases

Links have also been made between levels and specific locations of CD161 expressing cells in autoimmune and immune related diseases. In patients with

multiple sclerosis $CD161^{++}$ $CD8^{+}$ T cell levels were increased in the peripheral blood and were found in brain infiltrates (Annibali et al. 2011). In rheumatoid arthritis patients, $CD161^{++}$ $CD8^{+}$ T cells levels were decreased in the peripheral blood (Annibali et al. 2011). Increased levels of $CD161^{+}$ T cells have also been shown in the gut of patients with Crohn's disease (CD) and in the skin of patients with psoriasis (Cosmi et al. 2008).

1.2.1.4 Relationship between CD161 and T_H17/T_C17 cells

Interleukin 17 (IL-17) is a cytokine that induces a proinflammatory response along with inducing cells to produce other cytokines that amplify the acute inflammatory response. IL-17 production is the hallmark of $CD4^{+}$ T helper 17 (T_H17) cells and of $CD8^{+}$ (T_C17) cells (Murphy 2012). T_C17 cells would in theory be cytotoxic in nature; however, T_C17 cells have been shown to be low in the cytotoxic molecules granzyme B and perforin. This may indicate low killing ability for T_C17 cells.

CD161 protein expression is considered to be a marker for T_H17 (Cosmi et al. 2008). T_C17 cells have been shown to be restricted to $CD161^{+}$ populations (Maggi et al. 2010), and more specifically to the $CD161^{++}$ population (Billerbeck et al. 2010).

Recent studies have suggested that T_H17 cells are involved with the pathogenesis of immune-mediated diseases such as psoriasis, rheumatoid arthritis, MS, inflammatory bowel disease (IBD) and asthma (Tesmer et al. 2008). T_C17 cells have also been shown to sustain autoimmune disease progression in models of childhood type 1 diabetes (Saxena et al. 2012) and promote graft vs. host disease (Zhao et al. 2011). An increase in numbers of T_C17 cells were shown in peripheral

blood and synovial fluid of rheumatoid arthritis patients (Qu et al. 2013). However, T_C17 cells have also been shown to protect against lethal influenza challenge (Hamada et al. 2009).

1.2.2 CD161 Protein

The CD161 protein was found consistently on cell populations that "bridge" the innate and adaptive immune systems, which have been implicated in several disease states. Changes in CD161 protein expression levels have also been linked to several disease states. Therefore, understanding more about the CD161 protein itself is important to understanding how cells expressing CD161 react to or interact with various disease states.

The human protein CD161 encoded by the gene *KLRB1* is also known as killer cell lectin-like receptor subfamily B, member 1 (KLRB1), natural killer receptor protein 1 A (NKRP-1A) and less commonly C-type lectin domain 5 B (CLEC5B). CD161 is expressed by most NK cells along with subsets of T cells (including $CD4^+$, $CD8^+$, and double negatives), NKT cells, and immature thymocytes (Lanier et al. 1994; Poggi et al. 1996; Exley et al. 1998).

1.2.2.1 CD161 structure

The CD161 protein is a type II transmembrane C-type lectin-like protein found as a disulphide-linked homodimer. The molecular weight (mw) of the CD161 glycoprotein is ~40 kDa, which is reduced to ~26 kDa after the removal of N-linked oligosaccharides. CD161 is expressed on the majority of NK cells and ~24% of peripheral T cells.

The cDNA encoding CD161 is 738 base pairs with an open reading frame of 225 amino acids (aa). CD161 also contains the sequence similar to an

immunoreceptor tyrosine-based inhibition motif (ITIM), called a hemi-ITIM. The CD161 hemi-ITIM has substituted an alanine (A) -2 relative to the tyrosine (Y) in the ITIM, which normally contains isoleucine (I), valine (V), leucine (L) or serine (S) (Rosen et al. 2008). The alanine in this position is thought to decrease inhibitory potential of the ITIM sequence by inhibiting interaction with the tyrosine phosphatase SHP-1 (Burshtyn 1997).

1.2.2.1.1 Type II transmembrane protein

Type II transmembrane proteins are proteins that make a single pass through the lipid bilayer and the C-terminus (COOH) end of the protein is found in the extracellular space, while the N-terminus (NH_2) end of the protein is intracellular (Chou and Elrod 1999).

1.2.2.1.2 C-type lectin superfamily

The C-type lectin superfamily is a family of receptors that can have the capability to recognize pathogens, play a role in cell-cell communication, and recognize proteins or carbohydrates (Drickamer and Taylor 1993). The C-type refers to Ca^{+2} binding fold that was originally thought to be required for the function of the protein, which was binding carbohydrate sugars. The carbohydrate binding domains on the receptors were known as carbohydrate-recognition domains (CRDs). However, further studies revealed members of the family that were structurally related but did not bind carbohydrate sugars or that did not need Ca^{+2} to bind. These structurally related receptors were known as having C-type lectin-like domains (CTLDs) (reviewed Drickamer 1999). Proteins with CTLDs are widely represented amongst proteins mediating the innate immune response (Weis et al. 1998).

1.2.2.1.3 CD161 gene *KLRB1* location

The CD161 expressing gene *KLRB1* is found within the natural killer gene complex (NKC) (Yokoyama et al. 1991; Yabe et al. 1993) on chromosome 12 in humans and on chromosome 6 in mice (Lanier et al. 1994). The NKC is a region found on human chromosome 12 and mouse chromosome 6 where most of the proteins encoded in the region are receptors found on NK cells and they are generally type II transmembrane C-type lectins with highly related structures (Yokoyama and Plougastel 2003).

1.2.2.1.4 Homology of CD161

The human CD161 protein shows fairly low homology with other human proteins. CD161 shares the closest homology with NKG2A (natural killer group 2A) with 26% similarities. The next closest homologus proteins are human CD69 and mouse Ly49 with both sharing less than 26% homology. Human CD161 is the ortholog of the mouse NKRP1 family with which it shares 46% homology (Lanier et al. 1994).

1.2.2.2 Human Vs. Mouse CD161

1.2.2.2.1 Human CD161

The human CD161 (NKRP-1A) protein comes from the *KLRB1* gene. CD161 has been reported to bind two different proteins, lectin-like transcript 1 (LLT1) (Aldemir et al. 2005; Rosen et al. 2005) and proliferation-induced lymphocyte-associated receptor (PILAR)(Huarte 2008). CD161 has also been reported to bind to oligosaccharides (Bezouška et al. 1994; Christiansen et al. 2006). The functional impact of ligating human CD161 is unclear and discussed further in section Functional Effects of Human CD161 Ligation on page 31.

1.2.2.2.2 Mouse NKRP1 family

The ortholog of human CD161 (NKRP-1A) is the mouse NKRP1 protein family. The mouse NKRP1 family consists of seven different genes *Nkrp1a-g* (although *Nkrp1e* and possibly *Nkrp1g* are thought to be pseudogenes) (Plougastel et al. 2001; Carlyle et al. 2006). Of the five *Nkrp1* genes with known proteins, the proteins are expressed on different cells and have different functions. The ligands of this protein family are non-MHC ligands from the C-type lectin related (Clr) family, which encoded by genes also interspersed with the NKRP1 genes within the NKC (Plougastel, Dubbelde, and Yokoyama 2001; Iizuka et al. 2003).

The mouse NKRP1C protein is expressed on NK cells (Glimcher et al. 1977), NKT cells (MacDonald 1995), and possibly on activated $CD8^+$ T cells (Aust et al. 2009). The NKRP1C protein contains the alloantigen NK1.1, and NK1.1 is commonly used to mark NK cells in mice (Glimcher et al. 1977; Koo and Peppard 1984). However, it has been noted that some monoclonal antibodies (mAb) for NK1.1 also bind the NKRP1B protein (Kung et al. 1999; Carlyle et al. 2006). NKRP1C has a charged amino acid in the transmembrane region of the protein that associates with the Fcγ chain, which activates induction of cytolitic activity and cytokine secretion (Aust et al. 2009). The ligand for NKRP1C has not yet been defined (Figure 1.3).

The mouse proteins NKRP1A and NKRP1F are found on NK cells and have charged amino acids in their transmembrane regions, which induce NK cell cytolytic activity and are considered activating proteins (Aust et al. 2009). The ligand for NKRP1A is still unknown and NKRP1F has been shown to bind to Clr-g (Iizuka et al. 2003) and to Clr-x (Aust et al. 2009)(Figure 1.3).

Mouse proteins NKRP1B and NKRP1D are found on NK cells and lack a charged transmembrane residue. When cross-linked NKRP1B/D induce an inhibitory signal (Aust et al. 2009). The protein Clr-b has been shown to bind both NKRP1B and NKRP1D (Plougastel, Dubbelde, and Yokoyama 2001; Iizuka et al. 2003; Carlyle 2004) (Figure 1.3).

Figure 1.3

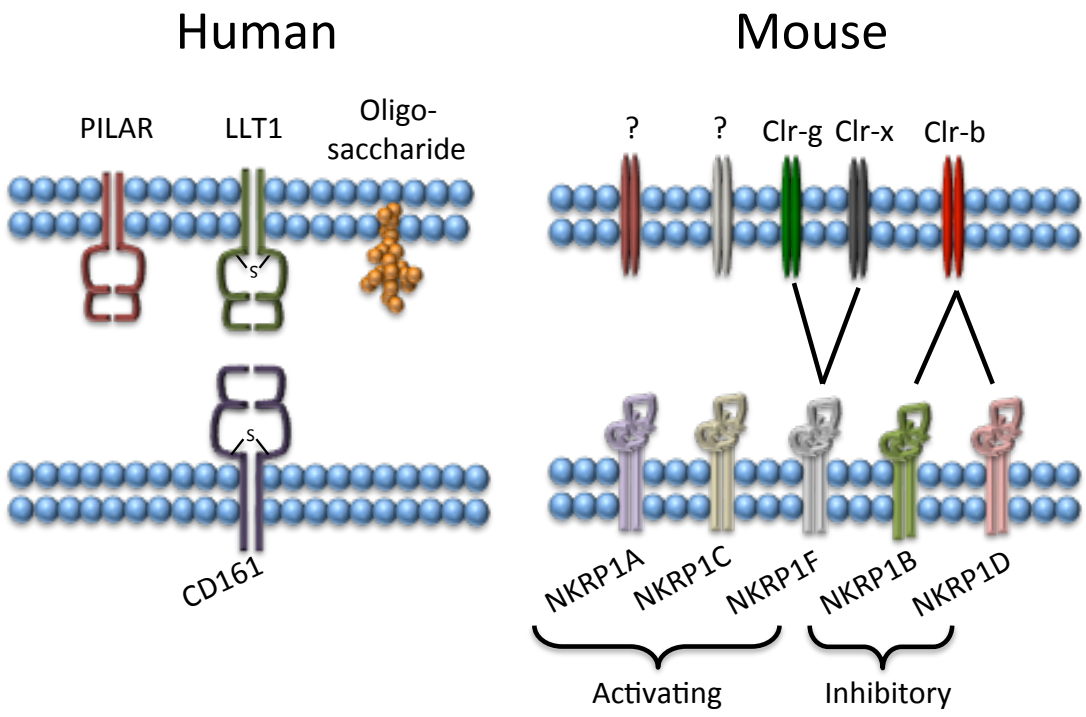

Human and Mouse proteins from the NKRP1 family and published ligands
Human CD161 has been described to bind PILAR, LLT1, and oligosaccharides. The mouse NKRP1 family has 5 known proteins. NKRP1A, NKRP1C, and NKRP1F are induce activating signals upon ligation. NKRP1A and NKRP1C have no known ligand, and NKRP1F binds Clr-g or Clr-x. NKRP1B and NKRP1D are both inhibitory and bind Clr-b. Adapted from Fergusson *et al.* 2011.

1.2.3 Ligands of Human CD161

Several ligands have been reported for human CD161. These include lectin-like transcript 1 (LLT1) (Aldemir et al. 2005; Rosen et al. 2005), proliferation-induced lymphocyte-associated receptor (PILAR) (Huarte et al. 2008), and oligosaccharides (Bezouška et al. 1994; Christiansen et al. 2006).

1.2.3.1 LLT1

The protein LLT1 is encoded by the gene *CLEC2D* and is also known as C-type lectin domain family 2 member D (CLEC2D), osteoclast inhibitory lectin (OCIL) and CLAX. LLT1 is a type II C-type lectin found on the NKC of human chromosome 12 (Boles et al. 1999). LLT1 is found on the cell surface as a glycosylated disulphide-linked homodimer (Rosen et al. 2008). Two different groups simultaneously identified LLT1 as a ligand for CD161 by (Aldemir et al. 2005; Rosen et al. 2005), and several other groups later confirmed this (Pozo et al. 2006; Germain et al. 2010; Kamishikiryo et al. 2011).

1.2.3.1.1 Binding kinetics

Binding analysis with surface plasmon resonance has shown LLT1 to bind CD161 with an affinity typical of proteins with interactions that mediate cell-cell recognition. LLT1 binds to CD161 with a low affinity, fast kinetics, small heat capacity, and entropically and enthalpically driven thermodynamics (Kamishikiryo et al. 2011).

1.2.3.1.2 Homology

Human LLT1 shows 43-48% homology with the mouse Clr protein family (Aldemir et al. 2005). LLT1 shares greater homology with some of the other human proteins also found in the human gene NKC including: activation induced C-type lectin (AICL) (59%), CD69 (56%), NKG2D (53%), and CD94 (51%))(Boles et al. 1999).

1.2.3.1.3 Location and function

Many studies have looked at the expression patterns of LLT1. When found in human osteoblastic cells, the LLT1 protein is called OCIL. In this environment OCIL

mRNA is constitutively expressed and the protein inhibited osteoclast formation and bone resorption (Hu et al. 2004). However, within peripheral blood cells there is little consensus on where and when LLT1 is expressed (See Table 1.1 for a summary of results). Reasons for the differences in results may be due to the method used to study LLT1 and the clone or type of antibody used. The functional impact of LLT1 binding its only known ligand CD161 will be discussed in section Functional Effects of Human CD161 Ligation on page 31.

Table 1.1 LLT1 Expression Patterns

Reference	Method	Antibodies	Cell type / Tissue
Boles 1999	Northern Blot	-	T, B and NK cells; Lymph node, thymus, spleen, LAK
Eichler 2001	RT-PCR	-	PMA-stimulated PBMCs
Zhou 2001	Northern blot, IHC, *In situ* hybridization	-	Osteoblasts; Liver, kidney, gut, heart, skeletal muscle
Iizuka 2003	RT-PCR	-	DCs, Macrophages (from bone marrow)
Carlyle 2004	FACS	mAb 4A6 (rat IgMκ)	Hematopoietic cells (no erythrocytes); Down-regulation in tumour cell lines
Mathew 2004	FACS	mAb L9.7	All monocytes, most B cells, few T and NK cells; PMA and IL-2 activated PBMCs
Hu 2004	RT-PCR	-	Osteoblasts, Upregulated with IL-1α and PGE_2
Rosen 2008	FACS, WB, RT-PCR	2F1, 4F68; mAb 402624 and 402659 (R&D); Rabbit anti-LLT1 antisera	Activated B cells and DCs
Germain 2010	FACS, RT-PCR, Real Time RT-PCR	2F1, 4F68; mAb 3480 (R&D); 4C7 (Abnova)	T and B cells, NK cells (low)
Germain 2011	FACS, WB, Real time RT-PCR	2F1, 4F68; mAB 3480 (R&D), 4C7 (Abnova)	No in resting PBMCs – upregulated with pathogen/IFN-γ stim

1.2.3.1.4 Splice variants

The *CLEC2D* gene has been shown to produce multiple slice variants. Six different splice variants have been identified, but only five produce a protein. Only splice variant 1 of *CLEC2D* creates the protein for LLT1 (Boles et al. 1999; Germain et al. 2010). Binding studies have also showed that only LLT1 and none of the other splice variants bind CD161 (Germain et al. 2010).

1.2.3.2 PILAR

The human protein proliferation-induced lymphocyte-associated receptor (PILAR) is a protein encoded by the gene *CLEC2A* and is also known as C-type lectin domain family 2 member A 1 (CLEC2A1), and keratinocyte-associated C-type lectin (KACL). The study by Spreu *et al*. that originally described the protein produced by the *CLEC2A* splice variant CLEC2A1, but did not name the protein or show binding of the protein (Spreu et al. 2007). A subsequent study by Huarte *et al*. named the protein made by CLEC2A1 as PILAR and described it as a ligand of CD161 (Huarte et al. 2008). After much of the work in this thesis on PILAR was completed, a follow-up study by Spreu *et al*. named the CLEC2A1 protein as KACL and described the protein as a ligand for NKp65 and not CD161 (Spreu et al. 2010).

The protein PILAR is encoded by the CLEC2A gene found in the NKC region of human chromosome 12. PILAR is a type II transmembrane C-type lectin with marked homology to other C-type lectins in the CLEC2 family encoded in the NKC. PILAR is glycoprotein with a molecular weight of ~30 kDa and is a 174 amino acids long. The amino acid sequence does not show any clear signalling motifs (Spreu et al. 2007). PILAR is expressed as a non-disulphide linked homodimer (Spreu et al. 2010).

1.2.3.2.1 Homology

The protein PILAR CTLD has 60.2% similarity with LLT1, 50.9% similarity with CD69, and 49.1% similarity with AICL (Spreu et al. 2007). No clear mouse ortholog has been described for PILAR. However, PILAR along with LLT1 both show a high degree of similarity to several *Clec2* mouse proteins (Huarte et al. 2008).

1.2.3.2.2 Expression

The expression patterns of PILAR are disputed between the two groups that have published studies. Spreu *et al*. showed cell surface expression of PILAR in high abundance on myeloid cell lines and in tissues such as the skin. This expression was later shown to be mainly restricted to keratinocytes. Spreu *et al*. also showed low levels of PILAR in PBMC, bone marrow, spleen, ovary and testis (Spreu et al. 2007; Spreu et al. 2010).

Huarte *et al*. showed expression of PILAR on $CD8^+$ T cells, $CD4^+$ T cells and B cells by PCR analysis. PILAR mRNA showed upregulation early after stimulation of the TCR. PCR analysis also showed PILAR to be constitutively expressed in the thymus and small intestine (Huarte et al. 2008).

1.2.3.2.3 Function of PILAR

The functional impact of ligation with PILAR is also contested. Huarte *et al*. demonstrate PILAR to have a role in dramatically increasing T cell expansion after ligation with CD161 (Huarte et al. 2008). On the other hand Spreu *et al*. show PILAR to stimulate cytotoxicity of NK cells after ligation with NKp65 (Spreu et al. 2010).

1.2.3.2.4 Splice variants

The gene that encodes PILAR has been shown to have at least 4 splice variants. There were two main splice variants, known as CLEC2A1 and CLEC2A2, and another version of each of these main variants that lacked the transmembrane domain encoding exon 2. CLEC2A1 is the variant that encodes PILAR. CLEC2A2 does not maintain homology with other C-type lectins at the C-terminal end of the CTLD, which may indicate a "wrecked" CTLD (Spreu et al. 2007).

1.2.3.2.5 Binding of CD161

PILAR was originally published by Huarte *et al*. to be a ligand of CD161 when immunoprecipitation experiments showed PILAR and CD161 being pulled down together, and binding was seen with soluble chimeric CD161 protein to PILAR transfected cells (Huarte et al. 2008). The subsequent study by Spreu *et al*. looking at binding of PILAR using ectodomains and tetramers did not show binding between PILAR and CD161 (Spreu et al. 2010). Two later studies also showed that the structures of PILAR and CD161 did not support binding between the proteins (Germain et al. 2010; Kamishikiryo et al. 2011).

1.2.3.3 Oligosaccharide

CD161 has also been shown to bind various oligosaccharides. Bezouska *et al*. showed CD161 (expressed by *E. coli* in a recombinant soluble form) bound several oligosaccharides with very high affinity in a calcium dependant manner. This study also showed that interactions between CD161 and the oligosaccharides could induce activation of targeted cell killing (Bezouška et al. 1994).

A more recent study by Christiansen *et al.* showed CD161 to bind oligosaccharides with the epitope Galα(1,3)Gal. Removing the terminal αGal epitope

and leaving a N-acetyllactosamine (NAcLac) xenoepitope increased binding with CD161. This study hypothesized that this NAcLac/CD161 binding may play a role in xenograft rejection (Christiansen et al. 2006).

1.2.4 Functional Effects of Human CD161 Ligation

Function effects of CD161 ligation has been studied by different groups using a range of different techniques. Some experimental setups use transfected or exogenous protein to trigger CD161, while others used different clones of αCD161 mAb. In some experiments the cells are activated with αCD3 or other stimulations, while others use resting cells. Some of the differences in experimental outcome may be due to these factors.

1.2.4.1 Functional Effect of CD161 ligation on NK cells

The functional effects seen after CD161 ligation on NK cells are consistent and generally accepted as being inhibitory. Studies found that ligation of CD161 through any means inhibited cytotoxicity towards target cells (Lanier et al. 1994; Poggi et al. 1998; Azzoni et al. 1998; Rosen et al. 2005; Aldemir et al. 2005), inhibited IFNγ production (Aldemir et al. 2005; Rosen et al. 2005), inhibited degranulation (CD107a) (Aldemir et al. 2005; Rosen et al. 2008), increased acid sphingomyelinase and transiently increased intracellular ceramide (Pozo et al. 2006).

1.2.4.2 Functional Effect of CD161 ligation on T cells

The functional effects of CD161 ligation on T cells are slightly less clear. Several studies have shown that CD161 ligation on T cells does not affect cytokine production especially IFNγ without also stimulating through αCD3 (Exley et al. 1998; Aldemir et al. 2005; Pozo et al. 2006). These studies also showed that

CD161 ligation with αCD3 stimulation increased IFNγ production (Exley et al. 1998; Aldemir et al. 2005; Pozo et al. 2006), increased proliferation (Exley et al. 1998; Pozo et al. 2006), but did not affect cytotoxicity (Exley et al. 1998).

However, a fourth study, by Rosen *et al.*, showed CD161 cross-linking with an αCD161 mAb on αCD3/ αCD28 stimulated T cells, resulted in a decrease in TNFα production, but had no affect on IFNγ production (Rosen et al. 2008). In addition, Rosen *et al.* used Staphylococcal Enterotoxin B (SEB) to stimulate cells with CD161 ligation and found no effect on TNFα or IFNγ production (Rosen et al. 2008). (See Table 4.1 on page 84 or Appendix Appendix 5 on page 219 for more detailed information)

1.3 Aims of this Thesis

- Design and produce the extracellular portions of CD161 ligands LLT1 and PILAR proteins for functional ligation experiments.
- Determine the expression patterns and stability of internal and surface CD161 expression.
- Use experimental model(s) to test functional effects of CD161 ligation by its natural protein ligands and monoclonal antibodies

Chapter 2 Material and Methods

2.1 Subjects

2.1.1 Subjects

All cells came from healthy donor leukocyte cones (NHS Blood and Transplant Services) or from healthy laboratory blood donors who gave informed consent.

2.2 Materials

2.2.1 Media

2.2.1.1 R10

RPMI 1640 with 10% FCS, 1mmol L-glutamine, 50,000U penicillin, and 50mg streptomycin (all Sigma)

2.2.1.2 RH10

RPMI 1640 with 10% Human Serum, 1mmol L-glutamine, 50,000U penicillin, and 50mg streptomycin (all Sigma)

2.2.1.3 MACs Buffer

PBS (phosphate buffered saline), 2mM EDTA (sigma), 0.5% FCS (sigma)

2.2.2 Soluble Protein

2.2.2.1 CLEC2A from Boston

The CLEC2A protein provided by Prof. Gordon Freeman are mIgG2a-IEGR-human CLEC2A, made with Hinge-mIgG2a with an Fc mutated to reduce FcR

binding, Linker of IEGR (Factor Xa cleavage site), and the extracellular lectin domain of hCLEC2A. The complete sequence of the protein is:

MRRMQLLLLIALSLALVTNSAEPRGPTIKPCPPCKCPAPNLEGGPSVFIFPPKIK
DVLMISLSPIVTCVVVDVSEDDPDVQISWFVNNVEVHTAQTQTHREDYNSTL
RVVSALPIQHQDWMSGKAFACAVNNKDLPAPIERTISKPKGSVRAPQVYVLP
PPEEEMTKKQVTLTCMVTDFMPEDIYVEWTNNGKTELNYKNTEPVLDSDGS
YFMYSKLRVEKKNWVERNSYSCSVVHEGLHNHHTTKSFSRTPGKIEGRKHA
KPVACSGDWLGVRDKCFYFSDDTRNWTASKIFCSLQKAELAQIDTQEDMEFL
KRYAGTDMHWIGLSRKQGDSWKWTNGTTFNGWFEIIGNGSFAFLSADGVHS
SRGFIDIKWICSKPKYFL.

2.2.3 Cell Lines

2.2.3.1 300-LLT1 and 300-Null cell lines

A cell line transfected with LLT1 (300-LLT1) and the parental cell line (300-Null) were provided by our collaborator Prof. Gordon Freeman. A western blot confirms the 300-LLT1 expressed in a LLT1 as a disulphide homodimer (Figure 4.1). The 300-LLT1 cell line also highly expressed LLT1 on the surface where the parental cell line 300-Null did not (Figure 4.2).

2.2.3.2 B cell line

The B cell line (BCL) used was an EBV immortalized primary B cells from a healthy donor. At resting state or when activated with various stimuli, LLT1 was not found up-regulated or present significantly on the surface of the B cell line (Figure 6.2).

2.3 Methods

2.3.1 PBMC Separation

Fresh PBMCs were obtained from heparanized blood or PBS diluted leukocyte cones layered over Lymphoprep™ separation medium (Axis Shield Diagnostics), then centrifugation for 24 min (no break at 2200 rpm. The PBMC layer was collected and washed twice with R10 (RPMI 1640 with 10% FCS, 1mmol L-glutamine, 50,000U penicillin, and 50mg streptomycin (all Sigma)), first for 7mins at 1700 rpm, then 10 min at 1500 rpm.

2.3.2 PBMC Freezing and Thawing

Freshly isolated PBMCs were frozen for later use in 90% FCS/ 10% DMSO solution. Cells were initially at -80°C and then frozen vials were transferred to liquid nitrogen (-180°C) after 1-3 days.

Frozen vials were thawed partially using a 37°C water bath and transferred into a 15ml falcon tube. R10 media with DNaseI (20U, Roche) was added and left on cells for 5 minutes. Cells were washed and re-suspended in R10.

2.3.3 Cell Selection

2.3.3.1 $CD8^+$ T cell Selection

$CD8^+$ T cells were isolated from PBMCs by positive selection with anti-CD8 magnetic beads (Miltenyi) using manual MS-columns (Miltenyi) following manufactures instructions. Purity was consistently >85%.

2.3.3.2 $CD8^+$ T cell Selection

$CD8^+$ T cells were isolated from PBMCs by positive selection with anti-CD8 magnetic beads (130-045-201) (Miltenyi) using manual MS-columns (130-042-201) (Miltenyi) following manufactures instructions. Purity was consistently >85%.

2.3.3.3 Anit-PE or Anti-FITC column selection

PBMCs were stained with PE or FITC conjugated antibodies and then bound with anti-PE (130-048-801) or anti-FITC (130-048-701) magnetic beads (Miltenyi). Cells were positively selected using manual MS-columns (130-042-201) (Miltenyi) following manufactures instructions.

2.3.4 Surface Stain, Intracellular Stain, and Flow Cytometry

Resting or stimulated cells were washed with PBS and then stained with fluorochrome-conjugated antibodies (see Appendix 6 on page 219) at room temperature for 30 minutes. Cells were then washed with PBS, and either fixed for surface only stains, or fixed and permeabilized. Cells are fixed (PBS containing 2% formaldehyde or using 1X Fixation/Permeabilization (ebioscience)) for 30 min at room temperature. Cells are then washed and permeabalized in 1X Permeabilization buffer (ebioscience) for 30 minutes. For intracellular staining fluorochrome-conjugated antibodies were added (see Appendix 6 on page 219) and incubated at room temperature for 30 min. Cells were then washed with PBS and re-suspended in PBS for FACS analysis. Samples were processed on a BD LSRII or Miltenyi MACSQuant and analyzed with FlowJo (Treestar) software. Samples were gated using forward and side scatter and live cells along with other cell markers. Lymphocytes were gated on forward and side scatter, single cells, live, and CD3 positive unless otherwise indicated.

2.3.4.1 FACS Gating Strategy

The gating strategy used in the FACS analysis in this thesis follows the basic gating strategy of gating for lymphocytes, single cells (SSC vs. FSC), live cells, and $CD3^+$ or $CD3^-$. $CD3^+$ cells were gated for $CD4^+$ or $CD8^+$ and then the T cells were gate on the listed in the experiment on antibodies such as CD161, Vα7.2, IFNγ, etc. $CD3^-$ cells were gated as listed in the experiment on antibodies such as CD161, CD19, or CD56.

Figure 2.1

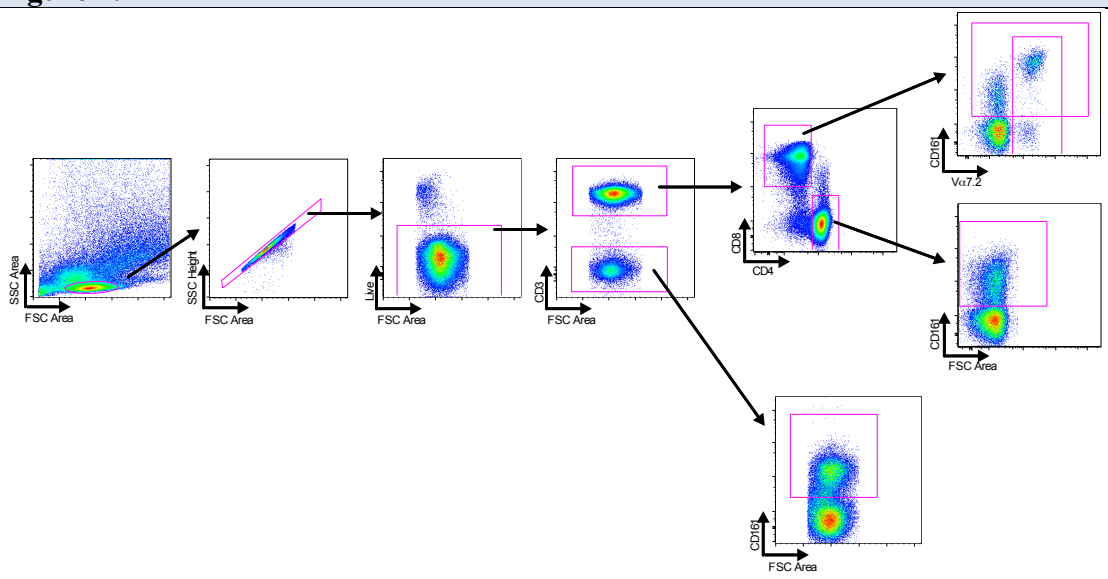

FACS Gating Strategy
Unless otherwise stated, cells are gated: Lymphocytes (SSC Area vs FSC Area), Single cells (FSC Height vs FSC Area), Live (Live vs FSC Area), $CD3^+$ or CD3- (CD3 vs FSC Area). CD3- cells may then be gated for $CD161^+$ (CD161 vs FSC Area). $CD3^+$ cells are gated $CD4^+$ or $CD8^+$ (CD8 vs CD4). $CD4^+$ cells may be gated for $CD161^+$ (CD161 vs FSC Area). $CD8^+$ cells may be gated for $CD161^+$, $V\alpha7.2^+$, or $CD161^+$ and $V\alpha7.2^+$ (CD161 vs Vα7.2).

2.3.5 Truncated Extracellular Protein Vector Production

The full protein sequence was obtained in a vector form (Origene or Source Bioscience). The intracellular, transmembrane, and extracellular regions were predicted using "DAS" - Transmembrane Prediction server (http://www.sbc.su.se/~miklos/DAS/). A truncated protein spanning only the extracellular region was designed using the predicted regions. Appropriate primers

were designed with Age1 and Kpn1 restriction sites and purchased (Eurofins MWG Operon). A PCR was then done using the designed primers and the Origene cDNA clone. The product was then run on a 1% agarose gel using electrophoresis, the band excised, and purified using QIAquik Gel Extraction kit (Qaigen). The purified PCR product was then digested with Age1 (New England Biolabs) and Kpn1 (New England Biolabs), and purified using QIAquick PCR Purification Kit (Qaigen). The digested PCR product was then ligated into a previously digested PHLsec vector using T4 ligase (New England Biolabs). The ligated PHLsec-PILAR vector was then transformed using XLII competent cells (Strategene) and plated on Ampacillin LB plates. Single colonies were picked and cultured in 2ml in a shaking 37°C incubator overnight. 4 hours into the overnight culture, a sample of each culture was then lysed and a PCR was run using the primers for the truncated protein. A gel was run of the PCRed lysates, to determine cultures with positive bands of the correct size. The overnight cultures with correct positive bands were then used for miniprep (Qaigen) or maxiprep (Qaigen) kits.

2.3.6 Transient Transfection

293T cells were plated in large petri dishes and grown to 90% confluency. For each plate of 293T cells, 5mls serum free Dulbeccos Modified Eagle Medium (DMEM), 100ul Polyethylenimine (PEI) (1mg/ml), and 50ug of vector were combined and incubated 10min at room temperature. Then 10ml of 2% fetal calf serum (FCS) DMEM was added. The 90% confluent 293T cell plates then had all media removed and replaced with 15ml of the above mix. The 293T cell plates were then incubated 3 hours in a 37°C incubator. An additional 10mls of 2% FCS DMEM was added and incubated at 37°C for 3-4 days or until the cells began to detach and

die. The media from the cells was then collected and any cells removed by centrifugation.

2.3.7 PCR

An appropriate amount of DNA template, 2.5ul each forward and reverse primers (designed for protein desired), 2ul dNTPs (Invitrogen), 5ul of PFU buffer (Promega), 1ul PFU DNA polymerase (Promega) and 36ul sterile distilled H_2O were mixed in a 0.2ul PCR tube. PCR cycling conditions were as follows: 95°C for 2 min, followed by 35 cycles of 30 s at 95°C, 1 min at 50°C, and 45 s at 72°C, with a final extension of 10 min at 72°C.

2.3.8 Sequencing

Sequencing was done bidirectionally using the ABI Prism BigDye Terminator system (Applied Biosystems) on an ABI 3100 DNA automated sequencer and appropriate primers.

2.3.9 Protein Purification

Supernatant media from the transient transfections was filtered with a 0.22um filter. Filtered supernatant was then added to 1L of 4°C binding buffer and run through a Nickel (Ni) column at 4°C. 4ml of Elution Buffer (500mM Imidazole, 50mM Tris pH8, 500mM NaCl) was added to the Ni column for 5 min. The elution buffer was then allowed through the column and collected. Protease inhibitors PMSF, Leupeptin, and Pepstatin were added and then the protein was dialyzed in gel filtration buffer (20 m*M* Tris pH 8.0, 150 m*M* NaCl) at 4°C overnight. The protein was analyzed and purified by gel-filtration chromatography with a 26/60 Superdex 75 column (GE Healthcare, Uppsala, Sweden). Eluted protein was immediately put on

ice and protease inhibitors PMSF, leupeptin, and pepstatin were added again at the same concentrations. Nanodrop was used to quantify the amount of protein collected.

2.3.10 SDS PAGE

Protein was added to 5X Loading Buffer (New England Bioscience) (Under reducing conditions, Bmercaptoethanol was also added). The mix was then heated at 95°C for 5 min before being loaded along with a Spectra5 protein ladder onto a SDS PAGE 15% acrylimide gel. Gels were run for 70-90 min at 200V.

2.3.11 Coomassie

SDS-PAGE gels were run and then stained in coomassie blue stain for 1 hour on a shaking table at room temperature. The add 30% methanol destain solution until bands are clearly visible.

2.3.12 PNGase F

Using Protein Deglycosylation Mix (New England Bioscience) manufacturer instructions were followed.

2.3.13 Western Blot

Cells were lysed with Pierce RIPA Lysis and extraction buffer (Thermo Scientific) including Complete, Mini Protease Inhibitor Cockatil Tablets (Roche). Lysates or protein suspensions were analysed in a NuPAGE® Novex 4–12% Bis-Tris Midi Gel w/ MOPS (Invitrogen) under reducing or non-reducing conditions. NuPAGE gels were transferred to Immobilon P nylon membrane using Bio-Rad transfer apparatus. The membrane was washed in dH2O before being blocked in a 3% BSA TBST solution. The membrane was then washed and stained with an appropriate primary. The membrane was then washed and stained with an appropriate

secondary HRP. Western blots were developed according to Amersham ECL western blotting chemiluminiscence detection system instructions (GE Healthcare).

2.3.14 Binding Protein and mAb to Plates

A mixture of 100ul PBS, αCD3 pure (BD) at 2.5ug/ml, αCD28 (BD) at 5ug/ml, and PILAR/CD161 proteins (see figure legend for concentrations) or αCD161 varying concentrations (see figure legends for concentrations) were mixed and added to a flat bottom ELISA plate (Greiner Bio-One Limited). The ELISA plate was incubated in the dark at room temperature overnight if using only antibodies, or for 1 hour at room temperature and then transferred to 4°C overnight if using protein. The plate was washed with PBS and then 200ul of 1X wash buffer (R&D 895126) was added at room temperature for 1-2 hours. The plate was then washed with PBS and 0.5-1 million cells and any unbound stimulations were added to each well of the ELISA plate and incubated at 37°C for 1 hour. BFA (Sigma) was added at 10ug/ml and incubated 4 hours to overnight. Cells were then recovered from the plate and 200ul of 2mM EDTA/PBS solution was added to each well of the ELISA plate and incubated at 37°C for 5 min. The 200ul EDTA/PBS was added to the cells, washed in PBS, and cells were stained.

2.3.15 Gene Microarray Processing

Cells for each sample were snap frozen and sent to Miltenyi Biotec where mRNA was extracted from the cells, converted into cRNA, probe hybridized, and then run on Agilent Whole Human Genome Oligo Microarray (two-color) chips. Agilent Feature Extraction Software (FES) was used to read out the image files from the microarray chips. The FES also made calculations to subtract background, normalize the data, and reject outliers.

2.3.15.1 Gene microarray P-value calculations

Statistical confidences (p-values) were calculated by Rosetta Resolver® (Rosetta Biosoftware) using a ratio calculation including an error model as described by Weng *et al.* (Weng et al. 2006). The p-values stated were calculated with the formula:

$$\text{p-value} = 1 - \text{Erf}\left[\frac{\left|\left(\text{Log(ratio)} / \text{Log (Error)}\right)\right|}{\sqrt{2}}\right]$$

Where Erf is the error function of a standard Gaussian distribution.

2.3.16 Real-time qPCR

1.1.1.1 First strand cDNA synthesis

Per sample, RNA, random primers, anchored primers and dNTPS were combined to form Master Mix 1 as described in Table 2.1. The reactions were heated by a thermal cycler (BioRad) and heated to 65°C for 5 minutes and then placed on ice for 2 minutes. Then 5X buffer, DTT RNase Out and Superscript III were combined to form Master Mix 2 as described in Table 2.1. Master mix 2 was then combined with the heated and cooled Master Mix 1. The entire mixture was then put back on the thermal cycler programed to run at 25ºC for 10minutes, 50ºC for 60 minutes, and 70ºC for 15minutes.

Table 2.1

Master Mix 1

Item	Concentration	ul
Random Primers	3Ug/ul	1
Anchored Primers	2.5ug/ul	0.3
dNTPS	10mM	1.25
RNA	1ng/ul	10
H2O		3.7
	Total	6.25

Master Mix 2

Item	Concentration	ul
5X Buffer	5X	5
0.1M DTT	0.1M	1.25
RNase Out	RNase Out	1.25
SSIII	200U/ul	1.25
	Total	8.75

Master Mix 1 and Master Mix 2

1.1.1.2 Real time qPCR

cDNA generated as described above was added to sterile distilled water, forward primer, reverse primer, the appropriate probe from the Roche universal probe library, and Faststart universal probe master (Roche) (2xMM) as described in Table 2.2. Samples were loaded into a 96-well Lightcycler 480 multiwell plate (Roche). The plate was run on the Lightcycler 480 96 well block (Roche) on the following cycle: 95ºC for 5 minutes and then 50 cycles of 95ºC for 10 seconds, 58ºC for 30 seconds, 72ºC for 10 seconds. Lightcycler 480 software (Roche) was used for running and analysis of the real time quantification of the PCR. The fold change was determined in relation to expression of the housekeeping gene HPRT using the 2-ΔΔCT method (Livak 2001).

Table 2.2

Item	Concentration	ul
ddH20		7.7
2xMM	2x	10
Forward Primer	10uM	1
Reverse Primer	10uM	1
Probe		0.3
cDNA	diluted	5
	Total volume	25ul

qPCR Master Mix

2.3.17 Irradiation

Cell lines were irradiated with 30 grays of radiation prior to any co-incubations.

2.3.18 T Cell Activation

2.3.18.1 T Cell Activation with CD3/28 Dynabeads

Dynabeads® Human T-Activator αCD3/28 beads (Life Technologies) were used at a 1:1 ratio (25ul/1 million cells). Beads were washed with MACS buffer and placed in EasySep™ magnet (Stemcell) for 2 minutes and buffer was poured off. Dynabeads were re-suspended in R10 and co-incubated at 37°C with cells at the appropriate concentration for the length of time specified. Dynabeads® were removed before flow cytometry by vigorously vortexing then put in EasySep™ magnet for 2 minutes and supernatant was then collected.

2.3.18.2 T Cell Activation with αBiotin Activation Beads

T Cell Activation/Expansion Kit (Miltenyi) was used to create the αbiotin activation beads. αBiotin activation beads were loaded following manufacturer instructions using biotin αCD3 and αCD28 provided with the kit, biotin αCD161 clone 191B8 (Miltenyi), and biotin IgG2a clone eBM2a (ebioscience). Combinations

of αCD3, αCD28, and αCD161 were loaded on beads at the final concentration of 10 μg/ml of each mAb on the bead. Beads were used at 5ul/1 million cells unless otherwise stated.

2.3.19 *E. coli* activation of B cell line

B cell lines (BCL) were either co-incubated with PFA-fixed *E. coli* at 10 BpC or were mock infected with the negative control at 10 BpC overnight in R10. The BCL were washed twice to remove any free *E. coli* before use.

2.3.20 Proliferation Assay

PBMCs were stained with 2.5μM CellTrace™ violet (CTV) (Life Technologies) for 10 minutes at room temperature followed by an addition of an equal volume of ice cold R10 to quench the reaction, and was kept on ice for another 5 minutes. The cells were then washed three times, transferring into new tubes between each wash. Before the last wash, the cells were left at 37°C for 5 minutes to allow excess dye to diffuse out. Cells were then re-suspended in RH10 at 2 x10^6/ml and plated in a 48 well flat bottom plate. Cells were incubated at 37°C for 5 days and then washed before staining.

2.3.21 FATAL Assay

The assay was based on the published VITAL assay (Hermans et al. 2004). Target B cell lines (BCL) were either co-incubated with PFA-fixed *E. coli* at 10 BpC or were mock infected with the negative control overnight. Cells were harvested and the *E. coli* pulsed BCLs were stained with CFSE (Invitrogen), while the negative control BCLs were stained with CTV (Invitrogen). CFSE BCLs were labeled with 100nM CFSE in PBS for 10 minutes at room temperature. CTV BCLs were labeled with 2.5μM CTV in PBS for 10 minutes at room temperature. The staining for both

dyes was followed by an addition of an equal volume of ice cold R10 to quench the reaction, and was kept on ice for another 5 minutes. The cells were then washed three times, transferring into new tubes between each wash. Before the last wash, the cells were left at 37°C for 5 minutes to allow excess dye to diffuse out. The CFSE-labeled cells and CTV-labeled cells were mixed at a 1:1 ratio prior to plating out.

$CD8^+$ T cells were isolated from PBMCs by positive selection with anti-CD8 magnetic beads (Miltenyi) using manual MS-columns (Miltenyi Effector cells were added to the wells at the indicated E:T ratio and cells were incubated overnight.

Following incubation, cells were harvested and washed in PBS before staining with a live-dead maker (Invitrogen) before being fixed and permeablised for the staining of extracellular and intracellular markers, as described above. Analysis was on gated live BCLs only. BCL gating was based on controls without any effector T cells added. Based on the percentage survival of $CFSE^{high}$ cells in wells containing no effectors (E:T=0:1), the expected frequency of target cells can be found:

$$\text{Expected ratio (ER)} = \frac{\%\ CFSE^{high}\ \text{cells}}{\%\ CTV^{high}\ \text{cells}}$$

Using this ratio, the % specific killing can be calculated:

$$\%\ \text{specific killing} = \left[\frac{100 \times (ER \times \%CTV^{high}) - \%CFSE^{high}\ \text{cells}}{(ER \times \%CTV^{high})} \right]$$

Chapter 3 Protein Production and Purification

3.1 Introduction

In order to properly look at the functional impact of signaling through CD161, it was necessary to understand where the signal comes from. CD161 has two published protein ligands: Lectin-Like Transcript 1 (LLT1) (Aldemir et al. 2005; Rosen et al. 2005) and Proliferation-Induced Lymphocyte-Associated Receptor (PILAR) (Huarte et al. 2008). Both LLT1 and PILAR were of interest as binding CD161 might induce different levels or types of signals. An example of this has been shown with CD94; when it is bound by NKG2A it induces an inhibitory signal, but when it is bound by NKG2C it induces an activating signal (Houchins et al. 1997).

To test the functional impact of CD161 signaling on T cells, I wanted to use both LLT1 and PILAR to ligate CD161. Stably transfected cell lines could be used for functional ligation experiments. However, if a clear effect of CD161 ligation was determined, I planned to follow this with binding and structural studies using these proteins. As soluble forms of these proteins could also be used for functional studies, I chose to start my project by designing and producing soluble versions of LLT1 and PILAR.

The design of soluble proteins began by studying the genes that express *CLEC2D* (LLT1) and *CLEC2A* (PILAR). Both *CLEC2D* and *CLEC2A*, along with *KLRB1* (CD161), are found in the natural killer cell gene complex (NKC) found on human chromosome 12 (Spreu et al. 2007; Boles et al. 1999; Lanier et al. 1994). The *CLEC2A* and *CLEC2D* genes are alternatively spliced and form multiple protein

isomers. The PILAR protein is encoded by isoform CLEC2A1 and the LLT1 protein is encoded by isoform 1(Spreu et al. 2007; Boles et al. 1999).

CD161, PILAR and LLT1 are all type II transmembrane proteins with an intracellular, a single transmembrane, and an extracellular domain (Spreu et al. 2007; Boles et al. 1999; Lanier et al. 1994). The type II indicates that the N-terminal region of the protein is found intracellularly and the C-terminal region is extracellular.

CD161, PILAR and LLT1 are also all C-type lectin-like proteins, which means they have an extracellular C-type lectin-like domain (Spreu et al. 2007; Boles et al. 1999; Lanier et al. 1994). The C-type lectin-like domain is evolutionarily similar to the Ca^{2+} dependent carbohydrate recognition domain seen in C-type lectins. However, the carbohydrate recognition domain of the lectin-like protein lacks critical residues needed to bind carbohydrates and the domain may bind other proteins instead (Weis et al. 1998). Many of the C-type lectin-like proteins with genes found in the NKC bind other C-type lectin-like proteins whose genes are also found in the NKC. Some of these receptor ligand pairs include NKp80/AICL (Roda-Navarro et al. 2000; Shum et al. 2002) NKG2A/CD94, NKG2C/CD94 (Houchins et al. 1991; Renedo et al. 1997).

3.2 Aims

- Produce a soluble form of the extracellular domain of the PILAR protein
- Produce a soluble form of the extracellular domain of the LLT1 protein

3.3 Material and Methods

3.3.1 Truncated Extracellular PILAR Vector Production

The full sequence CLEC2A cDNA clone (NM_001130711) Origene (SC325556) and CLEC2A cDNA clone (NM_013269.2) Origene (SC312389) were obtained. The intracellular, transmembrane, and extracellular regions were predicted using "DAS" - Transmembrane Prediction server (http://www.sbc.su.se/~miklos/DAS/). A truncated protein spanning only the extracellular region was designed using the predicted regions. Appropriate primers were designed with Age1 and Kpn1 restriction sites and purchased (Eurofins MWG Operon). A PCR was then done using the appropriate designed primers and the Origene cDNA clone. The product was then run on a 1% agarose gel using electrophoresis, the band excised, and purified using QIAquik Gel Extraction kit (Qaigen). The purified PCR product was then digested with Age1 (New England Biolabs) and Kpn1 (New England Biolabs), and purified using QIAquick PCR Purification Kit (Qaigen). The digested PCR product was then ligated into a previously digested PHLsec vector using T4 ligase (New England Biolabs). The ligated PHLsec-PILAR or PHLsec-LLT1 vector was then transformed using XLII competent cells (Strategene) and plated on Ampacillin LB plates. Single colonies were picked and cultured in 2ml in a shaking 37°C incubator overnight. 4 hours into the overnight culture, a sample of each culture was then lysed and a PCR was run using the primers for the truncated PILAR. A gel was run of the PCRed lysates, to determine cultures with positive bands of the correct size. The overnight cultures with correct positive bands were then used for miniprep (Qaigen) or maxiprep (Qaigen) kits.

3.3.2 Transient Transfection

293T cells were plated in large petri dishes and grown to ~90% confluency. For each plate of 293T cells, 5mls serum free Dulbeccos Modified Eagle Medium (DMEM), 100ul Polyethylenimine (PEI) (1mg/ml), and 50ug PHLsec-PILAR were combined and incubated 10min at room temperature (rt). Then 10ml of 2% fetal calf serum (FCS) DMEM was added. The 90% confluent 293T cell plates then had all media removed and replaced with 15ml of the above mix. The 293T cell plates were then incubated 3 hours in a 37°C incubator. An additional 10mls of 2% FCS DMEM was added and incubated at 37°C for 3-4 days or until the cells began to detach and die. The media from the cells was then collected and any cells removed by centrifugation.

3.3.3 PCR

PCR was completed using PFU DNA polymerase (Promega). The primers used were 5' – ATATATACCGGTTGGTCCAAGCATGCTAAACCTGTGG -3' and 5'- TTATTAGGTACCTAAAAAATATTTAGGTTTGCTGCAAATC- 3'. PCR cycling conditions were as follows: 95°C for 2 min, followed by 35 cycles of 30 s at 95°C, 1 min at 50°C, and 45 s at 72°C, with a final extension of 10 min at 72°C.

3.3.4 Sequencing

Sequenced bidirectionally using the ABI Prism BigDye Terminator system (Applied Biosystems) on an ABI 3100 DNA automated sequencer with the primers 5' – ATATATACCGGTTGGTCCAAGCATGCTAAACCTGTGG -3' and 5'- TTATTAGGTACCTAAAAAATATTTAGGTTTGCTGCAAATC- 3'

3.3.5 Protein Purification

Supernatant media from the transient transfections was centrifuged at 3000rpm for 15 min at 4°C. It was then filtered using vacuum pump and a prefilter, then re-filtered with a 0.22um filter. 500ml of filtered supernatant was then added to 1L of 4°C PBS. 1ml of nickel binding beads were loaded in a column and washed with protein binding buffer. The supernatant-binding buffer solution was then left to slowly drip through the Ni column at 4°C. Still at 4°C, the Ni column was washed with protein binding buffer. Then, 4ml of Elution Buffer (500mM Imidazole, 50mM Tris pH8, 500mM NaCl) was added to the column for ~5 min. The elution buffer was then allowed through the column and collected. Protease inhibitors PMSF (0.1mm), Leupeptin (1ug/ml), and Pepstatin (1ug/ml) were added to the protein at 1:1000 and then dialyzed in gel filtration buffer (20 m*M* Tris pH 8.0, 150 m*M* NaCl) at 4°C overnight. The protein was analyzed and purified by gel-filtration chromatography in gel filtration buffer with a 26/60 Superdex 75 column (GE Healthcare, Uppsala, Sweden). Eluted protein was immediately put on ice and protease inhibitors PMSF, leupeptin, and pepstatin were added again at the same concentrations. Nanodrop was used to quantify the amount of protein collected.

3.3.6 SDS PAGE

20ul of protein supernatant was added to 5ul of 5X Loading Buffer (New England Bioscience) (Under reducing conditions, Bmercaptoethanol was also added). The mix was then heated at 95°C for 5 min before being loaded along with a appropriate ladder onto a SDS PAGE 15% acrylimide gel. The gel was run for 70-90 min at 200V.

3.3.7 Coomassie

SDS-PAGE gels were run and then stained in coomassie blue stain for 1 hour on a shaking table at room temperature. The add 30% methanol destain solution until bands are clearly visible.

3.3.8 PNGase F

Using Protein Deglycosylation Mix (New England Bioscience) follow kit protocol (http://www.neb.com/nebecomm/products/protocol525.asp). Run samples on SDS-PAGE and coomassie stain.

3.3.9 Western Blot

Cells were lysed with Pierce RIPA Lysis and extraction buffer (Thermo Scientific) including Complete, Mini Protease Inhibitor Cockatil Tablets (Roche). Lysates or protein suspensions were analysed in a NuPAGE® Novex 4–12% Bis-Tris Midi Gel w/ MOPS (Invitrogen) under reducing or non-reducing conditions. NuPAGE gels were transferred to Immobilon P nylon membrane using Bio-Rad transfer apparatus. The membrane was washed in dH2O before being blocked in a 3% BSA TBST solution. The membrane was then washed and stained with an appropriate primary. The membrane was then washed and stained with an appropriate secondary HRP. Western blots were developed according to Amersham ECL western blotting chemiluminiscence detection system instructions (GE Healthcare).

3.3.10 PILAR protein provided by Gordon Freeman

The CLEC2A protein provided by Prof. Gordon Freeman was a mIgG2a-IEGR-human CLEC2A, made with Hinge-mIgG2a with an Fc mutated to reduce FcR binding, Linker of IEGR (Factor Xa cleavage site), and the extracellular lectin domain of hCLEC2A. A western of the PILAR protein confirmed the protein to be the

correct size based on the protein sequence (Figure 3.1). The complete sequence of the protein is:

MRRMQLLLLIALSLALVTNSAEPRGPTIKPCPPCKCPAPNLEGGPSVFIFPPKIK
DVLMISLSPIVTCVVVDVSEDDPDVQISWFVNNVEVHTAQTQTHREDYNSTL
RVVSALPIQHQDWMSGKAFACAVNNKDLPAPIERTISKPKGSVRAPQVYVLP
PPEEEMTKKQVTLTCMVTDFMPEDIYVEWTNNGKTELNYKNTEPVLDSDGS
YFMYSKLRVEKKNWVERNSYSCSVVHEGLHNHHTTKSFSRTPGKIEGRKHA
KPVACSGDWLGVRDKCFYFSDDTRNWTASKIFCSLQKAELAQIDTQEDMEFL
KRYAGTDMHWIGLSRKQGDSWKWTNGTTFNGWFEIIGNGSFAFLSADGVHS
SRGFIDIKWICSKPKYFL.

Figure 3.1

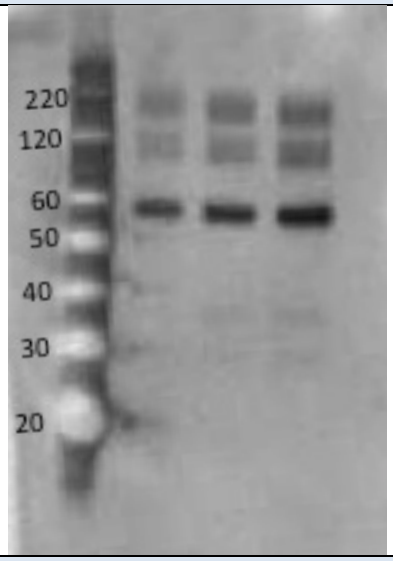

Western of PILAR protein provided by Prof. Gordon Freeman
Purified PILAR protein provided by Prof. Gordon Freeman was loaded on a western gel at 3 different concentrations.

3.4 Results

3.4.1 Predicted Extracellular Domains

3.4.1.1 LLT1 (CLEC2D) extracellular domain prediction

In order to produce soluble protein with extracellular domains of LLT1, I first determined the splice variant that produced the correct full-length protein and then determine what portion of the DNA sequence represented the extracellular domain.

Six different splice variants of *CLEC2D* have been shown, however, only 5 of which produced proteins. Lectin-like Transcript 1 (LLT1) was formed by the sequence of Isoform 1 (Boles et al. 1999; Germain et al. 2010). The LLT1 sequence was entered into the "DAS" - Transmembrane Prediction server to predict the transmembrane region of the protein. This result was compared with the published putative transmembrane region (Boles et al. 1999). The “DAS” prediction gave a slightly longer transmembrane region, so RANC was used as the beginning of the extracellular region for the soluble protein design to avoid including any of the transmembrane region (Table 3.1).

3.4.1.2 PILAR (CLEC2A) extracellular domain prediction

Spreu *et al*. first described the gene *CLEC2A* in a study that showed four different proteins could be produced by splice variants of the gene. Two main isoforms, CLEC2A1 and CLEC2A2, were found. A shortened version of each main isoform was also found that excluded the transmembrane region of the protein encoded on exon 2. The CLEC2A1 isoform contained most of the invariant amino acids associated with the CTLD of a C-type lectin. The C-terminal end of CLEC2A2 lacked significant homology with other C-type lectins and referred to as “wrecked”

(Spreu et al. 2007). The protein product from the CLEC2A1 isoform was later named proliferation-induced lymphocyte-associated receptor (PILAR) in a subsequent study (Huarte et al. 2008).

The CLEC2A1 sequence was entered into the "DAS" - Transmembrane Prediction server to predict the transmembrane region of the protein. This was then compared with the published putative transmembrane region (Spreu et al. 2007). The "DAS" predicted transmembrane region was slightly longer than the published region, so I used WSKH as the beginning of the extracellular region when I designed the soluble protein (Table 3.1).

Table 3.1

LLT1 (Isoform 1)	MHDSNNVEKDITPSELPANPGCLHSKEHSIKA**TLIWRLFFLIMFLTIIVCGM VAALSA**IRANCHQEPSVCLQAACPESWIGFQRKCFYFSDDTKNWTSSQRFC DSQDADLAQVESFQELNFLLRYKGPSDHWIGLSREQGQPWKWINGTEWTR QFPILGAGECAYLNDKGASSARHYTERKWICSKSDIHV
PILAR (CLEC2A1)	MINPELRDGRADGFIHRIVPKLIQNWKIG**LMCFLSIIITTVCIIMI**ATWSKHA KPVACSGDWLGVRDKCFYFSDDTRNWTASKIFCSLQKAELAQIDTQEDMEF LKRYAGTDMHWIGLSRKQGDSWKWTNGTTFNGWFEIIGNGSFAFLSADGV HSSRGFIDIKWICSKPKYFL

Predicted regions of LLT1 and PILAR
Transmembrane domain predicted using "DAS" - Transmembrane Prediction server (**http://www.sbc.su.se/~miklos/DAS/**) is underlined. The predicted transmembrane region published in (Boles et al. 1999) (LLT1) or (Spreu et al. 2007) (PILAR) is **bold.** The predicted extracellular region used in soluble protein production is shaded in grey.

3.4.1.3 Primer design for PILAR and LLT1 proteins

In order to produce the extracellular portions of the proteins, full-length DNA sequences were purchased in a plasmid vector for each protein. Primers were then designed for each end of the sequence of the desired extracellular domain of the protein. The primers included either an AgeI or a KpnI restriction site just outside the sequence desired for the extracellular protein domain (Table 3.2).

Table 3.2	
LLT1 Forward	5’ ATATATACCGGTAGAGCTAACTGCCATCAAGAGCCATC 3’
LLT1 Reverse	5’ TTATTAGGTACCGACATGTATATCTGATTTGGAACAAATCCA 3’
PILAR Forward	5’ ATATATACCGGTTGGTCCAAGCATGCTAAACCTGTGG 3’
PILAR Reverse	5’ TTATTAGGTACCTAAAAAATATTTAGGTTTGCTGCAAATC 3’

Primer design for LLT1 and PILAR protein extracellular domains
AgeI restriction site (red) and KpnI restriction site (blue)

3.4.1.4 PCR product of extracellular domains of LLT1 and PILAR

A PCR was performed using the appropriate designed primers and the product was run on an agarose gel to confirm the product was the correct size (Figure 3.2). The PCR product was then digested with AgeI and KpnI digestion enzymes. The digested product was run on an agarose gel, excised, and then gel extracted.

Figure 3.2

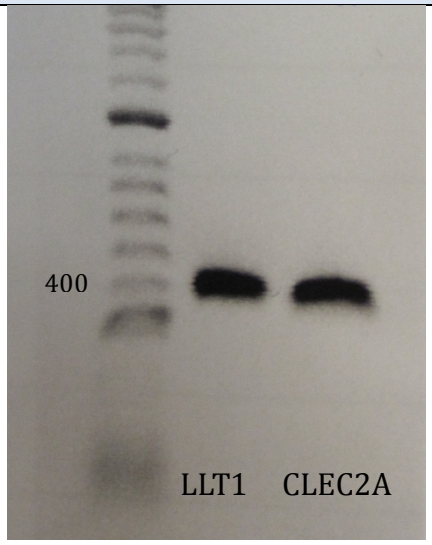

Gel from PCR of LLT1 and PILAR extracellular regions
PCR product from full length plasmid vectors fro LLT1 and PILAR along with primers designed for LLT1 extracellular domain (369bp) and PILAR extracellular domain (378bp) run on a 1% agarose gel with Hyperladder II.

3.4.2 PHL-sec Plasmid

3.4.2.1 PHL-sec plasmid design for transfections

A PHL-sec plasmid which contained a BirA tag (site for biotinylation), a His tag (site for Ni affinity purification), a secretion sequence, AgeI restriction site, KpnI restriction site, and Ampicillin resistance was obtained (Table 3.3). For the full sequence of PHL-sec see Appendix 2 on page 214. The PHL-sec plasmid was digested with AgeI and KpnI restriction enzymes to linearize the plasmid and remove any insert between the AgeI and KpnI. The plasmid was run on an agarose gel, excised and gel extracted.

Table 3.3

TCTTTTTCCTACAGCTCCTGGGCAACGTGCTGGTTGTTGTGCTGTCTCATCATTTTGGCAAAG
AATTGCGGCCGTCTCAGGCCGAATTCAAGCTTGCCACC**ATG**GGGATCCTTCCCAGCCCTGGGA
TGCCTGCGCTGCTCTCCCTCGTGAGCCTTCTCTCCGTGCTGCTGATGGGTTGCGTAGCTGAAA
CCGGT_Insert_GGTACCGGAGGTTCCGGTGGTTCCGGTCTGAATGATATCTTTGAAGCTCAGA
AGATTGAATGGCATGAAGGACGTACCAAGCACCACCATCACCATCACTAATGATCACTCGAG
ACTAGTATCGCGATAATTCACTCCTCAGGTGCAGGCTGCCTATCAGAAGGTGGTGGCTGGTG
TGGCCAATGCCCTGGCTCACAAATACC

Sequence of PHLsec-protein plasmid for transfections
A portion of the sequence of PHLsec vector. Start codon (underlined bold), secretion sequence (dark blue letters), AgeI restriction site (red), protein extracellular portion of protein (green), KpnI restriction site (light blue), BirA tag (grey), His tag (yellow), in frame stop codons (pink) Sequence information from (Aricescu et al. 2006)

3.4.2.2 Insertion of LLT1 and PILAR extracellular domain into PHL-sec plasmid

The digested PHL-sec plasmid and the digested PCR products for the extracellular domain of PILAR or LLT1 were ligated together. The ligation product was then transfected into competent cells and then plated on agarose petri dishes. Resulting colonies were picked and grown. After 4 hours of cell culture, samples were lysed and a PCR was run with the appropriate forward and reverse primers for

the PILAR or LLT1 protein fragment inserted into the PHL-sec. The PCR products were run on agarose gels and the samples positive for the correct size band indicated colonies of correctly transformed cells (Figure 3.3). One positive colony for each of the PHL-sec-LLT1 and PHL-sec-PILAR plasmids were grown in large quantities and the plasmids were isolated.

These plasmids were then sequenced in forward and reverse directions using the primers designed for the LLT1 and PILAR extracellular domains (Table 3.2). Sequencing confirmed that the designed extracellular portions of the proteins were properly inserted into the PHL-sec plasmids (see Appendix 1 on page 214 for confirmed sequences).

Figure 3.3

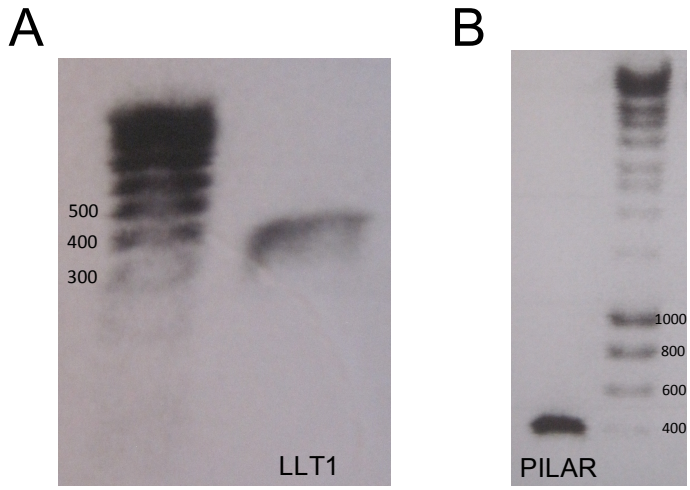

PCR confirming PHL-sec plasmids included LLT1 or PILAR inserts
(A) Cells transformed with PHL-sec LLT1 (369bp) insert plasmids were lysed and PCR was performed with LLT1 forward and reverse primers (Table 3.2) and run on an agarose gel with hyperladder II. **(B)** Cells transformed with PHL-sec PILAR (378bp) insert plasmids were lysed and put in a PCR with the PILAR forward and reverse primers (Table 3.2) and run on an agarose gel with hyperladder I

3.4.3 Transient Transfection

293T cells were grown to 90% confluence and then transiently transfected with the PHL-sec-LLT1 or the PHL-sec-PILAR plasmids. After transfection, the 293T cells were cultured for 3-4 days before the cell supernatants were collected. A

western blot was performed to confirm presence of a protein around the correct size. The 293 T cell transient transfections with PHL-sec-PILAR produced a protein around ~25-30 kDa (Figure 3.4). The 293 T cell transient transfections with PHL-sec-LLT1 did not show any clear protein production despite multiple transfections.

Figure 3.4

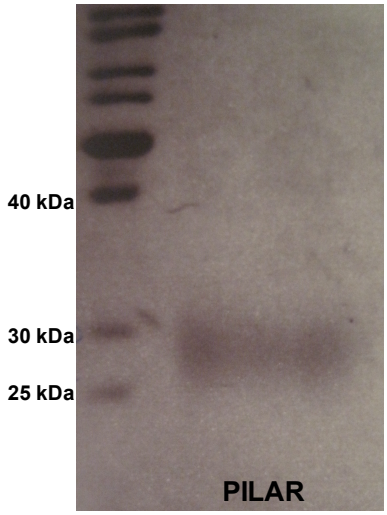

Western of PILAR from PHL-sec-PILAR transient transfection
Western blot of supernatant from cells transiently transfected with a PHL-sec-PILAR run with a PageRuler prestained protein ladder.

3.4.4 PILAR protein purification

Cell supernatant collected from transiently transfected cells was filtered to remove any remaining cells and then added to binding buffer and then run very slowly through a Nickel (Ni) column. The protein was then eluted from the Ni column and then dialyzed into gel filtration buffer. The PILAR protein was then purified by gel-filtration chromatography with a Superdex 75 column (Figure 3.5). The PILAR protein was collected in fractions as it came off of the Superdex column and quantified by nanodrop.

Figure 3.5

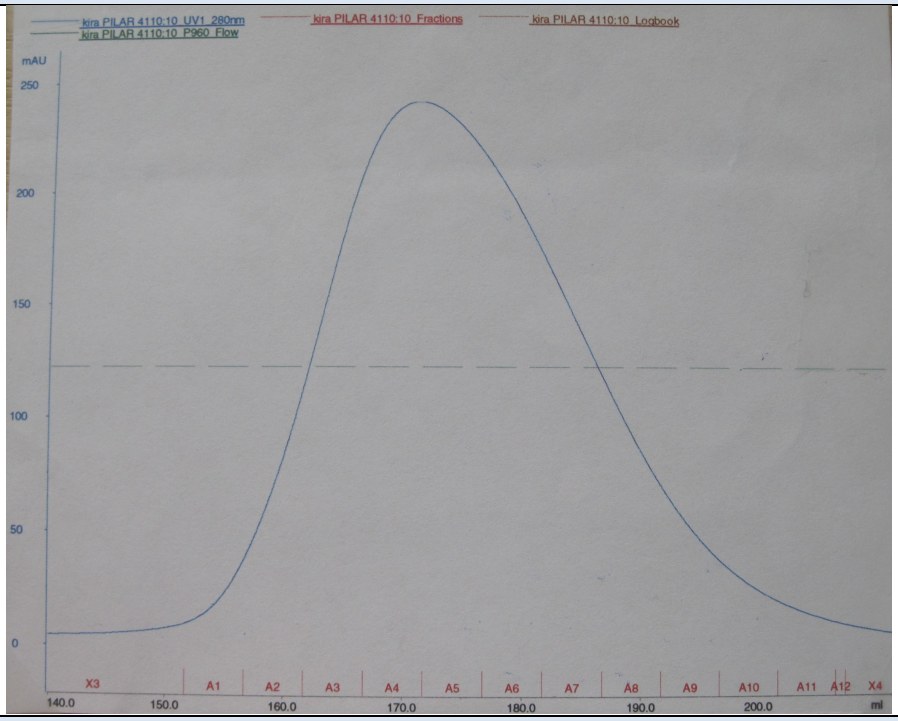

PILAR protein elution off Superdex column
Trace of the PILAR protein fractions as they are eluted from the gel-filtration chromatography with a 26/60 Superdex 75 column.

3.4.5 PILAR protein characteristics

3.4.5.1 Coomassie of sequential PILAR fractions from Superdex 75 column

It was noted that the trace of the PILAR protein fractions from the Superdex 75 column was broad and slightly skewed. Therefore, I investigated the fractions coming off the column more before combining and concentrating the fractions. Fractions 1-8 were run under reducing and non-reducing conditions on SDS-PAGE gels and then stained with coomassie blue. Under reducing conditions the PILAR fractions showed a clear size gradient from ~22 kDa to ~30 kDa (Figure 3.6). Non-reducing conditions showed the exact same size and gradient pattern (data not shown). Possible explanations for the size gradient seen could be due to differential glycosylation, or that 2 different but similar proteins that are very close in size (such as splice variants) could have been expressed.

Figure 3.6

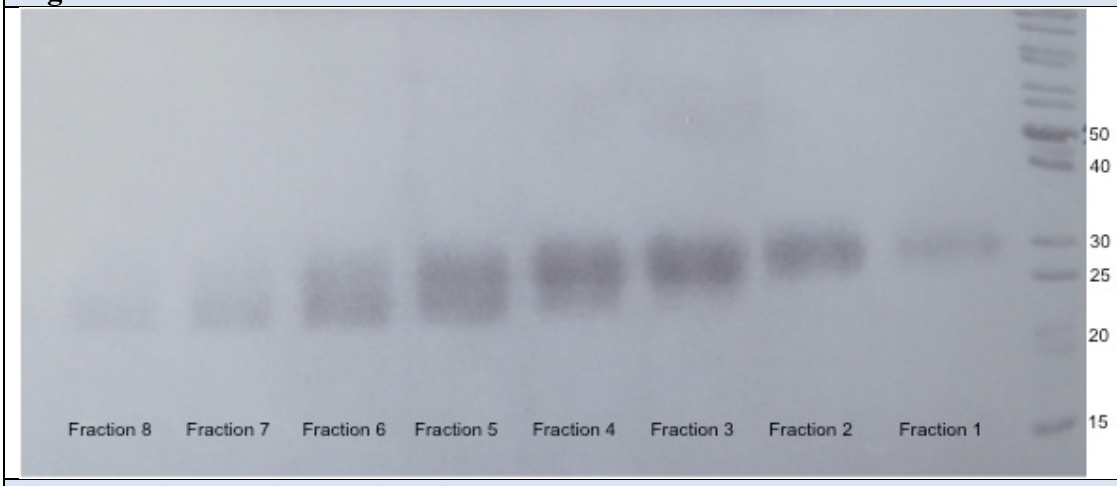

Coomassie of PILAR fractions from Superdex 75 column
Fractions 1-8 from the Superdex 75 column run on SDS-PAGE under reducing conditions and run with pageruler ladder. Gel was then stained with Coomassie blue and then destained until bands were clear.

3.4.5.2 Testing for differential glycosylation with PNGase F

One possible explanation for the size gradient seen in the fractions from the Superdex 75 column was differential glycosylation. The extracellular domain of PILAR contains 3 potential N-linked glycosylation sites (Spreu et al. 2007). Fraction 3 (one of the smallest fractions) and fraction 8 (the largest fraction) were treated with PNGase F to cleave any N-linked glycoproteins. The samples were then run by SDS-PAGE, and stained with coomassie blue. Both fractions 3 and 8 were ~18 kDa when treated with PNGase F (Figure 3.7), which corresponds to the predicted 18.6 kDa of the PILAR protein sequence.

Figure 3.7

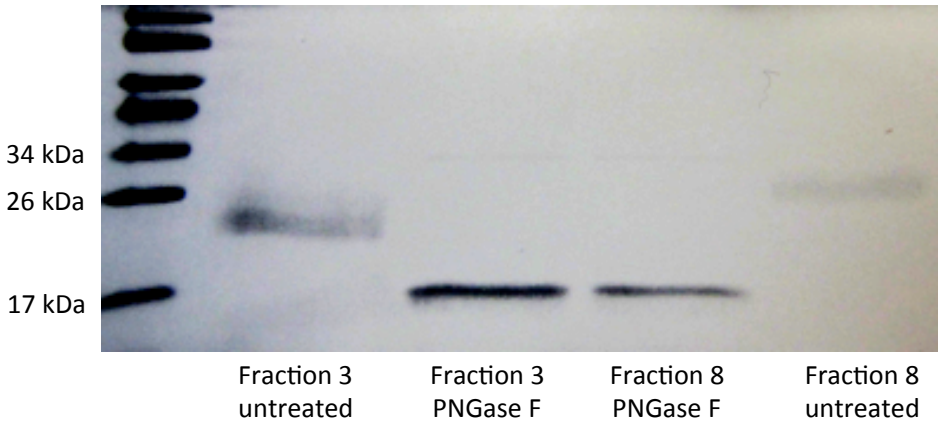

PNGase F treatment on fractions from Superdex column
Fractions 3 and 8 from the Superdex 75 column untreated or treated with PNGase F and run on SDS-PAGE. Run with Spectra Broad Range ladder. Gel was stained with Coomassie blue and then destained until bands were clear.

3.4.6 Binding pattern of conjugated PILAR protien

3.4.6.1 Conjugated PILAR protein binds $CD19^+$ cells

Huarte et al. reported PILAR was a ligand of CD161, which is found on most NK cells and some T cells (Huarte et al. 2008). I wanted to test if the PILAR protein produced bound PBMCs. I used Lightning-Link® (Innova) to fluorescently label PILAR-Oxford (PILAR protein I produced), PILAR-Boston (PILAR protein kindly provided by Gordon Freeman – see 3.3.10 on page 52), IgG protein, and LLT1 protein (Abnova). PILAR did not show binding to $CD3^+$ cells (Figure 3.8A). Both PILAR-Oxford and PILAR-Boston proteins bound a large percentage of $CD19^+$ cells, but the labeled IgG and LLT1 proteins did not (Figure 3.8B).

Figure 3.8

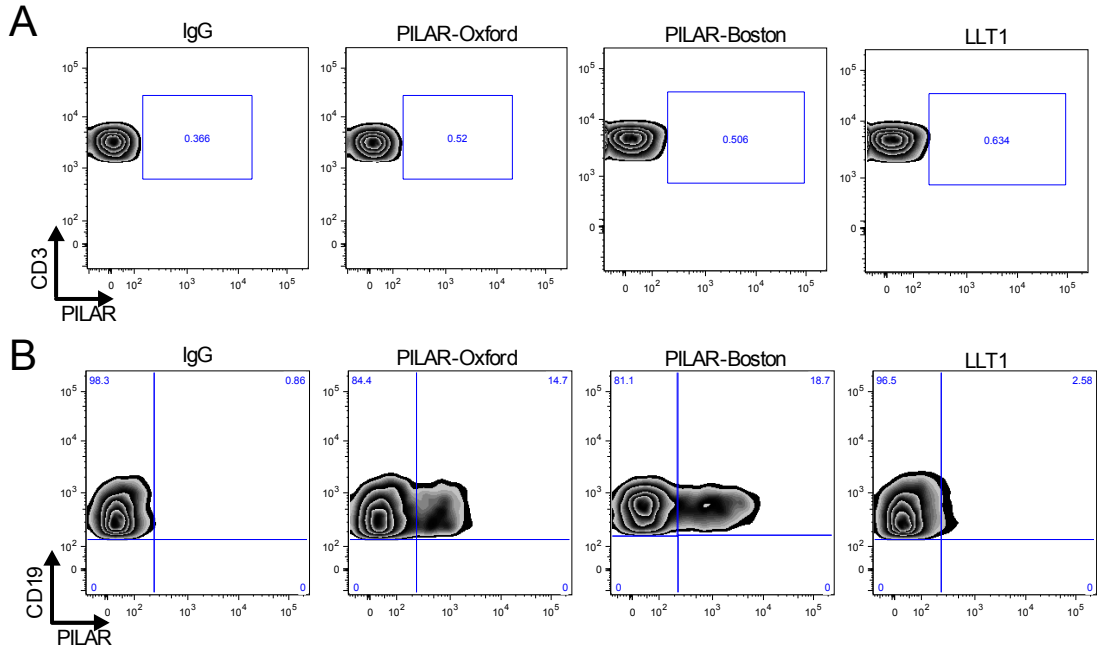

PILAR protein binds CD19$^+$ cells but not CD3$^+$ cells
(A) Lightning-Link® flourescently labeled PILAR-Oxford, PILAR-Boston (provided by Gordon Freman), IgG and LLT1 protein (Abnova) were co-incubated with PBMCs overnight. Cells were then stained surface and internally and analyzed by flow cytometry with PBMCs gated on CD3$^+$ cells **(B)** Lightning-Link® flourescently labeled PILAR-Oxford, PILAR-Boston (provided by Gordon Freman), IgG and LLT1 protein (Abnova) were co-incubated with PBMCs overnight. Cells were then stained surface and internally and analyzed by flow cytometry with PBMCs gated on CD3$^-$ cells
310811.jo 260811.jo PILAR funcitonal figures.pzfx

3.4.6.2 Maturation state of CD19$^+$ cells bound by PILAR protein

CD19$^+$ B cells can be divided based on the maturation state of the cell using IgD, CD38, and CD27 (Sanz et al. 2008). Since PILAR protein bound CD19$^+$ cells, I wanted to know if PILAR bound specifically to a certain maturation state. PBMCs were co-incubated with fluorescently labeled PILAR-Boston overnight and then stained for other markers. The maturation states of CD19$^+$PILAR$^+$ cells were compared to the entire CD19$^+$ cell population for enrichment of any specific state. CD19$^+$PILAR$^+$ cells stained with CD38 and IgD were enriched for virgin naïve, activated naïve, and pre-germinal center cells, but not specific for these populations. On CD27 and IgD stained cells, CD19$^+$PILAR$^+$ cells were enriched on but not specific to naïve and naïve unswitched memory populations (Figure 3.9).

Figure 3.9

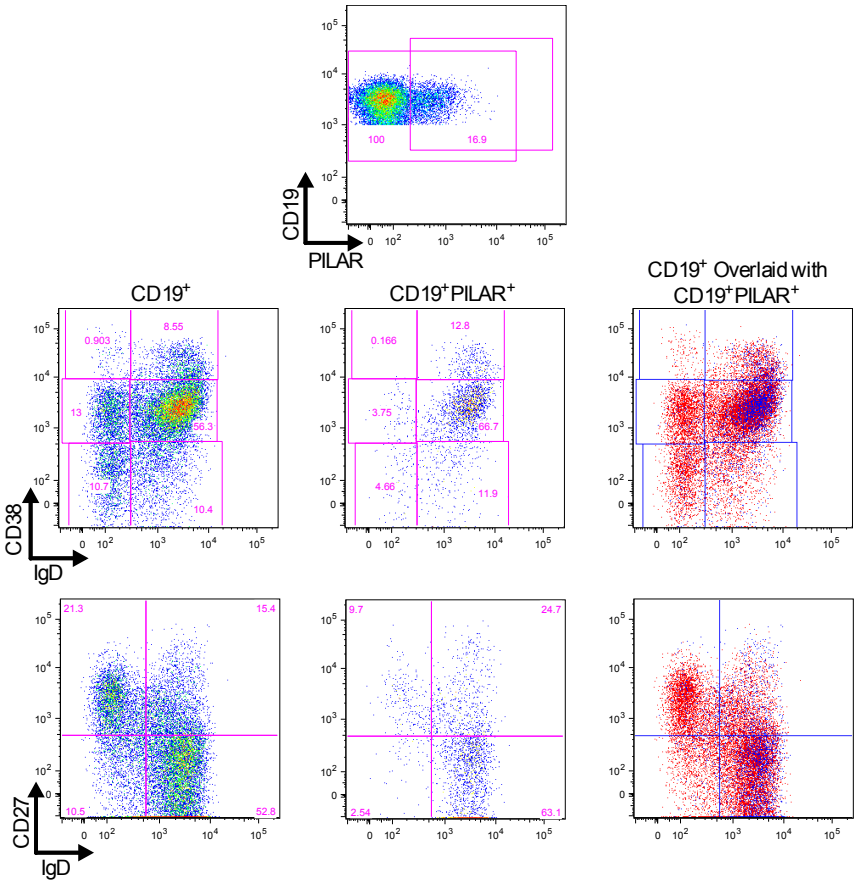

Maturation state of CD19$^+$ cells bound to fluorescently labeled PILAR protein
PBMCs co-incubated overnight with Lightning-Link® fluorescently labeled PILAR protein and stained with anit-IgD, anti-CD38 and anti-CD27 mAbs. Gated on CD3$^-$ CD19$^+$. Gating strategy for maturation states based on gating strategy described in Sanz *et al.* 2008. (Left) Total CD19$^+$ population (Middle) CD19$^+$PILAR$^+$ population (Right) Overlay of CD19$^+$ and CD19$^+$PILAR$^+$ populations
1881011b.jo PILAR funcitonal figures.pzfx

3.4.7 Functional Impact of PILAR ligation on CD8$^+$ T cells

PILAR has been proposed to be a ligand of CD161 (Huarte et al. 2008) however I was only able to show binding of fluorescently labeled PILAR protein to CD19$^+$ cells. It was possible that PILAR bound CD161 on T cells even though I was unable to show this. Therefore, I wanted to know if CD8$^+$ T cells showed any impact on IFNγ expression after co-incubation with PILAR protein. To test this, PILAR-Oxford, PILAR-Boston, or BSA was bound to a plate in a dose titration (11µg/ml to 0.14 µg/ml) along with a constant amount of αCD3 and αCD28 mAb. PBMCs were

incubated on the plate overnight and then stained. The IFNγ expression levels were normalized to the percentage of IFNγ production at the same level of plate bound BSA control. The expression of IFNγ was significantly decreased by the addition of PILAR-Boston ($p= 0.0091$) and PILAR-Oxford ($p= 0.017$) (Figure 3.10A). It was noted that the IFNγ expression levels decreased on both $CD161^{+/++}$ and $CD161^{-}$ cells (Figure 3.10B). The effect of PILAR on IFNγ expression lacked specificity towards $CD161^{+}$ T cells, which suggests that the effects of PILAR are not CD161 specific and therefore were not pursued further.

Figure 3.10

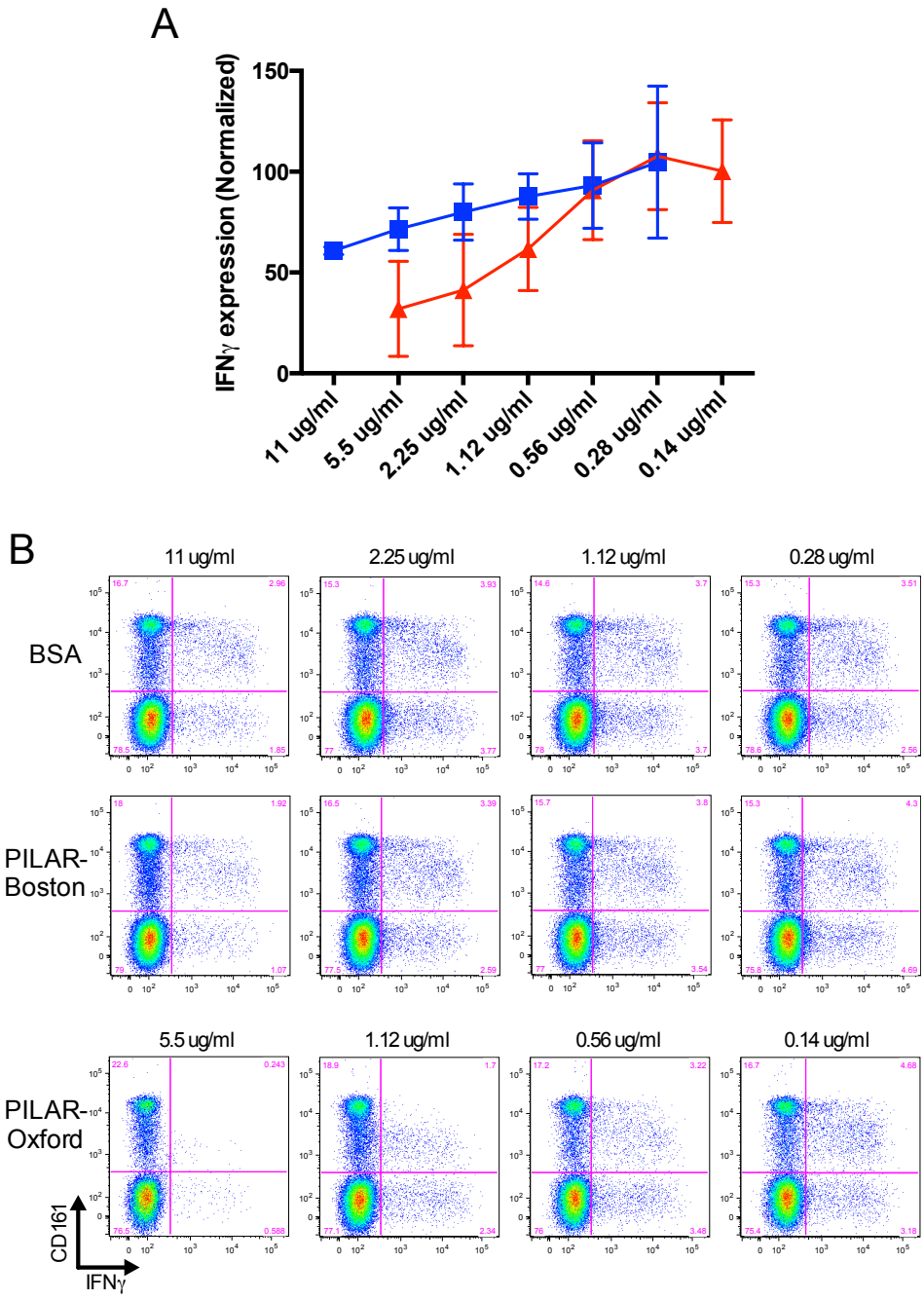

Impact of PILAR protein ligation on IFNγ expression on CD8$^+$ T cells
(A) PILAR protein I produced in Oxford (PILAR-Oxford), PILAR protein provided by Gordon Freeman's lab in Boston (PILAR-Boston), and BSA were bound to plates in a dose titration (11 µg/ml - 0.14mg/ml) along with αCD3 (2.5 µg/ml), αCD28 (2.5 µg/ml). PBMCs were incubated overnight in the protein bound plates and stained for IFNγ expression. IFNγ expression was normalized using the IFNγ expression level of the same concentration of the BSA control. PILAR-Boston (Blue) and PILAR-Oxford (Red). Statistical analysis: Friedman test with Dunn's multiple comparisons test. (n=4)
(B) Representative raw data from on donor shown in A.
PILAR functional IFNγ expression.pzfx 060810

3.5 Discussion

3.5.1 Why soluble protein instead of stable transfection?

In order to study the effects of CD161 binding its protein ligands LLT1 and PILAR, I needed a way of triggering CD161. If the CD161 signaling produced significant effects on T cells, I would have been interested in performing surface plasmon resonance (SPR) binding experiments and determine the structures using x-ray crystallography on the ligands. Although stably transfecting cell lines could be used for experiments on the functional effects of CD161 ligand binding, soluble protein would be necessary for SPR and crystallography. This thesis does not include SPR or x-ray crystallography, but I chose to design and produce a soluble version of LLT1 and PILAR to allow for these uses in the future.

3.5.2 Unable to produce LLT1 protein

Despite successfully ligating the extracellular domain of LLT1 into the PHL-sec plasmid, multiple attempts at transient transfection of 293 T cells with PHL-sec-LLT1 did not result in soluble protein in the cell supernatant. Western blots of the transfected cell supernatants were never positive for protein. There are many possible causes for the lack of protein, including the transfections did not work, that the protein was unstable and therefore degraded, or that the protein could not be properly secreted from the cell. Kamishikiryo *et al.* noted that wild type LLT1 tended to aggregate and they had to introduce mutations to help stabilize the soluble forms of LLT1 (Kamishikiryo et al. 2011).

Although the soluble extracellular domain of the LLT1 protein was unable to be produced, a soluble LLT1 protein was available commercially, and Gordon Freeman subsequently provided a stably transfected LLT1 cell line and a soluble Fc

fusion version of the protein. Due to this, I chose not to continue trying to express a soluble protein of the LLT1 extracellular domain.

3.5.3 Expression of PILAR protein

Transient transfection of 293T cells with the PHL-sec-PILAR plasmid did produce protein secreted into the cell supernatant. This was confirmed by western blot before the protein was purified using a Ni column and then a gel filtration chromatography column. The protein fractions that came out of the gel filtration column showed a broad and slightly skewed peak on the protein trace. This led me to question if the protein fractions were really the same size.

3.5.4 Differential glycosylation of PILAR

A SDS-PAGE gel of the first 8 fractions stained with coomassie blue showed the fractions ranged from ~22 to ~30 kDa in size. Reducing did not affect the size of the bands indicating the protein was not disulfide linked. The size range could be due to more than one protein of slightly different sizes being produced, or it could be due to differential glycosylation of one protein. Deglycosylation with PNGase F treatment on fraction 3 (~26-30 kDa) and on fraction 8 (~22-25 kDa) produced bands of ~18kDa for both fractions. The deglycosylation produced the same size bands, which indicated that the size difference was due to differential glycosylation of the protein. The ~18kDa size also fit well with the predicted size of 18.6 kDa for the extracellular portion of the PILAR protein designed. Together this data indicated that a single, differentially glycosylated, PILAR protein was produced.

3.5.5 Fluorescently labeled LLT1 protein did not bind $CD3^+$ cells

The LLT1 protein from Abnova was fluorescently labeled and used as a control in this experiment; however, unexpectedly LLT1 did not bind $CD3^+$ cells. A

closer inspection of the LLT1 protein from Abnova revealed that although the protein is marketed as the "Human CLEC2D full-length ORF," the protein ends where the splice variants diverge in sequence. This means the C terminal end of the protein was missing. The other isoforms of LLT1 do not bind CD161 and since the Abnova form of the protein ends at the divergence point, this suggests that the Abnova protein lacks crucial portions of the sequence necessary to bind CD161.

3.5.6 Fluorescently labeled PILAR protein binds $CD19^+$ cells

In their original study, Spreu *et al.* published the CLEC2A1 (PILAR) protein but did not indicate what the protein bound (Spreu et al. 2007). In a subsequent study Huarte *et al.* named the protein PILAR and showed PILAR signaled through CD161. The PILAR signaling through CD161 affected proliferation/apoptosis and secretion on T cells (Huarte et al. 2008).

To test if the PILAR protein produced could bind $CD161^+$ cells, PILAR protein was fluorescently labeled and co-incubated with resting PBMCs. The fluorescently labeled PILAR did not bind $CD3^+$ cells, which includes NK cells and T cells that express high levels of CD161 (Pozo et al. 2006; Billerbeck et al. 2010). Unexpectedly, the fluorescently labeled PILAR bound to a small percentage of $CD19^+$ cells.

Around the time this experiment was performed, Spreu *et al*. published another study on the protein produced by the CLEC2A1 (PILAR) splice variant, which they named keratinocyte-associated C-type lectin (KACL). This study showed KACL did not bind CD161, but KACL did bind the newly described NKp65 (Spreu et al. 2010). The PILAR/KACL protein was later described as not being a ligand of CD161 by several studies (Germain et al. 2010; Kamishikiryo et al. 2011; Li et al.

2013). No studies have been published on where NKp65 is expressed, therefore, NKp65 or an unknown ligand of PILAR may be expressed on $CD19^+$ cells.

3.5.7 Maturation state of $CD19^+PILAR^+$ cells

B cells express different protein markers and immunoglobulins as they progress through different development and activation stages (Y.-J. Liu and Arpin 1997; Sanz et al. 2008). If the $CD19^+PILAR^+$ cells bound only B cells in specific stages of development, this might give a clue to what PILAR binds or what function PILAR may have. Staining $CD19^+PILAR^+$ cells indicated that PILAR bound cells at all development stages, although cells were enriched for earlier development stages (naïve and naïve unswitched memory populations).

3.5.8 PILAR protein decreases IFNγ expression non-specifically

A study by Huarte *et al*. indicated that ligation of CD161 T cells by PILAR protein aided CD3 induced proliferation and increased T helper type 1 cytokines, including IFNγ (Huarte et al. 2008). Even though clear binding of PILAR could not be shown on $CD3^+$ cells, IFNγ expression tests were done to test the effect co-incubation of PBMCs with plate bound PILAR protein had on $CD8^+$ T cells. Two different PILAR proteins (PILAR-Oxford and PILAR-Boston), made with different designs and methods, showed a dose dependent decrease in IFNγ expression. The decrease in IFNγ expression was not specific to $CD161^+$ cells, as would be expected if PILAR signaled through CD161.

My findings in experiments on effects of PILAR protein on IFNγ expression on T cells directly contradict the findings of Haurte *et al* (Huarte et al. 2008). However, multiple studies indicated PILAR/KACL was not a ligand for CD161 (Spreu et al. 2010; Germain et al. 2010; Kamishikiryo et al. 2011; Li et al. 2013),

which may explain my discordant results. It is possible that the effect on $CD8^+$ T cell IFNγ expression by PILAR is a bystander effect of ligation with another ligand or cell type.

3.5.9 PILAR is not a ligand of CD161

PILAR could not be clearly shown to bind or have a specific effect on $CD161^+$ T cells in the experiments carried out and multiple other studies have also shown PILAR/KACL to not be a ligand of CD161 (Spreu et al. 2010; Germain et al. 2010; Kamishikiryo et al. 2011; Li et al. 2013). Therefore, PILAR was not studied as a ligand of CD161 during further experiments in this thesis.

3.6 Summary

- Soluble LLT1 protein could not be successfully produced in large quantities.
- Soluble PILAR protein was designed, produced in large quantities and purified.
- PILAR protein was differentially glycosylated.
- PILAR protein binds $CD19^+$ cells.
- PILAR protein decreases IFNγ expression on CD8+ T cells in CD161 non-specific way.
- These results plus recently published studies indicate PILAR is not a ligand of CD161.

Chapter 4 CD161 Expression Patterns on T cells

4.1 Introduction

CD161 (NKR-P1A) is a C type lectin encoded by the *KLRB1* gene found in the NK complex of human chromosome 12 (Lanier et al. 1994). CD161 is the only human ortholog for the murine receptor family known as NKPR1. This murine receptor family contains seven different genes *NKRP1a-e* (although *NKRP1e* and *NKRP1g* may be pseudogenes) (Plougastel et al. 2001; Carlyle et al. 2006). The proteins resulting from these genes have been shown to bind different ligands and induce activating or inhibitory signals (depending on the protein) upon ligation (Aust et al. 2009). The different mouse NKRP1 proteins and their ligands are described in 1.2.2.2 Human Vs. Mouse CD161 on page 23. Since multiple mouse NKRP1 genes exist with different functions, experiments in this thesis focus solely on human CD161.

In humans, CD161 is a protein expressed by most NK cells along with subsets of T cells (including $CD4^+$, $CD8^+$, and double negatives), NKT cells, and immature thymocytes (Lanier et al. 1994; Poggi et al. 1996; Exley et al. 1998). Multiple studies agree that on NK cells, ligation of CD161 inhibits the cytotoxicity of the NK cell (Lanier et al. 1994; Poggi et al. 1996; Azzoni et al. 1998; Aldemir et al. 2005; Rosen et al. 2005). There is much less agreement on function of CD161 ligation in T cells. Studies have shown ligating CD161 on T cells to increase (Exley et al. 1998; Aldemir et al. 2005; Pozo et al. 2006), not affect (Exley et al. 1998; Rosen et al. 2008) or decrease (Rosen et al. 2008) cytokine production. Therefore, I will focus on the function of CD161 in T cells.

In order to design experiments to test the function of CD161 on T cells, a clear understanding is needed of CD161 expression patterns. Not all T cell transmembrane proteins are expressed in a stable manner. Several proteins including the T cell receptor (TCR) (Valitutti et al. 1997; H. Liu et al. 2000; Escors et al. 2011), NKG2D (Groh et al. 2002), and CTLA-4 (Qureshi et al. 2011) have been shown to be downregulated after ligation. Therefore it was important to determine how ligation of CD161 affected the expression of CD161.

4.2 Aims

- To understand the expression patterns of CD161 in T cells.
- Determine if CD161 expression is stable upon ligation.
- If CD161 expression is not stable upon ligation, identify molecules to use as a marker to track cells capable of expressing CD161.

4.3 Materials and Methods

4.3.1 αCD161

Unless otherwise stated, any unbound αCD161 mAb added as a stimulation to an experiment will be the same clone and conjugated fluorochrome that was used when cells were stained for flow cytometer.

4.3.2 Subjects

All cells came from healthy donor leukocyte cones (NHS Blood and Transplant Services) or from healthy laboratory blood donors who gave informed consent.

4.3.3 LLT1 Transfected cell line

A cell line transfected with LLT1 (300-LLT1) and the parental cell line (300-Null) were provided by our collaborator Prof. Gordon Freeman. A western blot confirms the 300-LLT1 expressed in a LLT1 as a disulphide homodimer (Figure 4.1). The 300-LLT1 cell line also highly expressed LLT1 on the surface where the parental cell line 300-Null did not (Figure 4.2).

Figure 4.1

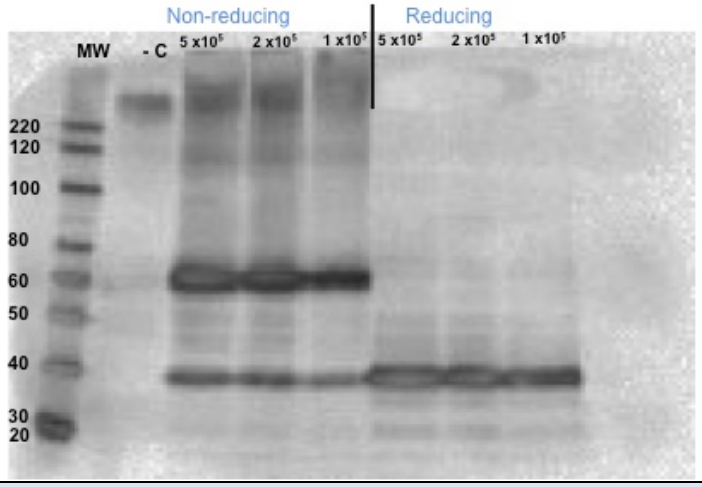

Size and mAb confirmation of LLT1 transfected cell line from GF lab
Western of 300-LLT1 cells lysed and run under non-reducing and reducing conditions and stained with anti-LLT1 goat polyclonal primary antibody and then HRP anti-goat secondary. A negative control (-C) of 300-Null cells, which did not express LLT1, was also included under non-reducing conditions.

Figure 4.2

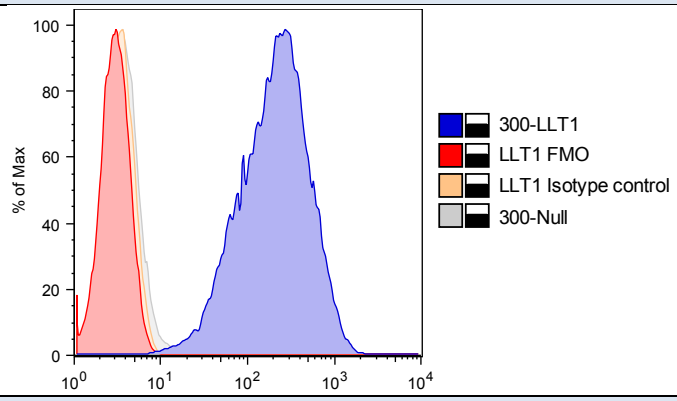

300-LLT1 transfectant expresses high levels of surface LLT1 and the parental 300-Null does not.
The LLT1 transfected cell line 300-LLT1 and the untransfected paternal cell line 300-Null surface stained for LLT1 (R&D) along with an isotype control and FMO for 300-LLT1.

4.3.4 CD8$^+$ T cell Selection

CD8$^+$ T cells were isolated from PBMCs by positive selection with anti-CD8 magnetic beads (Miltenyi) using manual MS-columns (Miltenyi) following manufactures instructions. Purity was consistently >85%.

4.3.5 Surface Stain, Intracellular Stain, and Flow Cytometry

Resting or stimulated cells were washed with PBS and then stained with fluorochrome-conjugated antibodies (see Appendix 6 on page 222) at room

temperature for 30 minutes. Cells were then washed with PBS, and either fixed for surface only stains, or fixed and permeabilized. Cells are fixed (PBS containing 2% formaldehyde or using 1X Fixation/Permeabilization (ebioscience)) for 30 min at room temperature. Cells are then washed and permeabalized in 1X Permeabilization buffer (ebioscience) for 30 minutes. For intracellular staining fluorochrome-conjugated antibodies were added (see Appendix 6 on page 222) and incubated at room temperature for 30 min. Cells were then washed with PBS and re-suspended in PBS for FACS analysis. Samples were processed on a BD LSRII or Miltenyi MACSQuant and analyzed with FlowJo (Treestar) software. Samples were gated using forward and side scatter and live cells along with other cell markers. Lymphocytes were gated on forward and side scatter, single cells, live, and CD3 positive unless otherwise indicated.

4.3.6 FACS Gating Strategy

The gating strategy used in the FACS analysis in this thesis follows the basic gating strategy of gating for lymphocytes, single cells (SSC vs. FSC), live cells, and $CD3^+$ or $CD3^-$. $CD3^+$ cells were gated for $CD4^+$ or $CD8^+$ and then the T cells were gate on the listed in the experiment on antibodies such as CD161, Vα7.2, IFNγ, etc. $CD3^-$ cells were gated as listed in the experiment on antibodies such as αCD161, αCD19, or αCD56.

Figure 4.3

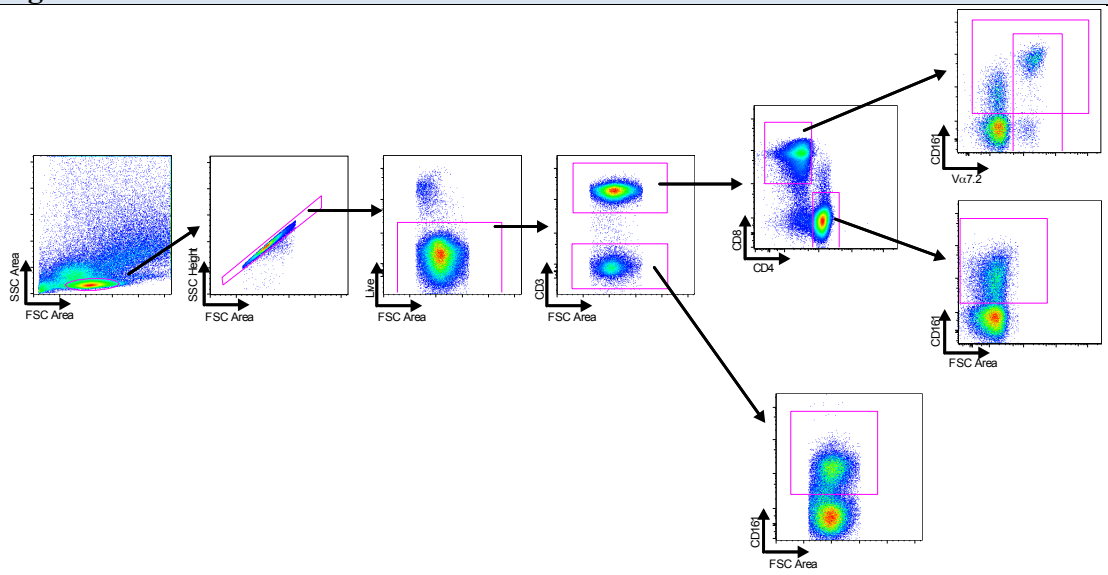

FACS Gating Strategy
Unless otherwise stated, cells are gated: Lymphocytes (SSC Area vs FSC Area), Single cells (FSC Height vs FSC Area), Live (Live vs FSC Area), $CD3^+$ or CD3- (CD3 vs FSC Area). CD3- cells may then be gated for $CD161^+$ (CD161 vs FSC Area). $CD3^+$ cells are gated $CD4^+$ or $CD8^+$ (CD8 vs CD4). $CD4^+$ cells may be gated for $CD161^+$ (CD161 vs FSC Area). $CD8^+$ cells may be gated for $CD161^+$, $V\alpha7.2^+$, or $CD161^+$ and $V\alpha7.2^+$ (CD161 vs Vα7.2).

4.4 Results

4.4.1 CD161 expression patterns on T cells

The staining pattern of CD161 on T cells was previously described with $CD4^+$ T cells having $CD161^-$ and $CD161^+$ populations (Takahashi, Dejbakhsh-Jones, and Strober 2006), and $CD8^+$ T cells were described as having $CD161^-$, $CD161^+$, and $CD161^{++}$ populations (Takahashi, Dejbakhsh-Jones, and Strober 2006; Billerbeck et al. 2010). After staining $CD3^+$ T cells with CD161 mAb I found the same pattern. $CD8^+$ T cells showed $CD161^-$, $CD161^+$, and $CD161^{++}$ populations and $CD3^+$ $CD8^-$ T cells showed the same pattern previously described for $CD4^+$ T cells, with $CD161^-$ and $CD161^+$ populations (Figure 4.4). $CD3^+$ $CD4^+$ T cells were stained to confirm $CD161^-$ and $CD161^+$ populations.

On T cells, $CD8^+$ $CD161^{++}$ T cells had the highest intensities of CD161 expression. Due to the high expression, experiments were focused on $CD8^+$ T cells, except when other populations were used for comparison.

Figure 4.4

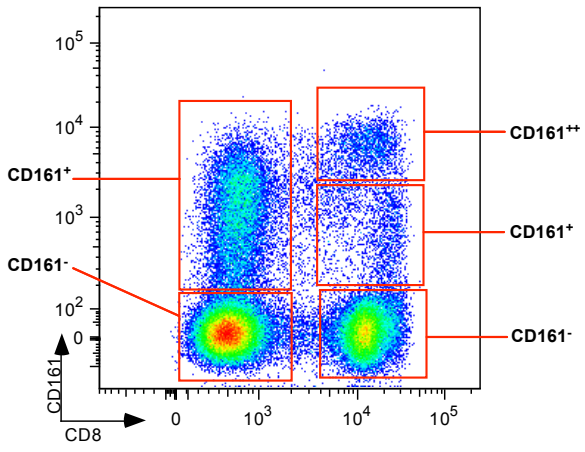

$CD3^+$ T cells stained on the surface and internally showing the different levels of CD161 expression. PBMCs gated on $CD3^+$ T cells and stained with αCD161 on surface and internally. $CD8^+$ cells show three levels of staining: $CD161^-$, $CD161^+$ and $CD161^{++}$. $CD8^-$ cells show two levels of staining $CD161^-$ and $CD161^+$ (same two level pattern is seen in $CD4^+$ cells).
Internal vs external stain and clone stains.pptx Chapter 4 (CD161) figures.pzfx

4.4.2 Surface vs Internal expression of CD161

Along with the knowledge of what cells expressed CD161, it was important to understand if CD161 was expressed on the surface, intracellularly, or in both places. αCD161 surface staining on $CD8^+$ T cells showed both $CD161^+$ and $CD161^{++}$ populations (Figure 4.5A). CD161 gMFI increased 39.5% with intracellular staining, which indicated high intracellular expression (Figure 4.5A-C). The percent of cells that only expressed CD161 internally could be calculated by subtracting the percent of cells $CD161^{+}/^{++}$ after surface only stain from the percent of cells $CD161^{+}/^{++}$ after surface and intracellular staining. This calculation indicated an average of 3.3% of $CD161^{+}/^{++}$ cells expressed CD161 only internally (Figure 4.5B,D). Based on this information, all future experiments were done with surface and intracellular staining unless otherwise stated.

Figure 4.5

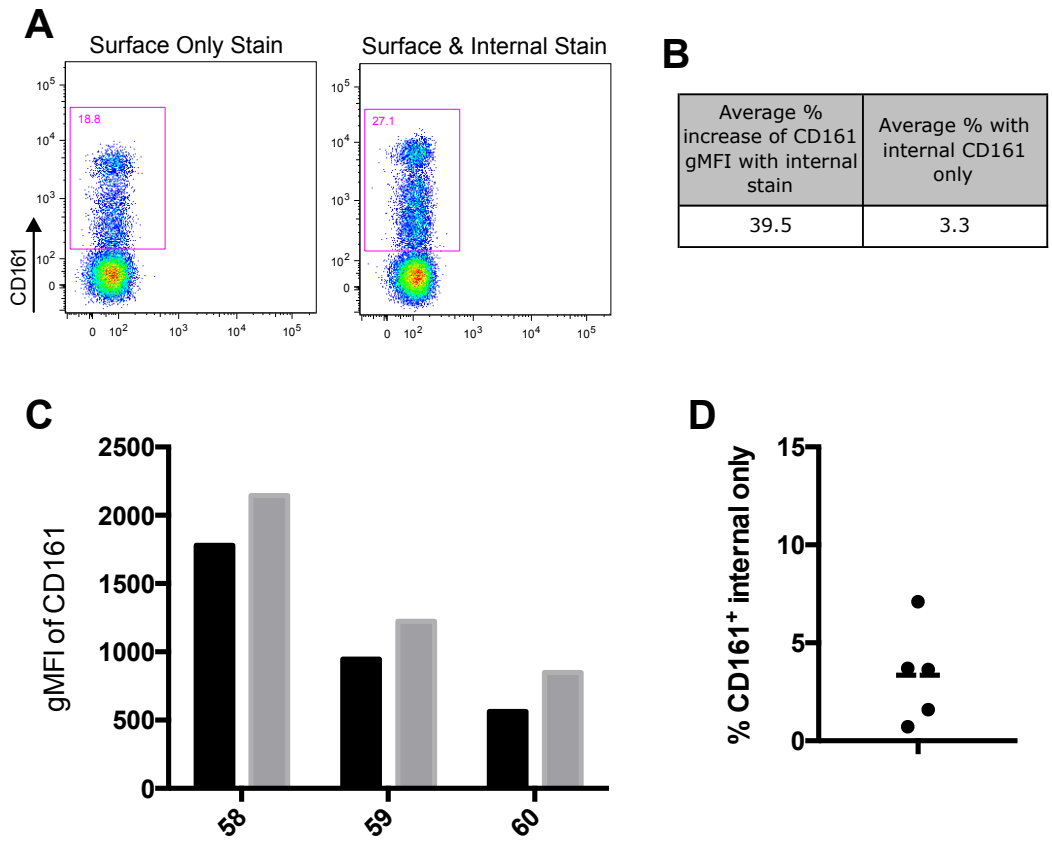

Differences in surface and internal expression of CD161 on CD8$^+$ T cells.
(A) PBMCs gated on CD8$^+$ T cells stained on the surface only or surface and intracellularly. **(B)** Average percent increase in CD161 gMFI on CD8$^+$ T cells with surface and internal staining compared with surface only staining (n=3). Average percent of CD8$^+$ T cells with only internal αCD161 staining (n=5) **(C)** Raw data for 3 donors showing CD161 gMFI on CD8$^+$ T cells stained on the surface only (black) or surface and internally stained (grey) **(D)** Raw data for percent of CD8$^+$ T cells stained with αCD161 internally only.
180512 thesis figure.jo 180512_3.xlsx 180512.pzf

4.4.3 CD161 staining decreases after cross-linking with plate bound CD161 mAb

Several previous studies showed a functional impact of cross-linking of αCD161 mAb on cells (Azzoni et al. 1998; Exley et al. 1998; Aldemir et al. 2005; Pozo et al. 2006). Therefore, I used plate bound pure αCD161 mAb or plate bound αIgG mAb to cross-link PBMCs overnight. Samples that were cross-linked with αCD161 mAb had much lower CD161 staining levels than cells cross-linked with

αIgG mAb (Figure 4.6). The decrease in CD161 staining was reflected in the CD161 gMFI and was dose dependent (Figure 4.7).

A possible explanation for this could be that upon cross-linking, CD161 is internalised and degraded. However, as the conjugated mAb used to stain the cells was the same clone as the unconjugated mAb used to cross-link CD161, any unconjugated mAb that had detached from the plate could block subsequent staining.

Figure 4.6

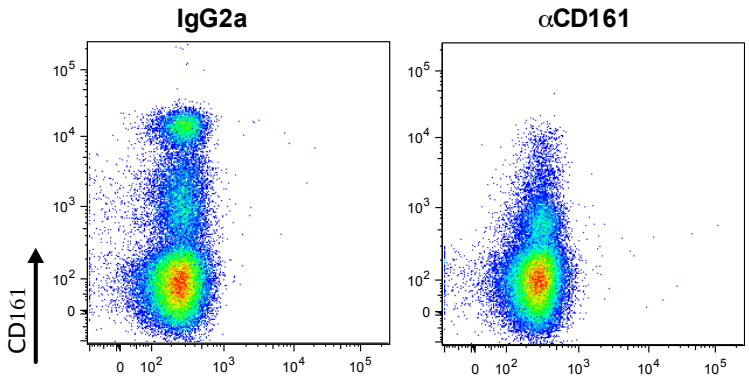

CD161 staining decreases after cross-linking with plate αCD161 mAb.
PBMCs gated on $CD8^+$ T cells incubated with plate bound unconjugated αCD161 or IgG2a mAb overnight. Cells were then surface and internally stained with αCD161-APC mAb.
Chapter 4 (CD161) figures.pzfx 060810

Figure 4.7

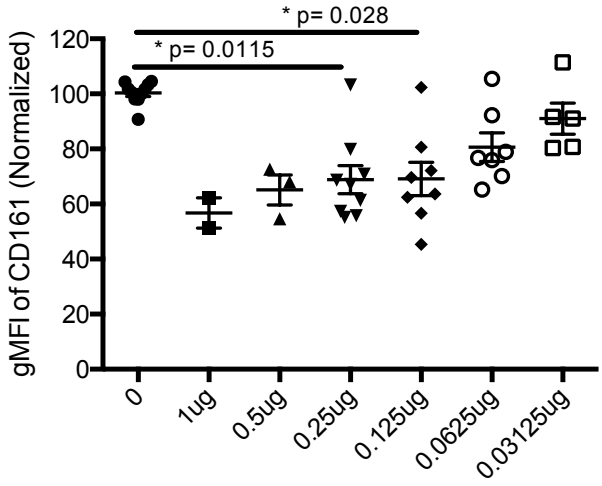

Reduced αCD161 staining after incubation with αCD161 mAb is dose dependent.
CD161 gMFI of PBMCs gated on $CD8^+$ $CD161^+$ T cells incubated for 16-18 hours with constant level of plate bound αCD3 (2.5ug/ml), αCD28 (2.5ug/ml), and a dose titration of plate bound unconjugated αCD161 mAb (1ug to 0.03125ug). Cells were then surface and internally stained with αCD161 mAb. The CD161 gMFI was normalized to the same dosage of plate bound IgG2a mAb (1ug to 0.03125ug). Statistical analysis: Friedman test with Dunn's multiple comparisons test.
Original aCD161 plate ICS data T.pzf

4.4.4 Unconjugated αCD161 mAb detached from plate could block binding

Due to concerns that the unconjugated αCD161 mAb from the plate remained bound to the cells and blocked subsequent staining with the same mAb clone, I tested for the presence of IgG on cells after incubation with plate bound mAb. Anti-IgG staining showed 10-18% of cells had mAb bound after incubation with plate bound mAb (Figure 4.8). This indicated mAb could detach from the plate, but cells were as likely to bind αCD3 and αCD28 mAbs detached from the plate as the αCD161 mAb. Since the αCD161 mAb could detach from the plate and block subsequent staining, I needed to develop a different way to measure CD161 expression.

Figure 4.8

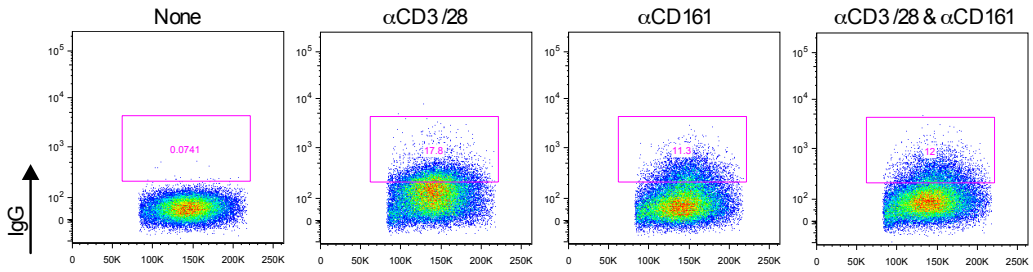

Pure αCD161 and αCD3/28 from plate may block staining.
PBMCs gated on $CD8^+$ T cells incubated with plate bound pure αCD161, αCD3 and αCD28 or all three mAb overnight. Cells were then surface stained with αIgG mAb to detect pure mAb bound to cells.
Chapter 4 (CD161) figures.pzfx

4.4.5 Do other αCD161 mAb clones have non-overlapping epitopes?

One way to get around the issue of detached mAb blocking proper staining, would be to use a different clone of αCD161 that bound a non-overlapping epitope for staining. Thus, I sequentially stained cells with two different αCD161 mAb clones to find two clones that showed complete dual staining and where the CD161 gMFI was not affected by a different clone already bound to the cells. Four different αCD161 clones were obtained and tested.

Cells initially stained with αCD161 clone DX12 showed a high degree of co-staining with clones Hp-3G10 and 191B8, suggesting the DX12 clone recognised a different epitope. However, when the order of clone staining was reversed, the cells no longer showed co-staining at high levels. The other clones tested had very low co-staining, suggesting very similar or overlapping epitopes (Figure 4.9). The resulting effects of on CD161 gMFI of the second αCD161 mAb clone in the co-staining experiments are summarized in Table 4.1. The αCD161 clone DX12 may bind a different epitope than Hp-3G10 and 191B8, but the addition of Hp-3G10 or 191B8 clones obstructed staining by the DX12 clone. This indicated that DX12 was not an ideal αCD161 mAb to use alongside 191B8 in experiments.

Figure 4.9

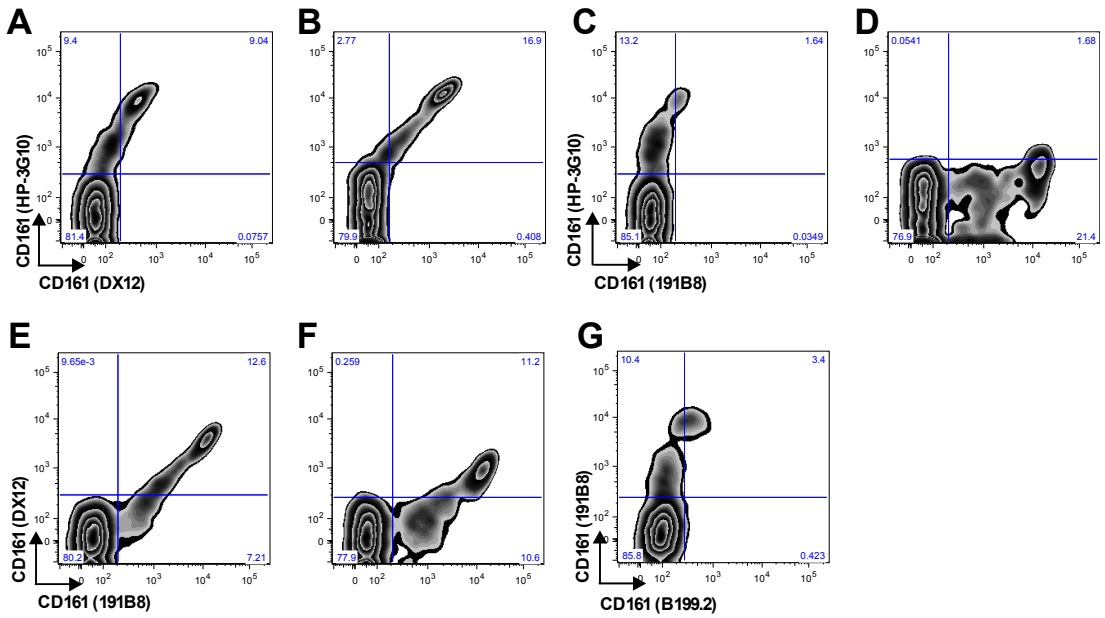

Sequentially staining with two different αCD161 mAb clones.
PBMCs gated on $CD8^+$ T cells surface stained with one clone of αCD161, washed and re-stained on the surface with a different αCD161 clone. **(A)** 1st HP-3G10, 2nd DX12 **(B)** 1st DX12, 2nd HP-3G10 **(C)** 1st HP-3G10, 2nd 191B8 **(D)** 1st 191B8, 2nd HP-3G10 **(E)** 1st DX12, 2nd 191B8 **(F)** 1st 191B8, 2nd DX12 **(G)** 1st 191B8, 2nd 199.2
071311_072311_2.jo Chapter 4 (CD161) figures.pzfx

Table 4.1

1st αCD161 mAb	2nd αCD161 mAb	% decrease in gMFI of 2nd αCD161 mAb compared to single stain
DX12	191B8	13.2
191B8	DX12	52.4
Hp-3G10	191B8	85.6
191B8	Hp-3G10	64.4
B199.2	191B8	19.8

Decrease in CD161 gMFI of the second αCD161 mAb clone in a sequentially surface stained reaction shows possible overlapping epitopes.
Brand of clones used: 191B8 (MACS), DX12 (BD), Hp-3G10 (Biolegend), B199.2 (Serotech)

4.4.6 αCD161 mAbs have different binding kinetics

The pattern of co-staining with the DX12 clone seemed slightly unusual until I noticed that the staining patterns of the different αCD161 mAb clones were not the

same within the same timeframes. The αCD161 clone DX12 had a much slower staining rate than the 191B8 clone (Figure 4.10). This differences in staining rate and variations in length of staining times during the co-staining experiments could lead to the unusual patterns seen. (Figure 4.9, Table 4.1). Due to these differences, the αCD161 clone 191B8 was used in all further experiments unless clearly stated otherwise.

Figure 4.10

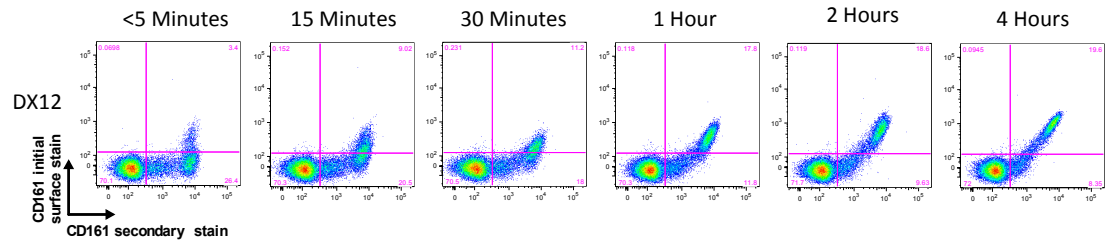

αCD161 mAb clones bind cells at different rates.
PBMCs gated on $CD8^+$ T cells surface stained with the clone αCD161 DX12 on APC for the time indicated (<5 minutes – 4 hours) and then stained again surface and internally with the αCD161 191B8 clone on PE for 30 minutes.
CD161 mAb clone staining time frame Chapter 4 (CD161) figures.pzfx

4.4.7 CD161 expression is downregulated by CD161 mAb cross-linking

Although antibodies blocking could explain some of the loss of $CD161^+$ T cells, it was also possible that CD161 expression was downregulated upon cross-linking. When APC conjugated αCD161 mAb or IgG2a was used to cross-link CD161 on cells and the same conjugated mAb was used to stain the cells, the αCD161 staining was still considerably reduced. This indicated a downregulation of both surface and intracellular expression of CD161 (Figure 4.11). Since CD161 expression was downregulated, an alternative method of tracking or isolating $CD161^+$ T cells was required.

Figure 4.11

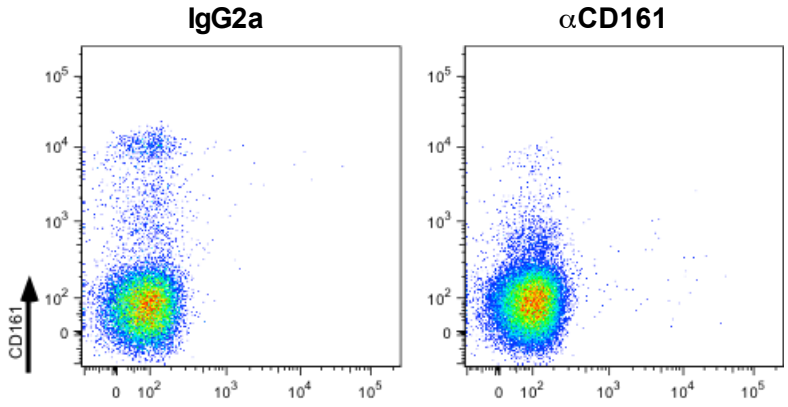

CD161 downregulation after incubation with αCD161 mAb.
PBMCs gated on $CD8^+$ T cells incubated with IgG2a-APC or αCD161-APC mAb (191B8) overnight. Cells were then stained again surface and internally with the same clone and fluorochrome.
Chapter 4 (CD161) figures.pzfx

4.4.8 CD26 is a poor marker for selection of $CD161^{+/++}$ cells.

The downregulation of CD161 expression upon cross-linking led to the need for another way to mark or isolate $CD161^{++}$ cells without using αCD161 mA. High expression of CD26 ($CD26^{++}$) was shown to be associated with $CD161^{++}$ expression in some T cell subsets (Bengsch et al. 2012; Hildebrandt et al. 2012). Although CD26 is expressed on resting T cells, it can be upregulated on other cell types with activation (De Meester et al. 1999). Thus, I isolated $CD26^+$ cells from resting PBMCs, by magnetic positive selection, to determine if this highly enriched for $CD161^{+/++}$ cells. CD26 selection from resting PBMCs showed limited enrichment of $CD161^{+/++}$ on $CD4^+$ or $CD8^+$ T cells. The enrichment was insufficient to use CD26 as a marker for CD161 (Figure 4.12).

Figure 4.12

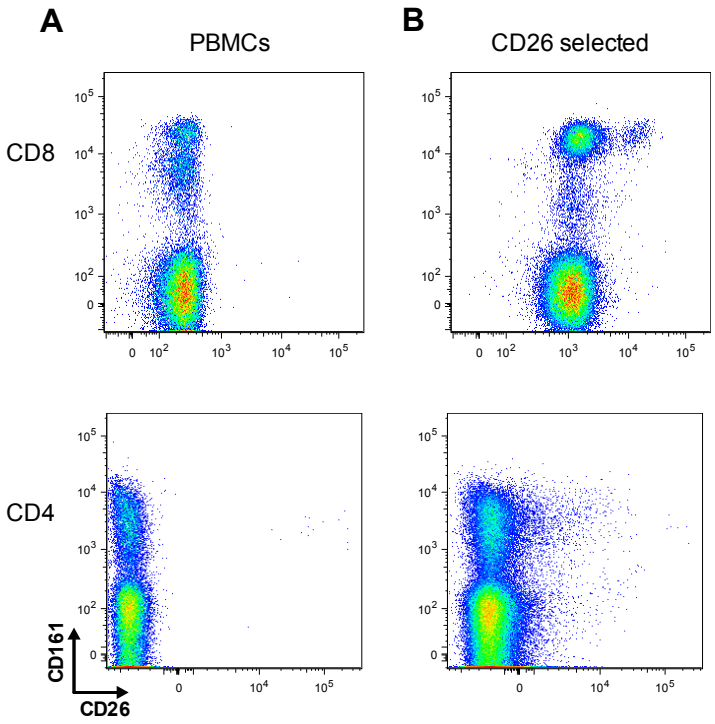

CD26 selection is an ineffective method of enriching CD161^{+} T cells.
(A) Resting PBMCs gated on CD3^{+} cells and CD8^{+} (top) or CD4^{+} (bottom) T cells **(B)** PBMCs that have been CD26 selected gated on CD3^{+} cells and CD8^{+} (top) or CD4^{+} (bottom) T cells.
280111.jo 280111_2 thesis.jo Chapter 4 (CD161) figures.pzfx

4.4.9 IL-18R is a good marker for selection of CD161^{++} CD8^{+} T cells

IL-18R was another molecule shown to be highly upregulated in CD161^{++} CD8^{+} T cells (Billerbeck et al. 2010). PBMCs were column selected for IL-18R and then stained to see the CD161 expression on the enriched cells. IL-18R selection highly (60-94%, n=3) enriched CD8^{+} T cells for CD161 positive cells, and the majority of the CD161 positive cells were CD161^{++}. On CD4^{+} T cells, IL-18R selection enriched for CD161^{+} cells to a lesser extent (30-50%, n=3) (Figure 4.13). The high levels of enrichment for CD161^{++} on CD8^{+} T cells by IL-18R selection made it a good candidate for co-staining or pre-selection of cells for experiments on CD161 cross-linking.

Figure 4.13

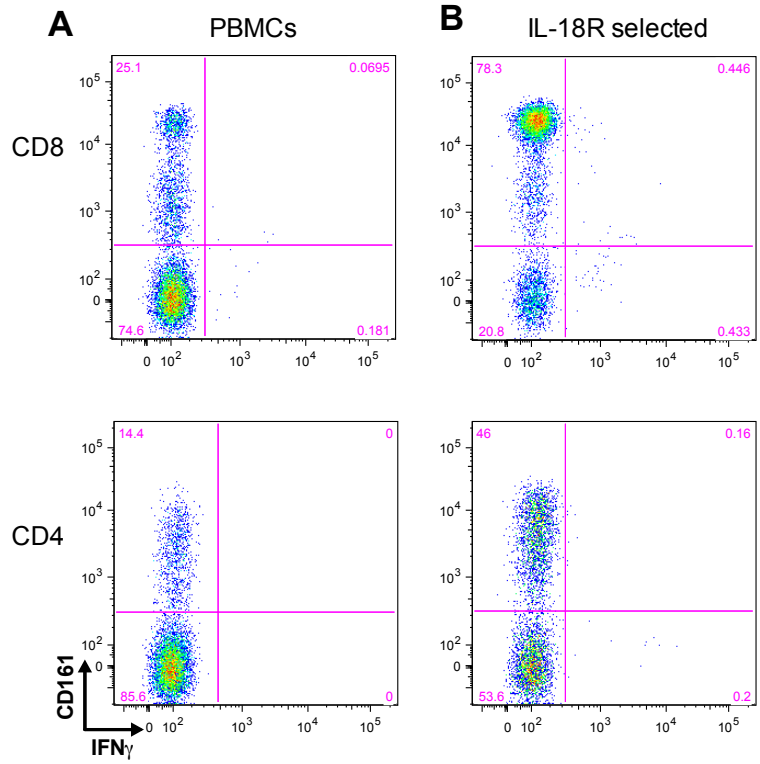

IL-18R selection enriches for CD161^{++} CD8^{+} T cells.
(A) Resting PBMCs gated on CD3^{+} cells and CD8^{+} (top) or CD4^{+} (bottom) T cells **(B)** PBMCs that have been selected for IL-18 receptor gated on CD3^{+} cells and CD8^{+} (top) or CD4^{+} (bottom) T cells. 181110c.jo Chapter 4 (CD161) figures.pzfx Chapter 4 (CD161) figures.pzfx

4.4.10 Vα7.2 highly co-stains CD8^{+} CD161^{++} cells

Around the same time the IL-18R selection experiments were carried out, Le Bourhis *et al.* showed Mucosal Associated Invariant T cells (MAIT), were mostly CD8^{+} CD161^{+} (Le Bourhis et al. 2010). MAIT cells were a population of mostly CD8^{+} CD161^{++} cells that expressed the invariant Vα7.2 version of the TCR α chain, and were suggested to be involved in antibacterial defence (Le Bourhis et al. 2010; Gold et al. 2010).

I stained PBMCs for Vα7.2 and CD161 to see the levels of co-expression. The majority of CD8^{+} T cells that expressed Vα7.2 were CD161^{++}, but few CD4^{+} T

cells expressed Vα7.2 and were not particularly enriched for $CD161^+$ (Figure 4.14).

The mean percentage of $CD8^+$ T cells that were MAIT cells was 67% (Figure 4.15).

Figure 4.14

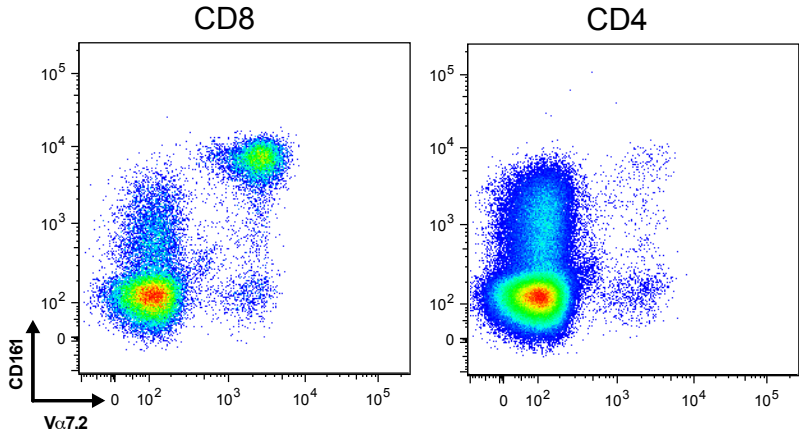

Vα7.2 is highly expressed on $CD161^{++}$ $CD8^+$ T cells but expression is limited on $CD4^+$ T cells.
Resting PBMCS gated on $CD3^+$ cells and $CD8^+$ (left) or $CD4^+$ (right) T cells stained with anti-Vα7.2 mAb.
CD161 va72 example.jo Chapter 4 (CD161) figures.pzfx

Figure 4.15

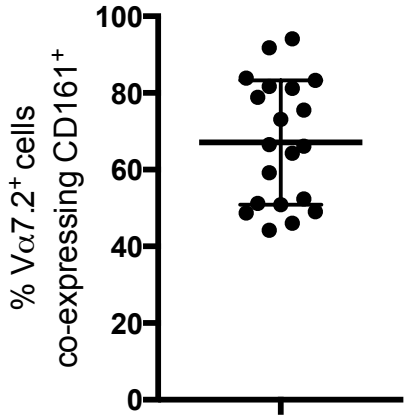

Median	66.3
25% Percentile	50.98
75% Percentile	81.58
Mean	67.1
SD	16.19
SE	3.62

Large porportion of $CD8^+$ $Vα7.2^+$ T cells co-express CD161.
Resting PBMCS gated on $CD8^+$ T cells. The percentage of $Vα7.2^+$ cells which co-express CD161 (n=20).
Va7.2 % CD161+.pzfx Va7.2 count % CD8.xlsx

4.4.11 Vα7.2 expression is not significantly affected by CD161 cross-linking

Vα7.2 is a chain of the TCR and activation of cells via the TCR can lead to the downregulation of the TCR (Valitutti et al. 1997; Y.-J. Liu and Arpin 1997; Escors et al. 2011). Therefore, it was important to determine if cross-linking affected Vα7.2 expression levels. PBMCs were cross-linked with αCD161 mAb for different timeframes (2-40 hours) then stained. The expression levels of Vα7.2 did not significantly change after cross-linking with αCD161 mAb (Figure 4.16). However, there was some indication that the downregulation of CD161 expression due to CD161 cross-linking was time dependent (Figure 4.16B).

Figure 4.16

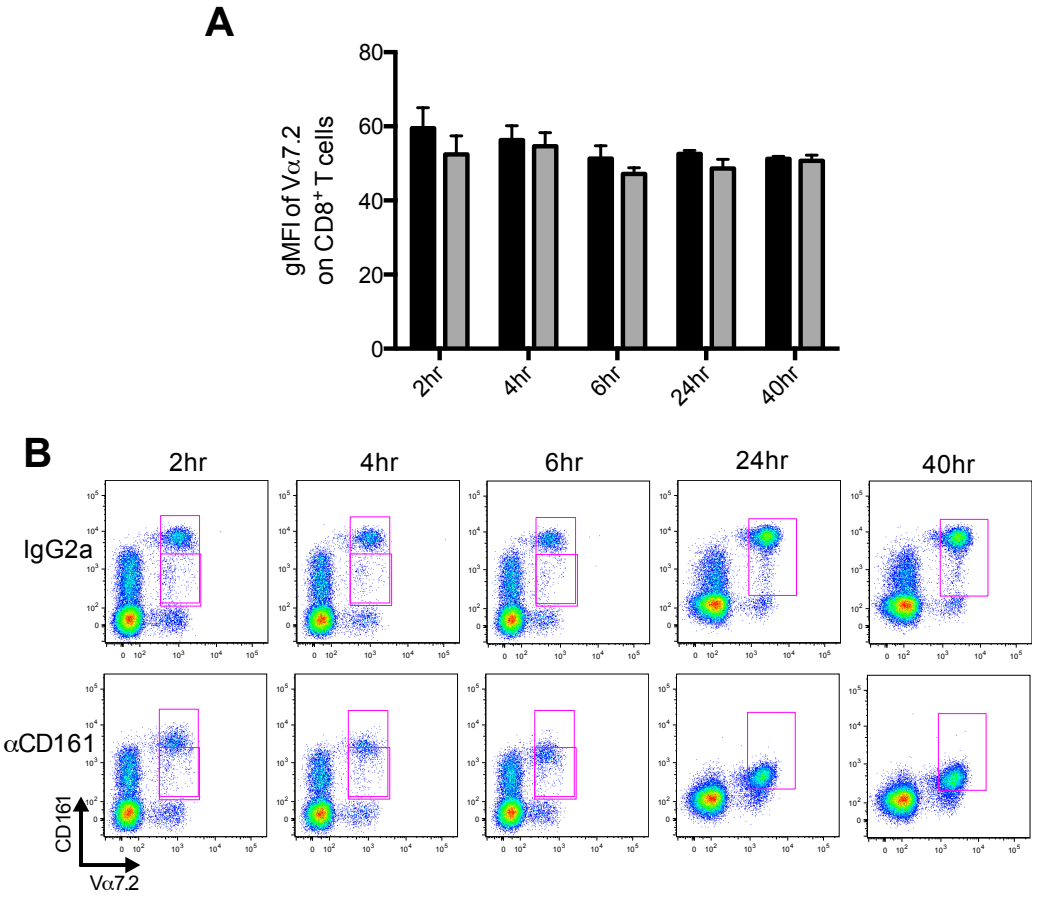

Vα7.2 expression does not significantly change with αCD161 mAb cross-linking.
(A) Vα7.2 gMFI on resting PBMCs gated on $CD8^+$ T cells which are co-incubated with αCD161 mAb (191B8) (0.25ug/ml) (grey) does not significantly change compared to IgG2a (0.25ug/ml) (black) at 2, 4, and 6 hours. **(B)** Representative raw data from one donor shown in A.
180512.pzf 180512 Thesis figure.jo

4.4.12 CD161 downregulation is time dependent

Previous experiments indicated that CD161 expression was downregulated after cross-linking with αCD161 mAb, and that the downregulation might be time dependent. To test if the downregulation was time dependent PBMCs were incubated with non-plate bound (free) αCD161-APC (clone 191B8) or IgG2a-APC mAbs for 1-40 hours before the staining was repeated. The $CD8^+$ $V\alpha7.2^+$ T cells showed a very clear time dependent downregulation of CD161 expression. It was also interesting to note, that CD8 $V\alpha7.2^-$ $CD161^+$ T cells, $CD4^+$ $CD161^+$ T cells, and even CD3- $CD161^+$ cells all showed a clear time dependent downregulation of CD161 expression (Figure 4.17).

Figure 4.17

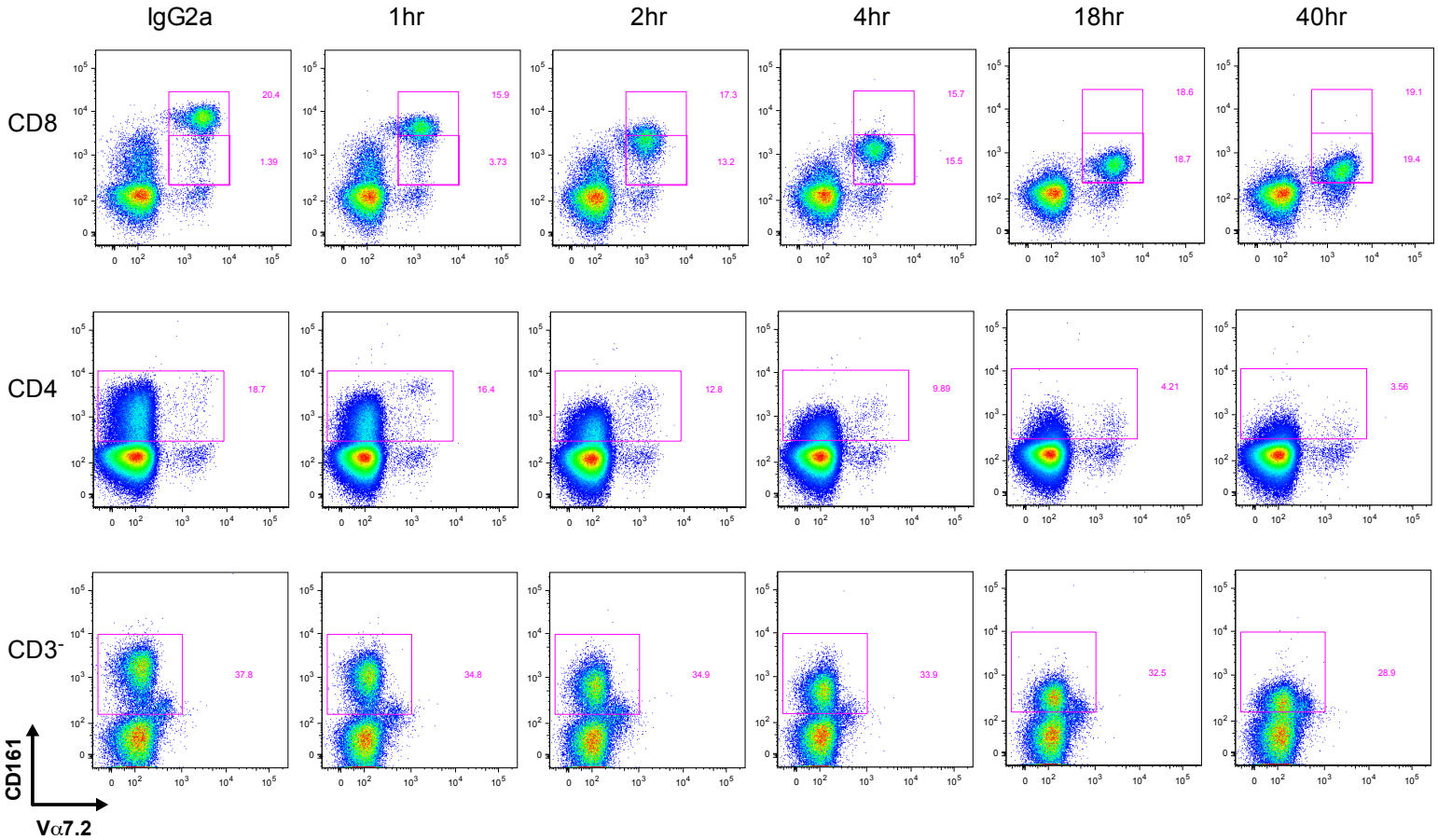

Downregulation of CD161 expression due to CD161 mAb cross-linking is time dependent.
CD161 stainging pattern of PBMCs co-incubated with IgG2a or αCD161 mAb (191B8) (1ug/ml) for time specified (1-40 hours). IgG2a is a representative graph of staining done at each time point. Gated on $CD3^+$ $CD8^+$ T cells (Top). Gated on $CD3^+$ $CD4^+$ T cells. (Middle). Gated on $CD3^-$ T cells. (Bottom)
150613 T CD161 time crash.jo Chapter 4 (CD161) figures.pzfx

4.4.13 αCD161 clones have different effects on time dependent downregulation

Earlier experiments showed a difference in the binding kinetics of how αCD161 clones DX12 and 191B8 bound to cells (Figure 4.10). Since the αCD161 mAb (191B8) cross-linking downregulated CD161 expression in a time dependent manner, would a different clone have the same effect on expression levels of CD161?

I first had to address what the staining patterns of αCD161 clones DX12 and 191B8 looked like over a longer time course. PBMCs were surface stained with the same concentrations of either DX12 or 191B8 αCD161 mAb for timeframes of <5 minutes – 40 hours. The cells were then surface stained with other cell markers, but not re-stained with CD161. The 191B8 clone stained cells quickly, but the staining levels started to decrease after 2 hours and had decreased substantially by 40 hours. The DX12 clone showed maximal staining at 4-6 hours, but the staining remained high for 24 hours before a possible decline around 40 hours (Figure 4.18).

The surface staining did not show what was happening to the intracellular CD161 expression. Samples at each time point (<5 minutes – 40 hours) were also stained again on the surface and intracellularly for CD161 and compared with control samples stimulated with IgG2a. αCD161 mAb clone 191B8 induced a significant decrease of CD161 expression ($p = 0.034$, $n=3$). The αCD161 mAb clone DX12 clone showed a much more moderate trend of decrease of CD161 expression, which might become statistically significant if more donors were tested (Figure 4.19).

Figure 4.18

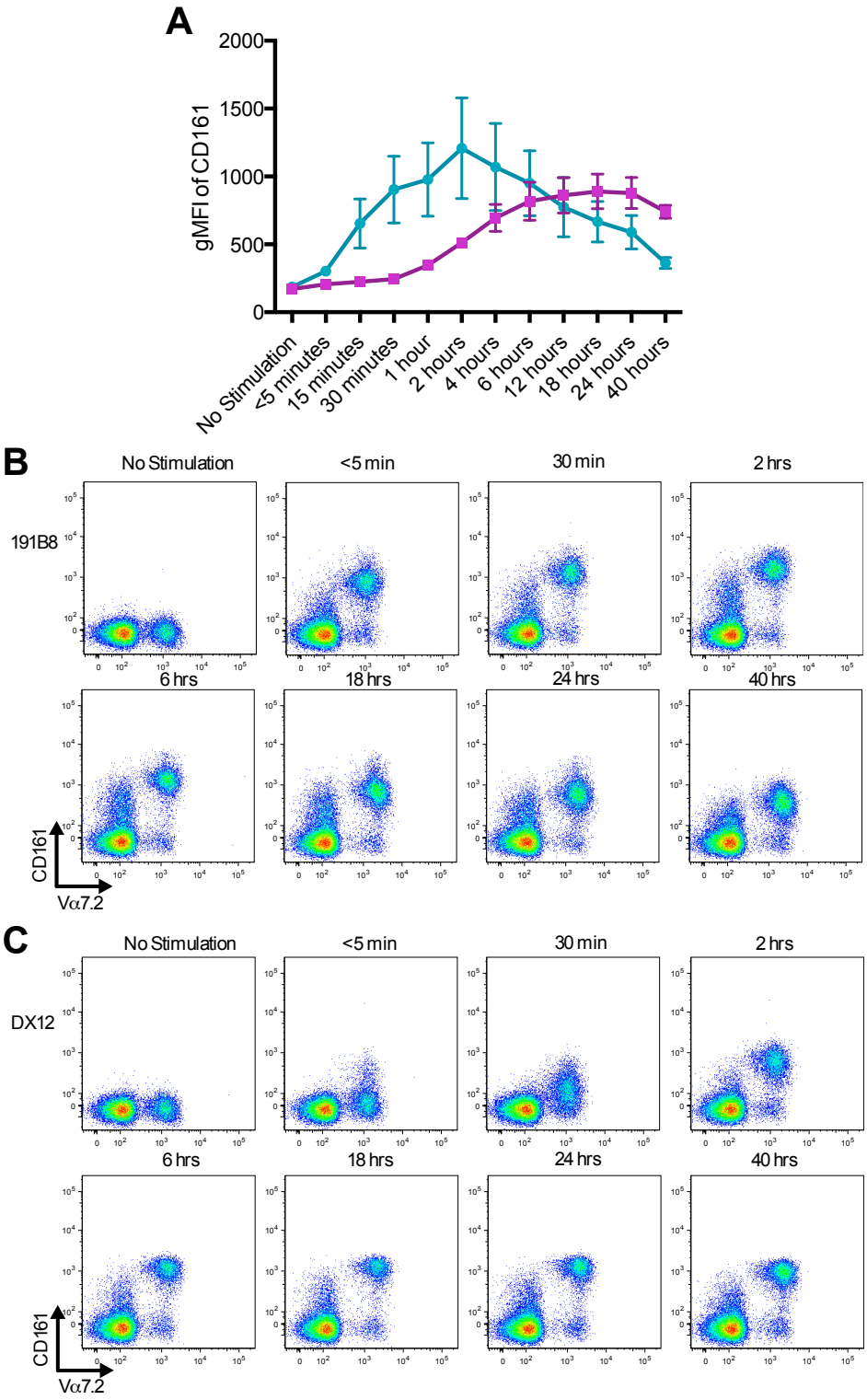

αCD161 mAb clones have different staining kinetics.
PBMCs gated on $CD8^+$ T cells surface stained for various lengths of time (<5 min – 40 hours) with either αCD161 clone 191B8 or clone DX12. **(A)** The CD161 gMFI of $CD8^+$ $V\alpha7.2^+$ $CD161^+$ T cells stained with αCD161 clone 191B8 (aqua) or DX12 (pink) to show the staining level after the time indicated (n=3). **(B)** Representative raw data of one donor stained with αCD161 mAb clone 191B8 shown in A. (C) Representative raw data of one donor stained with αCD161 mAb clone DX12 shown in A.
150612 T.pzf

Figure 4.19

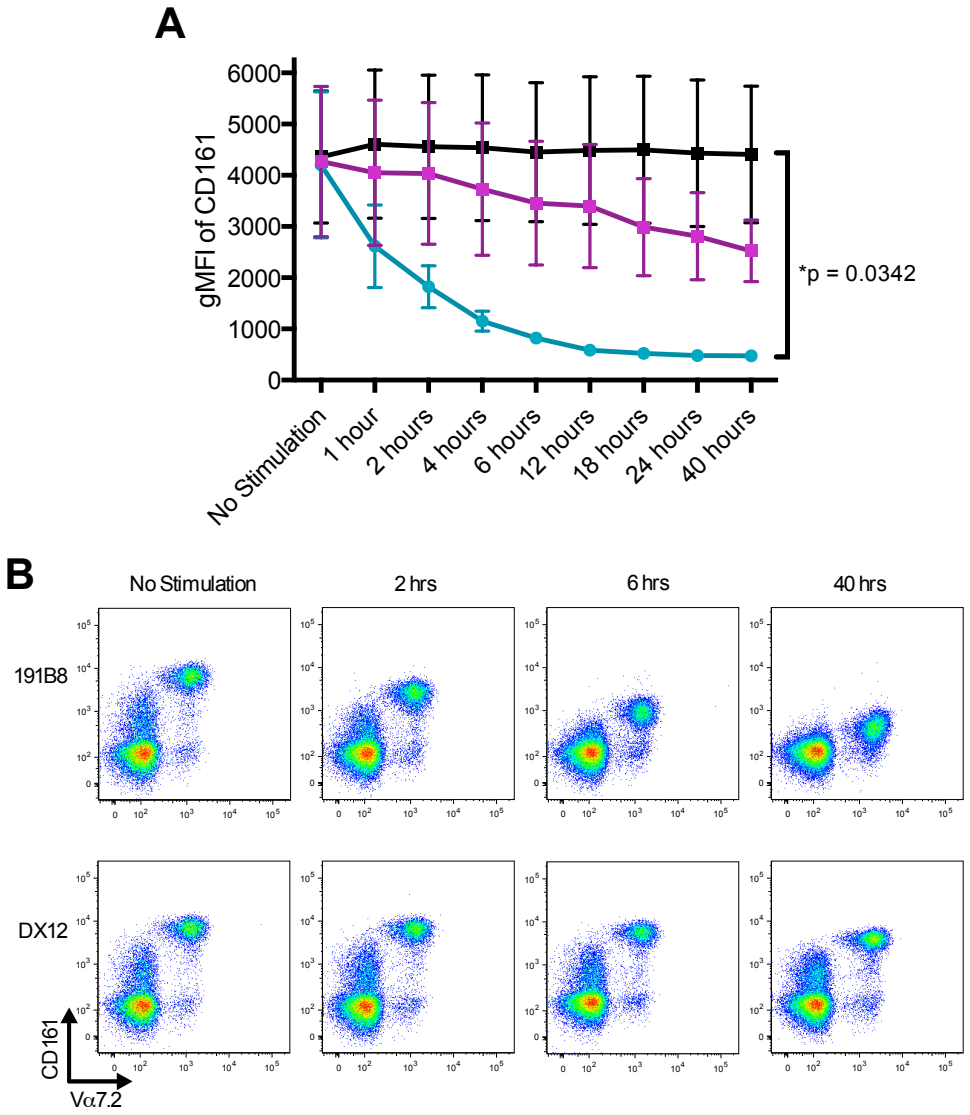

CD161 expression is downregulated at different rates depending on αCD161 mAb clone used for cross-linking.
(A) PBMCs cross-linked with αCD161 mAb clones 191B8 (aqua) or DX12 (pink), or IgG2a (black) for various lengths of time (1 – 40 hours). The CD161 gMFI is shown for cells gated on $CD8^+$ $V\alpha7.2^+$ $CD161^+$ T cells which have been restained surface and intracellularly with αCD161 clone 191B8. (n=3) **(B)** Representative raw data of cells cross-linked with αCD161 clone 191B8 (top) or with DX12 (bottom)for one donor shown in A.
150612 T.pzf

4.4.14 CD161 downregulation is dose dependent

Since the downregulation of CD161 expression was time dependent, I wanted to know if the downregulation was also dose dependent. I used a cell line transfected with LLT1 (300-LLT1) and the parental cell line 300-Null as a control. The PBMCs

were co-incubated with either 300-LLT1 or 300-Null cell lines at increasing concentrations (0-2x10^6) of cells overnight. The ligation of CD161 by 2x10^6 300-LLT1 cells induced significant downregulation (p= 0.008) of CD161 expression (Figure 4.20). This indicated that downregulation of CD161 occurred in a dose dependent manner.

Figure 4.20

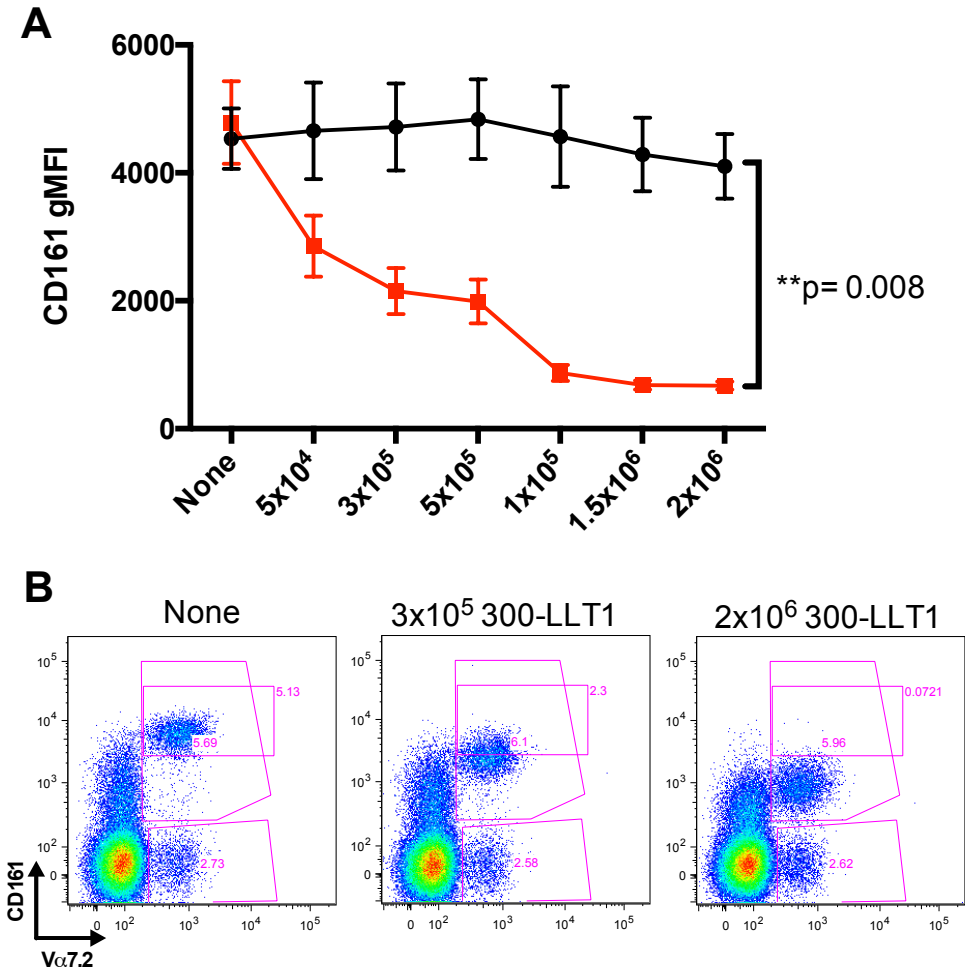

Downregulation of CD161 expression due to CD161-LLT1 ligation is dose dependent.
(A) Resting PBMCS (1x10^6) gated on $CD8^+$ $CD161^+$ $V\alpha7.2^+$ T cells co-cultured with increasing concentrations (0 - 2x10^6) of 300-Null cells (black) or 300-LLT1 cells (red) (n=3) Statistical analysis: Paired T-test **(B)** Representative raw data of one donor shown in A.
190412.pzf

4.4.15 CD161 expression improves after LLT1 ligation is removed in a time dependent manner

Downregulation of CD161 expression could be induced by αCD161 mAb and the natural ligand LLT1, but could the expression of CD161 recover after the removal of CD161 ligation? To address this, I took PBMCs and enriched for Vα7.2$^+$ cells. Then I co-incubated the Vα7.2$^+$ cells with 300-LLT1 or 300-Null cells for 3 hours. The 300 cell lines were then removed by re-enriching for the Vα7.2$^+$ cells. The re-enriched Vα7.2$^+$ cells were incubated for 0-48 hours before staining. The CD161 gMFI of the 300-LLT1 co-incubated cells were compared with 300-Null co-incubated cells at the same time point. The expression levels of CD161 recovered significantly over time after the removal of LLT1 ligation (Figure 4.21).

4.4.16 CD161 downregulation is not regulated from the mRNA level

Since CD161 ligation induces downregulation of CD161 expression, I wanted to know if the downregulation was regulated at the level of mRNA expression. To test this, PBMCs were enriched for CD8$^+$ T cells and then incubated with αCD161 (191B8) or IgG2a mAbs for 18 hours. A sample of each set of cells was stained for CD161 expression to confirm downregulation of CD161 expression (Figure 4.22). RNA was then extracted from the cells and used to produce cDNA. The cDNA was then used in real-time qPCR experiments. The real-time qPCR results did not show significant changes in mRNA expression between CD8$^+$ T cells with downregulated CD161 expression and cells without downregulated CD161 expression in any of the donors (Figure 4.23, Table 4.2).

Figure 4.21

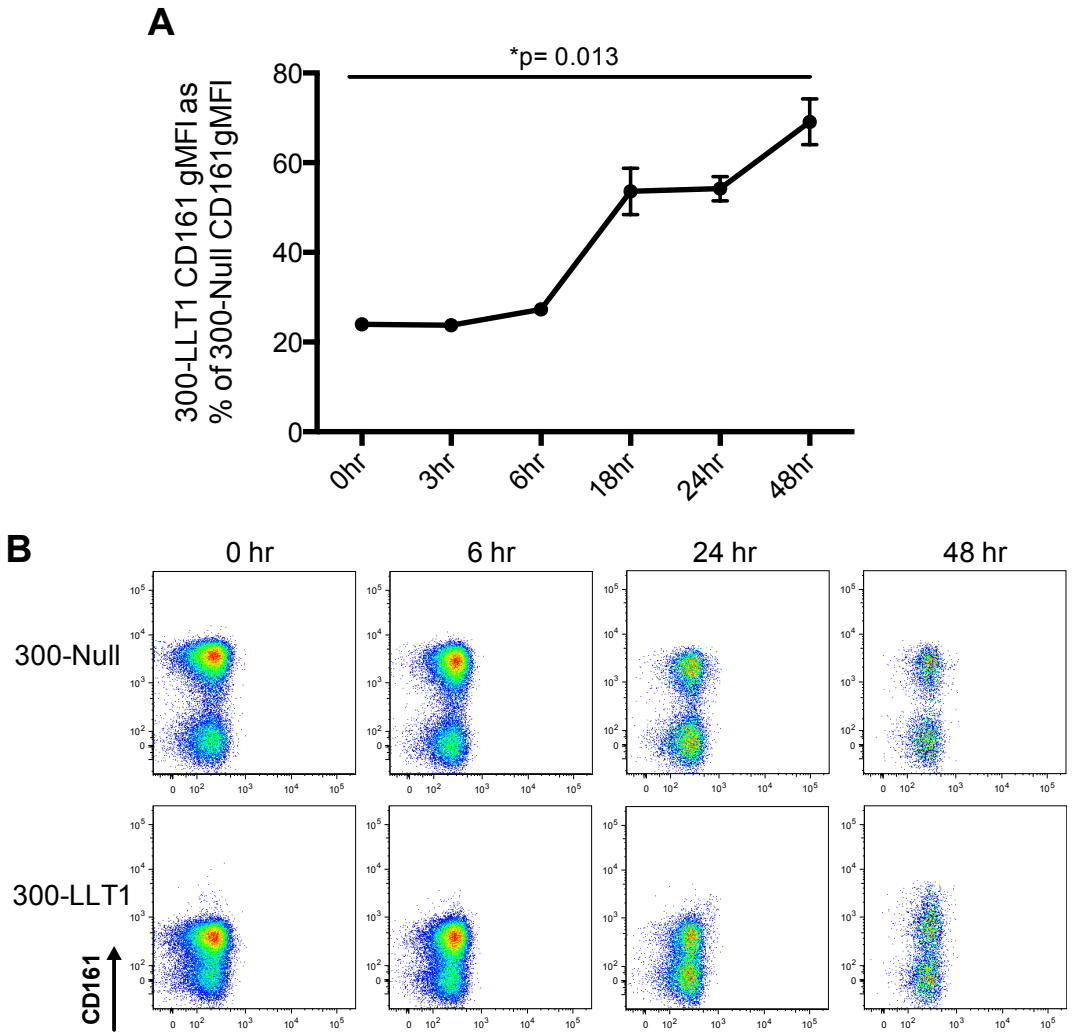

CD161 expression levels recover after removal of CD161 ligation.
PBMCs column selected for Vα7.2$^+$ cells, co-incubated with 300-LLT1 or 300-Null cells for 3 hours and then Vα7.2$^+$ cells are column selected again removing any 300-LLT1 or 300-Null cells. Re-selected cells were rested at 37°C for 0-48 hours then stained. **(A)** On CD8$^+$ Vα7.2$^+$ gated cells the percetage of the CD161 gMFI of 300-LLT1 co-incubated cells compared to the CD161 gMFI of 300-Null co-incubated cells was calculated for each timepoint. Statistical analysis: Friedman test with Dunn's multiple comparisons test. (n=3) **(B)** Representative raw data of cells co-incubated with 300-Null (top) or 300-LLT1 (bottom) for one donor shown in A.
040213.jo 040213.pzf

Figure 4.22

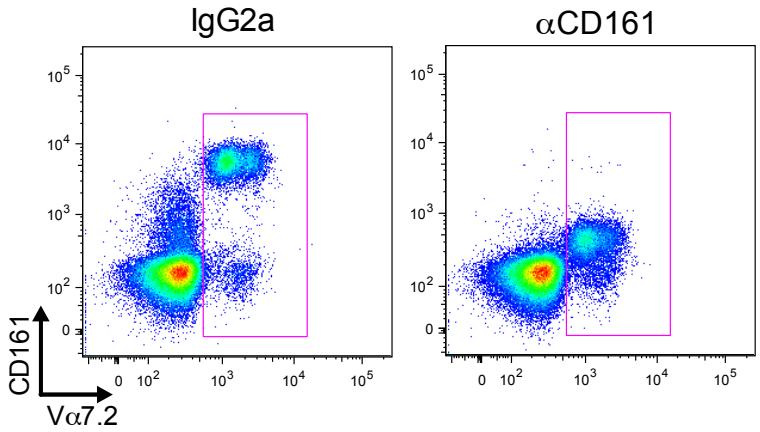

Cells used in real-time qPCR downregulated CD161 expression
PBMCs selected for CD8 and then incubated with αCD161 mAb or IgG2a mAb for 18 hours. A small sample of the cells were surface and internally stained, and the remaining cells were RNA extracted and used for real-time qPCR testing of CD161 expression. (See Figure 4.23-24) Representative raw data for one donor.
130612.jo 111012.pzf

Figure 4.23

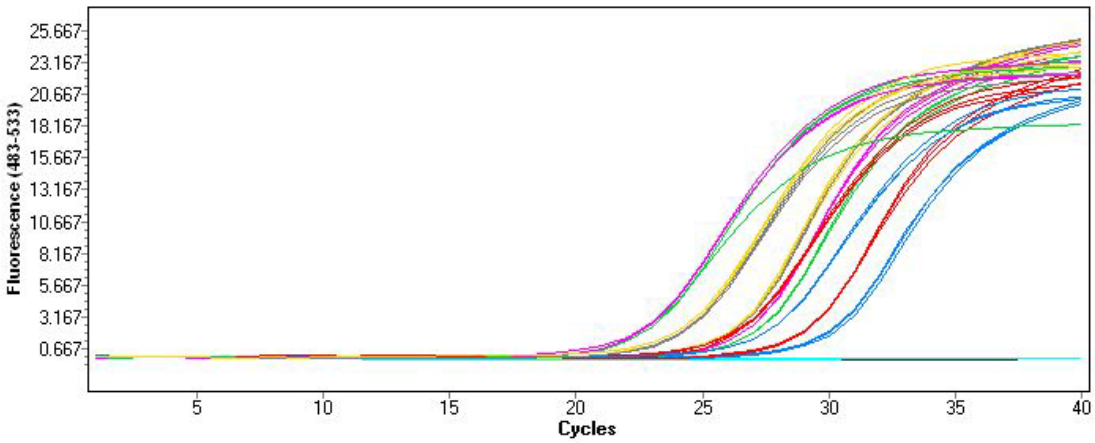

Traces from Real-Time qPCR of CD8 selected PBMCs stimulated with αCD161 or IgG2a mAb
Traces from one representative experiment of real-time qPCR from RNA extracted from CD161 ligated and unligated cells from 3 donors. See figure 4.24 for numerical output.

Table 4.2

Sample	Primers	C_T	Avg C_T	Δ C_T (GOI-HK)	ΔΔ C_T (CD161-IgG2a)	$2^{-\Delta\Delta CT}$ (Fold change)
64 IgG2a Stim	HPRT	29.59	29.70 ± 0.11			
64 IgG2a Stim	HPRT	29.80				
64 IgG2a Stim	HPRT	29.71				
64 IgG2a Stim	CD161	27.30	27.32 ± 0.03	-2.38 ± 0.11		
64 IgG2a Stim	CD161	27.35				
64 IgG2a Stim	CD161	27.32				
64 CD161 Stim	HPRT	28.68	28.71 ± 0.03		-0.16 ± 0.11	1.12 (1.03-1.21)
64 CD161 Stim	HPRT	28.73				
64 CD161 Stim	HPRT	28.72				
64 CD161 Stim	CD161	26.15	26.17 ± 0.02	-2.54 ±		
64 CD161 Stim	CD161	26.18				
64 CD161 Stim	CD161	26.18				
65 IgG2a Stim	HPRT	26.81	26.81 ± 0.01			
65 IgG2a Stim	HPRT	26.80				
65 IgG2a Stim	HPRT	26.81				
65 IgG2a Stim	CD161	22.59	22.43 ± 0.32	-4.38 ± 0.32		
65 IgG2a Stim	CD161	22.63				
65 IgG2a Stim	CD161	22.06				
65 CD161 Stim	HPRT	26.45	26.49 ± 0.04		0.33 ± 0.20	0.79 (0.69-0.91)
65 CD161 Stim	HPRT	26.49				
65 CD161 Stim	HPRT	26.52				
65 CD161 Stim	CD161	22.48	22.44 ± 0.07	-4.05 ± 0.08		
65 CD161 Stim	CD161	22.48				
65 CD161 Stim	CD161	22.36				
66 IgG2a Stim	HPRT	26.00	25.99 ± 0.02			
66 IgG2a Stim	HPRT	25.97				
66 IgG2a Stim	HPRT	26.00				
66 IgG2a Stim	CD161	24.06	24.09 ± 0.04	-1.90 ± 0.04		
66 IgG2a Stim	CD161	24.14				
66 IgG2a Stim	CD161	24.08				
66 CD161 Stim	HPRT	25.89	25.88 ± 0.02		0.06 ± 0.07	0.96 (0.91-1.01)
66 CD161 Stim	HPRT	25.89				
66 CD161 Stim	HPRT	25.86				
66 CD161 Stim	CD161	23.97	24.04 ± 0.10	-1.84 ± 0.10		
66 CD161 Stim	CD161	24.15				
66 CD161 Stim	CD161	24.00				
Neg Control RT-PCR	HPRT	0.00				
Neg Control RT-PCR	CD161	0.00				
Neg Control H_2O	HPRT	0.00				
Neg Control H_2O	CD161	0.00				

Fold change calculation of CD161 mRNA for Real-Time qPCR
Calculation of fold change in CD161 mRNA for Real-Time qPCR of CD8 selected PBMCs stimulated with αCD161 or IgG2a mAb using $2^{-\Delta\Delta CT}$. Formulas for calculations from Kenneth *et al*. 2001. (1 = no change mRNA, <1 = decrease mRNA, >1 = increase mRNA)
CD161_test_4_040712 analysis Thesis.xlsx 111012.pzf Chapter 4 (CD161) figures.pzfx

4.5 Discussion

4.5.1 CD161 expression patterns on T cells

The protein CD161 is expressed on NK and T cell subsets. Confirming previous observations from our group and others, I found that $CD4^+$ T cells could be divided into $CD161^-$ and $CD161^+$ populations of cells, while $CD8^+$ T cells could be divided into $CD161^-$, $CD161^+$ and $CD161^{++}$ populations (Takahashi, Dejbakhsh-Jones, and Strober 2006; Billerbeck et al. 2010).

4.5.2 Surface and intracellular staining of CD161

Surface expression of CD161 has been shown by many studies (Lanier et al. 1994; Aldemir et al. 2005; Pozo et al. 2006; Billerbeck et al. 2010). However, CD161 was also found intracellularly in readily detectable quantities, as intracellular staining increased CD161 gMFI by an average of almost 40%. A small percentage of cells were also positive for CD161 only intracellularly. Due to the high levels of intracellular CD161 expression, intracellular staining of CD161 was performed in all experiments unless otherwise stated.

4.5.3 CD161 staining decreased by αCD161 mAb cross-linking with unconjugated plate bound αCD161 mAb

Several previous studies used cross-linking of αCD161 mAb on cells to test functional consequences of CD161 cross-linking (Azzoni et al. 1998; Exley et al. 1998; Aldemir et al. 2005; Pozo et al. 2006). While setting up similar experiments, decreased CD161 staining on T cells was noticed after cross-linking with unconjugated plate bound αCD161 mAb. The decrease in CD161 staining with the plate bound mAb was dose dependent. The drop in CD161 staining was only partially

accounted for by the detachment of unconjugated mAb from the approximately 10-20% of cells that were shown to have unconjugated CD161 antibody bound. However the detachment of mAbs from the plate was not specific to αCD161 and also occurred with the αCD3 and αCD28 mAbs. Therefore, an alternative method of identifying $CD161^+$ cells was needed.

4.5.4 Staining CD161 with multiple clones of αCD161 mAb

To avoid blocked CD161 staining by unconjugated αCD161 mAb, a different αCD161 clone with a non-competing epitope could be used to stain the cells. At first, sequential staining experiments with the DX12 clone appeared to not interfere with the binding of 191B8 and Hp-3G10. However, staining the same clones in the reverse order significantly affected the binding of DX12. This could be due to the DX12 clone binding to a location on the CD161 protein that is made much less accessible when the CD161 has already been bound by the 191B8 or Hp-3G10 clones. No other pairs of clones with potentially non-competing epitopes were seen.

It was unexpected that the order the clones were bound would make a large difference in competition for the epitope. However, later experiments showed that the αCD161 clone DX12 bound to cells at a much slower rate than the αCD161 clone 191B8. This may not be due to a significantly different affinity of the antibody to its epitope, but a difference in the rate at which the epitope of the antibody is exposed. If the epitope is in a location where other molecules found in close proximity to the CD161 hinder access of the antibody, this might explain the slower binding time seen by the DX12 clone.

Thus, the DX12 clone may bind a different and non-competing epitope to the 191B8 clone. However, these issues combined made the αCD161 DX12 clone a less than ideal for co-staining with other αCD161 mAbs to identify $CD161^+$ T cells.

4.5.5 αCD161 mAb cross-linking downregulated CD161 expression

In previous experiments CD161 staining was reduced due to unconjugated αCD161 mAb blocking the binding of conjugated αCD161 mAb. To get around this problem, free APC-conjugated αCD161 mAb was used to cross-link $CD8^+$ T cells and then the cells were stained again with the same clone of αCD161-APC mAb. In this experiment CD161 staining was not blocked and a decrease was still seen in CD161 staining after cross-linking. This indicated that a downregulation of CD161 expression had occurred on the surface and intracellularly after cross-linking with αCD161 mAb.

Aldemir *et al*. previously showed a reduction in CD161 expression when LLT1 expressing cells were incubated with $CD161^+$ cells and noted this as similar to cross-linking using αCD161 mAb. This study suggested the reduction in expression happened quickly, the decrease in expression did not occur when transwells were used to prevent CD161 ligation by blocking cell-to-cell contact, and that fixation prevented the decrease in expression by stopping internalization of the CD161. However, the same study also noted the same αCD161 mAb clone (191B8) that reduced CD161 surface expression in a similar way to the natural ligand was also considered a blocking mAb (Aldemir et al. 2005). The reason for the contradiction in functional consequences of binding to the 191B8 is unclear.

CD161 downregulation upon ligation would not be unique, as several other T cell proteins decrease surface expression after ligation. TCR surface expression is

reduced after binding of its cognate MHC-peptide complex, although the exact mechanism of the decrease is debated (Valitutti et al. 1997; Liu et al. 2000; Escors et al. 2011). CLTA-4 surface expression is also reduced on T cells after binding CD80 or CD86, which inhibits the activation of CD28 (Qureshi et al. 2011). NKG2D, a C type lectin-like protein, is downregulated and degraded after ligation by a MIC ligand (Groh et al. 2002).

4.5.6 CD26 is a poor marker for CD161$^{+/++}$ T cells

Since CD161 expression is downregulated by CD161 cross-linking, another way of identifying the CD161$^{+/++}$ cells was needed. Some CD26^{++} T cells highly co-expressed CD161 (Bengsch et al. 2012; Hildebrandt et al. 2012), but cell activation also induced CD26 expression on other types of cells (De Meester et al. 1999). If resting CD26^{++} cells were highly enriched for CD161$^{+/++}$ T cells, then these cells could be isolated for functional experiments eliminating the need to effectively stain for CD161. However, magnetic enrichment of CD26^{+} cells did not significantly enrich for CD161$^{+/++}$ T cells.

4.5.7 CD8+ CD161++ T cells is significantly co-expressed IL-18R

The IL-18R was also shown to be highly upregulated on CD161^{++} CD8^{+} T cells (Billerbeck et al. 2010). Isolation of IL-18R^{+} cells greatly enriched for CD161^{++} CD8^{+} T cells (60-94%), and somewhat enriched for CD161^{+} CD4^{+} T cells (30-50%). This suggested that IL-18R expression would be a good co-marker in CD8^{+} T cells for ability to express CD161.

4.5.8 CD8^{+} CD161^{++} T cells significantly co-express Vα7.2^{+}

Around the same time IL-18R was found to be highly co-expressed on CD8^{+} CD161^{++} T cells, Le Bourhis *et al.* reported that on MAIT cells, also defined as

$CD161^{++}$, expressed the invariant Vα7.2 chain of the TCR (Le Bourhis 2010). This population represented approximately 70-80% of the $CD161^{++}$ $CD8^{+}$ T cells, and most of the $V\alpha7.2^{+}$ $CD8^{+}$ T cells were $CD161^{++\,++}$(Le Bourhis et al. 2010, Gold et al. 2010, Walker et al. 2012). Therefore, this allowed me to use the Vα7.2 expression as a marker of $CD161^{++}$ T cells, and track these cells as CD161 was downregulated.

4.5.9 Expression of Vα7.2 is not affected by αCD161 mAb cross-linking

The anti-Vα7.2 mAb binds a specific chain on the TCR, and TCRs can also be downregulated upon cell stimulation (Valitutti et al. 1997, Lui et al. 2000, Escors et al. 2011). Therefore, it was important to confirm that αCD161 cross-linking did not reduce the TCR expression as well. Experiments showed no significant change in Vα7.2 expression due αCD161 mAb cross-linking, making Vα7.2 a good candidate for tracking cells capable of CD161 expression.

4.5.10 αCD161 mAb induced downregulation of CD161 is time dependent

The experiments looking at Vα7.2 expression over time hinted that the αCD161 mAb cross-linking could downregulate CD161 expression in a time dependent manner. If the length of time that CD161 ligation occurs is important, then in the context of the human body it would be important to know not only where CD161 and its ligand can interact, but how long is CD161 in the presence of its ligand. Experiments showed αCD161 mAb (191B8) cross-linking induced CD161 downregulation in a time dependent manner.

Where the downregulation occurred over the course of time is also important. After ligation with αCD161 mAb the intracellular levels of CD161 begin to decrease even as the surface levels increase. This is mostly due to the continued fluorescence of the mAb as the stained but internalized CD161 proteins continue to fluoresce until the fluorochrome is fully degraded. However, it is possible that ligation of CD161 could change the amount of time CD161 is found on the surface before being recycled. With continued ligation the intracellular levels of CD161 continue to decrease and the surface levels of CD161 also begin to decline.

The time dependent downregulation of CD161 occurred on $CD4^+$ and $CD3^-$ cells as well, indicating that the downregulation of CD161 is not specific to $CD8^+$ T cells.

4.5.11 The αCD161 mAb clone used affects the time frame of CD161 downregulation

Since the downregulation was mAb mediated and different αCD161 mAb clones were shown to have differences in binding patterns, could cross-linking with a different clone change the pattern of CD161 downregulation? Interestingly, ligation with the αCD161 clone DX12 did not induce as much downregulation of CD161 as the 191B8 clone. Although αCD161 mAb DX12 ligation induced a downward trend in the intracellular levels of CD161, the surface levels did not appear to be significantly changed. Since intracellular downregulation of CD161 occurred prior to surface CD161 downregulation with 191B8, it is possible that DX12 could induce surface level downregulation if given a longer timeframe.

The differences seen between ligation with different clones of αCD161 indicate that the type or quality of ligation of CD161 may significantly affect the functional effects of CD161 ligation.

4.5.12 CD161 downregulation induced by CD161 ligation is dose dependent

Since CD161 downregulation is time dependent, could the downregulation also be dose dependent? In the context of the human body, this would indicate an importance of the quantity of ligand and CD161 interaction, which could dictate the level of CD161 downregulation seen.

I used natural ligand LLT1 to test for a dose dependent downregulation of CD161. Increasing the amount of the LLT1 transfected cell line (300-LLT1) co-incubated with PBMCs showed a significant dose dependent downregulation of CD161 compared with the untransfected 300-Null cell line. This indicated that ligation of CD161 with its natural ligand induced dose dependent downregulation.

In a disease state, if LLT1 or another unknown ligand of CD161 is significantly upregulated or downregulated by the disease, this could affect the levels of CD161 detected in that region. Interestingly, changes in CD161 expression have been noted in multiple disease states including hepatitis C virus, tuberculosis, multiple sclerosis, Crohn's disease, rheumatoid arthritis, and psoriasis (Billerbeck et al. 2010, Gold et al. 2010, Kleinschek et al. 2009, Annibali et al. 2011, et al. Cosmi 2008).

4.5.13 CD161 expression recovers after removal of CD161 ligation

Since ligation of αCD161 with mAb or LLT1 induced downregulation of CD161 expression, would the expression of CD161 recover if the stimulation were

removed? In experiments where LLT1-300 cells were co-incubated with Vα7.2$^+$ cells for 3 hours and then removed, the expression of CD161 was downregulated upon stimulation and then the expression levels of CD161 recovered in a time dependent manner. This indicates that CD161 expression can be specifically downregulated by ligation but expression levels recover after removal of the stimulus.

This has potential implications for the disease states where studies have shown CD161 levels to be increased or reduced in specific locations (Cosmi et al. 2008, Kleinschek et al. 2009, Annibali et al. 2011, Billerbeck et al. 2010, Cosgrove et al. 2013). In these disease states the levels of CD161 ligand may be altered inducing more or less downregulation of CD161 than would occur in a healthy state. If the disease state and any related changes in ligand expression discontinue, then the levels of CD161 expression should eventually return to more normal levels.

4.5.14 CD161 downregulation is not regulated at the mRNA level

Real-time qPCR showed the downregulation of CD161 on CD8$^+$ T cells to not be regulated at the level of mRNA. The post-translational regulation of CD161 may important in to the short timeframe necessary for downregulation. The post-translational nature of the regulation may play a role in the responsiveness of CD161 downregulation to the time and dose of ligation.

4.5.15 Model of CD161 downregulation

The main results of the effect of CD161 ligation by LLT1 or cross-linking with αCD161 mAb clone 191B8 were used to make a model of the process and timing of CD161 downregulation and recovery. After ligation of CD161 with either LLT1 or αCD161 mAb (1918B) the surface staining levels of CD161 may increase above the levels of antibody saturation levels (30 minutes post staining) and reach maximal

levels around the 2 hour time point as stained αCD161 mAb that has been internalized and is undergoing degradation still fluoresce. The intracellular levels of CD161 begin to decrease soon after ligation occurs: from within 30 minutes of ligation. The intracellular decrease of CD161 occurs even as the surface levels of CD161 staining are still building to maximal levels. After about 2 hours the surface levels of CD161 also begin to decrease. The surface and intracellular downregulation can continue until the cell is negative for CD161 or until the ligand is removed from the cell. After removal of the ligand, CD161 expression slowly begins to recover (Figure 4.24).

Although cross-linking with the αCD161 mAb DX12 does not show the same level of downregulation, it does appear to follow the model to a degree with the decrease in intracellular CD161 even if in the time frames tested surface expression of CD161 did not change greatly. More time may be necessary for a ligation similar to the DX12 clone to follow the entire downregulation model.

Figure 4.24

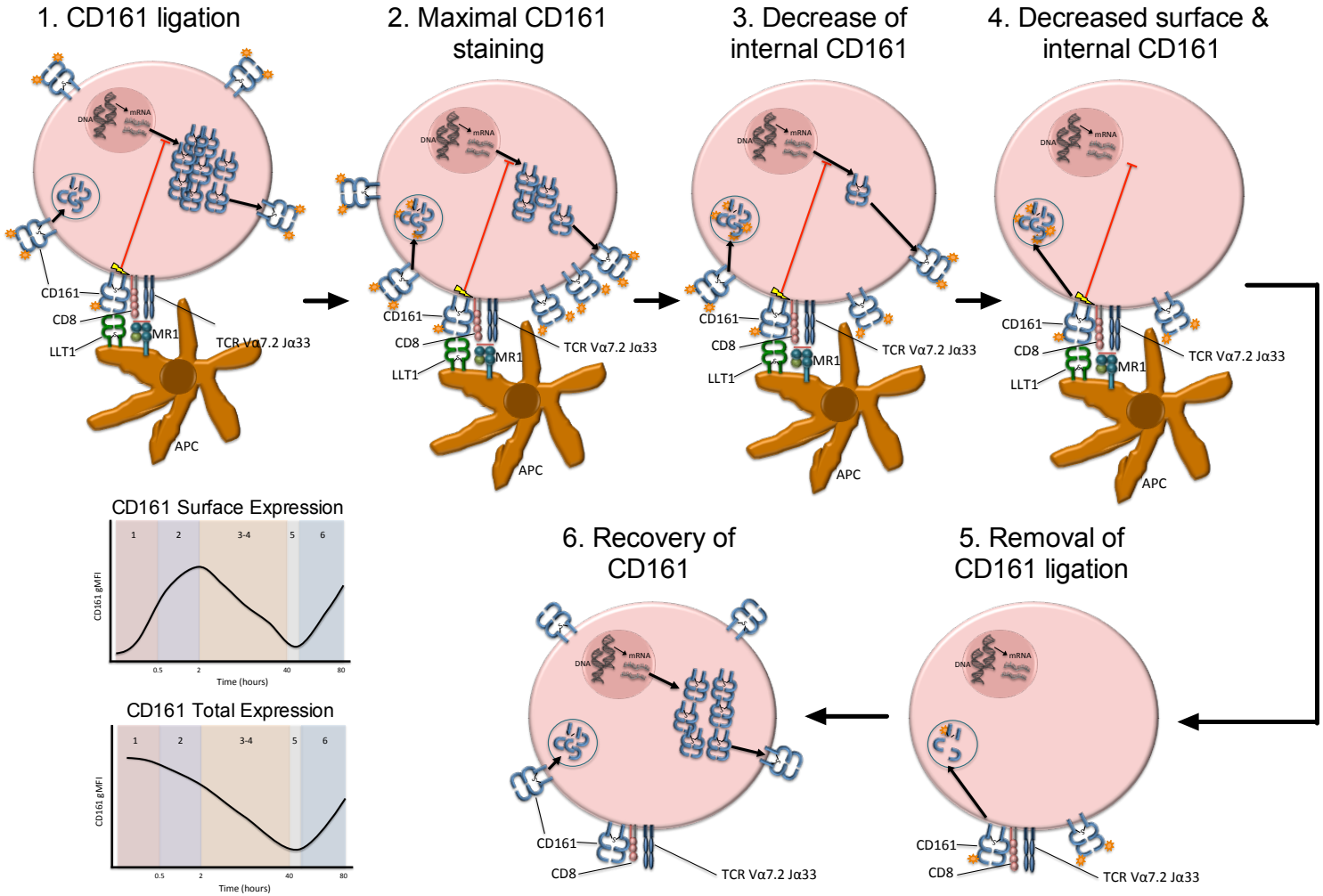

Model of CD161 downregulation based on ligation with αCD161 mAb (1918B) and LLT1

4.6 Summary

- CD161 is expressed on T cells and $CD8^+$ T cells have two positive populations while $CD4^+$ T cells have only one positive population.
- αCD161 mAb cross-linking induces a downregulation of CD161 expression.
- IL-18R and Vα7.2 are highly co-expressed on $CD8^+$ $CD161^{++}$ T cells and are good markers for tracking $CD161^{++}$ cells in functional experiments.
- The αCD161 mAb mediated downregulation of CD161 expression is time dependent.
- Different clones of αCD161 mAb induce different levels of CD161 downregulation.
- CD161 ligation with LLT1 induced downregulation of CD161 expression in a dose dependent manner.
- CD161 expression levels recovered over time from LLT1 induced down regulation when the LLT1 stimulus was removed.

- CD161 downregulation is not regulated at the mRNA level.

Chapter 5 Gene Microarray

5.1 Introduction

CD161 is a protein highly expressed on several cell types that are known for "bridging" the innate and adaptive immune system. Changes in the expression patterns of CD161 or locations of $CD161^+$ cells have been seen in specific disease states. Understanding how signaling through CD161 affects the function of cells may help elucidate the role $CD161^+$ cells play in disease pathogenesis.

In Chapter 4 the expression patterns of CD161 on T cells were examined. The expression of CD161 was found to be downregulated after the CD161 was ligated with its ligand LLT1 or with specific αCD161 mAbs. Alternate markers were also found that were also expressed on $CD161^+$ cells, allowing $CD161^+$ cells to be tracked even after downregulation of CD161. With this information, it is possible to study the effect CD161 ligation has on $CD161^+$ T cells.

Although many different approaches were available for looking at induction of functional effects of CD161 ligation, I chose to use a hypothesis-free approach examining mRNA expression by microarray. In this gene microarray mRNA from $CD161^+$ cells ligated with LLT1 were compared to mRNA from $CD161^+$ cells that were not ligated with LLT1.

5.2 Aims

- Design and carry out an appropriate gene microarray experiment to look for potential functional effects of CD161 ligation.
- Analyze gene microarray results and confirm significant findings with alternate experimental techniques.

5.3 Material and Methods

5.3.1 Type of Microarray

Many different types of microarray exist, but to look at the difference in gene expression after ligation of CD161, I chose to use a whole human genome oligo microarray. This type of microarray can be done with a one-color array or a two-color array.

In a one-color array, each mRNA sample is converted to cRNA then hybridized to a probe before running each sample on a separate microarray chip. The intensity results for each probe are compared with housekeeping genes or other internal controls and then statistically compared with results from other microarray chips.

In a two-color array, two samples from the same patient are used with each sample converted to cRNA and then hybridized to probes with different fluorophores before running both samples on the same microarray chip (Figure 5.1). The results from this type of chip come from computer analysis of both the color and the intensity of each probe (Figure 5.2).

Although a one-color array offers more flexibility in the way data is analyzed and the size of experiments, the two-color array allows more samples to be run on each chip, which reduces the cost. Under properly controlled conditions, the results of both types of arrays are equivalent (Patterson et al. 2006).

Figure 5.1

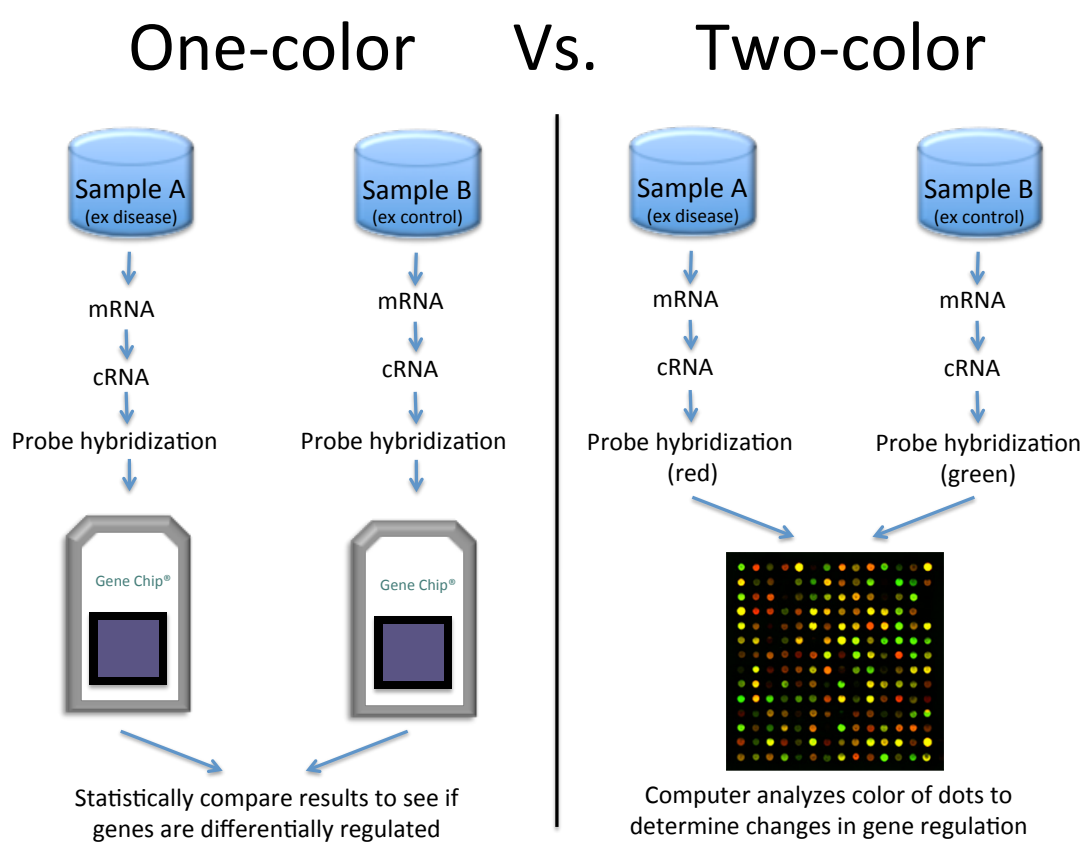

One-color Vs. Two-color Miroarrays
Schematic of the differences between one-color and two-color microarrays.
111012.pzf Lab meeting230113.pptx

Figure 5.2

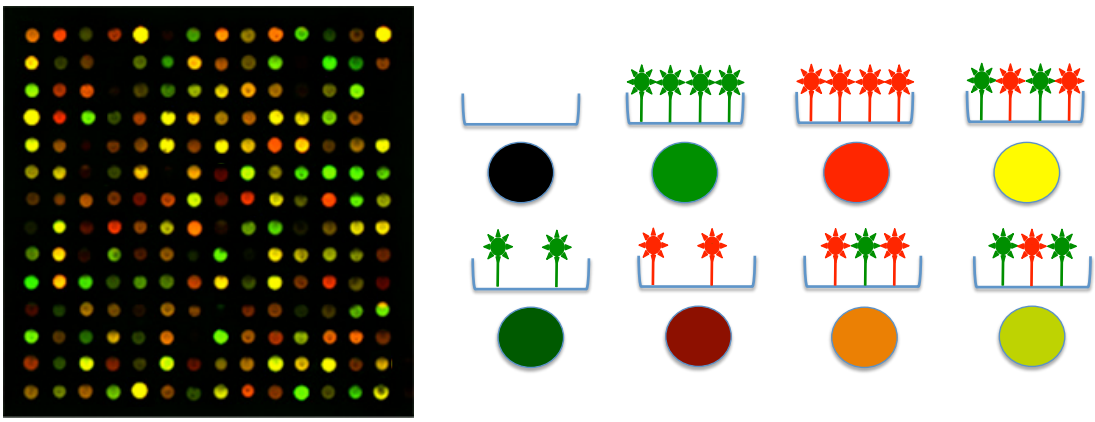

Color and intensity determination on Two-color microarrays
Schematic showing way color and intensity on two-color microarray chips are read.
111012.pzf Lab meeting 230113 Thesis.pptx

5.3.2 Gene Microarray Processing

Cells for each sample were snap frozen and sent to Miltenyi Biotec where mRNA was extracted from the cells, converted into cRNA, probe hybridized, and then run on Agilent Whole Human Genome Oligo Microarray (two-color) chips. Agilent Feature Extraction Software (FES) was used to read out the image files from the microarray chips. The FES also made calculations to subtract background, normalize the data, and reject outliers.

5.3.3 Gene microarray P-value calculations

Statistical confidences (p-values) were calculated by Rosetta Resolver® (Rosetta Biosoftware) using a ratio calculation including an error model as described by Weng *et al.* (Weng et al. 2006). The p-values stated were calculated with the formula:

$$\text{p-value} = 1 - \text{Erf}\left[\frac{\left(\text{Log(ratio)} / \text{Log (Error)} \right)}{\sqrt{2}} \right]$$

where Erf is the error function of a standard Gaussian distribution

5.4 Results

5.4.1 Experiment Design

This experiment was designed for analysis with a two-color microarray because this method allowed for the type of analysis needed between cells from the same patient and carried a lower cost than the same experiment using one-color microarray chips (see section 5.3.1 Type of Microarray on page 114).

Despite the fact that CD161 protein expression was downregulated, I was unable to show a change in CD161 expression at the mRNA level (See 4.4.16 on page 97). This hindered knowing what time frame of CD161 ligation was most appropriate for the gene microarray. I wanted to catch the early cascade of mRNA expression changes after CD161 ligation, and protein expression is downregulated within 30 minutes to 1 hour. Therefore, I chose to ligate CD161 for 2 hours and 5 hours.

Fresh PBMCs from four different donors were obtained and then selected for Vα7.2, using selection columns, to increase the percentage of $CD8^{+}$ $CD161^{++}$ T cells. The $V\alpha7.2^{+}$ cells were then co-incubated with either 300-Null or 300-LLT1 expressing cell lines for 2 or 5 hours. The cells were then sorted by flow cytometer for $CD3^{+}$ $CD8^{+}$ $V\alpha7.2^{+}$ cells. The cells were collected, a small sample was set aside for CD161 staining and the rest were flash frozen (Figure 5.3). The frozen cells were then sent to Miltenyi Biotec where the mRNA was extracted from the cells, converted into cRNA, probe hybridized, and then run on an Agilent Whole Human Genome Oligo Microarray (two-color).

Figure 5.3

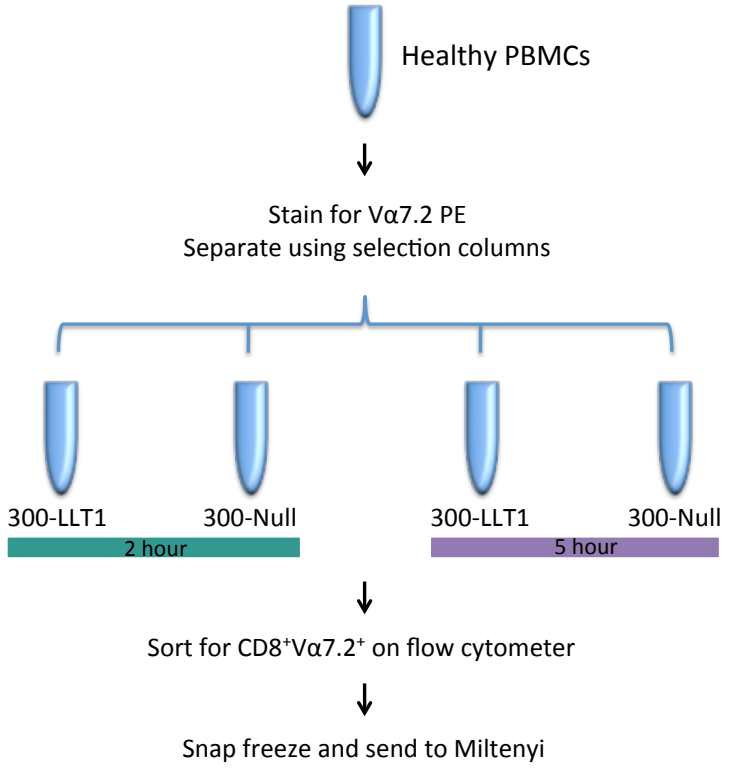

Schmatic of Experimental Design for Gene Microarray
The experimental design uses Healthy PBMCs from 4 donors that are stained for Vα7.2 using selection columns. The cells are then split into 4 groups and co-incubated with 300-LLT1 or 300-Null cells for either 2 hours or 5 hours. The cells were then sorted on CD3+ CD8+ Vα7.2+ cells by flow cytometer. Cells were then snap frozen and sent to Miltenyi Biotec.
111012.pzf Lab meeting 230113 Thesis.pptx

5.4.2 Microarray cells downregulated CD161 expression

Small samples from each final sorted sample were collected and then stained with CD161 before running on a flow cytometer. These samples confirmed that the expression levels of CD161 were significantly downregulated at both 2 hours ($p = 0.01$) and 5 hours ($p = 0.011$) (Figure 5.4). This indicated that significant ligation of CD161 occurred at both time points.

Figure 5.4

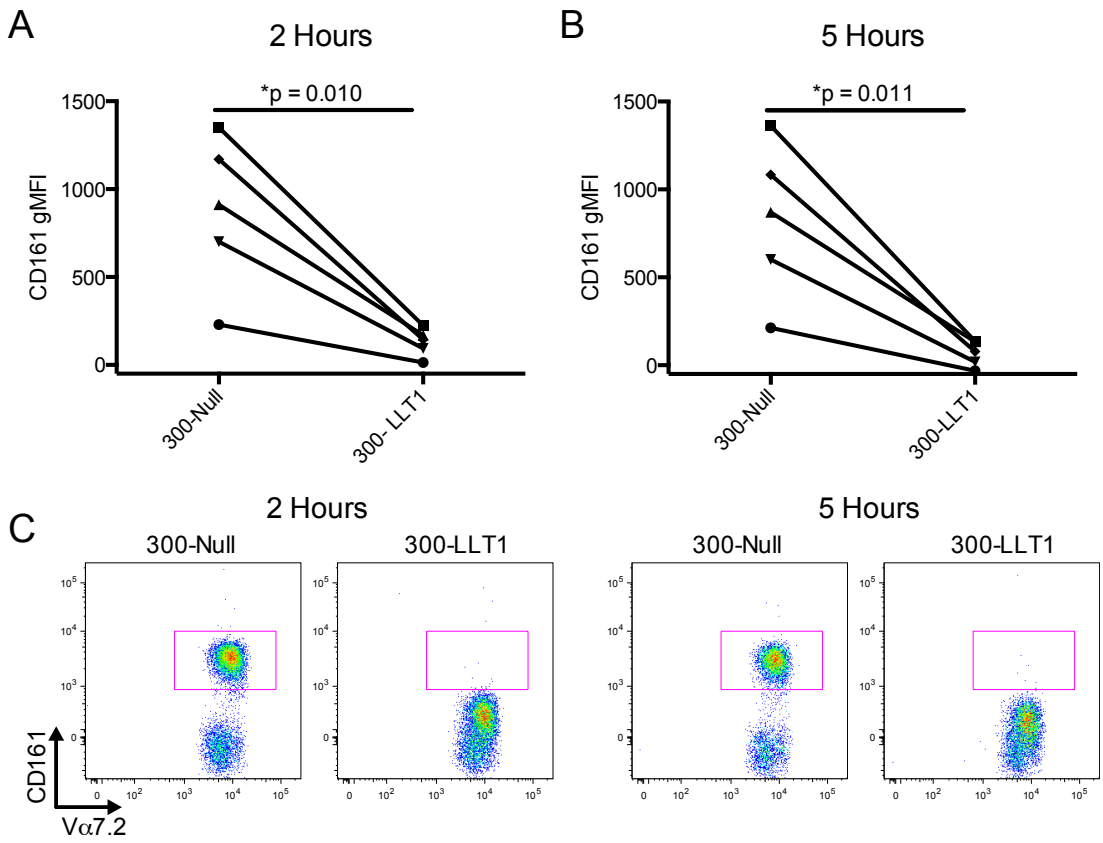

Downregulation of CD161 expression on cells used in gene microarray
Samples of cells used in gene microarray. **(A)** CD161 gMFI of $CD8^+$ $V\alpha7.2^+$ co-incubated with either 300-Null or 300-LLT1 cells for 2 hours and then surface and interally stained for CD161 and run on flow cytometer. Each line represents the paired results from a different healthy donor. Statistical analysis used: Paired T test **(B)** CD161 gMFI of $CD8^+$ $V\alpha7.2^+$ co-incubated with either 300-Null or 300-LLT1 cells for 5 hours and then stained for CD161 and run on flow cytometer. Each line represents the paired results from a different healthy donor. Statistical analysis used: Paired T test **(C)** Representative raw data from one donor used in A and B.
111012.pxf 111012.jo

5.4.3 Top Hit Gene lists

Miltenyi used Agilent Feature Extraction Software (FES) to read the intensities and ratios of the probes. The FES then subtracted background, normalized the data, and rejected outliers. The data was then processed by the Rosetta Resolver® software to create statistical confidences (p-values).

I wanted to compare the genes with the top p-values for all 4 of the donors tested. However, it is not accurate to directly compare p-values between gene chips

on the two-color arrays due to the p-value being a calculation of confidence based on the ratio between the two probes for that gene, the error calculated, and the error function of a standard Gaussian distribution (5.3.3 Gene microarray P-value calculations on page 116). A small p-value (<0.01) of this type indicates that the log-ratio is significantly larger than its error indicating it is differentially expressed (Weng et al. 2006). To indirectly compare the p-values of all four donors, the full list of probes for each donor was ranked from smallest p-value to largest p-value. Then the ranks for each probe were added for all four donors and then arranged from lowest to highest rank, which created a total rank order list. The top 30 ranked genes can be found in Table 5.1 for the 2 hour time point and Table 5.2 for the 5 hour time.

Of note in the top ranked genes, from both 2 hour and 5 hour time points, contain many histone genes that are upregulated. Unfortunately histones are modified post-translationally, which limits the information to be gathered from examining transcriptional regulation of these genes (Allfrey, Faulkner, and Mirsky 1964; Bannister and Kouzarides 2011). It is also worth noting that at the 5 hour time point, many heat shock related proteins are also significantly upregulated.

Table 5.1 Total Rank Order (Top 30) Microarray Gene List - 2 hour time point

Total Rank Order	Primary Sequence Name	Sequence Description	510 Fold Change	510 P-value	2006 Fold Change	2006 P-value	2069 Fold Change	2069 P-value	2076 Fold Change	2076 P-value
1	HIST2H4B	Homo sapiens histone cluster 2, H4b (HIST2H4B),	1.93	6.04E-09	2.91	3.32E-21	1.84	7.11E-08	3.06	4.26E-23
2	HIST1H2AB	Homo sapiens histone cluster 1, H2ab (HIST1H2AB)	3.06	5.12E-10	4.28	3.26E-13	2.26	1.17E-06	4.47	7.61E-14
3	TAT	Homo sapiens tyrosine aminotransferase (TAT), nuclear gene encoding mitochondrial protein, mRNA	-6.09	1.02E-07	-2.45	2.64E-07	-2.75	1.10E-11	-2.33	2.19E-13
4	HIST1H4I	Homo sapiens histone cluster 1, H4i (HIST1H4I),	1.79	2.66E-07	2.70	1.51E-18	1.71	1.89E-06	2.70	1.79E-18
5	HIST1H4H	Homo sapiens histone cluster 1, H4h (HIST1H4H),	2.25	4.08E-07	3.86	8.03E-13	2.31	2.14E-07	4.06	2.60E-13
6	MYB	Homo sapiens v-myb myeloblastosis viral oncogene homolog (avian) (MYB), transcript variant 2, mRNA	-1.99	1.11E-09	-1.76	5.23E-07	-1.91	9.74E-09	-1.83	9.95E-08
7	TET2	Homo sapiens tet methylcytosine dioxygenase 2 (TET2), transcript variant 2, mRNA [NM_017628]	2.38	1.78E-14	2.21	3.03E-12	2.38	1.63E-14	1.71	0.00004
8	ENSA	Homo sapiens endosulfine alpha (ENSA), transcript variant 8, mRNA [NM_207168]	1.83	9.90E-08	1.69	3.69E-06	2.79	1.37E-19	1.74	1.14E-06
9	PYCR1	Homo sapiens pyrroline-5-carboxylate reductase 1 (PYCR1), transcript variant 1, mRNA [NM_006907]	-2.60	4.94E-08	-3.13	1.43E-06	-2.44	7.18E-07	-4.74	2.21E-07
10	PDE2A	Homo sapiens phosphodiesterase 2A, cGMP-stimulated (PDE2A), transcript variant 1, mRNA	2.31	1.54E-13	2.62	1.72E-17	1.55	0.00011	2.82	5.48E-20
11	HIST1H2AH	Homo sapiens histone cluster 1, H2ah (HIST1H2AH), mRNA [NM_080596]	2.05	4.17E-06	3.51	6.08E-12	2.01	7.33E-06	4.13	1.76E-13
12	NR4A2	Homo sapiens nuclear receptor subfamily 4, group A, member 2 (NR4A2), mRNA [NM_006186]	2.71	1.34E-18	1.82	1.28E-07	1.95	3.43E-09	1.56	0.00009
13	PHLDB3	Homo sapiens cDNA FLJ40193 fis, clone TESTI2019430. [AK097512]	2.10	3.98E-06	2.33	4.29E-06	2.14	3.62E-06	2.31	6.62E-07
14	MAGEE1	Homo sapiens melanoma antigen family E, 1 (MAGEE1), mRNA [NM_020932]	-2.05	2.20E-10	-2.14	1.62E-11	-1.56	0.0001	-1.68	4.51E-06
15	HIST1H2BJ	Homo sapiens histone cluster 1, H2bj (HIST1H2BJ),	1.65	0.00001	1.67	0.00005	2.06	1.64E-10	1.73	1.14E-06
16	CD69	Homo sapiens CD69 molecule (CD69), transcript variant 1, mRNA [NM_001781]	1.95	3.42E-09	1.71	2.20E-06	1.55	0.0001	1.70	2.97E-06

17	MMD	Homo sapiens monocyte to macrophage differentiation-associated (MMD), mRNA	2.98	9.44E-10	1.87	0.00006	1.93	0.00003	1.99	0.00002
18	HIST1H4L	Homo sapiens histone cluster 1, H4l (HIST1H4L),	2.94	8.21E-09	11.10	1.24E-17	1.93	0.00055	8.73	2.73E-17
19	HIST1H2AJ	Homo sapiens histone cluster 1, H2aj (HIST1H2AJ),	2.00	7.80E-06	2.55	1.47E-08	1.76	0.00017	3.09	1.28E-10
20	HIST1H2AK	Homo sapiens histone cluster 1, H2ak (HIST1H2AK),	1.80	0.0001	2.56	1.39E-08	1.83	0.00007	2.92	4.82E-10
21	RNU2-2	Homo sapiens RNA, U2 small nuclear 2 (RNU2-2), small nuclear RNA [NR_002761]	1.52	0.00022	1.57	0.00006	1.96	2.48E-09	1.91	9.97E-09
22	ZNF331	zinc finger protein 331	2.05	8.36E-06	1.81	0.00012	2.28	3.59E-07	1.88	0.00005
23	CTH	Homo sapiens cystathionase (cystathionine gamma-lyase) (CTH), transcript variant 1, mRNA	1.86	3.75E-08	1.90	1.48E-08	1.60	0.00004	1.50	0.00033
24		lincRNA:chr12:105956302-105956716 forward strand	-2.24	0.0002	-2.90	3.27E-06	-2.65	0.00001	-2.90	1.60E-06
25	ZNF331	Homo sapiens zinc finger protein 331 (ZNF331), transcript variant 1, mRNA [NM_018555]	2.16	1.19E-06	1.98	0.00001	2.16	1.10E-06	1.66	0.00066
26	SIGMAR1	Homo sapiens sigma non-opioid intracellular receptor 1 (SIGMAR1), transcript variant 1, mRNA	-1.65	9.16E-06	-1.57	0.00008	-1.69	3.93E-06	-1.53	0.00016
27	WDR77	Homo sapiens WD repeat domain 77 (WDR77),	-1.59	0.00004	-1.55	0.00011	-1.89	1.77E-08	-1.54	0.00015
28	SLAMF6	Homo sapiens SLAM family member 6 (SLAMF6), transcript variant 2, mRNA [NM_052931]	-7.64	2.21E-20	-5.02	0.00004	-2.08	1.08E-10	-3.21	0.0015
29	MAN1B1	mannosidase, alpha, class 1B, member 1	2.91	1.02E-08	1.81	0.00066	2.35	5.55E-07	1.97	0.0001
30	LMTK2	Homo sapiens lemur tyrosine kinase 2 (LMTK2),	1.86	4.35E-08	1.50	0.00034	1.93	6.42E-09	1.81	0.00039

Table 5.2 Total Rank Order (Top 30) Microarray Gene List - 5 hour time point

Total Rank Order	Primary Sequence Name	Sequence Description	510 Fold Change	510 P-value	2006 Fold Change	2006 P-value	2069 Fold Change	2069 P-value	2076 Fold Change	2076 P-value
1	HSPA1B	Homo sapiens heat shock 70kDa protein 1B (HSPA1B), mRNA [NM_005346]	4.01	1.15E-34	3.26	1.76E-25	5.82	0	2.27	4.03E-13
2	ADM	Homo sapiens adrenomedullin (ADM), mRNA [NM_001124]	3.94	4.33E-19	2.38	1.71E-14	2.19	3.95E-12	2.67	3.61E-18
3	HSPA6	Homo sapiens heat shock 70kDa protein 6 (HSP70B') (HSPA6), mRNA [NM_002155]	3.25	2.03E-25	2.16	1.13E-11	4.02	1.00E-34	2.07	1.16E-10
4	HSPA1A	Homo sapiens heat shock 70kDa protein 1A (HSPA1A), mRNA [NM_005345]	3.99	2.40E-34	2.82	5.07E-20	4.10	9.59E-36	1.83	1.05E-07
5	HIST2H2BF	Homo sapiens histone cluster 2, H2bf (HIST2H2BF), transcript variant 1, mRNA [NM_001024599]	4.32	1.95E-11	5.78	3.95E-14	10.07	5.37E-16	2.75	2.76E-09
6	HIST2H2AA4	Homo sapiens histone cluster 2, H2aa4 (HIST2H2AA4), mRNA [NM_001040874]	1.97	2.15E-09	2.51	3.80E-16	3.84	1.47E-32	1.98	1.42E-09
7	RASD1	Homo sapiens RAS, dexamethasone-induced 1 (RASD1), transcript variant 1, mRNA [NM_016084]	3.34	4.19E-09	4.40	8.96E-14	4.20	2.94E-14	1.96	2.39E-09
8	DNAJB1	Homo sapiens DnaJ (Hsp40) homolog, subfamily B, member 1 (DNAJB1), mRNA [NM_006145]	2.39	1.49E-14	2.08	1.05E-10	2.48	1.09E-15	1.69	3.42E-06
9	DUSP1	Homo sapiens dual specificity phosphatase 1 (DUSP1), mRNA [NM_004417]	2.78	1.44E-19	1.81	1.69E-07	2.31	1.50E-13	1.67	5.37E-06
10	IFNG	Homo sapiens interferon, gamma (IFNG), mRNA [NM_000619]	2.36	3.09E-14	1.72	1.85E-06	2.87	1.28E-08	1.88	2.57E-08
11	RN18S1	Homo sapiens RNA, 18S ribosomal 1 (RN18S1), ribosomal RNA [NR_003286]	2.32	1.83E-07	-2.99	2.86E-10	-2.48	3.10E-08	2.66	5.28E-09
12	HIST1H2BG	Homo sapiens histone cluster 1, H2bg (HIST1H2BG), mRNA [NM_003518]	1.69	3.11E-06	2.16	1.05E-11	1.95	3.77E-09	1.89	2.10E-08
13		Unknown	2.25	3.94E-07	-2.94	4.23E-10	-2.05	4.32E-06	2.47	3.49E-08
14	HSPA8	heat shock 70kDa protein 8 [Source:HGNC Symbol;Acc:5241] [ENST00000532091]	2.26	1.48E-06	3.02	1.69E-09	2.49	1.08E-06	2.39	1.54E-07
15	MAGEE1	Homo sapiens melanoma antigen family E, 1 (MAGEE1), mRNA [NM_020932]	-1.93	6.95E-09	-1.58	0.00005	-1.78	3.81E-07	-1.87	2.97E-08

16	HIST3H2BB	Homo sapiens histone cluster 3, H2bb (HIST3H2BB), mRNA [NM_175055]	1.89	0.00006	2.02	5.34E-08	2.06	1.53E-10	2.11	3.83E-11
17	AKR7A2	Homo sapiens aldo-keto reductase family 7, member A2 (aflatoxin aldehyde reductase) (AKR7A2), mRNA [NM_003689]	-2.03	3.89E-10	-1.54	0.00015	-1.90	1.49E-08	-1.61	0.00003
18	DFNB31	deafness, autosomal recessive 31 [Source:HGNC Symbol;Acc:16361] [ENST00000374057]	2.46	1.80E-07	2.18	9.88E-07	2.24	1.27E-06	1.77	0.00016
19	SNORD3B-1	Homo sapiens small nucleolar RNA, C/D box 3B-1 (SNORD3B-1), small nucleolar RNA [NR_003271]	1.95	0.00001	2.32	1.70E-07	2.02	5.80E-06	2.36	1.18E-07
20	DOCK9	Homo sapiens dedicator of cytokinesis 9 (DOCK9), transcript variant 4, mRNA [NM_001130050]	1.92	7.97E-09	1.61	0.00002	2.04	2.96E-10	1.46	0.0008
21	HSPA6	Homo sapiens heat shock 70kDa protein 6 (HSP70B') (HSPA6), mRNA [NM_002155]	2.71	2.22E-08	2.07	7.04E-06	2.49	0.00009	2.25	9.81E-07
22		histone cluster 2, H2aa3 [Source:HGNC Symbol;Acc:4736] [ENST00000369161]	2.04	4.81E-06	1.86	0.00005	3.50	6.47E-12	1.79	0.00011
23	CXCL16	Homo sapiens chemokine (C-X-C motif) ligand 16 (CXCL16), transcript variant 2, mRNA [NM_001100812]	1.58	0.00006	2.69	2.34E-18	1.67	6.10E-06	1.87	2.09E-06
24	HMOX1	Homo sapiens heme oxygenase (decycling) 1 (HMOX1), mRNA [NM_002133]	-1.60	0.00003	-2.50	6.08E-16	-1.60	0.00004	-1.88	5.84E-07
25	HIST1H2BJ	Homo sapiens histone cluster 1, H2bj (HIST1H2BJ), mRNA [NM_021058]	1.69	3.55E-06	1.63	0.00002	1.62	0.00002	1.73	1.14E-06
26	EZH2	Homo sapiens enhancer of zeste homolog 2 (Drosophila) (EZH2), transcript variant 1, mRNA [NM_004456]	2.21	2.62E-12	1.74	9.25E-07	1.72	1.73E-06	1.43	0.00153
27	HIST1H2AB	Homo sapiens histone cluster 1, H2ab (HIST1H2AB), mRNA [NM_003513]	3.27	1.08E-10	1.72	0.00064	2.16	5.31E-06	2.71	5.78E-09
28	CAPZA1	Homo sapiens capping protein (actin filament) muscle Z-line, alpha 1 (CAPZA1), mRNA [NM_006135]	1.65	8.49E-06	1.62	0.00002	1.86	3.86E-08	1.49	0.00043
29	SPTBN1	Homo sapiens spectrin, beta, non-erythrocytic 1 (SPTBN1), transcript variant 2, mRNA [NM_178313]	1.83	8.88E-08	2.02	4.79E-10	2.08	1.04E-10	1.39	0.00411
30	ENOX2	Homo sapiens ecto-NOX disulfide-thiol exchanger 2 (ENOX2), transcript variant 2, mRNA [NM_182314]	-1.77	1.88E-06	-1.85	8.50E-07	-1.66	7.99E-06	-1.44	0.00117

5.4.4 Ingenuity Pathway Analysis

The microarray was performed with the hope of finding pathways of genes that might give an indication of the functional effects caused by CD161 ligation on T cells. Therefore, I used the software program Ingenuity Pathway Analysis (IPA) to help map out pathways of genes found the up or downregulated. Based on the imputed genes and parameters, IPA produced lists of top canonical pathways such as the one in Figure 5.5. It also gave a list of the genes that were found differentially regulated in these pathways (Table 5.3).

However, as in the Aldosterone Signaling in Epithelial Cells Pathway (Figure 5.5, Table 5.3), even the top pathways produced by IPA contained only a handful of genes identified in the array. When shown in a schematic of the pathway (Figure 5.6), the genes were unconnected or found only in the periphery of the pathway. This pattern was found for both 2 and 5 hour time points and did not change significantly even when using less stringent cutoffs in p-values or fold change.

Figure 5.5

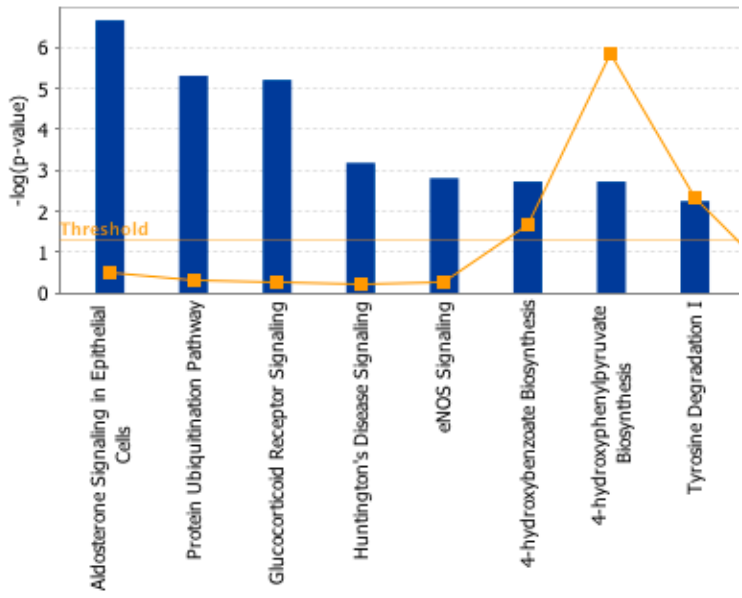

Ingenuity Top Cononical Pathways graph
Graph showing the top cononical pathways determined for the up and downregulation of genes from the gene mircroarray at the 5 hour time point.

Table 5.3

Ingenuity Canonical Pathways	-log(p-value)	Ratio	Molecules
Aldosterone Signaling in Epithelial Cells	6.65E00	4.17E-02	HSPA8,HSPA1A/HSPA1B,DUSP1,HSPE1,HSPA6,DNAJB1
Protein Ubiquitination Pathway	5.3E00	2.44E-02	HSPA8,IFNG,HSPA1A/HSPA1B,HSPE1,HSPA6,DNAJB1
Glucocorticoid Receptor Signaling	5.2E00	2.32E-02	HSPA8,IFNG,HSPA1A/HSPA1B,DUSP1,HSPA6,TAT
Huntington's Disease Signaling	3.17E00	1.83E-02	HSPA8,HSPA1A/HSPA1B,HSPA6,DNAJB1
eNOS Signaling	2.8E00	2.26E-02	HSPA8,HSPA1A/HSPA1B,HSPA6
4-hydroxybenzoate Biosynthesis	2.72E00	1.43E-01	TAT
4-hydroxyphenylpyruvate Biosynthesis	2.72E00	5E-01	TAT
Tyrosine Degradation I	2.24E00	2E-01	TAT

Ingenuity Cononical Pathway list of molecules and values
List of pathways and molecules from the top cononical pathways determined for the up and downregulation of genes from the gene mircroarray at the 5 hour time point.

Figure 5.6

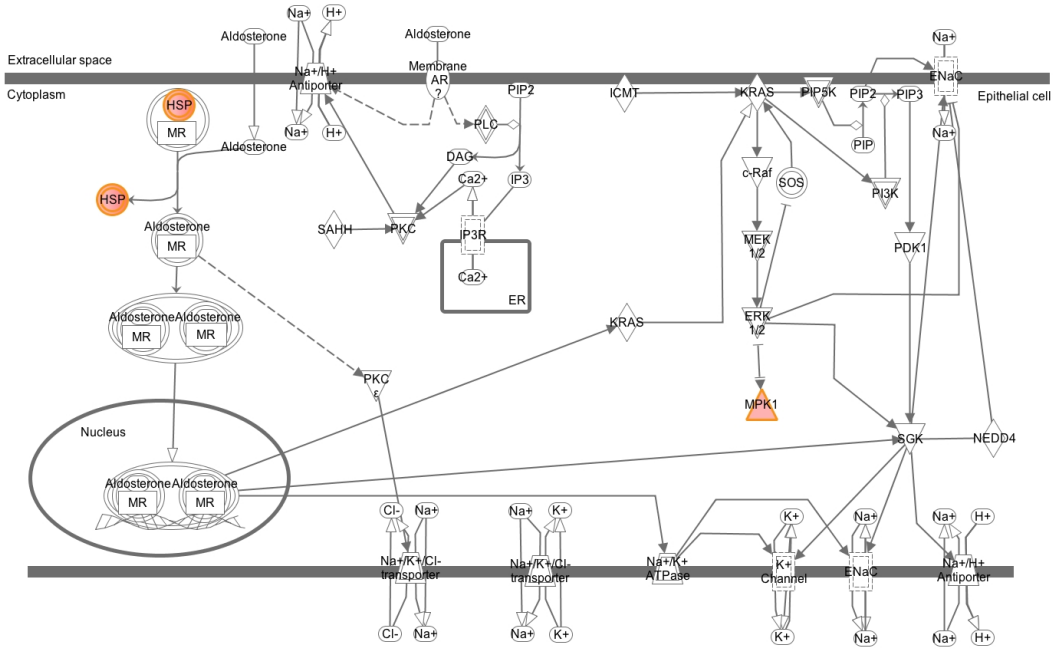

Schematic of Aldosterone Signaling in Epithelial Cells Pathway
Schematic of Aldosterone Signaling in Epithelial Cells Pathway. Proteins with downregulated genes from microarray in red outlined in orange. Proteins in grey are not up or downregulated in microarray but are part of the pathway. Figure produced by IPA.

5.4.5 Gene confirmation with Real-Time qPCR

From the lists of top ranked p-values at both 2 and 5 hours along with the pathway results from IPA, a list of genes was chosen for confirmation by real-time qPCR. The Universal ProbeLibray Assay Design Center by Roche was used to design appropriate primers for each gene that incorporated an appropriate probe (Table 5.4). The primers were then run through primer-BLAST (basic local alignment search tool) to confirm binding of the appropriate gene. Real time qPCR for the genes listed in Table 5.4 was then performed on cDNA extracted from cells that had been incubated with either 300-LLT1 or 300-Null cells for 5 hours. HPRT was used as a housekeeping gene and CD161 was used as a negative control.

Table 5.4

Name	Accession No.	Probe	F/R	Sequence
SLAMF6	NM_052931	5	For	aaggtctcaagcaccagtcttc
			Rev	ggggttaagctgctttgtga
HIST2H2BF	NM_001024599	65	For	tacaggtccttctccacagga
			Rev	tggaaccaagacagggttctt
HIST1H2AB	NM_003513	74	For	taaactcttggggcgtgtg
			Rev	gccttatgatggctctcagttt
HSPA1B	NM_005346	87	For	aagggtgtttcgttcccttt
			Rev	tagtgttttcgccaagcaaa
IFNy	NM_000619	21	For	ggcattttgaagaattggaaag
			Rev	tttggatgctctggtcatctt
DNAJB1	NM_006145	57	For	ggcctacgacgtgctcag
			Rev	gtgtagctgaaagaggtaccattg
HMOX1	NM_002133	15	For	ggcagagggtgatagaagagg
			Rev	agctcctgcaactcctcaaa
HSPA8	based off ENST	78	For	caactggcttgataagaatcagact
			Rev	cttggtgatgatggggttg
CXCL16	NM_00110812	55	For	ttcctatgtgctgtgcaagag
			Rev	caggtatataatgaaccggcaga
ADM	NM_001124	57	For	gcctgcccagacccttat
			Rev	gtagcgcttgactcggatg
CD161	NM_002258.2	15	For	aaatgcagtgtggacattcaa
			Rev	ctcggagttgctgccaata
RORC	NM_005060	69	For	cagcgctccaacatcttc
			Rev	ccacatctcccacatgga
HPRT	NM_000194.2	73	For	tgaccttgatttattttgcatacc
			Rev	cgagcaagacgttcagtcct

Primer sequences and probe numbers for Real-Time qPCR
Primers designed using Universal ProbeLibrary Assay Design Center by Roche
qPCR primers to order.xlsx

Unexpectedly, the results of the real-time qPCR experiments did not confirm the significant changes in expression seen in the gene microarray for any of the 11 non-control genes tested (Figure 5.7). This was seen despite the fact that the cells used in the real-time qPCR experiments did downregulate CD161, in a similar way to the downregulation seen in the gene microarray experiment (Figure 5.8). The real-time qPCR amplification curve traces showed good quality amplification curves (Figure 5.9) and the triplicates used in the experiment showed good reproducibility (Table 5.5).

Cells used for this the real-time qPCR experiments were treated the same way as cells in the gene microarray experiment with the exception of being re-selected by column instead of being sorted by flow cytometer. Some of the same donors used in the microarray experiment were also used in the Real-Time qPCR experiments.

Figure 5.7

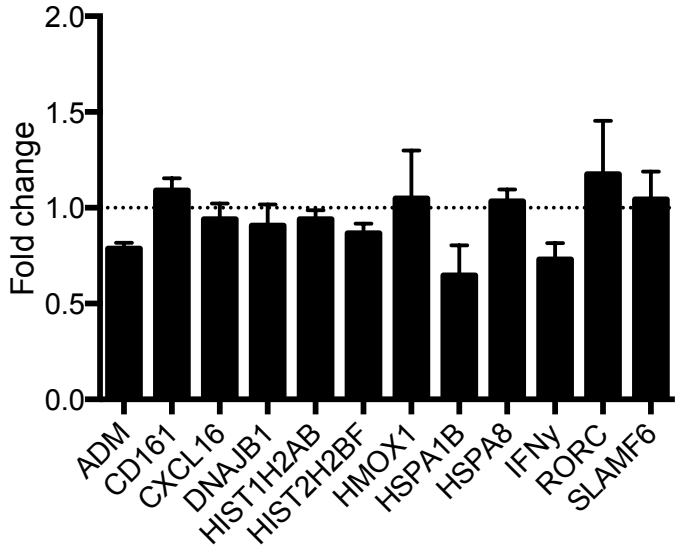

Fold change seen with Real-Time qPCR of genes significant in microarray analysis
$CD8^+$ $V\alpha7.2^+$ T cells were incubated with 300-LLT1 compared to 300-Null for 5 hours and then reselected with columns. mRNA was then extracted and real-time qPCR was performed on a selection of genes found as significant in gene microarray. (n=3) See Table 5.5 for the calculation of these values.
Microarray Confirm 5hr fresh.pzf

Figure 5.8

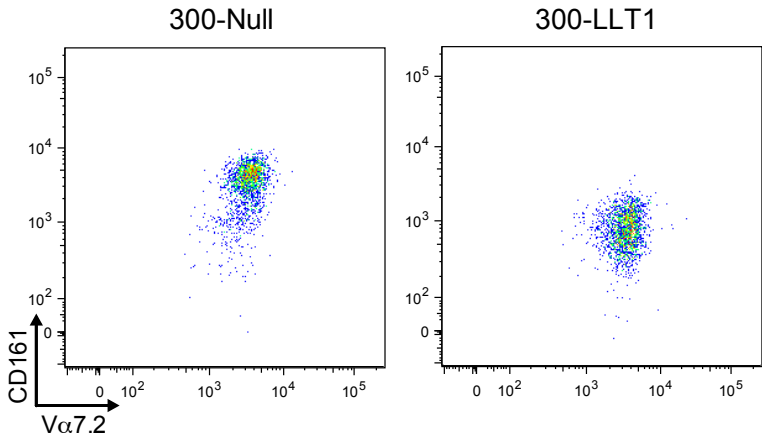

Downregulation of CD161 expression on cells used for Real-Time qPCR confirmation of microarray
Representative raw data of surface and internal stain of sample for one set of $CD8^+$ $V\alpha7.2^+$ T cells that were incubated with 300-LLT1 compared to 300-Null for 5 hours and then reselected with columns and used in Real-Time qPCR confirmation experiments.
050213.jo figures2.pzfx

Figure 5.9

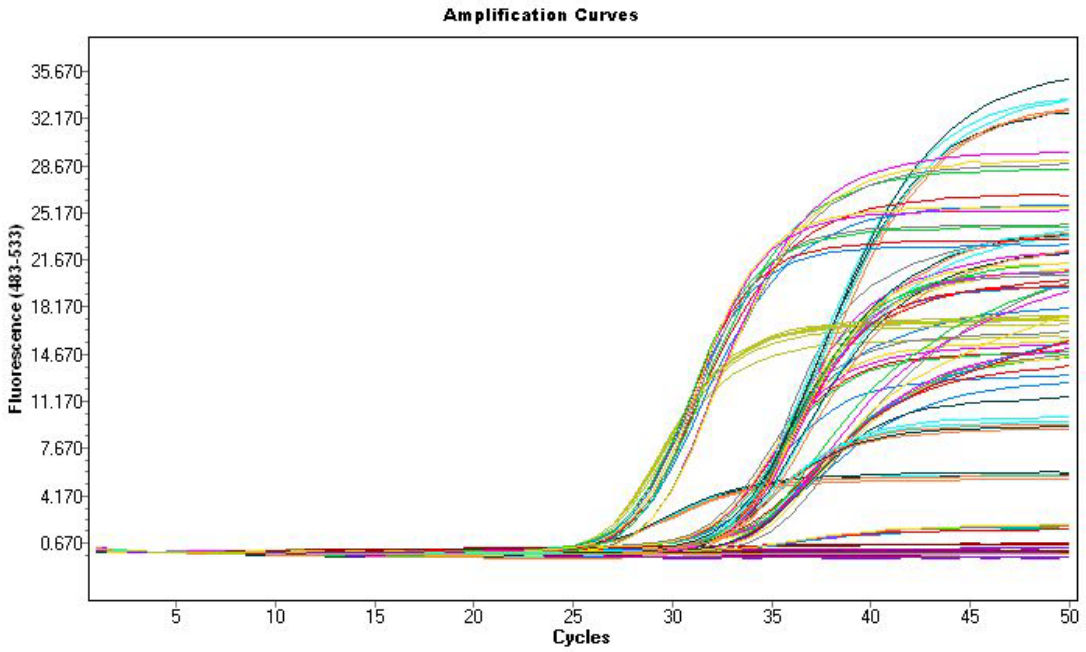

Real Time qPCR Amplification Curves
Amplification curves from Real Time qPCR of all genes listed in Table 5.4 for one donor.
Microarray Confirm 5hr fresh qPCR 2006_B.PDF

Table 5.5 Real Time qPCR fold change calculations

Primers	Stimu-lation	CT	Avg CT	Δ CT (GOI-HK)	ΔΔ CT (LLT1-Null)	2-ΔΔ CT (Fold change)
HPRT (HK)	Null	32.55	32.64 ± 0.08			
HPRT (HK)	Null	32.69				
HPRT (HK)	Null	32.68				
HPRT (HK)	LLT1	32.98	32.89 ± 0.12			
HPRT (HK)	LLT1	32.75				
HPRT (HK)	LLT1	32.93				
ADM	Null	32.85	32.84 ± 0.15	0.20 ± 0.17	0.32 ± 0.28	0.80 (0.66-0.97)
ADM	Null	32.69				
ADM	Null	32.99				
ADM	LLT1	33.46	33.41 ± 0.19	0.52 ± 0.22		
ADM	LLT1	33.20				
ADM	LLT1	33.56				
CD161	Null	26.30	26.30 ± 0.01	-6.34 ± 0.08	-0.28 ± 0.15	1.21 (1.09-1.34)
CD161	Null	26.30				
CD161	Null	26.29				
CD161	LLT1	26.29	26.27 ± 0.03	-6.62 ± 0.13		
CD161	LLT1	26.28				
CD161	LLT1	26.23				
CXCL16	Null	33.30	33.38 ± 0.09	0.74 ± 0.12	-0.01 ± 0.19	1.00 (0.88-1.15)
CXCL16	Null	33.36				
CXCL16	Null	33.47				
CXCL16	LLT1	33.58	33.62 ± 0.10	0.73 ± 0.15		
CXCL16	LLT1	33.55				
CXCL16	LLT1	33.73				
DNAJB1	Null	27.59	27.56 ± 0.03	-5.08 ± 0.08	0.12 ± 0.15	0.92 (0.83-1.02)
DNAJB1	Null	27.53				
DNAJB1	Null	27.55				
DNAJB1	LLT1	27.91	27.92 ± 0.02	-4.97 ± 0.12		
DNAJB1	LLT1	27.94				
DNAJB1	LLT1	27.91				
HIST1H2AB	Null	32.78	32.57 ± 0.22	-0.07 ± 0.23	-0.05 ± 0.27	1.03 (0.86-1.25)
HIST1H2AB	Null	32.34				
HIST1H2AB	Null	32.59				
HIST1H2AB	LLT1	32.76	32.77 ± 0.07	-0.12 ± 0.14		
HIST1H2AB	LLT1	32.71				
HIST1H2AB	LLT1	32.84				
HIST2H2BF	Null	33.57	33.46 ± 0.19	0.82 ± 0.20	0.20 ± 0.27	0.87 (0.72-1.05)
HIST2H2BF	Null	33.24				
HIST2H2BF	Null	33.56				
HIST2H2BF	LLT1	33.77	33.90 ± 0.14	1.01 ± 0.18		
HIST2H2BF	LLT1	33.89				
HIST2H2BF	LLT1	34.04				
HMOX1	Null	32.65	32.74 ± 0.08	0.10 ± 0.11	-0.04 ± 0.23	1.03 (0.88-1.21)
HMOX1	Null	32.80				
HMOX1	Null	32.77				
HMOX1	LLT1	33.05	32.94 ± 0.17	0.06 ± 0.21		
HMOX1	LLT1	32.75				
HMOX1	LLT1	33.03				
HSPA1B	Null	27.96	27.94 ± 0.11	-4.70 ± 0.13	0.59 ± 0.18	0.66 (0.59-0.75)
HSPA1B	Null	27.83				
HSPA1B	Null	28.04				
HSPA1B	LLT1	28.80	28.78 ± 0.03	-4.11 ± 0.13		
HSPA1B	LLT1	28.74				
HSPA1B	LLT1	28.80				

Primers	Stimu-lation	CT	Avg CT	Δ CT (GOI-HK)	ΔΔ CT (LLT1-Null)	2-ΔΔ CT (Fold change)
HSPA8	Null	26.45	26.46 ± 0.03	-6.18 ± 0.08	-0.14 ± 0.15	1.10 (0.99-1.23)
HSPA8	Null	26.44				
HSPA8	Null	26.50				
HSPA8	LLT1	26.61	26.57 ± 0.05	-6.32 ± 0.13		
HSPA8	LLT1	26.52				
HSPA8	LLT1	26.58				
IFNy	Null	33.34	33.50 ± 0.17	0.86 ± 0.18	0.51 ± 0.47	0.70 (0.51-0.97)
IFNy	Null	33.50				
IFNy	Null	33.67				
IFNy	LLT1	33.98	34.26 ± 0.42	1.37 ± 0.43		
IFNy	LLT1	34.74				
IFNy	LLT1	34.06				
RORC	Null	31.86	32.34 ± 0.97	-0.30 ± 0.97	-0.79 ± 0.98	1.73 (0.87-3.42)
RORC	Null	33.45				
RORC	Null	31.70				
RORC	LLT1	31.92	31.79 ± 0.11	-1.09 ± 0.16		
RORC	LLT1	31.72				
RORC	LLT1	31.74				
SLAMF6	Null	31.83	31.80 ± 0.07	-0.84 ± 0.10	-0.34 ± 0.17	1.26 (1.12-1.42)
SLAMF6	Null	31.72				
SLAMF6	Null	31.84				
SLAMF6	LLT1	31.75	31.71 ± 0.06	-1.18 ± 0.13		
SLAMF6	LLT1	31.64				
SLAMF6	LLT1	31.73				
HPRT (HK)	NC	0.00				
ADM	NC	0.00				
ADM	NC	0.00				
CD161	NC	0.00				
CD161	NC	0.00				
CXCL16	NC	0.00				
DNAJB1	NC	0.00				
HIST1H2AB	NC	0.00				
HIST2H2BF	NC	0.00				
HMOX1	NC	0.00				
HSPA1B	NC	0.00				
HSPA8	NC	0.00				
HSPA8	NC	0.00				
IFNy	NC	0.00				
RORC	NC	0.00				
SLAMF6	NC	0.00				

Real Time qPCR fold change calculations
Representative raw data and calculations of fold change of genes with real-time qPCR for one donor. Calculations are based on Livak et al. 2001.
Microarray confirm 5hr fresh qpcr 2006_B analysis.xlsx

5.4.6 Low Intensity Microarray Probe Signals

In an attempt to understand why the genes the microarray showed as significantly changed did not show significant change when tested by real-time qPCR, I looked at the microarray data closer. The log10 intensity scatterplots showed most

of the probes with a p-value of <0.01 to be at the lower intensities (Figure 5.10). It was noted that at very low intensity levels p-values of <0.01 are seen by many genes which are unchanged.

Figure 5.10

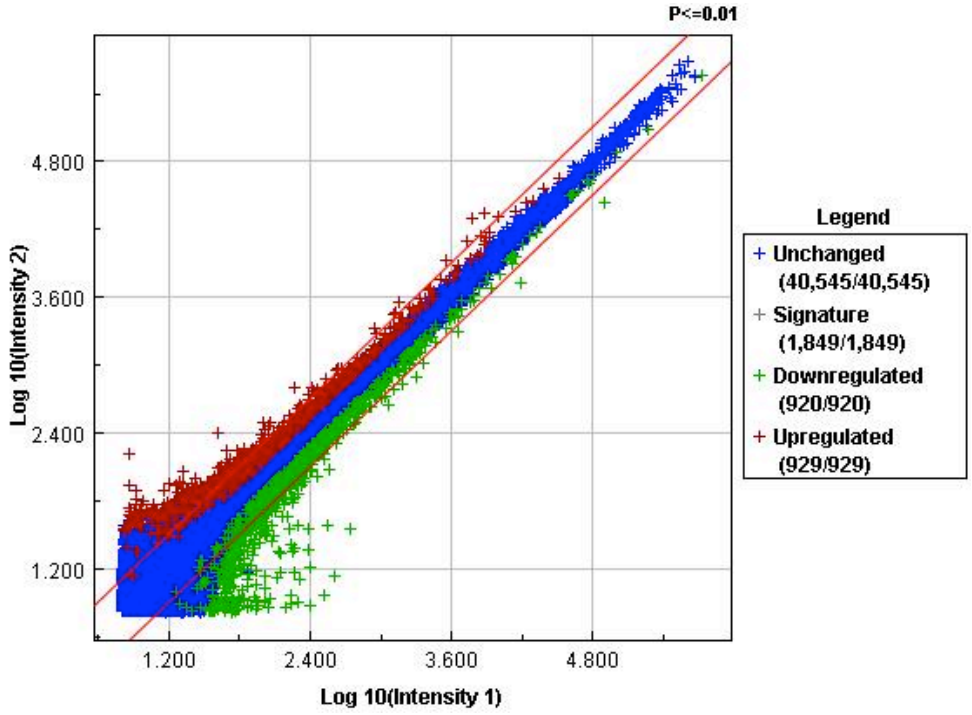

Log10 Intensity scatter plots
Representative scatterplot of the intensities of all genes tested in one donor at the 5 hour time point produced in Rosetta Biosoftware. Points in the space between the red lines indicates a p-value of greater than 0.01. For scatterplots of each individual donor see Appendix 3 on page 216. Figures.pzfx

I then went back to the intensity values of the probes for the genes tested by real-time qPCR and plotted these values. Many of the genes were represented by more than one probe. Most of the genes had at least one probe with very low intensities. Several of the probes showed intensities as low as 10 where the housekeeping gene HPRT was around 500-600 (Figure 5.1, Appendix 4 on page 217).

Figure 5.11

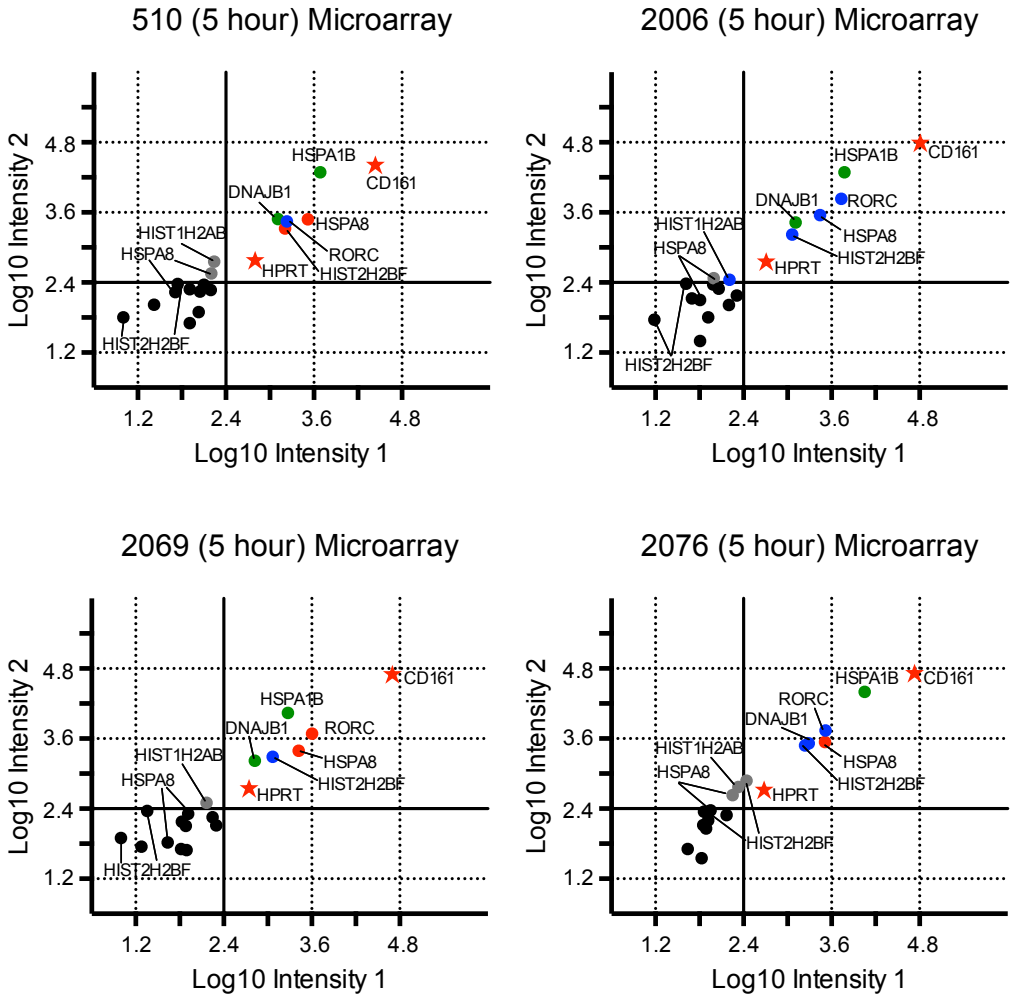

Log 10 intensity scatterplots of probes for the microarray genes tested by real-time qPCR
Log 10 intensity scatterplots for each donor at the 5 hour time point with each probe found for the genes tested by real-time qPCR. Control genes shown by stars, issues with quality of probe results shown by colors: p-value > 0.01 (red), < ±2 fold change (blue), p-value < 0.01 & > ±2 fold change (green), slighly low intensity for at least one fluorophore (grey), poor intensity (black). For values of each probe see (Asyali et al. 2004) on page (Asyali et al. 2004).
qPCR genes 1.pzf

A study by Asyali *et al*. showed that the ratio between fluorophores, which the p-value is based on, was unreliable when the fluorophore intensities were very low (Asyali et al. 2004). Based on this study along with looking at the intensity levels of different genes and the log10 intensity scatterplots of the entire gene sets, I chose the log10 intensity of 2.4 (~250) as a lower limit for the intensity of genes I wanted to examine.

I then re-evaluated the 5 hour time point data for all donors including the criteria of: p-value <0.01, > ±2 fold change, and intensity levels of both fluorophores > 250. Filtering with these criteria, only 7 sequences were positive in 3 or 4 of the donors (Table 5.6). Out of these sequences, one corresponds to an unknown gene and several others are genes for heat shock proteins including HSPA1B and DNAJB1, which did not show a significant change in expression when tested by real-time qPCR.

Table 5.6

Primary Sequence Name	Sequence Code	Sequence Description	Number Donors Positive
HSPA1A	A_23_P111132	Homo sapiens heat shock 70kDa protein 1A (HSPA1A), mRNA [NM_005345]	3
HSPA6	A_23_P114903	Homo sapiens heat shock 70kDa protein 6 (HSP70B') (HSPA6), mRNA [NM_002155]	4
DNAJB1	A_23_P90062	Homo sapiens DnaJ (Hsp40) homolog, subfamily B, member 1 (DNAJB1), mRNA [NM_006145]	3
RN18S1	A_33_P3390107	Homo sapiens RNA, 18S ribosomal 1 (RN18S1), ribosomal RNA [NR_003286]	4
SNORD3B-1	A_33_P3226542	Homo sapiens small nucleolar RNA, C/D box 3B-1 (SNORD3B-1), small nucleolar RNA [NR_003271]	3
	A_33_P3303394	Unknown	4
HSPA1B	A_33_P3415430	Homo sapiens heat shock 70kDa protein 1B (HSPA1B), mRNA [NM_005346]	3

List of probes at 5 hour time point that have 3+ donors with a p-value <0.01, fold change of +/-2, and intensities for both fluorophores of < 250
qPCR genes 1.xlsx

5.5 Discussion

The two-color gene microarray experiment was designed to look at the changes in genes seen shortly after ligation with CD161. The exact timeframe for ligation of CD161 for the microarray was uncertain. Therefore, I chose to include two different time points with the hope that at least one time point would show changes in pathways, which would be an indication of biological function. Ideally, the combination of both time points would show changes in similar pathways.

CD161 staining of a sample of the cells sent to Miltenyi for the gene microarray showed that CD161 was significantly downregulated after ligation with

LLT1 at both 2 hours and 5 hours. This indicated that the cells underwent changes even if no change was seen at the level of mRNA. Unfortunately, the CD161 downregulation was not regulated at the mRNA level, so the *KLRB1* gene could not be used as a positive control.

The initial list of results from each of the donors was ranked based on the p-values given for each probe. The results for each donor at a single time point were combined into a single rank order list for that time point. These lists showed the genes highly significant across all of the donors for each time point. It was noted that at the 2 and 5 hour time points that several histone related genes were found upregulated, and at the 5 hour time point several heat shock protein related genes are upregulated.

When the lists of top ranked genes were uploaded into the Ingenuity Pathway Analysis (IPA) software, several pathways were highlighted. However, closer inspection of these pathways showed often only a few genes were involved and these were often found on the periphery of the pathways. Despite looking at both 2 hour and 5 hour time points, using various stringencies on the fold change and p-value parameters, no pathways showed central significant changes due to ligation of CD161.

It was possible that single genes were more important in the functional effects of CD161 ligation, or that the time points chosen were not appropriate for catching a widespread or cascade effect through a specific pathway.

From the IPA results and from looking at the top ranked p-value lists from each time point, a selection of genes that showed highly significant p-values were chosen as the first round of genes to be confirmed by real-time qPCR. Unexpectedly, none of the selected genes showed a significant change in expression upon CD161

ligation. This result was repeated over several donors even though the samples were created in almost the exact same way as the samples for the microarray, including using some of the same donors. The main difference between the samples is that the microarray samples were sorted by a flow cytometer as the final step where the real-time qPCR samples were sorted by column for Vα7.2, which might have led to slightly lower purity.

In an attempt to understand why the real-time qPCR results did not match the microarray data, I re-examined the microarray data. Most of the genes that were significantly upregulated or downregulated had very low intensity responses as seen by the log10 scatterplots. It has been reported that results from microarray data with low intensity levels are much less reliable and prone to false positives (Asyali et al. 2004).

Further examination of the genes chosen for confirmation by real-time qPCR showed that many of these probes did have very low intensities. Some of the genes had more than one probe for the gene within the microarray. For several of the genes, the probes with very low intensities showed over 2 fold changes with significant p-values, but the probes with much higher intensities failed to show a 2 fold change or significant p-values.

In the context of a cell, the low intensity levels correspond to low levels of mRNA production. If a cell has regular small fluctuations in mRNA expression levels, for example from 10 copies to 25 copies of a specific mRNA, although this shows a 2.5 fold change, this level of change may not be specific to anything or biologically relevant. However, with over 40,000 genes tested some of these types of cells may have been highlighted by the microarray.

In an attempt to limit the number of likely false positives resulting from low intensity levels, the microarray data was re-analyzed after removing probes with low intensities. Using the criteria of <0.01 p-value, > ± 2 fold change, and intensities of >250 for the probes on both samples, only 7 probe sequences were found in 3 or more donors at the 5 hour time point. Of these, one probe was a completely unknown gene and two of the others were genes that failed to show changes in gene expression in earlier real-time qPCR experiments. Although more testing could be done on the genes found with stricter selection criteria at both 2 and 5 hours, the results failed to indicate a pathway linked to a biological function that could be clearly tested.

The lack of data indicating a clear biological functional change being induced on T cells after CD161 ligation may indicate that there is no signaling function. It is possible that a second stimulus, such at TCR stimulation, is required in order to induce a functional effect upon ligation of CD161- i.e. CD161 signaling acts as a modifier (inhibitor or amplifier) of a more potent signaling pathway. Further experiments of this kind could be carried out with activated T cells to determine if any clear transcriptional functional effect can be seen upon CD161 ligation, in addition to classical functional assays.

5.6 Summary

- Data from a gene microarray of CD161 ligated T cells compared to non-ligated cells showed no clear and significant change in any gene pathways.
- Although the gene microarray showed many genes to have significant changes in expression due to CD161 ligation, the selected genes often had low intensity levels and changes in expression could not be seen with real-time qPCR experiments.
- These data together indicate that CD161 ligation on its own may downregulate CD161 protein expression, but ligation alone does not affect the cell at the mRNA level.

Chapter 6 CD161 Functional Effects

6.1 Introduction

CD161 (NKR-P1A) is a protein that is highly expressed on NK, NKT, and T cells, to the extent that it is considered a phenotypic marker on NK and NKT cells. (Pozzo et al. 2006) CD161 is highly expressed on cells that "bridge" the adaptive and innate immune system. Changes in CD161 expression levels have been seen in many disease states including multiple sclerosis (Annibabli et al. 2011), psoriasis (Cosmi et al. 2008), and Crohn's disease (Kleinschek et al. 2009; Billerbeck et al. 2010). Understanding the functional consequences of CD161 ligation on cells could lead to a greater understanding of what role CD161 plays in disease states.

There is a consensus in the literature that CD161 ligation on NK cells induced inhibition of cytotoxicity (Lanier et al. 1994; Poggi et al. 1998; Azzoni et al. 1998; Rosen et al. 2005; Aldemir et al. 2005), decreased cytokine production (Aldemir et al. 2005; Rosen et al. 2008), and decreased degranulation (Aldemir et al. 2005).

However, it is unclear what the role of CD161 ligation on T cells. T cell studies have shown CD161 ligation to increase cytokine production (Exley et al. 1998; Aldemir et al. 2005; Pozzo et al. 2006), no impact on cytokine production (Exley et al. 1998; Rosen et al. 2008) or decrease cytokine production (Rosen et al 2008). Studies have also shown CD161 ligation on T cells to not effect cytotoxicity (Exley et al. 1998) and increase proliferation (Pozo et al. 2006). These T cell ligation experimental results are summarized in Table 6.1.

Expression patterns of CD161 on T cells and the dynamics of CD161 cell expression were discussed in Chapter 4. Then, in Chapter 5 a gene microarray of

CD161 ligated non-activated $CD8^+$ T cells failed to show a clear functional impact on the regulation mRNA. One explanation for this was that CD161 signaling could act as a modifier of a more potent signaling pathway, thus a second stimulus to the cell would be required to see a functional impact of CD161 signaling. Thus, I looked at potential functional effects of CD161 ligation in several classical functional assays in the areas of cytokine production, cytotoxicity, proliferation, and cell death.

Table 6.1

Paper	CD161 Ligation Method	Experimental Findings
Exley 1998	αCD161 mAb	• αCD3 stimulated $CD4^+V\alpha24^{invt}$ cells increased IL-4, IFNγ production, and proliferation • PMA/I stimulated $CD4^+V\alpha24^{invt}$ cells showed no difference in IL-4 or IFNγ production • No effect on cytotoxicity
Aldemir 2005	αCD161 mAb LLT1 P815	• αCD3 stimulated increased IFNγ production • Unstimulated cells no effect seen • αCD3 stimulated increased IFNy production
Pozo 2006	αCD161 mAb	• αCD3 stimulated increased IFNγ • Unstimulated cells no IFNγ effect seen • Increased proliferation
Rosen 2008	αCD161 mAb	• SEB activated cells no effect on IFNγ or TNFα • αCD3/28 activated cells no effect on IFNγ and decrease in TNFα

CD161 in Literature

6.2 Aims

Study the functional effects of CD161 ligation on $CD8^+$ $CD161^+$ $V\alpha7.2^+$ (MAIT) cells in the areas of:

- Production of key cytokines
- Cytotoxicity
- Proliferation
- Cell Death

6.3 Material and Methods

6.3.1 αCD161 mAb staining

Unless otherwise stated, any unbound αCD161 mAb added as a stimulation to an experiment will be the same clone and conjugated fluorochrome that was used when cells were stained for flow cytometer.

6.3.2 Subjects

All cells came from healthy donor leukocyte cones (NHS Blood and Transplant Services) or from healthy laboratory blood donors who gave informed consent.

6.3.3 Binding mAb to Plates

A mixture of 100ul PBS, αCD3 pure (BD) at 2.5ug/ml, αCD28 (BD) at 5ug/ml, and αCD161 varying concentrations (see figure legends for concentrations) were mixed and added to a flat bottom ELISA plate (Greiner Bio-One Limited). The ELISA plate was incubated in the dark at room temperature overnight if using only antibodies. The plate was washed with PBS and then 200ul of 1X wash buffer (R&D 895126) was added at room temperature for 1-2 hours. The plate was then washed with PBS and 0.5-1 million cells and any unbound stimulations were added to each well of the ELISA plate and incubated at 37°C for 1 hour. BFA (Sigma) was added at 10ug/ml and incubated 4 hours to overnight. Cells were then recovered from the plate and 200ul of 2mM EDTA/PBS solution was added to each well of the ELISA plate and incubated at 37°C for 5 min. The 200ul EDTA/PBS was added to the cells, washed in PBS, and cells were stained.

6.3.4 $CD8^+$ T cell Selection

$CD8^+$ T cells were isolated from PBMCs by positive selection with αCD8 magnetic beads (Miltenyi) using manual MS-columns (Miltenyi) following manufactures instructions. Purity was consistently >85%.

6.3.5 Irradiation

Irradiated cell lines were irradiated with 30 grays of radiation prior to any co-incubations.

6.3.6 αCD3/28 Dynabeads

Dynabeads® Human T-Activator αCD3/28 beads (Life Technologies) were used at a 1:1 ratio (25ul/1 million cells). Correct amount of beads were calculated and washed in 5ml FACS tube with MACS buffer (PBS, 2mM EDTA, 0.5% FCS). Tube was placed in appropriate sized EasySep™ magnet (Stemcell) for 2 minutes and buffer was poured off. Dynabeads were re-suspended in R10 and co-incubated at 37°C with cells at the appropriate concentration for the length of time specified. Cells were re-suspended in MACS buffer in 5ml FACS tubes. Tubes were vigorously vortexed then put in appropriate sized EasySep™ magnet for 2 minutes. Supernatant was then collected, washed in PBS and stained.

6.3.7 αBiotin Activation Beads Design

T Cell Activation/Expansion Kit (Miltenyi) was used to create the αbiotin activation beads. αBiotin activation beads were loaded following manufacturer instructions using biotin αCD3 and αCD28 provided with the kit, biotin αCD161 clone 191B8 (Miltenyi), and biotin IgG2a clone eBM2a (ebioscience). αCD3, αCD28, and αCD161 were loaded on beads at the final concentration of 10 μg/ml of each mAb

on the bead (Figure 6.1). Beads were used at 5ul/1 million cells unless otherwise stated.

Figure 6.1

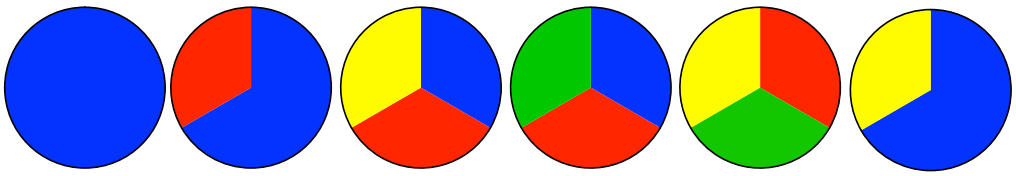

	IgG2a	αCD3	αCD3/161	αCD3/28	αCD3/28/161	αCD161
IgG2a	+	+	+	+	-	+
αCD3	-	+	+	+	+	-
αCD28	-	-	-	+	+	-
αCD161	-	-	+	-	+	+

αBiotin Activation Beads Design
Antibodies loaded to give 10ug/ml of αCD3, αCD28, or αCD161 mAb on the bead at the final concentration of 10 µg/ml with IgG2a used to fill rest of the bead.
Bead mAb porportions.pzfx

6.3.8 B cell line

The B cell line (BCL) used was an EBV immortalized primary B cells from a healthy donor. At resting state or when activated with various stimuli, LLT1 was not found up-regulated or present significantly on the surface of the B cell line (Figure 6.2)

Figure 6.2

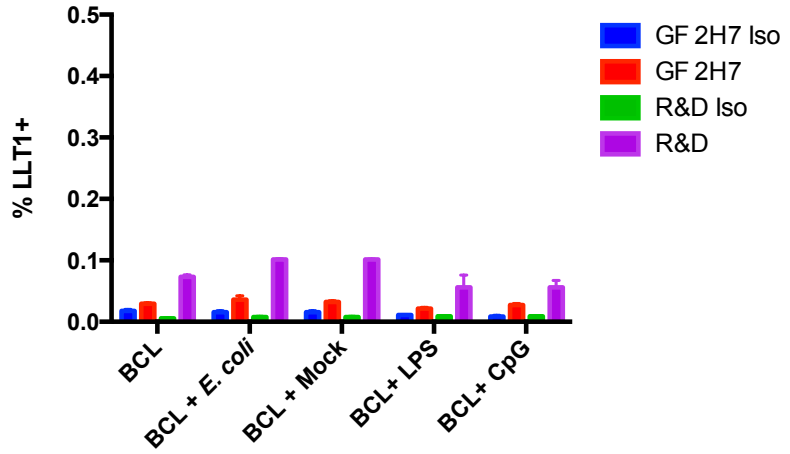

Activated B cell line (BCL)
Levels of LLT1 protein found on the surface of a B cell line at resting or after *E. coli* (10 BcP), Mock *E. coli* (10 BcP), LPS or CPG activation overnight. LLT1 clone 2H7 from Gordon Freeman Lab, Isotype for clone 2H7, hCLEC2D clone 402659 R&D, Isotype for clone R&D 402659.
170613 BCL LLT1 expression.pzfx

6.3.9 *E. coli* activation of B cell line

B cell lines (BCL) were either co-incubated with PFA-fixed *E. coli* at 10 BpC or were mock infected with the negative control at 10 BpC overnight in R10. The next day BCL were washed twice to remove any free *E. coli* before use.

6.3.10 FACS Gating Strategy

The gating strategy used in the FACS analysis in this thesis follows the basic gating strategy of gating for lymphocytes, single cells (SSC vs. FSC), live cells, and $CD3^+$ or $CD3^-$. $CD3^+$ cells were gated for $CD4^+$ or $CD8^+$ and then the T cells were gate on the listed in the experiment on antibodies such as CD161, Vα7.2, IFNγ, etc. $CD3^-$ cells were gated as listed in the experiment on antibodies such as CD161, CD19, or CD56 (Figure 6.3).

Figure 6.3

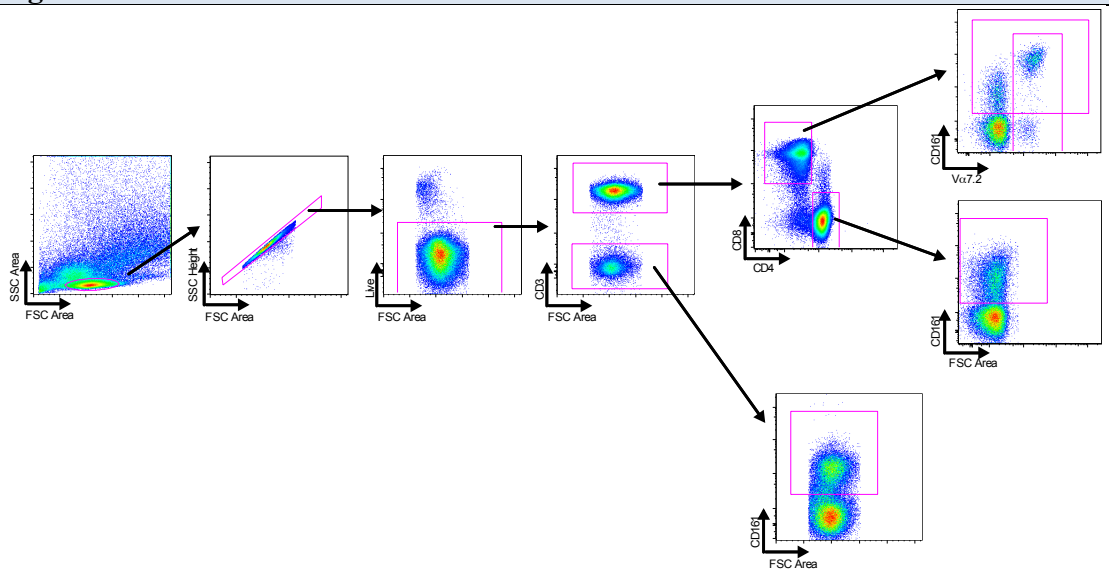

FACS Gating Strategy
Unless otherwise stated, cells are gated: Lymphocytes (SSC Area vs FSC Area), Single cells (FSC Height vs FSC Area), Live (Live vs FSC Area), $CD3^+$ or CD3- (CD3 vs FSC Area). CD3- cells may then be gated for $CD161^+$ (CD161 vs FSC Area). $CD3^+$ cells are gated $CD4^+$ or $CD8^+$ (CD8 vs CD4). $CD4^+$ cells may be gated for $CD161^+$ (CD161 vs FSC Area). $CD8^+$ cells may be gated for $CD161^+$, $V\alpha7.2^+$, or $CD161^+$ and $V\alpha7.2^+$ (CD161 vs Vα7.2).

6.3.11 Proliferation Assay

PBMCs were stained with 2.5µM CellTrace™ violet (CTV) (Life Technologies) for 10 minutes at room temperature followed by an addition of an equal volume of ice cold R10 to quench the reaction, and was kept on ice for another 5 minutes. The cells were then washed three times, transferring into new tubes between each wash. Before the last wash, the cells were left at 37°C for 5 minutes to allow excess dye to diffuse out. Cells were then re-suspended in RH10 at 2 $x10^6$/ml and plated in a 48 well flat bottom plate. Cells were incubated at 37°C for 5 days and then washed before staining.

6.3.12 FATAL Assay

The assay was based on the published VITAL assay (Hermans et al. 2004). Target B cell lines (BCL) were either co-incubated with PFA-fixed *E. coli* at 10 BpC

or were mock infected with the negative control overnight. Cells were harvested and the *E. coli* pulsed BCLs were stained with CFSE (Invitrogen), while the negative control BCLs were stained with CTV (Invitrogen). CFSE BCLs were labeled with 100nM CFSE in PBS for 10 minutes at room temperature. CTV BCLs were labeled with 2.5μM CTV in PBS for 10 minutes at room temperature. The staining for both dyes was followed by an addition of an equal volume of ice cold R10 to quench the reaction, and was kept on ice for another 5 minutes. The cells were then washed three times, transferring into new tubes between each wash. Before the last wash, the cells were left at 37°C for 5 minutes to allow excess dye to diffuse out. The CFSE-labeled cells and CTV-labeled cells were mixed at a 1:1 ratio prior to plating out.

$CD8^+$ T cells were isolated from PBMCs by positive selection with αCD8 magnetic beads (Miltenyi) using manual MS-columns (Miltenyi). Effector cells were added to the wells at the indicated E:T ratios, in duplicates. An αMR1-blocking antibody (Clone 26.5) was used at 5μg/ml for blocking experiments, and cells were incubated overnight.

Following incubation, cells were harvested and washed in PBS before staining with a live-dead maker (Invitrogen) before being fixed and permeablised for the staining of extracellular and intracellular markers, as described above. Analysis was on gated live BCLs only. BCL gating was based on controls without any effector T cells added. Based on the percentage survival of $CFSE^{high}$ cells in wells containing no effectors (E:T=0:1), the expected frequency of target cells can be found:

$$\text{Expected ratio (ER)} = \frac{\%\ CFSE^{high}\ \text{cells}}{\%\ CTV^{high}\ \text{cells}}$$

Using this ratio, the % specific killing can be calculated:

$$\% \text{ specific killing} = \left[\frac{100 \times (ER \times \%CTV^{high}) - \%CFSE^{high} \text{ cells}}{(ER \times \%CTV^{high})} \right]$$

6.3.13 Statistics

Unless otherwise stated all stats were calculated using GraphPad Prism 5 or 6 in the following way: If n ≥8 a D'Agostino & Pearson omnibus normality test was performed. If the samples passed with alpha ≥0.05 then a Repeated measures one-way ANOVA with Geisser-Greenhouse correction and Bonferroni's multiple comparison tests was performed to get the p-value. If n ≤8 or if n ≥8 but fails the D'Agostino & Pearson omnibus normality test with alpha ≤0.05 a Friedman test with Dunn's multiple comparisons test was performed to get the p-value.

6.4 Results

Previous studies showed various effects of CD161 ligation or cross-linking on the production of cytokines, namely IFNγ and TNFα, on T cells (Exley et al. 1998; Aldemir et al. 2005; Pozo et al. 2006; Rosen et al. 2008). Therefore, I started with experiments designed to determine if CD161 ligation affected the cytokine production on activated $CD3^+$ $CD8^+$ T cells.

6.4.1 $CD8^+$ T cells cross-linked with plate bound αCD161 mAb decreased IFNγ expression at some concentrations

PBMCs stimulated overnight with plate bound αCD3 (2.5ug/ml) and αCD28 (5ug/ml) mAbs and a dose titration of αCD161 (1ug to 0.03125ug) mAb were stained intracellularly for IFNγ production. For $CD8^+$ cells, a statistically significant ($p = 0.002$) decrease in total IFNγ production was found at the αCD161 mAb concentration of 0.25ug, but there was no significant difference at the other concentrations tested (Figure 6.4). For $CD4^+$ gated cells, there was no statistically significant difference in total IFNγ production at any concentration of αCD161 mAb (Figure 6.5).

However, these experiments were performed prior to understanding the dynamics of CD161 expression after signaling, as described in Chapter 4, which made it difficult to track the $CD161^+$ cells without either IL-18R or Vα7.2. Thus, total CD4 or CD8 IFNγ production was measured, and the higher concentrations of αCD161 mAb (1ug and 0.5ug), were not used in most experiments due to the extent of CD161 gMFI downregulation.

Figure 6.4

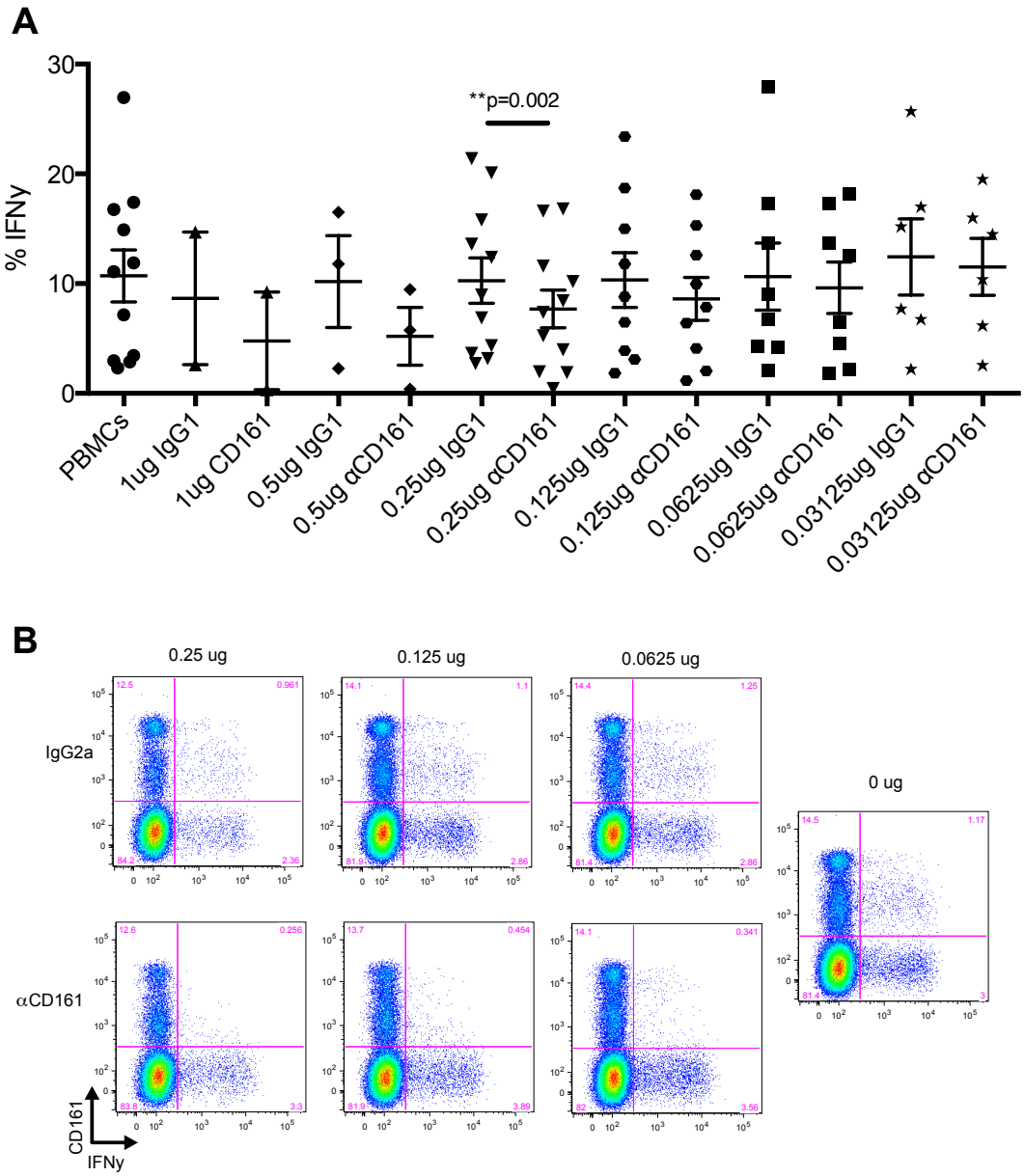

Total CD8$^+$ IFNy expression decreases with cross-linking of plate bound αCD161 mAb at some concentrations

(A) Expression of IFNy by PBMCs incubated for 16-18 hours with constant level of plate bound αCD3 (2.5ug/ml), αCD28 (2.5ug/ml), and a dose titration of plate bound αCD161 or IgG2a mAb (1ug to 0.03125ug). All cells gated on CD8$^+$ (n= 2 to 11). Statistical analysis used: One way ANOVA with Bonferroni's multiple comparison correction **(B)** Representative raw data for one donor for plate bound αCD161 mAb concentrations of 0.25ug, 0.125ug, 0.0625ug, and 0ug.
Original aCD161 plate ICS data T.pzf 101407.jo

Figure 6.5

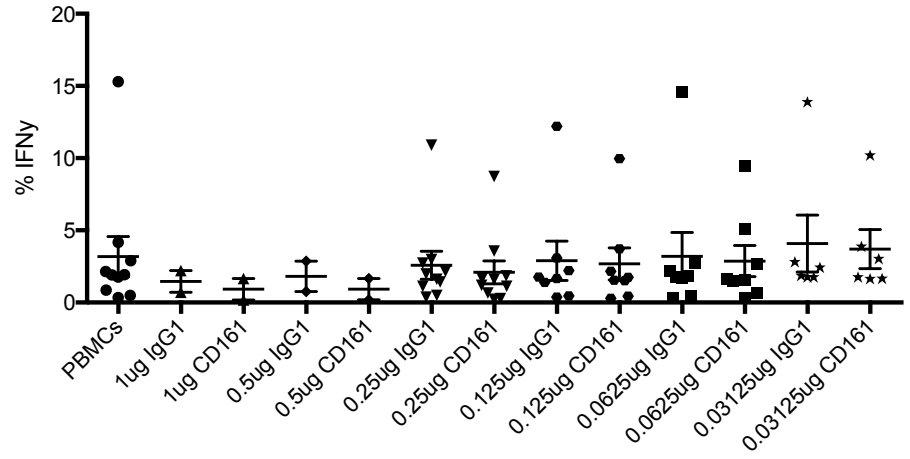

Total $CD4^+$ IFNy expression was not affected by cross-linking with αCD161 mAb
Expression of IFNy by PBMCs incubated for 16-18 hours with constant level of plate bound αCD3 (2.5ug/ml), αCD28 (2.5ug/ml), and a dose titration of plate bound αCD161 or IgG2a mAb (1ug to 0.03125ug). All cells gated on $CD4^+$. (n= 2 to 11)
Original aCD161 plate ICS data T.pzf

6.4.2 CD161 ligation of MAIT cells did not affect IFNγ or TNFα expression regardless of ligation or activation methods used

With the ability to use Vα7.2 staining to track $CD8^+$ $CD161^{++}$ $Vα7.2^+$ (MAIT) cells, the previous experiments could be repeated greater specificity by including only the cells directly affected by CD161 ligation in the calculations of cytokine production.

The next series of experiments tested IFNγ and TNFα expression, with plate bound, bead and free mAb forms of cell stimulation, in addition to CD161 cross-linking with mAb or LLT1 expressed on a transfected cell line. PBMCs gated on $CD8^+$ $Vα7.2^+$ $CD161^+$ had a greater decrease in gMFI of CD161 with free mAb or LLT1 transfected cell lines than with cell cross-linked with plate bound αCD161 (Figure 6.6A). Despite the downregulation of CD161, the expression levels of IFNγ and TNFα remained constant, regardless of the method used to ligate CD161 (Figure 6.6B-C).

6.4.3 CD161 ligation of $CD4^+$ T cells decreased IFNγ expression with plate bound stimulation but not other forms of stimulation

$CD4^+$ $CD161^+$ cells could not easily be tracked with Vα7.2 so total $CD4^+$ IFNγ and TNFα expression were measured. The $CD4^+$ cells showed downregulation of CD161 gMFI similar to $CD8^+$ cells (Figure 6.7A). $CD4^+$ cells showed a statistically significant decrease in IFNy ($p = 0.01$) when the αCD3/28 and αCD161 mAb stimuli were all plate bound, but not with any other type of stimulation (Figure 6.7B). There was no statistically significant difference seen in TNFα expression (Figure 6.7C).

6.4.4 Cross-linking of CD161 on MAIT cells stimulated with a biotin activation beads increased expression of IFNγ and TNFα

The only statistically significant differences or trends in IFNγ and TNFα production were when a combination of both αCD3/28 activation and plate bound αCD161 was used. Thus, I chose to look at another method of activation where αCD3/28 and αCD161 would be presented together to the target cells. Thus, I designed a set of αbiotin activation beads with various combinations of αCD3, αCD28, and αCD161 (For design see Figure 6.1 on page 144).

PBMCs were enriched for $CD8^+$ cells to ensure activated B cells, which might express LLT1, were removed. The αbiotin activation beads were co-incubated with the $CD8^+$ selected cells for 18 hours. A statistically significant increase in IFNγ ($p = 0.0002$) and in TNFα ($p = 0.012$) production was seen when αCD161 was added to the αCD3/28 beads, but no significant difference was seen without TCR stimulation or with αCD3 stimulation alone (Figure 6.8).

Figure 6.6

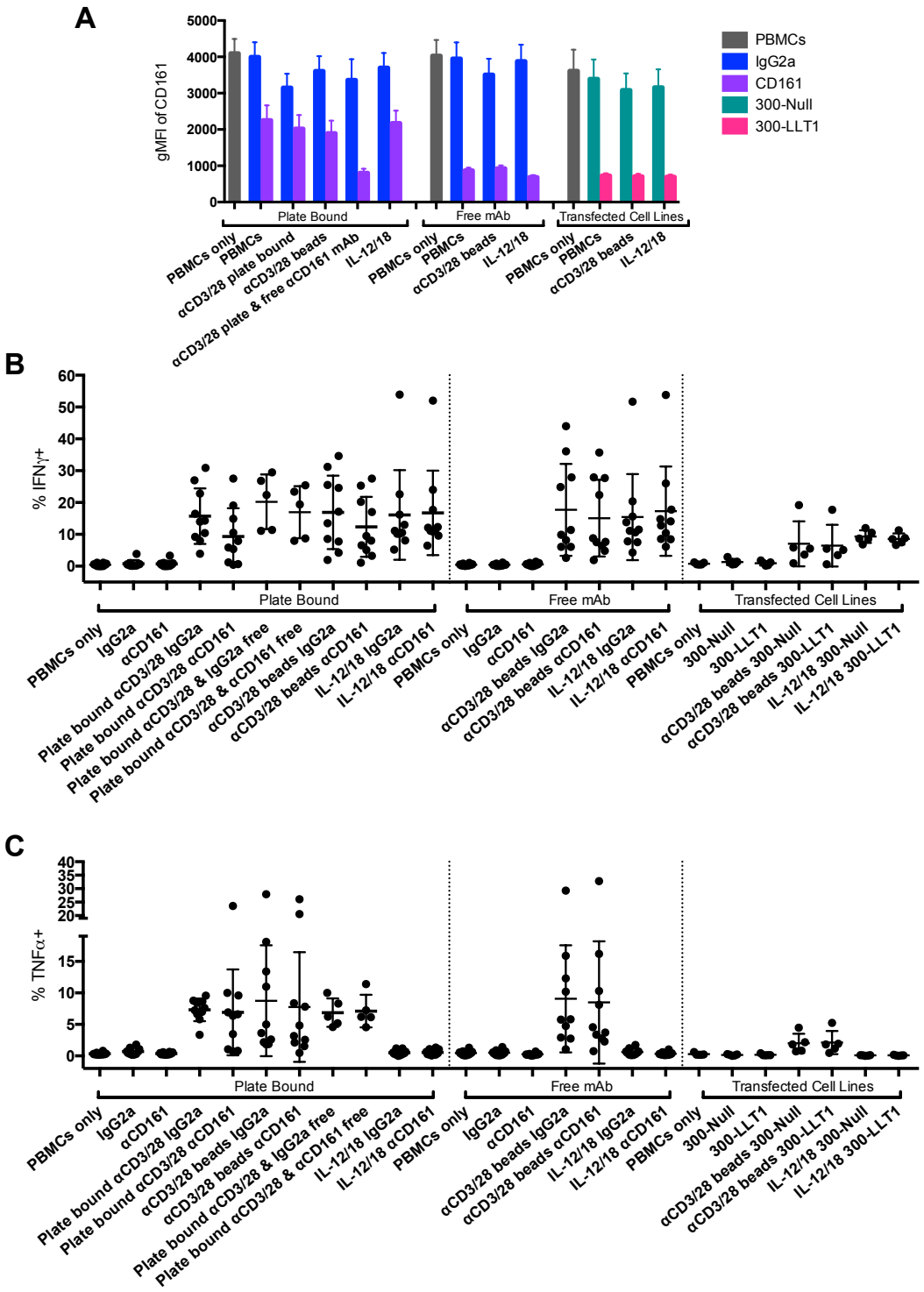

CD161 ligation on CD8$^+$ Va7.2$^+$ CD161$^+$ (MAIT) cells does not affect IFNγ or TNFα expression
PBMCs incubated for 16-18 hours with plate bound αCD3 (2.5ug/ml) αCD28 (5ug/ml), IL-12 (50ng/ml) IL-18 (50ng/ml), or αCD3/28 beads (Dynabead) and incubated with plate bound IgG2a or αCD161 mAb (0.25ug), free IgG2a or αCD161 APC conjugated mAb (0.25ug/ml), or an irradiated 300 Line or 300-LLT1 transfected cell line at a 3:1 PBMC to cell line ratio. All samples gated on CD8$^+$ CD161$^+$ Va7.2$^+$ cells. Statistical analysis: Friedman test with Dunn's multiple comparisons test. (n= 5 or 10) **(A)** CD161 gMFI of MAIT cells **(B)** IFNγ expression by MAIT cells **(C)** TNFα expression by MAIT cells.
240413 150513 IFNy ICS T.pzfx

Figure 6.7

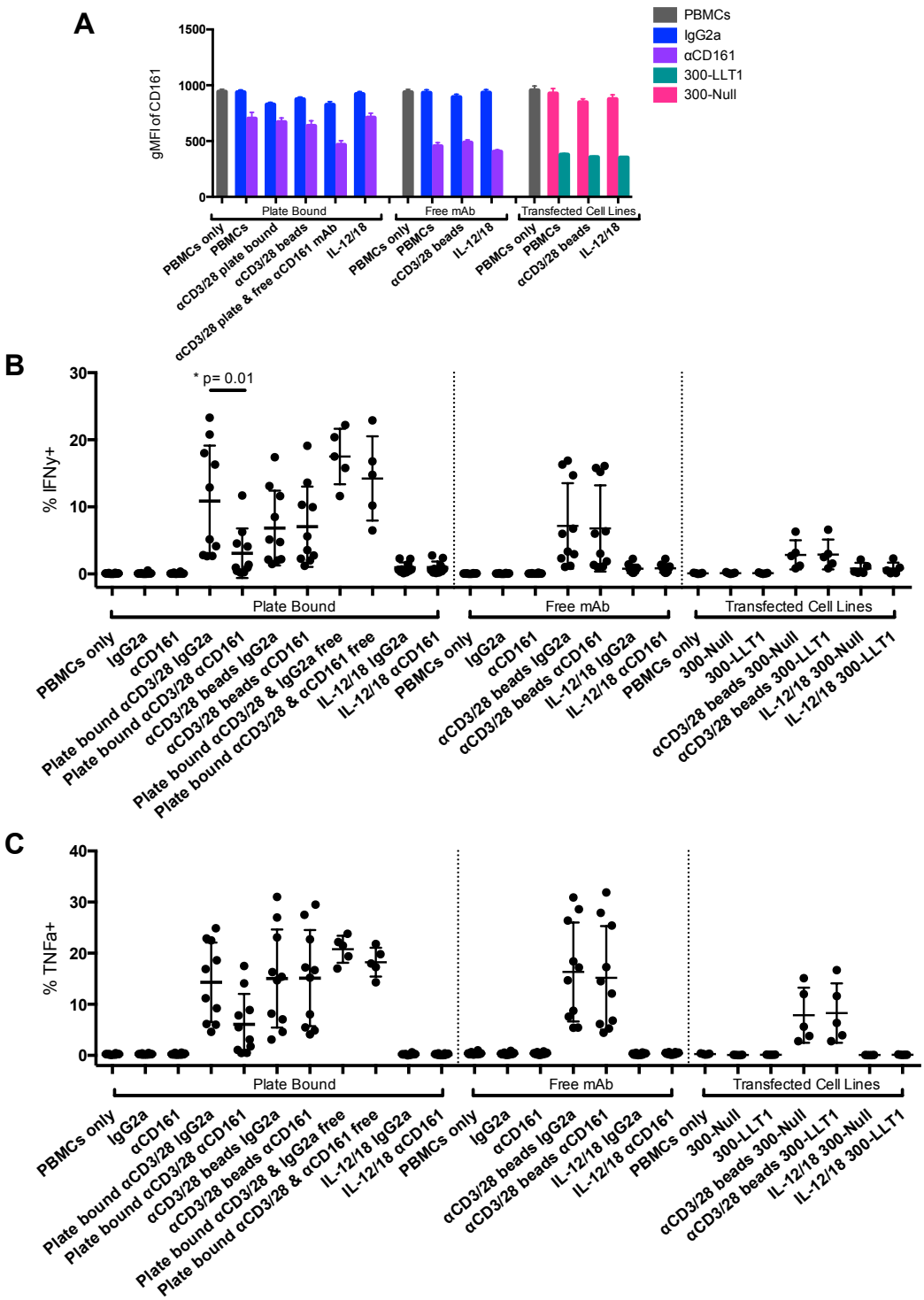

$CD4^+$ $CD161^+$ IFNγ expression decreased with plate bound CD161 ligation but not other formats of ligation and TNFα expression was not affected

PBMCs incubated for 16-18 hours with plate bound αCD3 (2.5ug/ml) αCD28 (5ug/ml), IL-12 (50ng/ml) IL-18 (50ng/ml), or αCD3/28 beads (Dynabead) and incubated with plate bound IgG2a or αCD161 mAb (0.25ug), free IgG2a or αCD161 APC conjugated mAb (0.25ug/ml), or an irradiated 300-Null or 300-LLT1 transfected cell line at a 3:1 PBMC to cell line ratio. All samples gated on $CD4^+$ $CD161^+$ cells. Statistical analysis: Friedman test with Dunn's multiple comparisons test. (n= 5 or 10)
(A) CD161 gMFI of MAIT cells **(B)** IFNγ expression by MAIT cells **(C)** TNFα expression by MAIT cells.
240413 150513 IFNy ICS T.pzfx

Figure 6.8

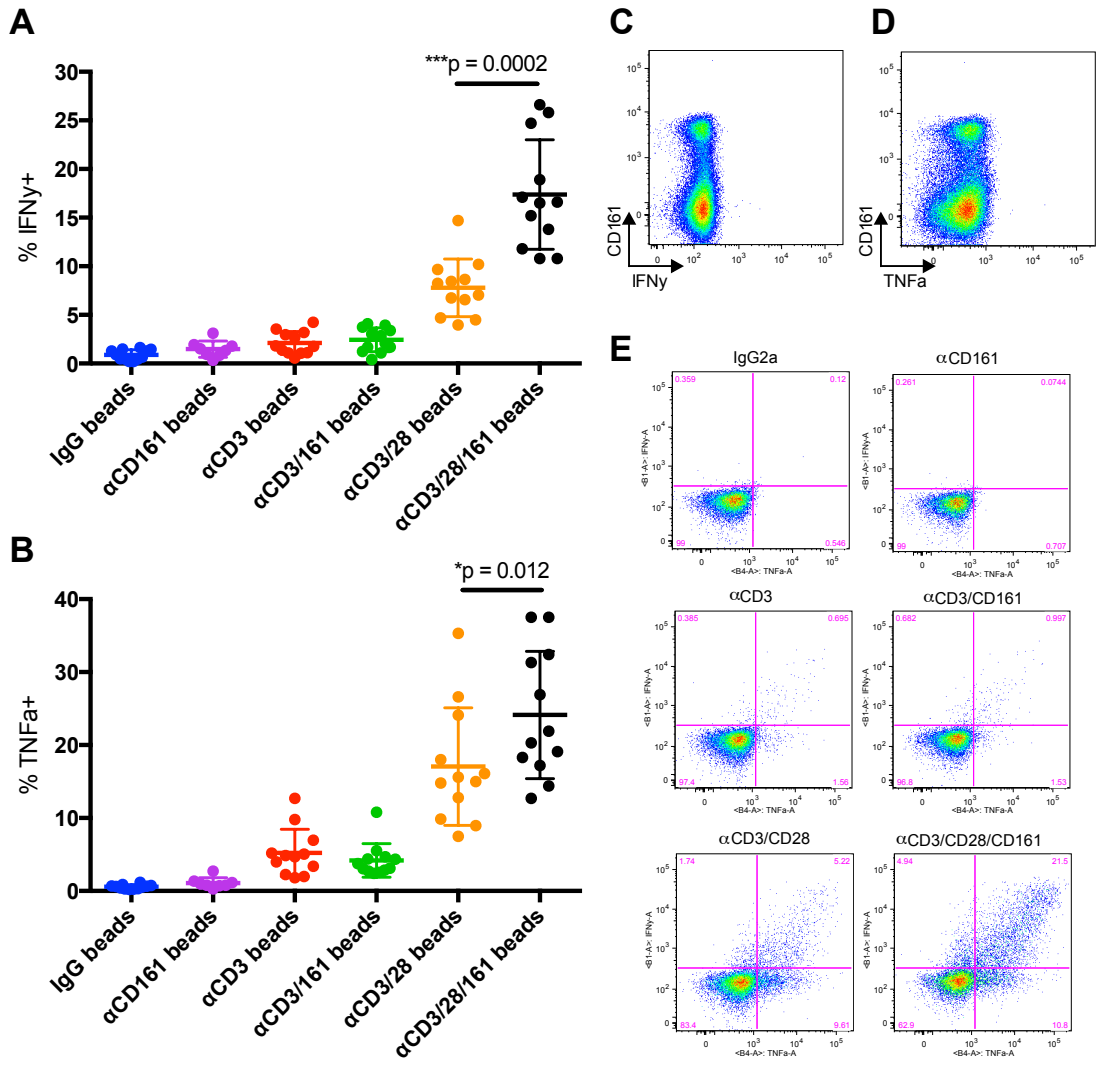

CD161 cross-linking with αbiotin beads increased IFNy and TNFa expression
$CD8^+$ selected cells gated on $Va7.2^+$ cells in response to αbiotin activation beads (see material and methods Figure 6.1 for bead design on page 144) Statistical analysis: One way ANOVA with Bonferroni's multiple comparisons **(A)** IFNy expression (n= 5 or 10) **(B)** TNFa expression (n= 5 or 10) **(C & D)** $CD8^+$ selected cells activated by IgG2a beads **(E)** Representative raw data of one donor for each bead in A & B
250613 & 120713 IFNy ICS beads.pzfx 120713 IFNy TNFa ICS.jo

6.4.5 Bead bound CD161 cross-linking of $CD8^+$ T cells stimulated with IL-12 + IL-18 does not affect IFNγ expression

Since putting both the CD3/28 stimulation and the αCD161 cross-linking mAb in the same location increased the effect of the CD161 ligation, I wanted to know if this increased affect occurred with IL-12 + IL-18 activated cells. Interestingly, $CD4^+$

and $CD8^+$ $V\alpha7.2^+$ cells stimulated with both IL-12 + IL-18 showed no difference in IFNγ expression when cross-linked with bead bound αCD161 mAb compared to bead bound IgG2a mAb(Figure 6.9 A,C). The lack of affect on IFNγ occurred despite a decrease in CD161 gMFI with CD161 cross-linking (Figure 6.9 B,D).

Figure 6.9

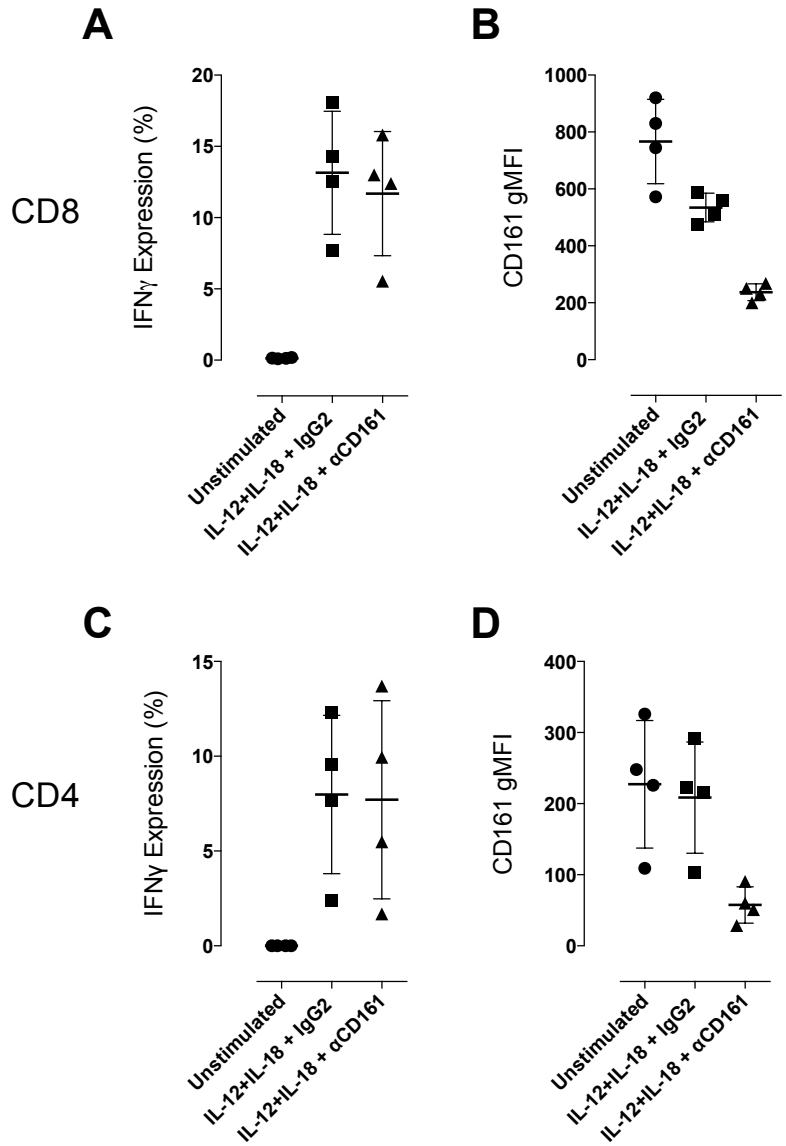

Bead bound αCD161 cross-linking of IL-12+IL-18 stimulated MAIT cells does not affect IFNγ expression

PBMCs unstimulated or stimulated with bead bound αCD161 or IgG2a mAb (see material and methods Figure 6.1 for bead design on page 144) and IL-12+IL-18. (n= 4) **(A)** $CD8^+$ $V\alpha7.2^+$ T cells IFNy expression **(B)** $CD8^+$ T cells gMFI of CD161 **(C)** $CD4^+$ T cells IFNy expression **(D)** $CD4^+$ T cells gMFI of CD161

IL-12_18 abiotin bead IFNy and TNFa expression.pzfx

6.4.6 CD161 cross-linking did not induce changes in IL-22 expression

$CD161^+$ $CD4^+$ and $CD8^+$ cells have been shown to be capable of producing IL-22. However, I found it difficult to induce large amounts of IL-22 from $CD161^+$ cells, especially from $CD8^+$ cells in the short-term timeframes I was interested in. Despite trying multiple time points including 5 hours and overnight stimulations and different permeabilization methods, αCD3/28 stimulations did not induce much IL-22 despite clearly inducing activation and IFNγ (Figure 6.10). PMA/I activation produced slightly more IL-22, especially in the $CD4^+$ cells. However, a large portion of the $CD8^+$ $CD161^{++}$ or $V\alpha7.2^+$ cells died and made it very difficult to measure IL-22 production. When $CD8^+$ selected cells were activated with αbiotin activation beads or PMA/I, no statistically significant differences were found when αCD161 mAb was added (Figure 6.11).

Figure 6.10

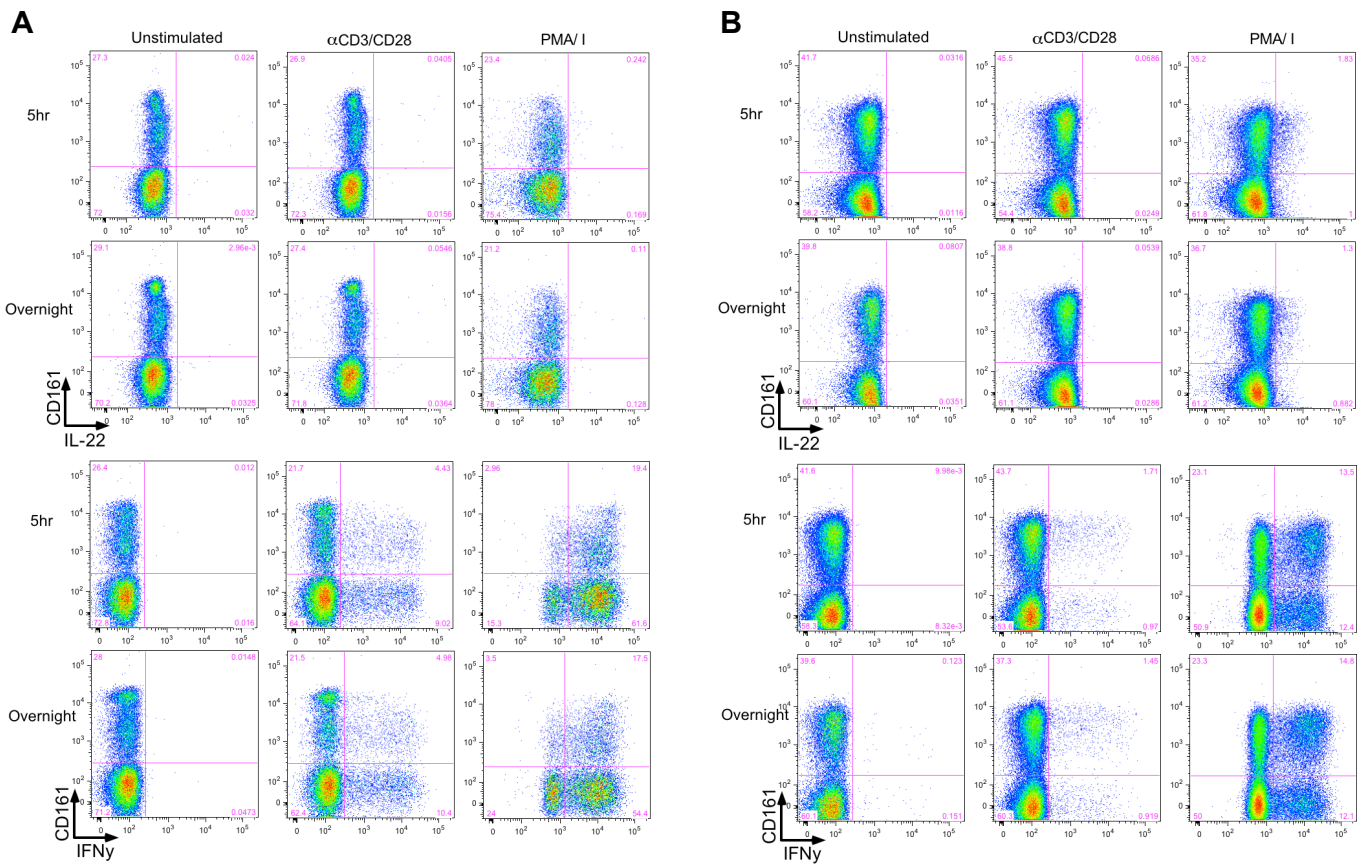

IL-22 expression levels were low on activated CD8$^+$ and CD4$^+$ T cells
(A) IL-22 production by PBMCs stimulated with plate bound αCD3/28mAb (18 hours) or PMA/I for (top) 5 hours or (bottom) overnight (18-20 hours) gated on CD8$^+$ cells. **(B)** IL-22 production by PBMCs stimulated with plate bound αCD3/28 mAb (18 hours) or PMA/I for (top) 5 hours or (bottom) overnight (18-20 hours)gated on CD4$^+$ cells.
030910 IL-22.jo

Figure 6.11

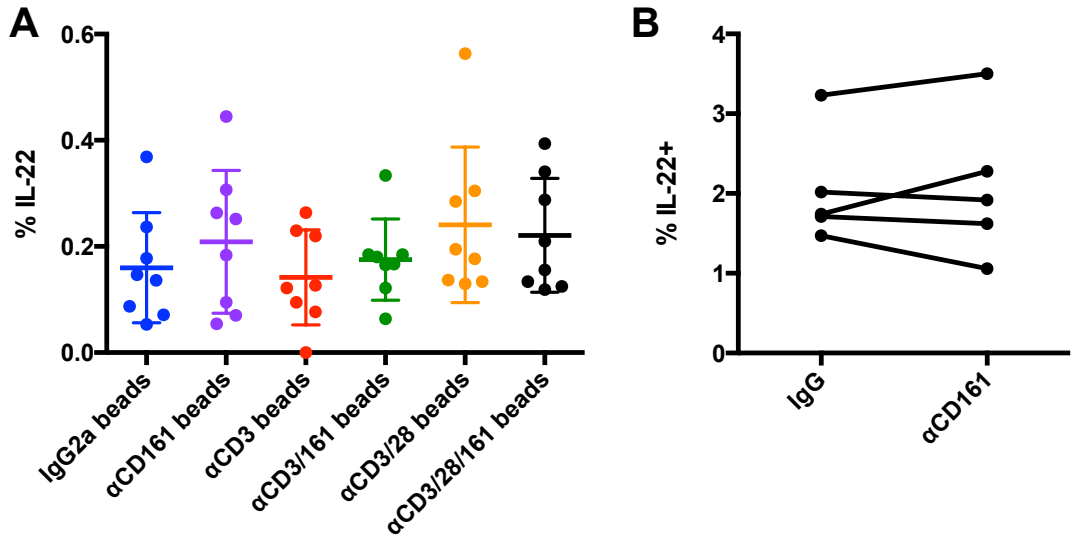

CD161 cross-linking did not affect IL-22 expression when activated by αbiotin activation beads or PMA/I
(A) IL-22 production by $CD8^+$ selected cells gated on $Va7.2^+$ cells in response to activation beads (see material and methods Figure 6.1 for bead design on page 144) (n= 8) for 18 hours. **(B)** IL-22 production by $CD8^+$ selected cells gated on $Va7.2^+$ cells in response to PMA/I for 5 hours.
120713 PMA/I IL-17 IL-22.pzfx 120713 TCR IL-22 IL-17.pzfx

6.4.7 CD161 cross-linking did not induce changes in IL-17a expression

$CD161^+$ T cells have also shown to be capable of producing IL-17a. However, I found it difficult to get $CD8^+$ cells to express large amounts (Figure 6.12) despite trying multiple short-term time frames and permeabilization methods. When $CD8^+$ selected cells were stimulated with activation beads or PMA/I, no statistically significant differences were found when CD161 was added (Figure 6.12).

Figure 6.12

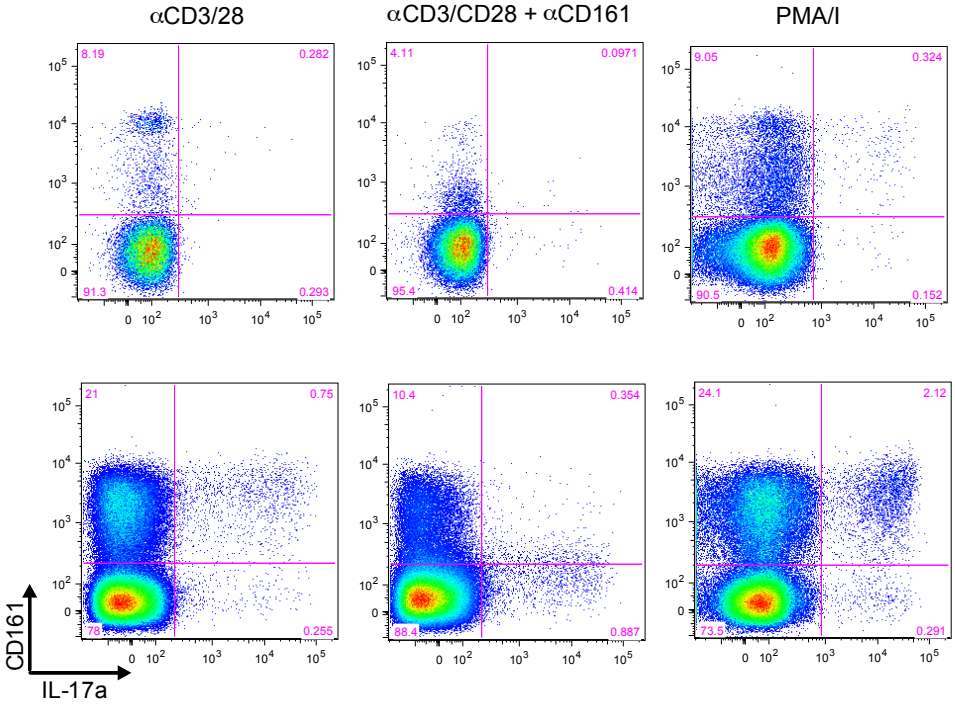

IL-17a expression levels were low on activated CD8$^+$ and CD4$^+$ T cells
IL-17a production by PBMCs stimulated with plate bound αCD3/28 mAb, αCD161 mAb (18 hours) or PMA/I (5 hours) Gated on (top) CD8$^+$ or (bottom) CD4$^+$
220710.jo

Figure 6.13

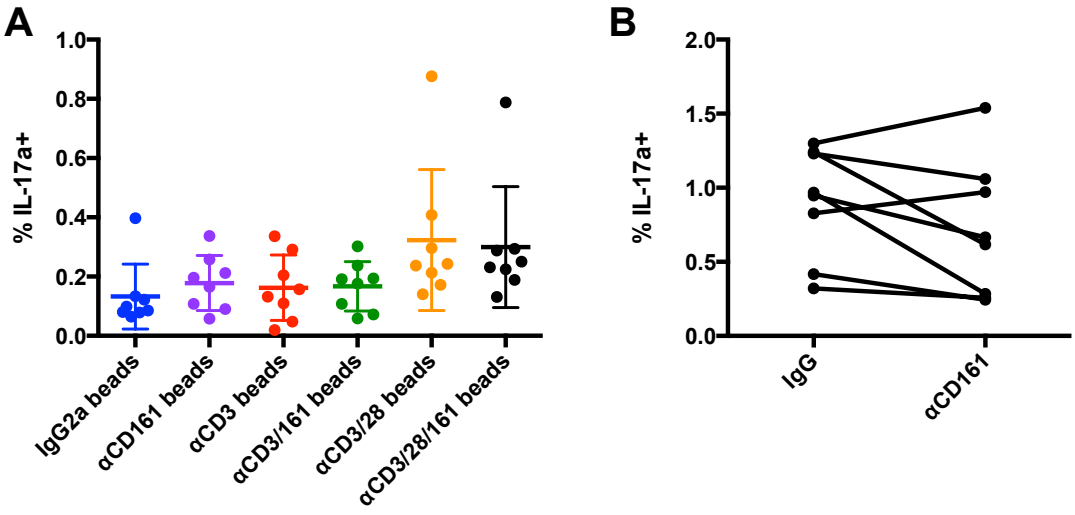

CD161 cross-linking did not affect IL-17a expression when activated by αbiotin activation beads or PMA/I
(A) IL-17a production by CD8$^+$ selected cells gated on Va7.2$^+$ cells in response to activation beads (see material and methods Figure 6.1 for bead design on page 144) (n= 8) for 18 hours. **(B)** IL-17a production by CD8$^+$ selected cells gated on Va7.2$^+$ cells in response to PMA/I for 5 hours.
120713 PMA/I IL-17 IL-22.pzfx 120713 TCR IL-22 IL-17.pzfx

6.4.8 CD161 ligation increased specific killing by activated MAIT cells

Since cytotoxic $CD8^+$ cells are known for the ability to kill infected cells, I wanted to determine if CD161 ligation had an affect on the killing ability of $CD8^+$ $CD161^+$ cells. In the FATAL assay, B cell line (BCL) activated overnight with *E. coli* up-regulates MR1 and activates $CD8^+$ cells in an MR1 dependent manner. MR1 triggers through the Vα7.2 TCR receptor on $CD8^+$ $CD161^+$ T (MAIT) cells and this leads to specifically activated $CD161^{++}$ cells (Treiner et al. 2003).

BCLs were incubated overnight with PFA fixed *E. coli* or a mock *E. coli*. The next day *E. coli* treated BCLs were stained with CFSE and mock *E. coli* treat BCLs were stained with CTV. The *E. coli* and the mock activated and stained BCL cells were mixed at a 1:1 ratio and added to PBMCs. IgG2a, CD161 or aMR1 mAb were added to the PBMC/BCL mixture and then incubated for 16-18 hours before staining. The expected ratio between CFSE and CTV stained BCLs was determined from control wells and then the specific killing was calculated. (For formula see Material and Methods section 2.3.20 FATAL Assay on page 45) The specific killing significantly increased ($p= 0.0129$) with the addition of αCD161 mAb and significantly decreased ($p = 0.0072$) with addition of αMR1 mAb (Figure 6.14).

Figure 6.14

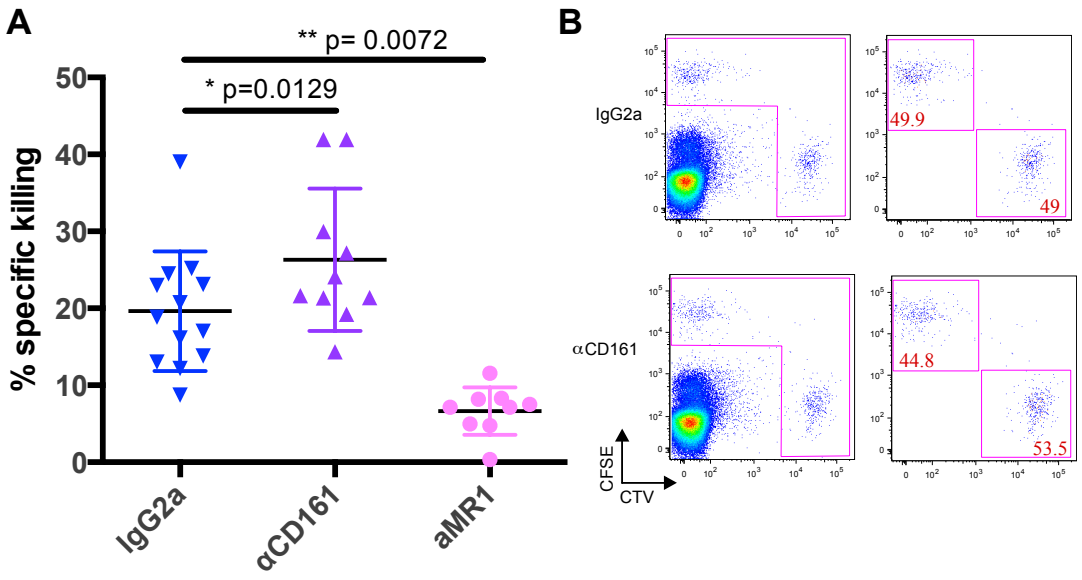

CD161 ligation in FATAL Assay increased specific killing
CD8$^+$ selected cells co-incubated with *E. coli* or mock activated BCL overnight with IgG2a (0.5ug/ml), αCD161 mAb (0.5ug/ml), or αMR1 mAb (5ug/ml) **(A)** Specific killing. Statistical analysis: One way ANOVA with Bonferroni's multiple comparisons **(B)** Representative raw data from one donor. All cells (left) BCL only (right) E. coli stained with CFSE and mock E. coli stained with CTV
FATAL inhibitors 5 T.pzfx 010513 FATAL.jo

6.4.9 CD161 cross-linking increased degranulation (CD107a) and activation (CD69) of CD8$^+$ T cells

Since addition of CD161 increased the specific killing by CD8$^+$, cells I looked at possible mechanisms for the increased killing. Degranulation was measured by staining of CD107a and the activation level was measured by staining of CD69. PBMCs were activated with αCD3/28 Dynabeads and IgG2a or αCD161 mAb. The addition of αCD161 mAb statistically significantly increased the degranulation ($p = 0.0001$) and levels of CD69 activated cells ($p = 0.0158$) (Figure 6.15).

I wanted to see if the increases seen in degranulation and activation, with the addition of αCD161 mAb, were more dramatic if the αCD161 mAb was presented in the same location as the TCR stimulus. Therefore, the αbiotin activation beads were used to activate CD8$^+$ selected cells. CD69 levels increased significantly ($p = 0.001$)

for αCD3/161 beads compared to αCD3 beads, and increased slightly (p = 0.023) for αCD3/28/161 beads compared to αCD3/28 beads (Figure 6.16A, E). CD107a increased slightly (p= 0.013) for αCD3/161 beads compared to αCD3 beads, and significantly (p = 0.0003) for αCD3/28/161 beads compared to αCD3/28 beads (Figure 6.16B, E).

Figure 6.15

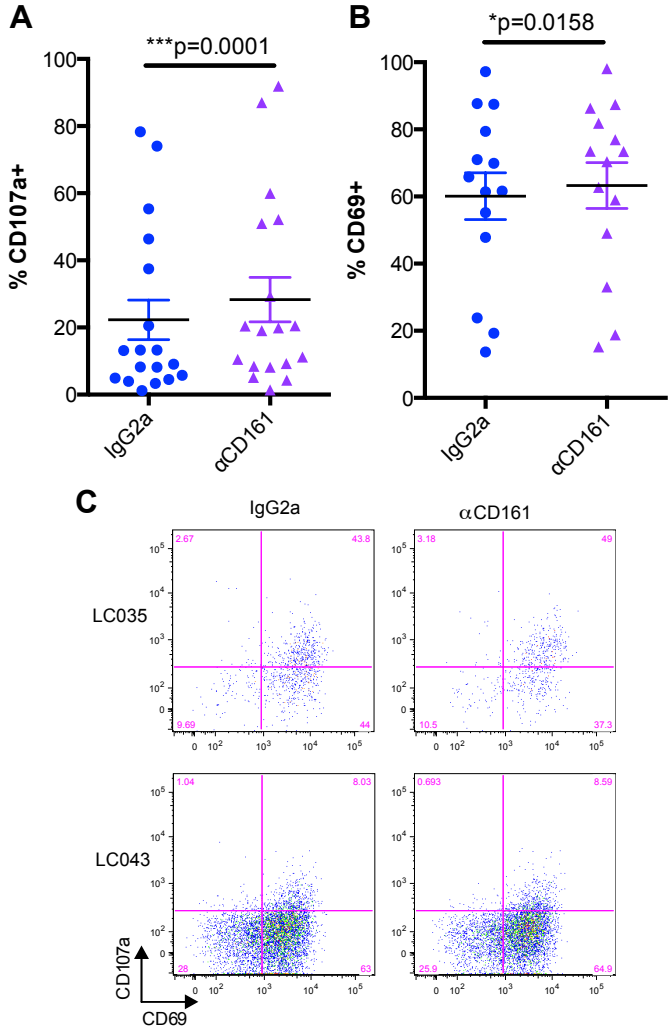

CD161 cross-linking with free αCD161 mAb increased CD107a and CD69 expression
PBMCs co-cultured with αCD3/28 Dynabeads along with IgG2a-APC or αCD161-APC mAbs and stained intracellularly. All samples gated on $CD8^+$ $CD161^+$ $Va7.2^+$ cells. Statistical analysis: Paired T test **(A)** Degranulation shown by staining levels of CD107a (n=18) **(B)** Activation levels shown by CD69 (n=14) **(C)** Representative raw data from two donors.
220313 degranulation T.pzf

Figure 6.16

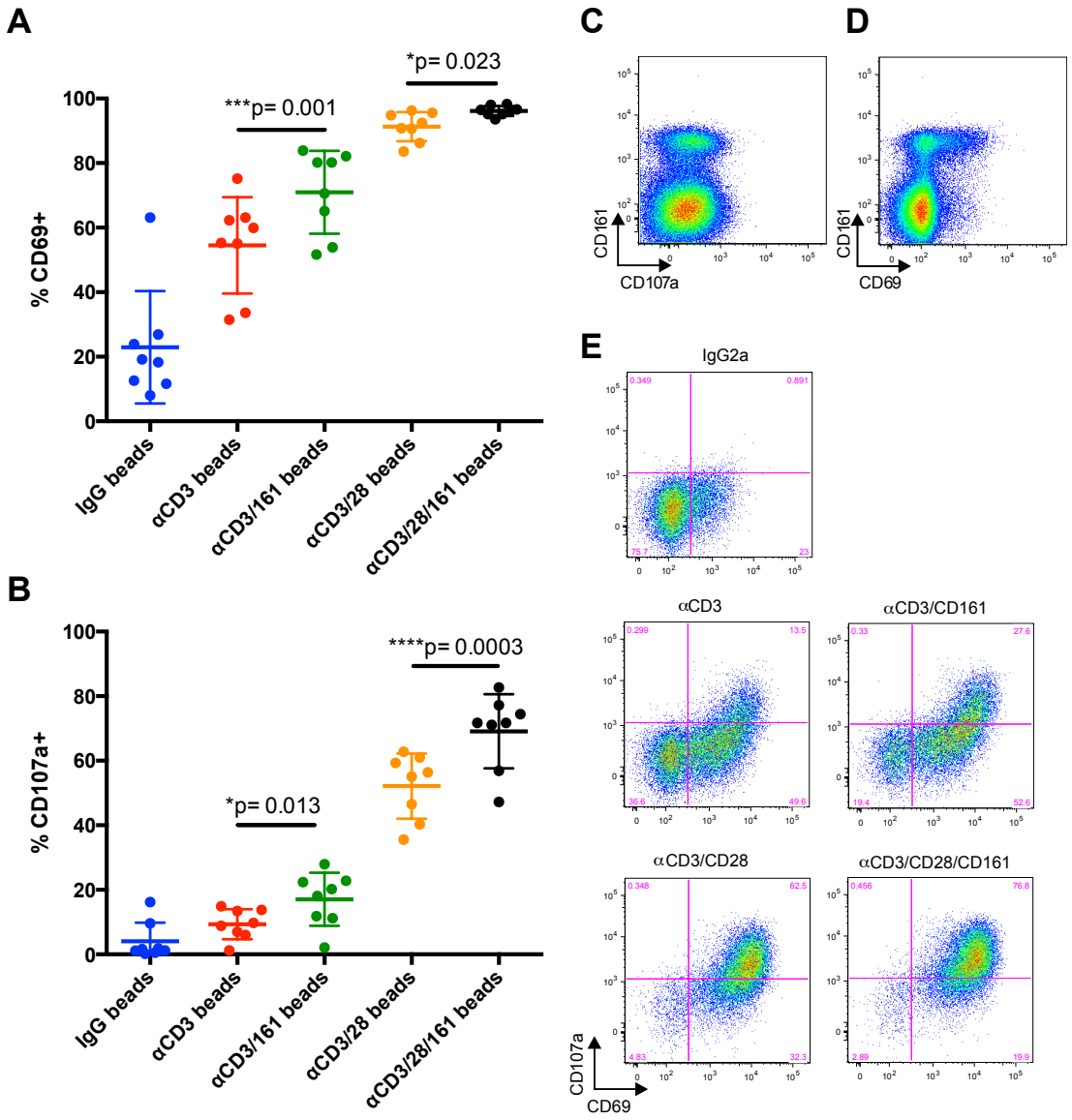

CD161 cross-linking with αbiot activation beads increased CD107a and CD69 expression
$CD8^+$ selected cells gated on $Va7.2^+$ cells in response to αbiotin activation beads (see material and methods Figure 6.1 for bead design on page 144) Statistical analysis: One way ANOVA with Bonferroni's multiple comparisons **(A)** CD69 expression (n= 8) **(B)** CD107a expression (n= 8) **(C & D)** $CD8^+$ selected cells activated by IgG2a beads **(E)** Representative raw data of one donor for each bead in A & B
250613 Degranulation.pzfx 250613 Degranulation.jo

6.4.10 CD161 ligation increased Granzyme B expression

The increase in degranulation led to the question of what type and how much granzyme or perforin cells were releasing. This was first tested using the same activation setup found in the FATAL assay with $CD8^+$ selected cells being activated

by *E. coli* activated BCLs with the addition of either IgG2a or αCD161 mAb overnight. The addition of αCD161 mAb increased Granzyme B ($p = 0.029$) (Figure 6.17).

I was also interested to see if the level of activation made a difference in how αCD161 mAb affected the levels of granzymes and perforin. It was noted that $CD161^+$ $V\alpha7.2^+$ cells did not express Granzyme B or expressed it at very low levels compared to other $CD8^+$ cells at resting or with $CD3^+$ activation. However, with αCD3/28 activation, Granzyme B was expressed (Figure 6.18A, C). αCD3/28/161 beads significantly increased ($p= 0.0081$) the level of Granzyme B production compared to αCD3/28 beads. Granzyme B production was not changed with the addition of αCD161mAb to the beads with the other activation conditions. (Figure 6.18A, E)

6.4.11 CD161 ligation had no effect on perforin expression

In the FATAL assay setup addition of αCD161 mAb had no effect on the expression levels of perforin (Figure 6.17).

When αBiotin activations beads were used to activate $CD8^+$ enriched cells, levels of perforin production were slightly more variable between patients at the resting state, but were not changed significantly at any of the activation conditions with the addition of αCD161 mAb to the beads. However, the levels of perforin production did increase significantly ($p= 0.0015$) between αCD3 beads and αCD3/28 beads (Figure 6.18B, E).

6.4.12 CD161 ligation decreased Granzyme A expression

When αBiotin activations beads were used to activate $CD8^+$ enriched cells, it was noted that MAIT cells had very high at Granzyme A levels at resting (Figure

6.19A-B). Granzyme A levels decreased (p= 0.0003) for αCD3/28 beads compared to αCD3 beads. Granzyme A levels were also significantly decreased (p = 0.0008) with αCD3/28/161 beads compared to αCD3/28 beads, but no significant change with addition of αCD161 was seen at any other activation conditions (Figure 6.19).

6.4.13 CD161 ligation decreased Granzyme K expression with αBiotin bead activation but not with FATAL assay

It was noted that MAIT cells of most donors had fairly high Granzyme K levels at resting. (Figure 6.20A-B)

In the FATAL assay setup addition of αCD161 mAb had no effect on the expression levels of Granzyme K (Figure 6.17). However, when αBiotin activations beads were used to activate $CD8^+$ enriched cells Granzyme K levels decreased (p< 0.0001) for αCD3/28 beads compared to αCD3 beads. Granzyme K levels were significantly decreased (p = 0.017) with αCD3/28/161 beads compared to αCD3/28 beads, but no significant change was seen with addition of αCD161 at any other activation conditions (Figure 6.20).

Figure 6.17

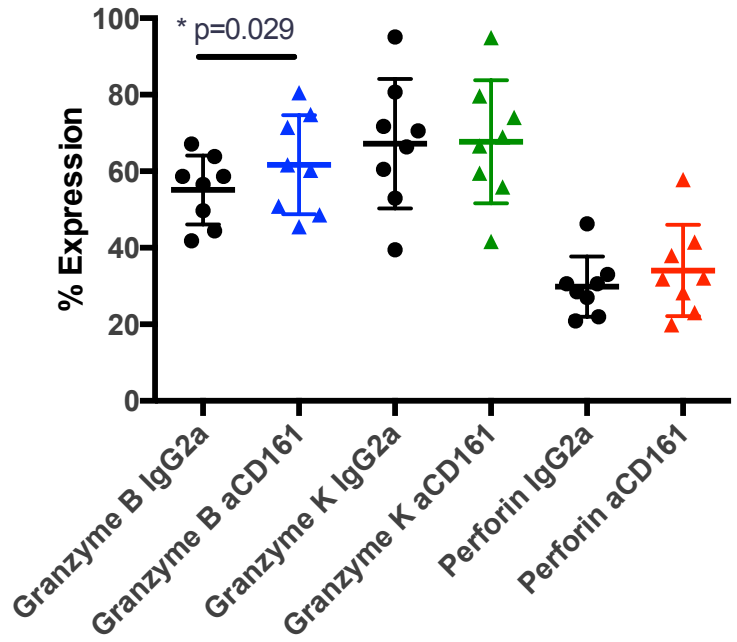

CD161 cross-linking increased Granzyme B expression on cells activated with *E. coli* activated B cells

PBMCs co-cultured with an *E. coli* activated B cell line along with IgG2a or αCD161 mAbs and stained surface and internally with Granzyme B, Granzyme K or Perforin. Samples gated on $CD8^+$ $CD161^+$ $Va7.2^+$ cells. Statistical analysis: One way ANOVA with Bonferroni's multiple comparisons (n=8)

010513 Granzyme T.pzfx

Figure 6.18

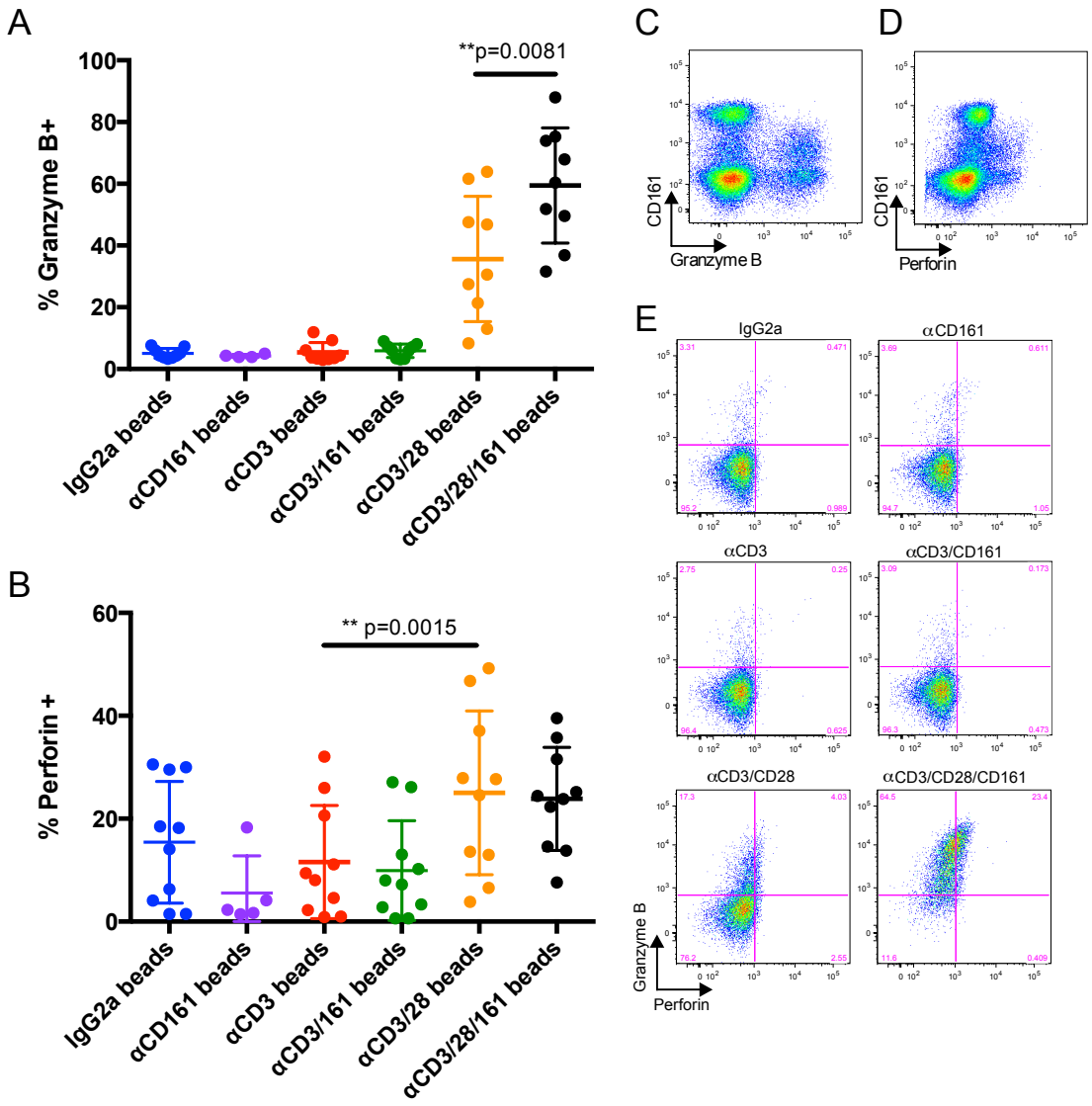

CD161 cross-linking with αbiotin activation beads increased Granzyme B expression and had no effect on Perforin expression

$CD8^+$ selected cells gated on $Va7.2^+$ cells in response to αbiotin activation beads (see material and methods Figure 6.1 for bead design on page 144) for 18hr Statistical analysis: One way ANOVA with Bonferroni's multiple comparisons **(A)** Granzyme B expression (n= 5 or 10) **(B)** Perforin expression (n= 5 or 10) **(C)** Raw data of $CD8^+$ selected cells activated by IgG2a beads and stained for Granzyme B. **(D)** Raw data of $CD8^+$ selected cells activated by IgG2a beads and stained for Perforin. **(E)** Representative raw data of $Va7.2^+$ $CD8^+$ cells stained for Granzyme B and Perforin for one donor for each bead in A & B

200613 & 120713 Granzyme.pzfx 120703 Granzyme B.jo

Figure 6.19

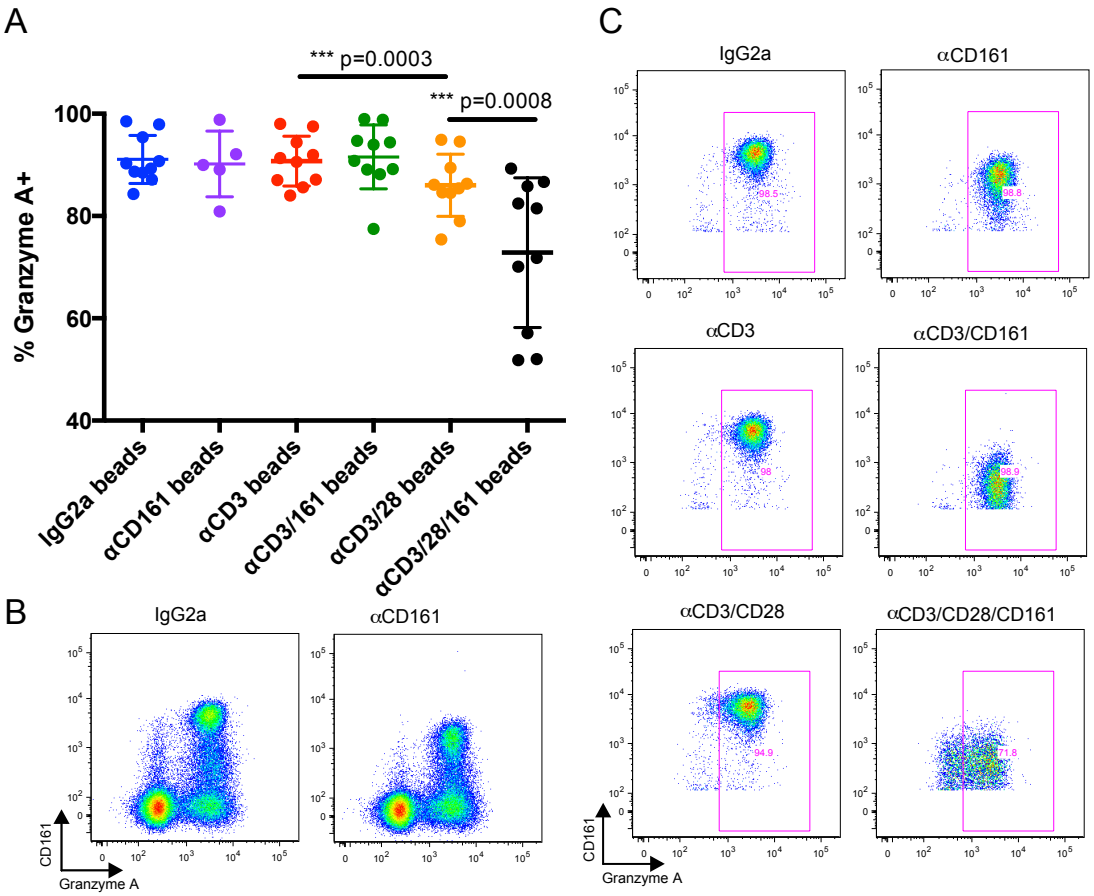

CD161 cross-linking with αbiotin activation beads decreased Granzyme A expression
(A) CD8 selected cells gated on Va7.2^{+} cells in response to activation beads (see material and methods Figure 6.1 for bead design on page 144) for 18hr and stained surface and internally for Granzyme A expression (n= 5 or 10) Statistical analysis: One way ANOVA with Bonferroni's multiple comparisons **(B)** CD8^{+} selected cells activated by IgG2a (left) or αCD161 (right) beads and stained surface and internally for Granzyme A expression **(C)** Representative raw data of Va7.2^{+} CD8^{+} cells from one donor stained for Granzyme A for each bead in A
200613 & 120713 Granzyme.pzfx 120713 Granzyme A.

Figure 6.20

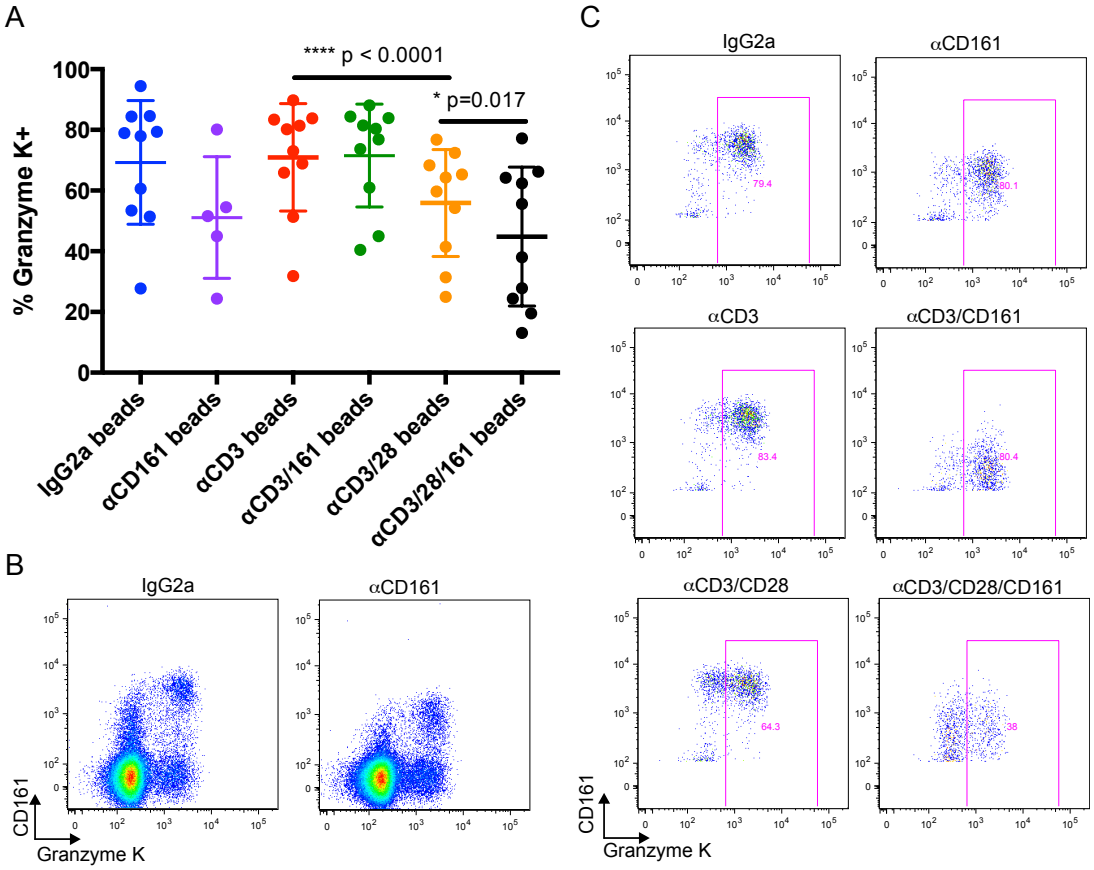

CD161 cross-linking with αbiotin activation beads decreased Granzyme K expression
(A) CD8 selected cells gated on Va7.2$^+$ cells in response to activation beads (see material and methods Figure 6.1 for bead design on page 144) for 18hr and stained surface and internally for Granzyme K expression (n= 5 or 10) Statistical analysis: One way ANOVA with Bonferroni's multiple comparisons **(B)** CD8$^+$ selected cells activated by IgG2a (left) or αCD161 (right) beads and stained surface and internally for Granzyme K expression **(C)** Representative raw data of Va7.2$^+$ CD8$^+$ cells from one donor stained for Granzyme K for each bead in A
200613 & 120713 Granzyme.pzfx 120713 Granzyme K.jo

6.4.14 CD161 ligation reduced MAIT cell proliferation

To determine if ligation of CD161 had an impact on the proliferative response of CD161$^+$ CD8$^+$ cells, CTV stained PBMCs were co-incubated with irradiated 300-Null or 300-LLT1 cell lines and nothing, αCD3/28 Dynabeads, IL-12, or IL-12/IL-18 for 5 days. Resting cells and cells activated with IL-12/IL-18 did not proliferate well. IL-12 alone induced low amounts of proliferation and αCD3/28 Dynabeads induced large amounts of proliferation. The addition of 300-LLT1 cells slightly reduced proliferation in αCD3/28 Dynabead activated cells ($p = 0.0337$) and in IL-12 activated

cells (p = 0.0205). No statistically significant change was seen for resting or IL-12/IL-18 stimulated cells (Figure 6.21). It was noted that although the total amount of proliferation was reduced, the number of rounds of replication did not change significantly (Figure 6.21B).

Figure 6.21

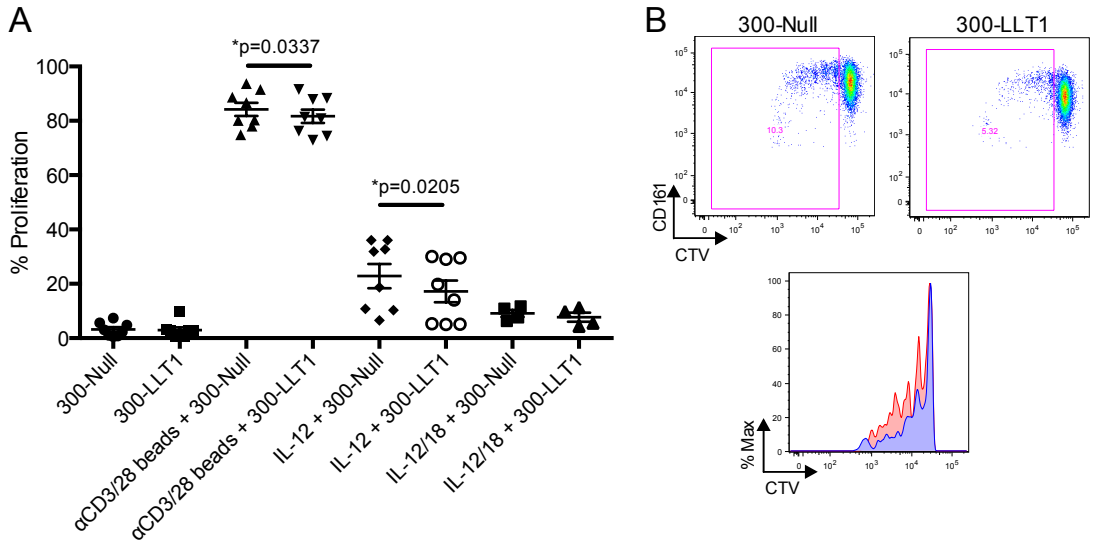

CD161 ligation with LLT1 decreased proliferation on αCD3/28 stimulated MAIT cells
(A) PBMCs stained with CTV to track cell proliferation and co-cultured with 300 or LLT1 cell line and indicated activation (αCD3/28 Dynabeads, IL-12, IL-12/18) for 5 days. **(B)** (Top) Representative raw data of IL-12 activated 300 and LLT1 from one donor and stained with CTV to track cell proliferation. Samples gated on $CD8^+$ $CD161^+$ $Va7.2^+$ cells. (Bottom) Overlay of the proliferation portion of 300 (red) and LLT1 (blue) from above.
260313 010513 T.pzf 010513 Proliferation.jo

I looked at the proliferative response again using the αbiotin activation beads. Resting cells did not proliferate much, but beads with both αCD3 and αCD3/28 induced good proliferation by PBMCs. αCD3/161 beads decreased proliferation (p = 0.0072) compared to αCD3 beads, and αCD3/28/161 decreased (p = 0.017) compared to αCD3/28 beads (Figure 6.22). It was noted that the rounds of proliferation undergone did not significantly change with the addition of αCD161, even when the total proliferation amounts were reduced (Figure 6.22C).

Figure 6.22

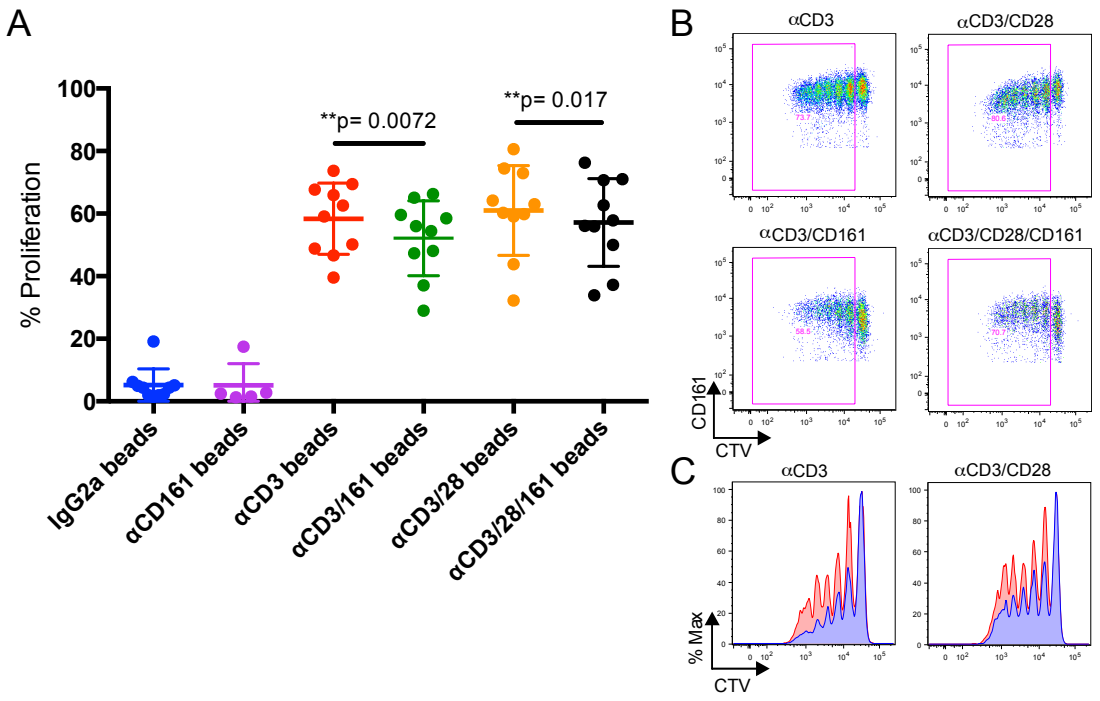

CD161 cross-linking with αbiotin activation beads decreased proliferation on MAIT cells stimulated with αCD3 or αCD3/28
(A) Proliferation of $CD8^+$ selected cells stained with cell tracker violet (CTV) to track cell proliferation and co-cultured with αbiotin activation beads (see material and methods Figure 6.1 for bead design on page 144) for 5 days. Cells gated on $Va7.2^+$ cells **(B)** Representative raw data of one donor for activations in A surface stained for CTV and surface and internally for CD161. **(C)** Overlay of the proliferation gate in the stated stimulation bead (red) and stimulation bead with αCD161 added (blue) as seen in raw data from B.
260613 170713 proliferation.pzfx 260613 Proliferation.jo

6.4.15 CD161 cross-linking increased MAIT cell apoptosis

The decrease in total proliferation, without a decrease in rounds of proliferation, led to concern that the decrease in proliferation was due to cell death instead of changes in proliferative capacity. This was of particular concern as $CD161^+$ $Vα7.2^+$ cells have been shown to be prone to activation induced cell death. (Cosgrove 2013) Thus, I tested the levels of activated caspase 3 in activated cells, as a marker for live cells undergoing apoptosis. PBMCs were co-incubated with *E. coli* activated BCL or mock activated BCL along with nothing, a positive control Staurosporine, IgG2a mAb or αCD161 mAb. With the addition of αCD161 mAb, the amount of activated caspase 3 increased significantly ($p = 0.0004$) for $CD161^+$ $Vα7.2^+$ cells

(Figure 6.23). However, it was particularly interesting to note that amount of activated caspase 3 was significantly lower on Vα7.2$^-$ than Vα7.2$^+$ cells and αCD161 mAb did not significantly change activated caspase 3 levels for CD161$^+$ Vα7.2$^-$ cells (Figure 6.23A).

Figure 6.23

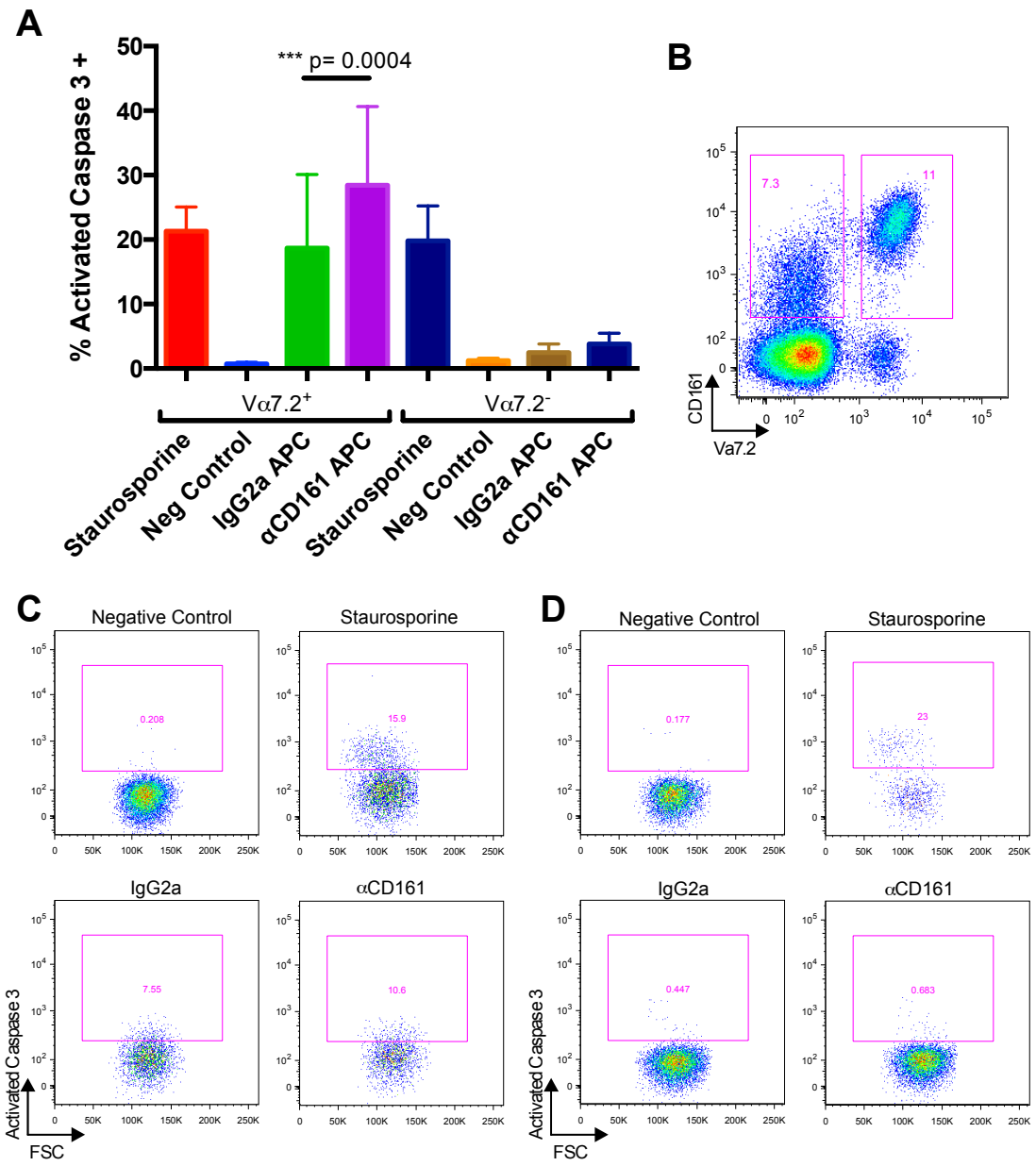

CD161 cross-linking increased activated caspase 3 on MAIT cells stimulated with *E. coli* activated B cells

(A) PBMCs co-cultured with an *E. coli* activated B cell line along with positive control Staurosporine, negative control, IgG2a-APC or αCD161-APC free mAbs for 24 hours and then stained for activated caspase 3. Samples gated on $CD8^+$ $CD161^+$ $V\alpha7.2^+$ or $V\alpha7.2^-$ cells. **(B)** Representative raw data of $CD8^+$ of $V\alpha7.2^+$ and $V\alpha7.2^-$ gates used in A. **(C)** Raw data graphs of $V\alpha7.2^+$ from one donor in A. **(D)** Raw data graphs of $V\alpha7.2^-$ from one donor in A.
220513 Caspase 3.pzfx 220513 Caspase 3.jo (B) 260613 Proliferation.jo

The effect of CD161 cross-linking on activated caspase 3 was tested again on $CD8^+$ selected cells co-incubated for 18 hours with an activation bead set and staurosporine as a positive control. αCD3 beads did not induce more activated

caspase 3 compared to resting cells but αCD3/28 beads did induce activated caspase 3. αCD3/28/161 significantly increased (p = 0.0036) activated caspase 3 levels compared to αCD3/28 alone (Figure 6.24).

Figure 6.24

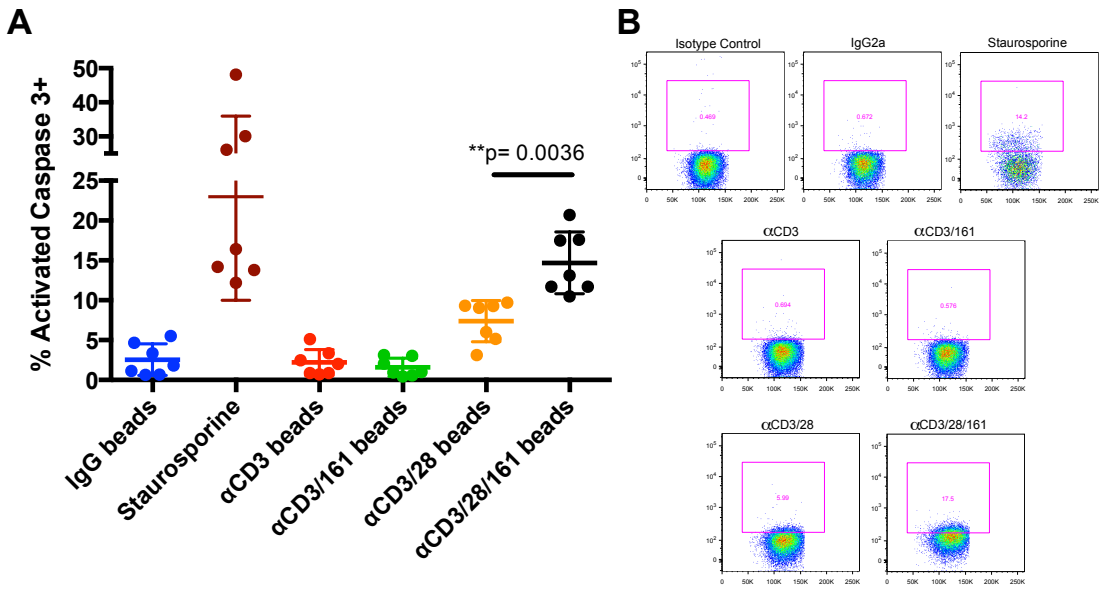

CD161 cross-linking with αbiotin activation beads increased activated caspase 3 on MAIT cells stimulated with αCD3/28

(A) Activated Caspase 3 expression by CD8 selected cells gated on Va7.2^{+} cells in response to αbiotin activation beads (see material and methods Figure 6.1 for bead design on page 144) for 18hr and stained for activated Caspase 3. (n= 7) **(B)** Representative raw data of one donor for each bead in A and isotype control.

Caspase3 250613.pzfx 250613 Caspase3.jo

6.5 Discussion

6.5.1 The effects of CD161 ligation on IFNγ and TNFα expression

Previously published investigations on the effect of CD161 ligation on T cells have been conflicting. Exley *et al*. found CD161 ligation increased IL-4 and IFNγ production, or had no effect on cytokine production depending on the stimulation used for the cells (Exley et al. 1998). Aldemir *et al*. and Pozzo *et al*. found increased IFNγ production (Aldemir et al. 2005; Pozzo et al 2006). Rosen *et al*. 2008 found no effect on IFNγ and TNFα or a decrease in TNFα depending on the type of stimulation used (Rosen 2008).

Based on Exley *et al.* and Pozzo *et al*., early experiments were designed using plate bound CD3, CD28 and CD161 looking at IFNγ production (Exley et al. 1998; Pozzo et al. 2006). Cells cross-linked with αCD161 mAb alone did not produce IFNγ. αCD3/28 stimulated $CD8^+$ cells indicated that specifically at 0.25ug of αCD161 mAb could inhibit IFNγ production. However, a similar inhibition was not seen in $CD4^+$ cells. This led to me to question to the validity of the inhibition. The lack of activation by αCD161 mAb alone agrees with Aldemir *et al*., but is opposite to what was seen when αNK1.1 mAb is cross-linked on mouse NKR-$P1^+$ cells (Aldemir et al. 2005; Arase et al. 1996). Furthermore, there was also an issue with the reproducibility of the assays.

To address these concerns alternative methods were tested:

- Activation using IL-12/IL-18, αCD3/28 Dynabeads or free αCD161 mAb, were compared to plate bound αCD161 mAb.
- CD161 cross-linking with LLT1 expressing cell line, 300-LLT1, and

the control cell line 300-Null were compared with αCD161 mAb.

- To improve the analysis of the IFNγ expressing cells I took advantage of a newly available anti-Vα7.2 mAb that allowed the specific identification of the $CD161^{++}$ MAIT cell population.

None of the methods tested resulted in a statistically significant change in IFNγ or TNFα production for $CD8^+$ $CD161^+$ $V\alpha7.2^+$ (MAIT) cells. However, activation using the αCD3/28 Dynabeads and CD161 cross-linking with the free αCD161 mAb, consistently resulted in a lower IFNγ expression, although this never reached statistical significance. Furthermore, the reduction in the IFNγ production was also observed in the $CD4^+$ T cell population, further reinforcing this possibility.

This raised the question of a possible effect being stronger when the CD161 ligation was in the context of TCR stimulation. If the impact by CD161 ligation could only be seen when this occurred directly with TCR stimulus, this might explain the lack of an effect seen by Exley *et al*. when they used PMA/I (Exley et al. 1998). To address this, activation beads, with either αCD3 or αCD3/28 mAb bound, were generated and onto which the αCD161 mAb as added. Surprisingly, under these conditions a very clear statistically significant increase in production of IFNγ and TNFα was observed. This was reproducible over multiple patients in independent experiments, and using different batches of beads. Although this result appears to be opposite of the results found using the plate bound αCD161 mAb, technically these data were more reproducible and the effect was statistically stronger. Furthermore, this also follows published results of increased cytokine production when any significant change was seen (Exley et al. 1998; Aldemir et al. 2005; Pozzo et al. 2006).

The differences in IFNγ production seen between plate bound and bead bound activation may be due to the concentrations of αCD161 or αCD3/28 being different. The plate bound experiments had 0.25ug of αCD161 mAb plated and the activation beads had αCD161 mAb at the concentration of 10ug/ml. In future experiments, beads with lower concentrations of αCD3, αCD28, and αCD161 could be used to further examine this question.

Experiments using PBMCs stimulated with IL-12 and IL-18 showed no effect on IFNγ expression when bead bound αCD161 mAb was used to cross-link CD161. This suggested that the type of stimulation, and not just the concentration of the αCD161 cross-linking mAb, was important in determining the effect cross-linking CD161 had on a T cell. Specifically the T cell required an activation signal from an activated TCR, although it is possible that alternate cell activation signals could exist that would allow similar effects on cytokine expression.

6.5.2 IL-22 and IL-17a expression was low and not clearly affected by CD161 cross-linking

Although IL-22 and IL-17a can be produced by $CD8^{+}$ $CD161^{++}$ cells, under the short-term stimulations and conditions used, the levels of production found were extremely low. With the extremely low levels of production, any inhibition in production by CD161 would be very difficult to observe and any increases might be hidden if the levels were artificially low due to technical issues. Based on this it is difficult to make any clear conclusions about the effect to CD161 ligation on IL-22 or IL-17a production.

6.5.3 CD161 cross-linking increased specific cell killing in the FATAL Assay

$CD8^+$ T cells are known for the ability to be cytotoxic. The FATAL assay was chosen for its ability to specifically activate the $CD8^+$ $CD161^{++}$ cells in the assay and test the killing capacity of only $CD161^{++}$ cells against bacterially activated cells. The FATAL assay showed $CD8^+$ $CD161^{++}$ cells are capable of killing, and ligation with αCD161 mAb, significantly increased the killing capacity of these cells. The specificity of this was further confirmed by the ability of αMR1 mAb to block the killing capacity of the $CD8^+$ $CD161^{++}$ cells.

6.5.4 Degranulation and Activation were increased by CD161 ligation

With increased specific killing upon CD161 ligation, I wanted to test possible mechanisms behind this. Degranulation (CD107a) was increased, along with the level of activation (as determined by CD69 expression), when T cells were activated by the αCD3/28 Dynabeads in the presence of the αCD161 mAb compared with αCD3/28 Dynabeads alone.

A second method of cell activation, through αbiotin activation beads, confirmed the increased degranulation and activation when αCD161 mAb was added. CD69 expression increased more between αCD3 and αCD3/161 beads than with αCD3/28 and αCD3/28/161. The lower increase with αCD3/28/161 might be due to CD69 levels being extremely high to begin with; so increased activation could only increase CD69 expression slightly. However, CD107a expression increased to a much larger degree between αCD3/28 beads and αCD3/28/161 beads than between αCD3 beads and αCD3/161 beads.

CD161 ligation enhanced the activation levels or expression levels of cells slightly above what the cell would normally do at that level of stimulation instead of inducing production of a specific molecule. This indicated that the role of CD161 ligation acted as a co-stimulatory molecule in a similar fashion as CD28, but the co-stimulatory effects of CD161 ligation were less potent than CD28.

6.5.5 The effects of CD161 ligation on Granzymes and Perforin Expression

Degranulation is a marker for cytotoxicity, but relies on the presence of the effector molecules such as perforin and granzymes found within the granules to actually induce the cytotoxicity. Therefore, the type and quantities of granzymes and perforin produced by the cells was important. Previous studies have shown $CD8^+$ $CD161^+$ cells to produce low levels of Granzyme B (Northfield et al. 2008; Billerbeck et al. 2010), and the levels of perforin produced are contested (Takahashi et al 2006; Northfield et al. 2008; Billerbeck et al. 2010). However, using the same stimulation as the FATAL assay, E. coli stimulated BCL, Granzyme B, perforin and Granzyme K were all produced by $CD8^+$ $CD161^+$ $V\alpha7.2^+$ (MAIT) cells. The addition of αCD161 mAb further increased the levels of Granzyme B, but no significant changes were seen in perforin or Granzyme K expression.

The αbiotin activation beads were used to further examine the production of granzymes and perforin. At rest $CD8^+$ $CD161^+$ $V\alpha7.2^+$ cells did not express Granzyme B, perforin levels were slightly variable, however, Granzymes A and K were highly expressed. This follows what was previously published (Takahashi et al. 2006; Northfield et al. 2008; Billerbeck et al. 2010). The addition of αCD3 activation alone did not change this profile significantly. However, αCD3/28 activation did

significantly change the profile. Granzyme B production increased significantly and Granzymes A and K production decreased significantly. This indicated that the change in production levels required very specific types of activation, such as the activation signals that occur with TCR stimulation. CD161 ligation further enhanced the increases or decreases already seen with the TCR activation signal.

This follows what was seen in a microarray published by Billerbeck *et al*. where PMA/I activated $CD8^+$ $CD161^{++}$ cells significantly increased Granzyme B mRNA, and significantly decreased Granzymes A and K mRNA when compared to resting $CD8^+$ $CD161^{++}$ cells (Billerbeck et al. 2010). This also adds to the theory that CD161 ligation induces a co-stimulatory effect on T cells.

6.5.6 Proliferation of MAIT cells was inhibited by CD161 ligation

Takahashi *et al*. showed αCD3/28 stimulated $CD8^+$ $CD161^+$ cells to not proliferate at all (Takahashi et al. 2006), and another study indicated that $CD161^+$ cells proliferated but less so than $CD161^-$ cells (Northfield et al. 2008). I found $CD8^+$ $CD161^{++}$ cells did proliferate with αCD3/28 or αCD3 stimulation, although not as well as $CD8^+$ $CD161^-$ cells. Our group has also found that $CD8^+$ $CD161^{++}$ cells readily proliferate in response to IL-12 stimulation. However, when IL-12 was combined with IL-18, the proliferation was inhibited (unpublished data).

Ligation of CD161, by both LLT1 and αCD161 mAb, decreased proliferation levels when the activation of the stimulus induced proliferation. Interestingly, the reduction in proliferation appeared to come from a reduction in the number of cells proliferating but not the number of rounds of replication replicating cells underwent. This led to the questioning if the lower proliferation levels were due to fewer cells initiating proliferation or cell death left fewer cells able to proliferate. MAIT cells

have been shown to be prone to activation induced cell death (Cosgrove et al. 2013), thus I examined the levels of apoptosis that occurred.

6.5.7 CD161 ligation increased apoptosis on MAIT cells

The proportion live of cells undergoing apoptosis was examined by staining for activated caspase 3. $CD8^+$ $CD161^+$ $V\alpha7.2^+$ (MAIT) cells activated with either *E. coli* activated BCL or αCD3/28 activation beads expressed activated caspase 3. CD161 ligation further increased the levels of activated caspase 3 expressed by MAIT cells. Interestingly, $CD8^+$ $CD161^+$ $V\alpha7.2^-$ cells did not highly express activated caspase 3 upon activation with *E. coli* activated BCL or αCD3/28 activation beads, and CD161 ligation also did not increase expression levels.

Since the activated caspase 3 experiment was gated on live cells the experiment showed the cells undergoing apoptosis but not yet "dead". The potential exists for many cells to have already died causing the actual amount of death to be underestimated.

6.5.8 Summary of Functional effects of CD161 ligation on activated $CD8^+$ T cells

The most robust and repeatable results from this chapter indicated that CD161 ligation induced increased levels of IFNγ expression, TNFα expression, activation (CD69), Granzyme B expression, degranulation and apoptosis along with decreased Granzyme A expression, Granzyme K expression, and proliferation (Figure 6.25).

Figure 6.25

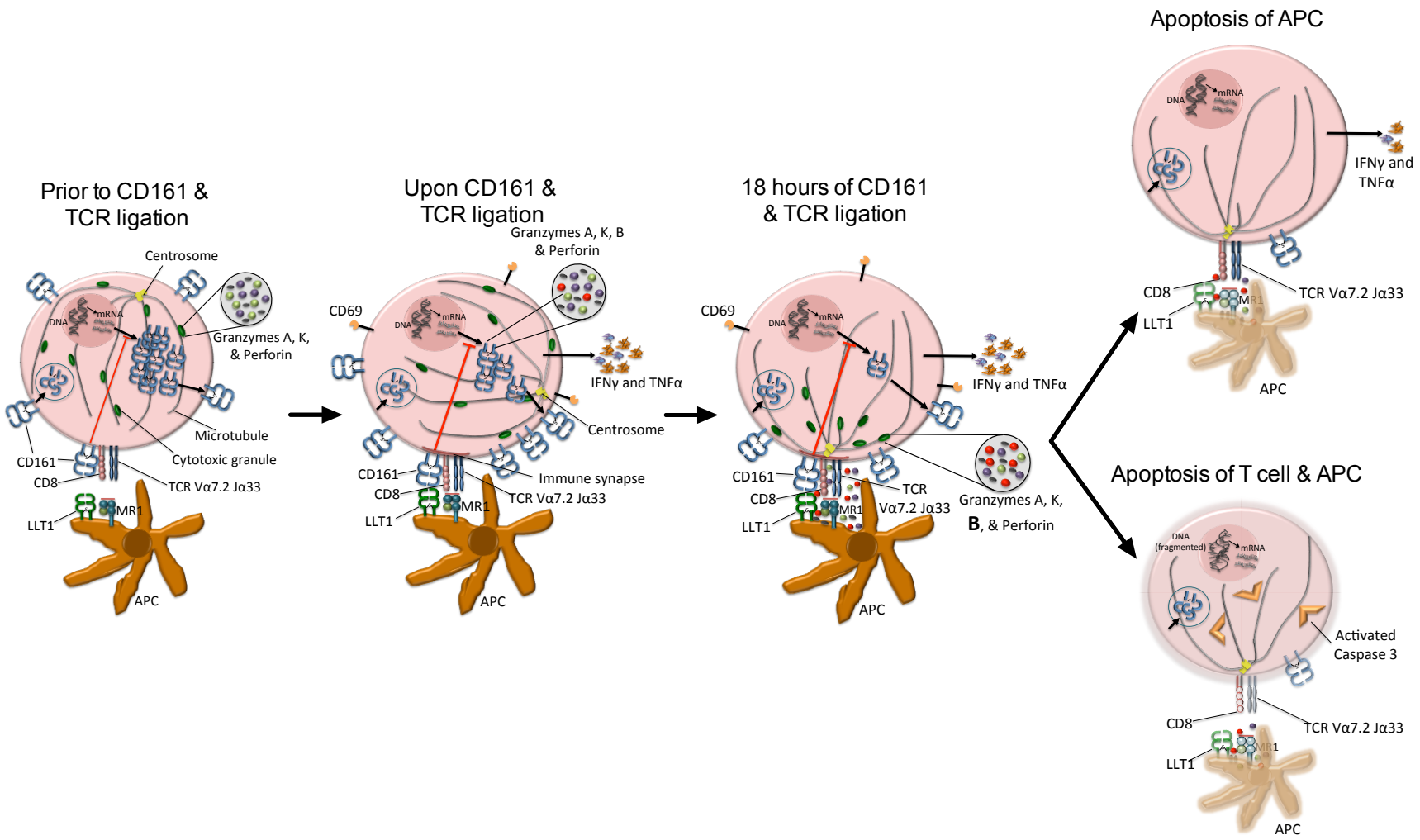

Summary of functional effects of CD161 ligation on MAIT cells

6.5.9 Potential Mechanism for functional effects CD161 ligation on T cells

On the surface, the induction of increased cytokine production, activation and degranulation upon CD161 ligation seemed at odds with decreased proliferation and increased apoptosis. However, this discrepancy could be explained by CD161 ligation inducing an increase of ceramide and the effects ceramide had on a cell.

Pozzo *et al*. 2006 found that ligation of CD161, through αCD161 mAb, induced an increase in acid sphingomyelinase (aSMase) and the increased aSMase activity was linked with increased N-acyl-sphin-gosine (ceramide) (Pozzo et al. 2006). At low levels with short-term exposure ceramide increased cell activation, increased TCR expression (Menné et al. 2000) and prevented apoptosis (Flores et al. 1998). The increase in cell activation was suggested to be due to ceramide increasing lipid membrane fluidity and formation of lipid rafts. Lipid rafts can help bring co-stimulatory molecules together, quickly and in a protected environment. This allowed for increased signaling or lowering of the threshold necessary for signaling (Viola 2001, Grassmé et al. 2001, Cremesti et al. 2001).

If the increased ceramide promotes lipid rafts that decreased the TCR threshold signal required or boosted the availability of co-stimulatory molecules, this would explain the co-stimulatory effect seen with CD161 ligation, which was weaker than the CD28 co-stimulatory effect. This would also explain the need for a TCR activation signal and why IL-12+ IL-18 stimulated cells showed no difference in cytokine production upon CD161 ligation.

However, the effects of ceramide on cells appeared to be dose and time dependent. At high levels or with long-term exposure ceramide inhibited proliferation

(O'Byrne 2000), increased AICD, increased apoptosis (Flores et al. 1998), activated caspases, and downregulated TCR expression (Menné et al. 2001). Interestingly, one study showed high levels of ceramide inhibited proliferation, but the inhibition was to the early stages of proliferation and the ceramide did not abrogate all signals from the TCR, including the up-regulation of CD69 (O'Byrne & Sansom 2000).

The time and dose effects could also explain the seemingly contradictory finding that CD161 ligation decreased proliferation. The proliferation experiments were done with 5 days of high levels of CD161 stimulation, which would likely induce extremely high ceramide levels. The non-physiological levels of CD161 ligation that occurred with αCD161 mAb binding all available surface CD161 or LLT1 transfected cell lines incubated with enriched $CD8^+$ T cells at a 1:1 ratio could also induce higher than normal ceramide levels.

These high dosage effects of ceramide might have skewed the results to indicate more inhibition of proliferation and more apoptosis from CD161 ligation than would normally be seen. However, the potential for these inhibitory results may reflect what is possible if LLT1 is highly expressed in a tissue or in a disease state. More testing would need to be done to determine the levels of ceramide induced by CD161 expression, and at what thresholds of ceramide activation or inhibition responses occur in T cells.

The theory that CD161 ligation increased ceramide levels could explain the results reported in this chapter of increased levels of cytokine production, activation, degranulation and cell death along with decreased proliferation. This further supports the conclusion that CD161 ligation leads to a co-stimulatory modification of TCR signaling.

6.6 Summary

Functional experiments on CD161 ligation of T cells had the following results:

- CD161 cross-linking $CD8^+$ T cells with plate bound αCD3/28 and αCD161 mAb showed a statistically significant inhibition IFNγ production, but this could not be repeated with statistical significance using a more technically accurate experiment with $CD8^+$ $V\alpha7.2^+$ $CD161^+$ T (MAIT) cells.
- CD161 cross-linking of $CD8^+$ $V\alpha7.2^+$ T cells stimulated αbiotin activation beads (αCD3 or αCD3/28) statistically significantly increased IFNγ and TNFα production.
- IL-17a or IL-22 expression levels were low and CD161 ligation showed no impact on IFNγ expression.
- CD161 cross-linking significantly increased specific killing of $CD8^+$ $V\alpha7.2^+$ $CD161^+$ T (MAIT) cells.
- CD161 ligation significantly increased degranulation (CD107a) and activation (CD69) in $CD8^+$ $V\alpha7.2^+$ T cells.
- CD161 ligation significantly increased Granzyme B expression and decreased Granzymes A & K expression. This was an enhancement of the expression changes that normally occur at that level of cell activation.
- CD161 ligation induced no significant change in Perforin expression in $CD8^+$ $V\alpha7.2^+$ T cells.
- CD161 ligation decreased proliferation in $CD8^+$ $V\alpha7.2^+$ $CD161^+$ T (MAIT) cells.
- CD161 cross-linking increased cell apoptosis as indicated by activated caspase 3 in $CD8^+$ $V\alpha7.2^+$ T cells.

The strongest and most reproducible of these results together indicated that ligation of high levels of CD161 on $CD8^+$ $V\alpha7.2^+$ $CD161^+$ T (MAIT) cells led to a co-stimulatory signal that was dependent on a concurrent TCR activation signal.

Chapter 7 Conclusions

7.1 Summary of Experimental Results

This thesis has investigated the functional consequences of CD161 ligation on T cells. In the first investigative chapter soluble ligand of CD161 was designed, produced, and initial binding and functional tests were carried out. In the second investigative chapter the kinetics of CD161 expression patterns on T cells were studied. In the third investigative chapter a gene microarray was conducted comparing T cells with ligated CD161 with T cells that were not ligated. In the final investigative chapter, activated T cells were studied for functional changes upon CD161 ligation.

7.1.1 Production of Soluble CD161 ligands

Two protein ligands were reported to bind CD161: LLT1 and PILAR. Soluble versions of the external domains of both proteins were designed. A soluble, differentially glycosylated version of the PILAR protein was produced and purified. I was unable to produce enough soluble LLT1 protein for purification. However, alternate sources of LLT1 protein were available both commercially and from a collaborator.

Unexpectedly, the soluble PILAR protein did not bind to $CD3^+$ cells, but did bind to $CD19^+$ cells. Further investigation showed PILAR binding predominately, but not exclusively, to B cells with more immature maturation states. Co-incubating activated $CD8^+$ T cells with soluble PILAR protein induced a decrease in IFNγ expression. However, the decrease in IFNγ was not specific to $CD161^+$ cells.

Since PILAR did not bind $CD3^+$ cell, which includes T cells, and the decrease in IFNγ was non-specific to $CD161^+$ T cells, this indicated that PILAR might not functionally bind $CD161^+$ T cells. Around the same time as these results were discovered, several other studies were published indicating that PILAR was not a ligand of CD161 (Spreu et al. 2010; Germain et al. 2010; Kamishikiryo et al. 2011). Based on these results, the functional effects of PILAR ligation on $CD161^+$ T cells were not pursued further.

7.1.2 CD161 expression patterns on T cells

CD161 is expressed on both $CD4^+$ and $CD8^+$ T cells. $CD8^+$ T cells had populations of $CD161^+$ and $CD161^{++}$ cells. $CD8^+$ $CD161^+$ T cells express CD161 on the surface, but also express significant amounts internally.

Ligation of CD161 induced both time and dose dependent downregulation of surface and internal CD161 expression. Downregulation of CD161 occurred when CD161 was ligated with LLT1 protein, and when cells were cross-linked by CD161 mAbs. However, the rate and strength of the downregulation was dependent on the clone of the αCD161 mAb used. After ligation-induced CD161 downregulation, removal of the ligand led to recovery of CD161 expression levels. Interestingly, the downregulation of CD161 protein expression was not regulated at the level of mRNA expression.

7.1.3 Gene microarray analysis of the effects of CD161 ligation on $CD8^+$ $V\alpha7.2^+$ T cells

Since CD161 ligation induced downregulation of CD161 expression without further cell activation required, a gene microarray was performed that compared non-

activated $CD8^+$ $V\alpha7.2^+$ T cells CD161 ligated by LLT1 to cells without CD161 ligated. IPA software analysis of the microarray results did not show any pathways where central parts of the pathway were clearly up or downregulated.

From the microarray, a subset of genes with highly ranked p-values were chosen for confirmation by real-time qPCR. However, significant upregulation or downregulation of gene expression could not be confirmed for any of the chosen genes.

Further analysis of the gene microarray data showed most of the highly significant responses had probes that were found at very low intensities. Low intensity fluorescence of probes significantly increases the chances of false positives (Patterson et al. 2006). When the microarray data was re-evaluated, discounting probes with low intensity values, very few genes were significantly changed. Of these, two had already been tested by real-time qPCR and were not significantly changed, indicating the genes were false positives.

The lack of reliably differentially expressed genes leading to clearly activated protein pathway(s) or groups of genes with similar functions indicated that CD161 ligation, in the absence of additional co-activation of the cells, did not have a major functional affect on T cells. Therefore, the gene microarray results were not perused further.

7.1.4 Functional effects of CD161 ligation on activated $CD8^+$ $V\alpha7.2^+$ T cells

Although no clear functional effect of CD161 ligation could be determined from the gene microarray of non-activated $CD8^+$ $V\alpha7.2^+$ T cells, functional effects of CD161 ligation could be seen on TCR stimulated $CD8^+$ $V\alpha7.2^+$ T cells.

The expression levels of IFNγ and TNFα significantly increased when αCD161 mAb induced ligation occurred in the same location as TCR simulation. Interestingly, when cells were activated with IL-12 and IL-18, αCD161mAb stimulation did not significantly affect IFNγ or TNFα expression. This indicated that the functional effects on cytokine production by $CD8^+$ $V\alpha7.2^+$ T cells required specific stimulation, such as TCR, in close proximity to CD161 ligation.

In the context of TCR stimulation, CD161 ligation also induced significantly increased levels of CD69 expression and degranulation. Along with significantly increased degranulation, the levels of Granzyme B expression significantly increased, while Granzyme A and Granzyme K levels significantly decreased. A similar pattern of changing granzyme expression occurred in αCD3 and αCD28 activated cells; however, the addition of CD161 ligation further increased the rate of change in granzyme expression. Along with the change in granzyme expression, there was significant increase in the cytotoxic ability of the $CD8^+$ $V\alpha7.2^+$ T cells.

Also co-stimulation via the TCR and CD161 resulted in a significant decrease in the levels of proliferation by the $CD8^+$ $V\alpha7.2^+$ $CD161^+$ T cells, as determined by CTV dilution assay. However, the decreased proliferation might have been due the cells undergoing significantly more apoptosis, which was marked by increased activated caspase 3.

7.1.5 Summary of all results

In total, the results of all of the investigative chapters combined indicated that CD161 ligation, on TCR activated $CD8^+$ $V\alpha7.2^+$ T cells, and functioned as a specific co-stimulatory molecule, which increased the kinetics or levels of activation of the cells. It is possible that the increased activation occurred through a lowering of the TCR activation threshold of the cell. The increased activation due CD161 ligation required TCR signaling, as CD161 signaling alone had no affect on the cells, nor was an increased activation seen in cells activated with IL-12 + IL-18.

7.2 Caveats of this study

As with most experimental studies, there are caveats that must be taken into account when applying the results from this study. The three main caveats of this study are: 1) that the experiments in were conducted with non-physiological levels of activation, 2) that the study focused on LLT1 or αCD161 mAbs to ligate CD161, but other unknown ligands with alternate functional effects may exist, and 3) that in-vitro experiments do not always accurately predict effects in-vivo.

7.2.1 Non-physiological levels of activation were used

The experiments in this thesis were conducted with cells that were activated at much higher levels than a physiological level. When CD161 was ligated, either a LLT1 transfected cell line or αCD161 mAbs were used. The LLT1 transfected cell lines over-expressed surface LLT1 at much higher level than has been found in activated or resting PBMCs. The LLT1 transfected cell lines were also used at ratios of up to 1:1 with T cells, which is unlikely to happen within the body. The αCD161 mAbs used bind to CD161 with a much higher affinity than LLT1 or other natural

ligands are likely to, and therefore have the possibility of sending a much stronger signal compared to a natural ligand would.

Also, in most of the experiments, the TCR was stimulated with αCD3 and αCD28 mAbs at high levels of concentration. The levels of activation used were chosen for the ability to induce strong cytokine secretion or other activation effects of the T cells for the study. However, this does not accurately reflect common physiological levels of activation since cross-linking mAb were added at saturation levels and LLT1 transfected cells were used in ratios of up to 1:1 with enriched $CD8^+$ T cells.

The effects of CD161 ligation with weaker signals or on cells which have lower levels of activation may lead to different functional outcomes compared to those described in this study.

7.2.2 LLT1 may not be the only ligand of CD161

PILAR was originally thought to be a ligand of CD161, but several studies have shown PILAR to not bind CD161 (Spreu et al. 2010; Germain et al. 2010; Kamishikiryo 2011). The data in this study also support PILAR not binding CD161. However, it is possible that LLT1, which showed similar results to the αCD161 mAbs tested, may not be the only ligand of CD161. Other ligands may induce alternate effects upon ligation of CD161. An example of another C type lectin that has ligands with opposite functional effects is CD94. When CD94 binds NKG2a it induces an inhibitory signal, while CD94 binding NKG2C induces an activating signal (Houchins et al. 1997).

CD161 has also been shown to bind to various oligosaccharides (Bezouška et al. 1994; Christiansen et al. 2006), and although this was not examined in this thesis,

it is possible that oligosaccharides could block or modify the binding affinity of CD161 for protein ligands.

7.2.3 In-vitro experiments do not always accurately reflect in-vivo effects

Despite well-designed in-vitro experiments, results do not always accurately reflect in-vivo effects. One classic example was the phase I trial of TGN1412 that occurred at Northwick Park. The in-vitro data on human PBMCs with the CD28 superagonist did not show any major cytokine release or proliferative responses. However, when the drug was given to volunteers, it induced life-threatening systemic release of pro-inflammatory cytokines (reviewed by Hünig 2012).

After the tragedy of the TGN1412 trial, a closer inspection of the pre-clinical data showed that there were failures in the pre-clinical data analysis and in the design of the animal testing models. There was also not enough consideration given to data from other superantigens such as the αCD3 OKT3 mAb (Horvath et al. 2012). The TGN1412 trial serves as a reminder, that drugs that activate the immune system must be tested extremely carefully before giving to humans due to the high danger of life-threatening systemic reactions that can occur.

Under the experimental conditions in this thesis, CD161 ligation induced co-stimulatory type effects in CD8+ Vα7.2 T cells. However, under different or more physiological conditions, CD161 ligation may induce other effects.

7.3 Model of CD161 ligation on activated MAIT ($CD8^+$ $V\alpha7.2^+$) T cells

When CD161 ligation occurs in the context of TCR stimulation on MAIT ($CD8^+$ $V\alpha7.2^+$) T cells, the MAIT cells undergo enhanced activation. The enhanced activation occurred specifically in the context of TCR stimulation, so the CD161 acted as a co-stimulatory molecule.

The effects of the CD161 co-stimulation on MAIT cells include:

- increased IFNγ, TNFα, CD69 and granzyme B, and activated caspase 3 expression
- decrease in granzyme A and K expression
- increased degranulation, apoptosis, and specific killing
- decrease in proliferation

These effects on the MAIT cell are found in detail in Chapter 6 and summarized in 6.6 on page 186.

The MAIT cell uses this increased activation state to kill APCs that display MR1 and its antigen. In the experiments found in Chapter 6, the specific killing assays used the APCs as both the presentation cells and the target cells. However, in-vivo this may or may not be accurate.

Therefore, I propose a model where the increased activation induced by co-stimulation from CD161 and TCR ligation induces apoptosis of an APC or the APC and the MAIT cell by one of two pathways, which are not mutually exclusive (Figure 7.1).

In pathway 1 the MAIT cell binds an APC presenting antigen bound to MR1 and expressing LLT1. The MAIT cell and the APC maintained contact in an immune synapse as the MAIT cell become fully activated. The activated MAIT cell

degranulates and releases the granzymes and perforin from granules, which induced apoptosis of the APC. In some cases the MAIT cell also undergo apoptosis due to increased activated caspase 3 expression.

In pathway 2 the MAIT cell bound an APC presenting both antigen bound to MR1 and LLT1. Post-activation the MAIT cell, but then detaches from the MAIT cell, and targets infected cells presenting MR1 loaded with antigen. These activated MAIT cell are then able to quickly form an immune synapse with the alternate APC and degranulate, killing the target cell. However, MAIT cells, which are prone to apoptosis due to increased activated caspase 3 expression, are also vulnerable to undergo activation induced apoptosis.

Figure 7.1

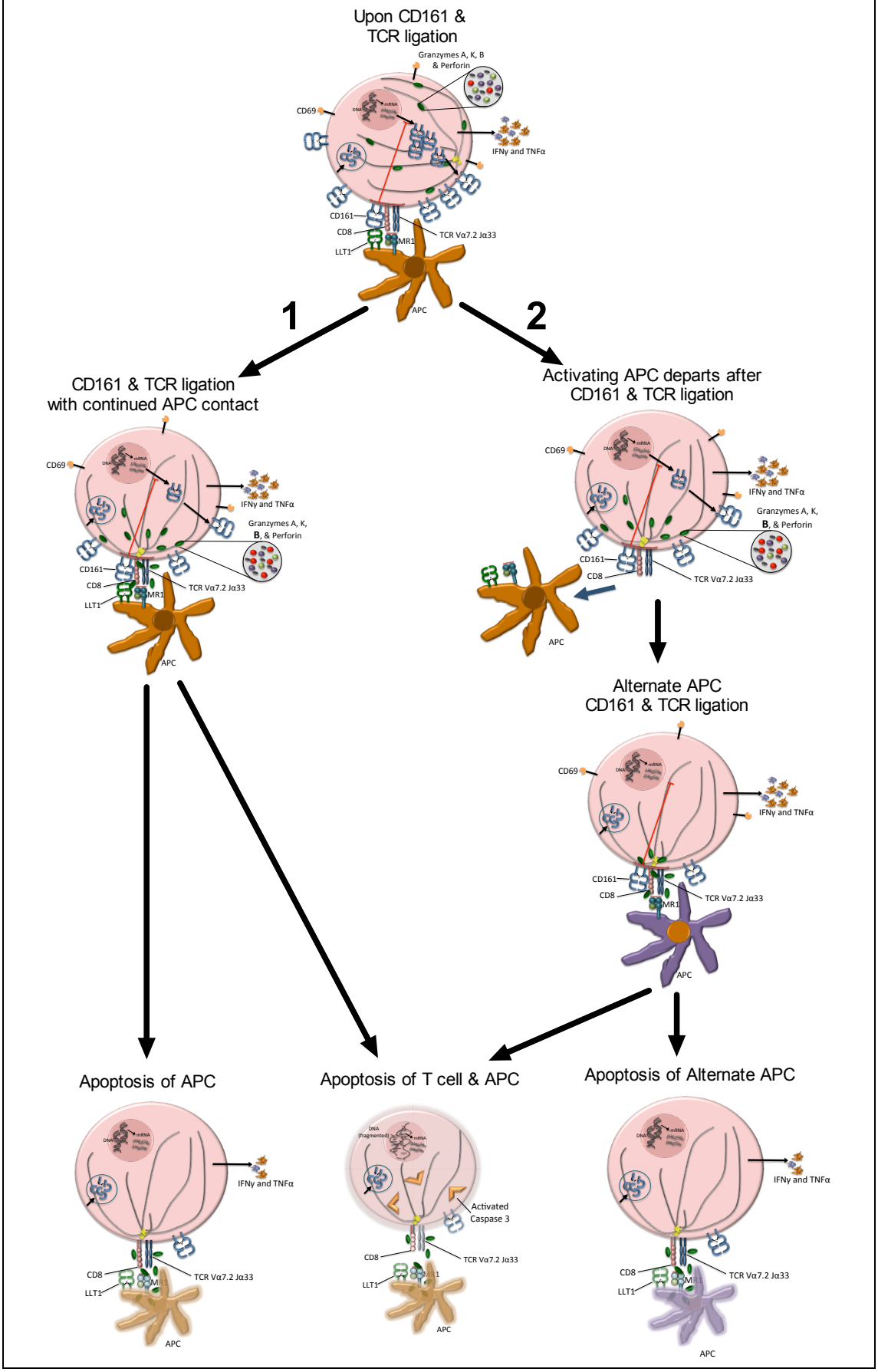
Upon CD161 & TCR ligation
Granzymes A, K, B & Perforin
CD69
IFNγ and TNFα
CD161
CD8
TCR Vα7.2 Jα33
LLT1
APC
1
2
CD161 & TCR ligation with continued APC contact
Activating APC departs after CD161 & TCR ligation
Granzymes A, K, B, & Perforin
Alternate APC CD161 & TCR ligation
Apoptosis of APC
Apoptosis of T cell & APC
Apoptosis of Alternate APC
Activated Caspase 3

Model of functional effects of TCR and CD161 ligation (figure on previous page)
In the proposed model, the TCR and CD161 must first be ligated by MR1 containing antigen and LLT1 on an APC. The MAIT ($CD8^+$ $V\alpha7.2^+$) T cell begins activation with increasing IFNγ and TNFα production, increasing granzyme B expression while decreasing granzyme A and K expression. CD69 increases and the cell begins the process of preparing for degranulation. Then one of two pathways can be followed. **(Pathway 1)** The MAIT cell remains bound to the APC, CD161 downregulation and increased degranulation occurs. Then the APC undergoes apoptosis, or both the MAIT cell and the APC undergo apoptosis. **(Pathway 2)** The MAIT cell detaches from the activating APC and the MAIT cell continues the activation process and downregulation of CD161. The MAIT cell then binds an alternative APC presenting MR1 and antigen. Then the alternative APC undergoes apoptosis or both the alternative APC and the MAIT cell undergo apoptosis.
Models.pzfx drawing figures.pptx

7.4 Future directions

As with any study, there are always more experiments that would be useful in order to better understand the results already obtained. Below are the experiments or questions following from my results that I would study in the future if given the opportunity.

- **What happens to CD161 when expression is downregulated after CD161 ligation?** In Chapter 4, it was shown that CD161 expression was downregulated after CD161 ligation on TCR activated T cells, and the regulation did not occur at the mRNA level. Further experiments could be done to study what happens to cause the downregulation of CD161 and what signals or pathways are involved. These types of experiments would be important if CD161 is targeted for treatments in any of the diseases that show changes in CD161 expression.
- **What is the effect of CD161 ligation on MAIT cells in the physiological context of APC presenting the MR1 and natural ligand along with LLT1 expression?** The experiments in this thesis were all carried out with both TCR activation and CD161 ligation occurring at levels much greater than the physiological levels. Further experiments are needed to understand what effects physiological levels of CD161 ligation has on T cells activated with MR1 and its

natural ligand. These effects of CD161 ligation at physiological levels may be very different to the results in this thesis, and it would be important to know before trying to design any type of disease treatment related to CD161.

- **Perform co-localization imaging of CD161 and TCR in the context of the immune synapse.** Since CD161 ligation in the same proximity to TCR stimulation was required for functional effects of the CD161 ligation to be seen it was hypothesized that CD161 was present in the immune synapse. Co-localization imaging experiments could confirm the location of CD161 within the synapse and provide information on the effects of CD161 downregulation on the immune synapse.
- **In what locations and under what conditions is LLT1 expressed?** Understanding the context in which CD161 could encounter LLT1 in order to be ligated would help explain what role does increased activation of $CD161^+$ T cells play in the immune system. The expression and regulation of LLT1 remains unclear. Therefore, a comprehensive study in this area would necessary to put the interaction between CD161 and LLT1 into proper context.

Overall, this study of CD161 has revealed an unexpected property of T cell co-stimulation for cytokine release and killing. Since $CD161^+$ T cells form an important component of the T cell repertoire in health and disease, this could have significance in vivo, although much further work to test this hypothesis in specific disease states is clearly needed

References

Aldemir, Hatice, Virginie Prod'homme, Marie-Jeanne Dumaurier, Christelle Retiere, Gwenola Poupon, Julie Cazareth, Franck Bihl, and Veronique M Braud. 2005. “Cutting Edge: Lectin-Like Transcript 1 Is a Ligand for the CD161 Receptor..” *The Journal of Immunology* 175 (12) (December 15): 7791–7795.

Allfrey, V G, R Faulkner, and A E Mirsky. 1964. “Acetylation and Methylation of Histones and Their Possible Role in the Regulation of RNA Synthesis..” *Proceedings of the National Academy of Sciences of the United States of America* 51 (May): 786–794.

Alt, F W, E M Oltz, F Young, J Gorman, G Taccioli, and J Chen. 1992. “VDJ Recombination..” *Immunology Today* 13 (8) (August): 306–314. doi:10.1016/0167-5699(92)90043-7.

Annibali, Viviana, Giovanni Ristori, Daniela F Angelini, Barbara Serafini, Rosella Mechelli, Stefania Cannoni, Silvia Romano, et al. 2011. “CD161(High)CD8+T Cells Bear Pathogenetic Potential in Multiple Sclerosis..” *Brain : a Journal of Neurology* 134 (Pt 2) (February): 542–554. doi:10.1093/brain/awq354.

Arase, H, N Arase, and T Saito. 1996. “Interferon Gamma Production by Natural Killer (NK) Cells and NK1. 1+ T Cells Upon NKR-P1 Cross-Linking..” *The Journal of Experimental Medicine* 183 (5): 2391–2396.

Aricescu, Alexandru Radu, Wai-Ching Hon, Christian Siebold, Weixian Lu, Philip Anton van der Merwe, and Edith Yvonne Jones. 2006. “Molecular Analysis of Receptor Protein Tyrosine Phosphatase Mu-Mediated Cell Adhesion..” *The EMBO Journal* 25 (4) (February 22): 701–712. doi:10.1038/sj.emboj.7600974.

Asyali, Musa H, Mohamed M Shoukri, Omer Demirkaya, and Khalid S A Khabar. 2004. “Assessment of Reliability of Microarray Data and Estimation of Signal Thresholds Using Mixture Modeling..” *Nucleic Acids Research* 32 (8): 2323–2335. doi:10.1093/nar/gkh544.

Aust, Jonathan G, Frances Gays, Katarzyna M Mickiewicz, Ella Buchanan, and Colin G Brooks. 2009. “The Expression and Function of the NKRP1 Receptor Family in C57BL/6 Mice..” *Journal of Immunology (Baltimore, Md. : 1950)* 183 (1) (July 1): 106–116. doi:10.4049/jimmunol.0804281.

Azzoni, L, O Zatsepina, B Abebe, I M Bennett, P Kanakaraj, and B Perussia. 1998. “Differential Transcriptional Regulation of CD161 and a Novel Gene, 197/15a, by IL-2, IL-15, and IL-12 in NK and T Cells.” *The Journal of Immunology* 161 (7): 3493–3500.

Bannister, A J, and T Kouzarides. 2011. “Cell Research - Abstract of Article: Regulation of Chromatin by Histone Modifications.” *Cell Research*.

Bauer, S, V Groh, J Wu, A Steinle, J H Phillips, L L Lanier, and T Spies. 1999. “Activation of NK Cells and T Cells by NKG2D, a Receptor for Stress-Inducible MICA..” *Science (New York, N.Y.)* 285 (5428) (July 30): 727–729.

Bengsch, Bertram, Bianca Seigel, Tobias Flecken, Julia Wolanski, Hubert E Blum, and Robert Thimme. 2012. “Human Th17 Cells Express High Levels of Enzymatically Active Dipeptidylpeptidase IV (CD26)..” *Journal of Immunology (Baltimore, Md. : 1950)* 188 (11) (June 1): 5438–5447.

doi:10.4049/jimmunol.1103801.
Bezouška, K, C T Yuen, J O'Brien, R A Childs, W Chai, A M Lawson, K Drbal, A Fiserova, M Posíšil, and T Feizi. 1994. "Oligosaccharide Ligands for NKR-P1 Protein Activate NK Cells and Cytotoxicity."
Billerbeck, E, Y H Kang, L Walker, H Lockstone, S Grafmueller, V Fleming, J Flint, et al. 2010. "Analysis of CD161 Expression on Human CD8+ T Cells Defines a Distinct Functional Subset with Tissue-Homing Properties." *Proceedings of the National Academy of Sciences* 107 (7) (February 16): 3006–3011. doi:10.1073/pnas.0914839107.
Boles, K S, R Barten, P R Kumaresan, J Trowsdale, and P A Mathew. 1999. "Cloning of a New Lectin-Like Receptor Expressed on Human NK Cells.." *Immunogenetics* 50 (1-2) (October): 1–7.
Burshtyn, D N. 1997. "A Novel Phosphotyrosine Motif with a Critical Amino Acid at Position -2 for the SH2 Domain-Mediated Activation of the Tyrosine Phosphatase SHP-1." *Journal of Biological Chemistry* 272 (20) (May 16): 13066–13072. doi:10.1074/jbc.272.20.13066.
Carlyle, J R. 2004. "Missing Self-Recognition of Ocil/Clr-B by Inhibitory NKR-P1 Natural Killer Cell Receptors." *Proceedings of the National Academy of Sciences* 101 (10) (March 1): 3527–3532. doi:10.1073/pnas.0308304101.
Carlyle, James R, Aruz Mesci, Belma Ljutic, Simon Belanger, Lee-Hwa Tai, Etienne Rousselle, Angela D Troke, Marie-France Proteau, and Andrew P Makrigiannis. 2006. "Molecular and Genetic Basis for Strain-Dependent NK1.1 Alloreactivity of Mouse NK Cells.." *The Journal of Immunology* 176 (12) (June 15): 7511–7524.
Cavallari, M, S El Daker, and T Beddoe. 2013. "Butyrophilin 3A1 Binds Phosphorylated Antigens and Stimulates Human [Gamma][Delta] T Cells." *Nature*.
Chaix, J, M S Tessmer, K Hoebe, and N Fuséri. 2008. "Cutting Edge: Priming of NK Cells by IL-18." *The Journal of …*.
Chang, Woo-Sung, Ji-Yeon Kim, Yeon-Jeong Kim, Yun-Sun Kim, Jung-Mi Lee, Miyuki Azuma, Hideo Yagita, and Chang-Yuil Kang. 2008. "Cutting Edge: Programmed Death-1/Programmed Death Ligand 1 Interaction Regulates the Induction and Maintenance of Invariant NKT Cell Anergy.." *Journal of Immunology (Baltimore, Md. : 1950)* 181 (10) (November 15): 6707–6710.
Chiba, Asako, Ryohsuke Tajima, Chiharu Tomi, Yusei Miyazaki, Takashi Yamamura, and Sachiko Miyake. 2012. "Mucosal-Associated Invariant T Cells Promote Inflammation and Exacerbate Disease in Murine Models of Arthritis.." *Arthritis and Rheumatism* 64 (1) (January): 153–161. doi:10.1002/art.33314.
Chou, K C, and D W Elrod. 1999. "Prediction of Membrane Protein Types and Subcellular Locations.." *Proteins* 34 (1) (January 1): 137–153.
Christiansen, Dale, Effie Mouhtouris, Julie Milland, Alessandra Zingoni, Angela Santoni, and Mauro S Sandrin. 2006. "Recognition of a Carbohydrate Xenoepitope by Human NKRP1A (CD161).." *Xenotransplantation* 13 (5) (September): 440–446. doi:10.1111/j.1399-3089.2006.00332.x.
Chua, Wei-Jen, Sojung Kim, Nancy Myers, Shouxiong Huang, Lawrence Yu, Daved H Fremont, Michael S Diamond, and Ted H Hansen. 2011. "Endogenous MHC-Related Protein 1 Is Transiently Expressed on the Plasma Membrane in a Conformation That Activates Mucosal-Associated Invariant T Cells.." *Journal*

of Immunology (Baltimore, Md. : 1950) 186 (8) (April 15): 4744–4750. doi:10.4049/jimmunol.1003254.

Chua, Wei-Jen, Steven M Truscott, Christopher S Eickhoff, Azra Blazevic, Daniel F Hoft, and Ted H Hansen. 2012. "Polyclonal Mucosa-Associated Invariant T Cells Have Unique Innate Functions in Bacterial Infection.." *Infection and Immunity* 80 (9) (September): 3256–3267. doi:10.1128/IAI.00279-12.

Ciccone, E, D Pende, O Viale, A Than, C Di Donato, A M Orengo, R Biassoni, S Verdiani, A Amoroso, and A Moretta. 1992. "Involvement of HLA Class I Alleles in Natural Killer (NK) Cell-Specific Functions: Expression of HLA-Cw3 Confers Selective Protection From Lysis by Alloreactive NK Clones Displaying a Defined Specificity (Specificity 2).." *The Journal of Experimental Medicine* 176 (4) (October 1): 963–971.

Cooper, M D, and M N Alder. 2006. "The Evolution of Adaptive Immune Systems." *Cell*.

Coppieters, K, P Dewint, K Van Beneden, P Jacques, S Seeuws, G Verbruggen, D Deforce, and D Elewaut. 2007. "NKT Cells: Manipulable Managers of Joint Inflammation.." *Rheumatology (Oxford, England)* 46 (4) (April): 565–571. doi:10.1093/rheumatology/kel437.

Coquet, J M, and S Chakravarti. 2008. "Diverse Cytokine Production by NKT Cell Subsets and Identification of an IL-17–Producing CD4– NK1. 1– NKT Cell Population." In.

Cosgrove, Cormac, James E Ussher, Andri Rauch, Kathleen Gärtner, Ayako Kurioka, Michael H Hühn, Krista Adelmann, et al. 2013. "Early and Nonreversible Decrease of CD161++ /MAIT Cells in HIV Infection.." *Blood* 121 (6) (February 7): 951–961. doi:10.1182/blood-2012-06-436436.

Cosmi, L, R De Palma, V Santarlasci, L Maggi, M Capone, F Frosali, G Rodolico, et al. 2008. "Human Interleukin 17-Producing Cells Originate From a CD161+CD4+ T Cell Precursor." *Journal of Experimental Medicine* 205 (8) (July 28): 1903–1916. doi:10.1084/jem.20080397.

Cosmi, Lorenzo, Laura Maggi, Veronica Santarlasci, Manuela Capone, Elisa Cardilicchia, Francesca Frosali, Valentina Querci, et al. 2010. "Identification of a Novel Subset of Human Circulating Memory CD4+ T Cells That Produce Both IL-17A and IL-4." *Journal of Allergy and Clinical Immunology* 125 (1) (January): 222–230.e4. doi:10.1016/j.jaci.2009.10.012.

Cremesti, A, F Paris, H Grassme, N Holler, J Tschopp, Z Fuks, E Gulbins, and R Kolesnick. 2001. "Ceramide Enables Fas to Cap and Kill.." *The Journal of Biological Chemistry* 276 (26) (June 29): 23954–23961. doi:10.1074/jbc.M101866200.

Crowe, Nadine Y, Jonathan M Coquet, Stuart P Berzins, Konstantinos Kyparissoudis, Rachael Keating, Daniel G Pellicci, Yoshihiro Hayakawa, Dale I Godfrey, and Mark J Smyth. 2005. "Differential Antitumor Immunity Mediated by NKT Cell Subsets in Vivo.." *The Journal of Experimental Medicine* 202 (9) (November 7): 1279–1288. doi:10.1084/jem.20050953.

Croxford, J Ludovic, Sachiko Miyake, Yi-Ying Huang, Michio Shimamura, and Takashi Yamamura. 2006. "Invariant v(Alpha)19i T Cells Regulate Autoimmune Inflammation.." *Nature Immunology* 7 (9) (September): 987–994. doi:10.1038/ni1370.

De Meester, I, S Korom, J Van Damme, and S Scharpé. 1999. "CD26, Let It Cut or Cut It Down.." *Immunology Today* 20 (8) (August): 367–375.

Diefenbach, Andreas, Elena Tomasello, Mathias Lucas, Amanda M Jamieson, Jennifer K Hsia, Eric Vivier, and David H Raulet. 2002. “Selective Associations with Signaling Proteins Determine Stimulatory Versus Costimulatory Activity of NKG2D..” *Nature Immunology* 3 (12) (December): 1142–1149. doi:10.1038/ni858.

Doyle, C, and J L Strominger. 1987. “Interaction Between CD4 and Class II MHC Molecules Mediates Cell Adhesion..” *Nature* 330 (6145) (November): 256–259. doi:10.1038/330256a0.

Drickamer, K. 1999. “C-Type Lectin-Like Domains..” *Current Opinion in Structural Biology* 9 (5) (October): 585–590.

Drickamer, K, and M E Taylor. 1993. “Biology of Animal Lectins..” *Annual Review of Cell Biology* 9: 237–264. doi:10.1146/annurev.cb.09.110193.001321.

Dusseaux, Mathilde, Emmanuel Martin, Nacer Serriari, Isabelle Péguillet, Virginie Premel, Delphine Louis, Maud Milder, et al. 2011. “Human MAIT Cells Are Xenobiotic-Resistant, Tissue-Targeted, CD161hi IL-17-Secreting T Cells..” *Blood* 117 (4) (January 27): 1250–1259. doi:10.1182/blood-2010-08-303339.

Ekkens, M J, D J Shedlock, E H Jung, and A Troy. 2007. “Th1 and Th2 Cells Help CD8 T-Cell Responses.” *Infection and …*.

Escors, David, Christopher Bricogne, Frederick Arce, Grazyna Kochan, and Katarzyna Karwacz. 2011. “On the Mechanism of T Cell Receptor Down-Modulation and Its Physiological Significance..” *The Journal of Bioscience and Medicine* 1 (1) (January).

Exley, M, S Porcelli, M Furman, J Garcia, and S Balk. 1998. “CD161 (NKR-P1A) Costimulation of CD1d-Dependent Activation of Human T Cells Expressing Invariant v Alpha 24 J Alpha Q T Cell Receptor Alpha Chains..” *The Journal of Experimental Medicine* 188 (5) (September 7): 867–876.

Fairfax, Kirsten A, Axel Kallies, Stephen L Nutt, and David M Tarlinton. 2008. “Plasma Cell Development: From B-Cell Subsets to Long-Term Survival Niches..” *Seminars in Immunology* 20 (1) (February): 49–58. doi:10.1016/j.smim.2007.12.002.

Fergusson, Joannah R, Vicki M Fleming, and Paul Klenerman. 2011. “CD161-Expressing Human T Cells..” *Frontiers in Immunology* 2: 36. doi:10.3389/fimmu.2011.00036.

Flores, I, C Martinez-A, Y A Hannun, and I Mérida. 1998. “Dual Role of Ceramide in the Control of Apoptosis Following IL-2 Withdrawal..” *The Journal of Immunology* 160 (7) (April 1): 3528–3533.

Georgel, Philippe, Mirjana Radosavljevic, Cécile Macquin, and Seiamak Bahram. 2011. “The Non-Conventional MHC Class I MR1 Molecule Controls Infection by Klebsiella Pneumoniae in Mice..” *Molecular Immunology* 48 (5) (February): 769–775. doi:10.1016/j.molimm.2010.12.002.

Germain, C, F Bihl, S Zahn, G Poupon, M J Dumaurier, H H Rampanarivo, S B Padkjaer, P Spee, and V M Braud. 2010. “Characterization of Alternatively Spliced Transcript Variants of CLEC2D Gene.” *Journal of Biological Chemistry* 285 (46) (November 5): 36207–36215. doi:10.1074/jbc.M110.179622.

Germain, Claire, Anders Meier, Teis Jensen, Perrine Knapnougel, Gwenola Poupon, Anne Lazzari, Anne Neisig, et al. 2011. “Induction of Lectin-Like Transcript 1 (LLT1) Protein Cell Surface Expression by Pathogens and Interferon-Γ Contributes to Modulate Immune Responses..” *Journal of*

Biological Chemistry 286 (44) (November 4): 37964–37975. doi:10.1074/jbc.M111.285312.

Glimcher, L, F W Shen, and H Cantor. 1977. "Identification of a Cell-Surface Antigen Selectively Expressed on the Natural Killer Cell.." *The Journal of Experimental …*.

Godfrey, Dale I, and Mitchell Kronenberg. 2004. "Going Both Ways: Immune Regulation via CD1d-Dependent NKT Cells.." *The Journal of Clinical Investigation* 114 (10) (November): 1379–1388. doi:10.1172/JCI23594.

Gold, Marielle C, and David M Lewinsohn. 2013. "Co-Dependents: MR1-Restricted MAIT Cells and Their Antimicrobial Function.." *Nature Reviews. Microbiology* 11 (1) (January): 14–19. doi:10.1038/nrmicro2918.

Gold, Marielle C, Stefania Cerri, Susan Smyk-Pearson, Meghan E Cansler, Todd M Vogt, Jacob Delepine, Ervina Winata, et al. 2010. "Human Mucosal Associated Invariant T Cells Detect Bacterially Infected Cells.." *PLoS Biology* 8 (6): e1000407. doi:10.1371/journal.pbio.1000407.

Goldfinch, Nick, Peter Reinink, Timothy Connelley, Ad Koets, Ivan Morrison, and Ildiko Van Rhijn. 2010. "Conservation of Mucosal Associated Invariant T (MAIT) Cells and the MR1 Restriction Element in Ruminants, and Abundance of MAIT Cells in Spleen.." *Veterinary Research* 41 (5) (September): 62. doi:10.1051/vetres/2010034.

Gordon, Siamon. 2003. "Alternative Activation of Macrophages.." *Nature Reviews. Immunology* 3 (1) (January): 23–35. doi:10.1038/nri978.

Grassme, H, A Jekle, A Riehle, H Schwarz, J Berger, K Sandhoff, R Kolesnick, and E Gulbins. 2001. "CD95 Signaling via Ceramide-Rich Membrane Rafts.." *The Journal of Biological Chemistry* 276 (23) (June 8): 20589–20596. doi:10.1074/jbc.M101207200.

Groh, V, R Rhinehart, J Randolph-Habecker, M S Topp, S R Riddell, and T Spies. 2001. "Costimulation of CD8alphabeta T Cells by NKG2D via Engagement by MIC Induced on Virus-Infected Cells.." *Nature Immunology* 2 (3) (March): 255–260. doi:10.1038/85321.

Groh, Veronika, Jennifer Wu, Cassian Yee, and Thomas Spies. 2002. "Tumour-Derived Soluble MIC Ligands Impair Expression of NKG2D and T-Cell Activation.." *Nature* 419 (6908) (October 17): 734–738. doi:10.1038/nature01112.

Hamada, Hiromasa, Maria de la Luz Garcia-Hernandez, Joyce B Reome, Sara K Misra, Tara M Strutt, Kai K McKinstry, Andrea M Cooper, Susan L Swain, and Richard W Dutton. 2009. "Tc17, a Unique Subset of CD8 T Cells That Can Protect Against Lethal Influenza Challenge.." *Journal of Immunology (Baltimore, Md. : 1950)* 182 (6) (March 15): 3469–3481. doi:10.4049/jimmunol.0801814.

Harty, J T, A R Tvinnereim, and D W White. 2000. "CD8+ T Cell Effector Mechanisms in Resistance to Infection.." *Annual Review of Immunology* 18: 275–308. doi:10.1146/annurev.immunol.18.1.275.

Hermans, Ian F, Jonathan D Silk, Jianping Yang, Michael J Palmowski, Uzi Gileadi, Corinna McCarthy, Mariolina Salio, Franca Ronchese, and Vincenzo Cerundolo. 2004. "The VITAL Assay: a Versatile Fluorometric Technique for Assessing CTL- and NKT-Mediated Cytotoxicity Against Multiple Targets in Vitro and in Vivo." 285 (1) (February 1): 25–40. doi:10.1016/j.jim.2003.10.017.

http://eutils.ncbi.nlm.nih.gov/entrez/eutils/elink.fcgi?dbfrom=pubmed&id=14871532&retmode=ref&cmd=prlinks.

Hewitt, Eric W. 2003. "The MHC Class I Antigen Presentation Pathway: Strategies for Viral Immune Evasion.." *Immunology* 110 (2) (October): 163–169.

Hildebrandt, Martin, Dorothea Dijkstra, Hella Gollasch, Kerstin Daemen, Maja Stevanovic-Meyer, and Wolf-Dieter Ludwig. 2012. "Apheresis-Related Enrichment of CD26++ T Lymphocytes: Phenotypic Characterization and Correlation with Unfavorable Outcome in Autologous Hematopoietic Progenitor Cell Transplantation.." *Transfusion* 52 (4) (April): 765–776. doi:10.1111/j.1537-2995.2011.03351.x.

Horvath, Christopher, Laura Andrews, Andreas Baumann, Lauren Black, Diann Blanset, Joy Cavagnaro, Kenneth L Hastings, et al. 2012. "Storm Forecasting: Additional Lessons From the CD28 Superagonist TGN1412 Trial.." *Nature Reviews. Immunology* 12 (10) (October): 740–author reply 740. doi:10.1038/nri3192-c1.

Houchins, J P, L L Lanier, E C Niemi, J H Phillips, and J C Ryan. 1997. "Natural Killer Cell Cytolytic Activity Is Inhibited by NKG2-a and Activated by NKG2-C.." *The Journal of Immunology* 158 (8) (April 15): 3603–3609.

Houchins, J P, T Yabe, C McSherry, and F H Bach. 1991. "DNA Sequence Analysis of NKG2, a Family of Related cDNA Clones Encoding Type II Integral Membrane Proteins on Human Natural Killer Cells.." *The Journal of Experimental Medicine* 173 (4) (April 1): 1017–1020.

Hu, Yun Shan, Hong Zhou, Damian Myers, Julian M W Quinn, Gerald J Atkins, Chi Ly, Christine Gange, et al. 2004. "Isolation of a Human Homolog of Osteoclast Inhibitory Lectin That Inhibits the Formation and Function of Osteoclasts.." *Journal of Bone and Mineral Research : the Official Journal of the American Society for Bone and Mineral Research* 19 (1) (January): 89–99. doi:10.1359/JBMR.0301215.

Huang, Shouxiong, Susan Gilfillan, Sojung Kim, Bruce Thompson, Xiaoli Wang, Andrea J Sant, Daved H Fremont, Olivier Lantz, and Ted H Hansen. 2008. "MR1 Uses an Endocytic Pathway to Activate Mucosal-Associated Invariant T Cells.." *Journal of Experimental Medicine* 205 (5) (May 12): 1201–1211. doi:10.1084/jem.20072579.

Huarte, E, J R Cubillos-Ruiz, Y C Nesbeth, U K Scarlett, D G Martinez, X A Engle, W F Rigby, P A Pioli, P M Guyre, and J R Conejo-Garcia. 2008. "PILAR Is a Novel Modulator of Human T-Cell Expansion." *Blood* 112 (4) (May 13): 1259–1268. doi:10.1182/blood-2007-12-130773.

Hünig, Thomas. 2012. "The Storm Has Cleared: Lessons From the CD28 Superagonist TGN1412 Trial.." *Nature Reviews. Immunology* 12 (5) (May): 317–318. doi:10.1038/nri3192.

Iizuka, Koho, Olga V Naidenko, Beatrice F M Plougastel, Daved H Fremont, and Wayne M Yokoyama. 2003. "Genetically Linked C-Type Lectin-Related Ligands for the NKRP1 Family of Natural Killer Cell Receptors.." *Nature Immunology* 4 (8) (August): 801–807. doi:10.1038/ni954.

Jewett, A, and B Bonavida. 1995. "Interferon-Alpha Activates Cytotoxic Function but Inhibits Interleukin-2-Mediated Proliferation and Tumor Necrosis Factor-Alpha Secretion by Immature Human Natural Killer Cells.." *Journal of Clinical Immunology* 15 (1) (January): 35–44.

Joyce, Sebastian, and Luc Van Kaer. 2008. "Invariant Natural Killer T Cells Trigger

Adaptive Lymphocytes to Churn Up Bile.." *Cell Host & Microbe* 3 (5) (May 15): 275–277. doi:10.1016/j.chom.2008.04.007.

Joyee, Antony George, Hongyu Qiu, Shuhe Wang, Yijun Fan, Laura Bilenki, and Xi Yang. 2007. "Distinct NKT Cell Subsets Are Induced by Different Chlamydia Species Leading to Differential Adaptive Immunity and Host Resistance to the Infections.." *The Journal of Immunology* 178 (2) (January 15): 1048–1058.

Kadowaki, N, S Ho, S Antonenko, R W Malefyt, R A Kastelein, F Bazan, and Y J Liu. 2001. "Subsets of Human Dendritic Cell Precursors Express Different Toll-Like Receptors and Respond to Different Microbial Antigens.." *The Journal of Experimental Medicine* 194 (6) (September 17): 863–869.

Kamishikiryo, Jun, Hideo Fukuhara, Yuki Okabe, Kimiko Kuroki, and Katsumi Maenaka. 2011. "Molecular Basis for LLT1 Protein Recognition by Human CD161 Protein (NKRP1A/KLRB1).." *Journal of Biological Chemistry* 286 (27) (July 8): 23823–23830. doi:10.1074/jbc.M110.214254.

Kjer-Nielsen, Lars, Onisha Patel, Alexandra J Corbett, Jérôme Le Nours, Bronwyn Meehan, Ligong Liu, Mugdha Bhati, et al. 2012. "MR1 Presents Microbial Vitamin B Metabolites to MAIT Cells.." *Nature* 491 (7426) (November 29): 717–723. doi:10.1038/nature11605.

Kleinschek, M A, K Boniface, S Sadekova, J Grein, E E Murphy, S P Turner, L Raskin, et al. 2009. "Circulating and Gut-Resident Human Th17 Cells Express CD161 and Promote Intestinal Inflammation." *Journal of Experimental Medicine* 206 (3) (March 16): 525–534. doi:10.1084/jem.20081712.

Koo, G C, and J R Peppard. 1984. "Establishment of Monoclonal Anti-Nk-1.1 Antibody.." *Hybridoma* 3 (3): 301–303.

Kung, S K, R C Su, J Shannon, and R G Miller. 1999. "The NKR-P1B Gene Product Is an Inhibitory Receptor on SJL/J NK Cells.." *The Journal of Immunology* 162 (10) (May 15): 5876–5887.

Lanier, L L, C Chang, and J H Phillips. 1994. "Human NKR-P1A. a Disulfide-Linked Homodimer of the C-Type Lectin Superfamily Expressed by a Subset of NK and T Lymphocytes." *The Journal of Immunology* 153 (6): 2417–2428.

Le Bourhis, Lionel, Emmanuel Martin, Isabelle Péguillet, Amélie Guihot, Nathalie Froux, Maxime Coré, Eva Lévy, et al. 2010. "Antimicrobial Activity of Mucosal-Associated Invariant T Cells.." *Nature Immunology* 11 (8) (August): 701–708. doi:10.1038/ni.1890.

Le Bourhis, Lionel, Lucia Guerri, Mathilde Dusseaux, Emmanuel Martin, Claire Soudais, and Olivier Lantz. 2011. "Mucosal-Associated Invariant T Cells: Unconventional Development and Function.." *Trends in Immunology* 32 (5) (May): 212–218. doi:10.1016/j.it.2011.02.005.

Li, Yili, Qian Wang, Sharon Chen, Patrick H Brown, and Roy A Mariuzza. 2013. "Structure of NKp65 Bound to Its Keratinocyte Ligand Reveals Basis for Genetically Linked Recognition in Natural Killer Gene Complex.." *Proceedings of the National Academy of Sciences* 110 (28) (July 9): 11505–11510. doi:10.1073/pnas.1303300110.

Liang, Shujuan, Haiming Wei, Rui Sun, and Zhigang Tian. 2003. "IFNalpha Regulates NK Cell Cytotoxicity Through STAT1 Pathway.." *Cytokine* 23 (6) (September 21): 190–199.

Liu, H, M Rhodes, D L Wiest, and D A Vignali. 2000. "On the Dynamics of TCR:CD3 Complex Cell Surface Expression and Downmodulation.." *Immunity* 13 (5) (November): 665–675.

Liu, Yong-Jun, and Christophe Arpin. 1997. “Germinal Center Development.” *Immunological Reviews* 156 (1) (April): 111–126. doi:10.1111/j.1600-065X.1997.tb00963.x.

Livak, K J, and T D Schmittgen. 2001. “Analysis of Relative Gene Expression Data Using Real-Time Quantitative PCR and the 2(-Delta Delta C(T)) Method..” *Methods (San Diego, Calif.)* 25 (4) (December): 402–408. doi:10.1006/meth.2001.1262.

Ljunggren, H G, and K Kärre. 1990. “In Search of the ‘Missing Self’: MHC Molecules and NK Cell Recognition..” *Immunology Today* 11 (7) (July): 237–244.

López-Botet, M, M Llano, F Navarro, and T Bellón. 2000. “NK Cell Recognition of Non-Classical HLA Class I Molecules..” *Seminars in Immunology* 12 (2) (April): 109–119. doi:10.1006/smim.2000.0213.

Maccario, R, M G Revello, P Comoli, D Montagna, F Locatelli, and G Gerna. 1993. “HLA-Unrestricted Killing of HSV-1-Infected Mononuclear Cells. Involvement of Either Gamma/Delta+ or Alpha/Beta+ Human Cytotoxic T Lymphocytes..” *The Journal of Immunology* 150 (4) (February 15): 1437–1445.

MacDonald, H R. 1995. “NK1.1+ T Cell Receptor-Alpha/Beta+ Cells: New Clues to Their Origin, Specificity, and Function..” *The Journal of Experimental Medicine* 182 (3) (September 1): 633–638.

Maggi, Laura, Veronica Santarlasci, Manuela Capone, Anna Peired, Francesca Frosali, Sarah Q Crome, Valentina Querci, et al. 2010. “CD161 Is a Marker of All Human IL-17-Producing T-Cell Subsets and Is Induced by RORC..” *European Journal of Immunology* 40 (8) (August): 2174–2181. doi:10.1002/eji.200940257.

Martin, Emmanuel, Emmanuel Treiner, Livine Duban, Lucia Guerri, Hélène Laude, Cécile Toly, Virginie Premel, et al. 2009. “Stepwise Development of MAIT Cells in Mouse and Human..” *PLoS Biology* 7 (3) (March 10): e54. doi:10.1371/journal.pbio.1000054.

Matsuda, Jennifer L, Thierry Mallevaey, James Scott-Browne, and Laurent Gapin. 2008. “CD1d-Restricted iNKT Cells, the ‘Swiss-Army Knife’ of the Immune System..” *Current Opinion in Immunology* 20 (3) (June): 358–368. doi:10.1016/j.coi.2008.03.018.

Mattner, Jochen, Kristin L Debord, Nahed Ismail, Randal D Goff, Carlos Cantu, Dapeng Zhou, Pierre Saint-Mezard, et al. 2005. “Exogenous and Endogenous Glycolipid Antigens Activate NKT Cells During Microbial Infections..” *Nature* 434 (7032) (March 24): 525–529. doi:10.1038/nature03408.

Medzhitov, R, and C A Janeway. 1997. “Innate Immunity: the Virtues of a Nonclonal System of Recognition..” *Cell* 91 (3) (October 31): 295–298.

Menné, C, J P Lauritsen, J Dietrich, J Kastrup, A M Wegener, N Odum, and C Geisler. 2000. “Ceramide-Induced TCR Up-Regulation..” *The Journal of Immunology* 165 (6) (September 15): 3065–3072.

Miyazaki, Yusei, Sachiko Miyake, Asako Chiba, Olivier Lantz, and Takashi Yamamura. 2011. “Mucosal-Associated Invariant T Cells Regulate Th1 Response in Multiple Sclerosis..” *International Immunology* 23 (9) (September): 529–535. doi:10.1093/intimm/dxr047.

Moretta, A, M Vitale, C Bottino, A M Orengo, L Morelli, R Augugliaro, M Barbaresi, E Ciccone, and L Moretta. 1993. “P58 Molecules as Putative Receptors for Major Histocompatibility Complex (MHC) Class I Molecules in Human

Natural Killer (NK) Cells. Anti-P58 Antibodies Reconstitute Lysis of MHC Class I-Protected Cells in NK Clones Displaying Different Specificities.." *The Journal of Experimental Medicine* 178 (2) (August 1): 597–604.

Murphy, K M. 2012. "Janeway's Immunobiology 8th Ed.."

Northfield, John W, Victoria Kasprowicz, Michaela Lucas, Nadine Kersting, Bertram Bengsh, Arthur Kim, Rodney E Phillips, et al. 2008. "CD161 Expression on Hepatitis C Virus-Specific CD8+ T Cells Suggests a Distinct Pathway of T Cell Differentiation." *Hepatology* 47 (2) (January 7): 396–406. doi:10.1002/hep.22040.

O'Byrne, D, and D Sansom. 2000. "Lack of Costimulation by Both Sphingomyelinase and C2 Ceramide in Resting Human T Cells.." *Immunology* 100 (2) (June): 225–230.

Oo, Ye Htun, Vanessa Banz, Dean Kavanagh, Evaggelia Liaskou, David R Withers, Elizabeth Humphreys, Gary M Reynolds, et al. 2012. "CXCR3-Dependent Recruitment and CCR6-Mediated Positioning of Th-17 Cells in the Inflamed Liver.." *Journal of Hepatology* 57 (5) (November): 1044–1051. doi:10.1016/j.jhep.2012.07.008.

Ozinsky, A, D M Underhill, J D Fontenot, A M Hajjar, K D Smith, C B Wilson, L Schroeder, and A Aderem. 2000. "The Repertoire for Pattern Recognition of Pathogens by the Innate Immune System Is Defined by Cooperation Between Toll-Like Receptors.." *Proceedings of the National Academy of Sciences of the United States of America* 97 (25) (December 5): 13766–13771. doi:10.1073/pnas.250476497.

Parekh, V V, S Lalani, S Kim, R Halder, M Azuma, H Yagita, V Kumar, L Wu, and L Van Kaer. 2009. "PD-1/PD-L Blockade Prevents Anergy Induction and Enhances the Anti-Tumor Activities of Glycolipid-Activated Invariant NKT Cells." *Journal of Immunology (Baltimore, Md. : 1950)* 182 (5) (March 1): 2816–2826. doi:10.4049/jimmunol.0803648.

Parham, P. 2005. "Immunogenetics of Killer Cell Immunoglobulin-Like Receptors." *Molecular Immunology*.

Peterfalvi, Agnes, Eva Gomori, Tamas Magyarlaki, Jozsef Pal, Miklos Banati, Andras Javorhazy, Julia Szekeres-Bartho, Laszlo Szereday, and Zsolt Illes. 2008. "Invariant Valpha7.2-Jalpha33 TCR Is Expressed in Human Kidney and Brain Tumors Indicating Infiltration by Mucosal-Associated Invariant T (MAIT) Cells.." *International Immunology* 20 (12) (December): 1517–1525. doi:10.1093/intimm/dxn111.

Piccirillo, C A, and E M Shevach. 2001. "Cutting Edge: Control of CD8+ T Cell Activation by CD4+ CD25+ Immunoregulatory Cells." *The Journal of Immunology*.

Pillai, Asha B, Tracy I George, Suparna Dutt, Pearline Teo, and Samuel Strober. 2007. "Host NKT Cells Can Prevent Graft-Versus-Host Disease and Permit Graft Antitumor Activity After Bone Marrow Transplantation.." *The Journal of Immunology* 178 (10) (May 15): 6242–6251.

Plougastel, B, C Dubbelde, and W M Yokoyama. 2001. "Cloning of Clr, a New Family of Lectin-Like Genes Localized Between Mouse Nkrp1a and Cd69.." *Immunogenetics* 53 (3) (April): 209–214.

Plougastel, B, K Matsumoto, C Dubbelde, and W M Yokoyama. 2001. "Analysis of a 1-Mb BAC Contig Overlapping the Mouse Nkrp1 Cluster of Genes: Cloning of Three New Nkrp1 Members, Nkrp1d, Nkrp1e, and Nkrp1f.."

Immunogenetics 53 (7) (September): 592–598. doi:10.1007/s002510100367.
Poggi, A, P Costa, E Tomasello, and L Moretta. 1998. "IL-12-Induced Up-Regulation of NKRP1A Expression in Human NK Cells and Consequent NKRP1A-Mediated Down-Regulation of NK Cell Activation.." *European Journal of Immunology* 28 (5) (May): 1611–1616. doi:10.1002/(SICI)1521-4141(199805)28:05<1611::AID-IMMU1611>3.0.CO;2-6.
Poggi, A, P Costa, L Morelli, C Cantoni, N Pella, F Spada, R Biassoni, et al. 1996. "Expression of Human NKRP1A by CD34+ Immature Thymocytes: NKRP1A-Mediated Regulation of Proliferation and Cytolytic Activity.." *European Journal of Immunology* 26 (6) (June): 1266–1272. doi:10.1002/eji.1830260613.
Poggi, A, P Costa, M R Zocchi, and L Moretta. 1997. "Phenotypic and Functional Analysis of CD4+ NKRP1A+ Human T Lymphocytes. Direct Evidence That the NKRP1A Molecule Is Involved in Transendothelial Migration.." *European Journal of Immunology* 27 (9) (September): 2345–2350. doi:10.1002/eji.1830270932.
Porcelli, S, C E Yockey, M B Brenner, and S P Balk. 1993. "Analysis of T Cell Antigen Receptor (TCR) Expression by Human Peripheral Blood CD4-8-Alpha/Beta T Cells Demonstrates Preferential Use of Several v Beta Genes and an Invariant TCR Alpha Chain.." *The Journal of Experimental Medicine* 178 (1) (July 1): 1–16.
Pozo, David, Mar Valés-Gómez, Nasim Mavaddat, Sharon C Williamson, Susan E Chisholm, and Hugh Reyburn. 2006. "CD161 (Human NKR-P1A) Signaling in NK Cells Involves the Activation of Acid Sphingomyelinase.." *The Journal of Immunology* 176 (4) (February 15): 2397–2406.
Qu, Ning, Mingli Xu, Izuru Mizoguchi, Jun-ichi Furusawa, Kotaro Kaneko, Kazunori Watanabe, Junichiro Mizuguchi, Masahiro Itoh, Yutaka Kawakami, and Takayuki Yoshimoto. 2013. "Pivotal Roles of T-Helper 17-Related Cytokines, IL-17, IL-22, and IL-23, in Inflammatory Diseases.." *Clinical & Developmental Immunology* 2013: 968549. doi:10.1155/2013/968549.
Qureshi, Omar S, Yong Zheng, Kyoko Nakamura, Kesley Attridge, Claire Manzotti, Emily M Schmidt, Jennifer Baker, et al. 2011. "Trans-Endocytosis of CD80 and CD86: a Molecular Basis for the Cell-Extrinsic Function of CTLA-4.." *Science (New York, N.Y.)* 332 (6029) (April 29): 600–603. doi:10.1126/science.1202947.
Rajewsky, K, I Förster, and A Cumano. 1987. "Evolutionary and Somatic Selection of the Antibody Repertoire in the Mouse.." *Science (New York, N.Y.)* 238 (4830) (November 20): 1088–1094.
Renedo, Mónica, Ignacio Arce, Antonio Rodríguez, Marta Carretero, Lewis L Lanier, Miguel López-Botet, and Elena Fernández-Ruiz. 1997. "The Human Natural Killer Gene Complex Is Located on Chromosome 12p12-P13." *Immunogenetics* 46 (4): 307–311.
Rinkevich, B. 1999. "Invertebrates Versus Vertebrates Innate Immunity: in the Light of Evolution.." *Scandinavian Journal of Immunology* 50 (5) (November): 456–460.
Roda-Navarro, Pedro, Ignacio Arce, Mónica Renedo, Kate Montgomery, Raju Kucherlapati, and Elena Fernández-Ruiz. 2000. "HumanKLRF1, a Novel Member of the Killer Cell Lectin-Like Receptor Gene Family: Molecular Characterization, Genomic Structure, Physical Mapping to the NK Gene

Complex and Expression Analysis." *European Journal of Immunology* 30 (2) (February): 568–576. doi:10.1002/1521-4141(200002)30:2<568::AID-IMMU568>3.0.CO;2-Y.

Rosen, David B, Jayaram Bettadapura, Mohammed Alsharifi, Porunelloor A Mathew, Hilary S Warren, and Lewis L Lanier. 2005. "Cutting Edge: Lectin-Like Transcript-1 Is a Ligand for the Inhibitory Human NKR-P1A Receptor.." *The Journal of Immunology* 175 (12) (December 15): 7796–7799.

Rosen, David B, Wei Cao, Danielle T Avery, Stuart G Tangye, Yong-Jun Liu, J P Houchins, and Lewis L Lanier. 2008. "Functional Consequences of Interactions Between Human NKR-P1A and Its Ligand LLT1 Expressed on Activated Dendritic Cells and B Cells.." *The Journal of Immunology* 180 (10) (May 15): 6508–6517.

Sallusto, F, D Lenig, R Förster, M Lipp, and A Lanzavecchia. 1999. "Two Subsets of Memory T Lymphocytes with Distinct Homing Potentials and Effector Functions.." *Nature* 401 (6754) (October 14): 708–712. doi:10.1038/44385.

Sallusto, F, M Cella, and C Danieli. 1995. "Dendritic Cells Use Macropinocytosis and the Mannose Receptor to Concentrate Macromolecules in the Major Histocompatibility Complex Class II Compartment: …." *The Journal of …*.

Sanz, Iñaki, Chungwen Wei, F Eun-Hyung Lee, and Jennifer Anolik. 2008. "Phenotypic and Functional Heterogeneity of Human Memory B Cells.." *Seminars in Immunology* 20 (1) (February): 67–82. doi:10.1016/j.smim.2007.12.006.

Savina, A, and S Amigorena. 2007. "Phagocytosis and Antigen Presentation in Dendritic Cells." *Immunological Reviews*.

Saxena, Amit, Sabine Desbois, Nadège Carrié, Myriam Lawand, Lennart T Mars, and Roland S Liblau. 2012. "Tc17 CD8+ T Cells Potentiate Th1-Mediated Autoimmune Diabetes in a Mouse Model.." *Journal of Immunology (Baltimore, Md. : 1950)* 189 (6) (September 15): 3140–3149. doi:10.4049/jimmunol.1103111.

Sciammas, R, and J A Bluestone. 1999. "TCRgammadelta Cells and Viruses.." *Microbes and Infection / Institut Pasteur* 1 (3) (March): 203–212.

Sciammas, R, R M Johnson, A I Sperling, W Brady, P S Linsley, P G Spear, F W Fitch, and J A Bluestone. 1994. "Unique Antigen Recognition by a Herpesvirus-Specific TCR-Gamma Delta Cell.." *The Journal of Immunology* 152 (11) (June 1): 5392–5397.

Shum, Benny P, Laura R Flodin, David G Muir, Raja Rajalingam, Salim I Khakoo, Sophia Cleland, Lisbeth A Guethlein, Markus Uhrberg, and Peter Parham. 2002. "Conservation and Variation in Human and Common Chimpanzee CD94 and NKG2 Genes.." *The Journal of Immunology* 168 (1) (January 1): 240–252.

Spreu, J, S Kuttruff, V Stejfova, K M Dennehy, B Schittek, and A Steinle. 2010. "Interaction of C-Type Lectin-Like Receptors NKp65 and KACL Facilitates Dedicated Immune Recognition of Human Keratinocytes." *Proceedings of the National Academy of Sciences* 107 (11) (March 16): 5100–5105. doi:10.1073/pnas.0913108107.

Spreu, Jessica, Eike C Kienle, Birgit Schrage, and Alexander Steinle. 2007. "CLEC2A: a Novel, Alternatively Spliced and Skin-Associated Member of the NKC-Encoded AICL–CD69–LLT1 Family." *Immunogenetics* 59 (12) (November 29): 903–912. doi:10.1007/s00251-007-0263-1.

Starr, T K, and S C Jameson. 2003. “Positive and Negative Selection of T Cells.” *Annual Review of …*.

Takahashi, T, M Nieda, Y Koezuka, A Nicol, S A Porcelli, Y Ishikawa, K Tadokoro, H Hirai, and T Juji. 2000. “Analysis of Human v Alpha 24+ CD4+ NKT Cells Activated by Alpha-Glycosylceramide-Pulsed Monocyte-Derived Dendritic Cells..” *The Journal of Immunology* 164 (9) (May 1): 4458–4464.

Takahashi, Tsuyoshi, Sussan Dejbakhsh-Jones, and Samuel Strober. 2006. “Expression of CD161 (NKR-P1A) Defines Subsets of Human CD4 and CD8 T Cells with Different Functional Activities..” *The Journal of Immunology* 176 (1) (January 1): 211–216.

Tang, Xiaolei, Igor Maricic, and Vipin Kumar. 2007. “Anti-TCR Antibody Treatment Activates a Novel Population of Nonintestinal CD8αα+TCRαβ+ Regulatory T Cells and Prevents Experimental Autoimmune Encephalomyelitis.” *Journal of Immunology (Baltimore, Md. : 1950)* 178 (10) (May 15): 6043–6050.

Tang, Xiaolei, Igor Maricic, Nikunj Purohit, Berge Bakamjian, Lisa M Reed-Loisel, Tara Beeston, Peter Jensen, and Vipin Kumar. 2006. “Regulation of Immunity by a Novel Population of Qa-1-Restricted CD8αα+TCRαβ+ T Cells.” *The Journal of Immunology* 177 (11) (December 1): 7645–7655.

Terabe, Masaki, and Jay A Berzofsky. 2008. “Chapter 8 the Role of NKT Cells in Tumor Immunity.” In *Advances in Cancer Research*, 101:277–348. Advances in Cancer Research. Elsevier. doi:10.1016/S0065-230X(08)00408-9.

Tesmer, Laura A, Steven K Lundy, Sujata Sarkar, and David A Fox. 2008. “Th17 Cells in Human Disease..” *Immunological Reviews* 223 (June): 87–113. doi:10.1111/j.1600-065X.2008.00628.x.

Thorbecke, G J, A R Amin, and V K Tsiagbe. 1994. “Biology of Germinal Centers in Lymphoid Tissue..”

Tonegawa, S. 1983. “Somatic Generation of Antibody Diversity..” *Nature* 302 (5909) (April 14): 575–581.

Trapani, Joseph A, and Mark J Smyth. 2002. “Functional Significance of the Perforin/Granzyme Cell Death Pathway..” *Nature Reviews. Immunology* 2 (10) (October): 735–747. doi:10.1038/nri911.

Treiner, Emmanuel, Livine Duban, Seiamak Bahram, Mirjana Radosavljevic, Valerie Wanner, Florence Tilloy, Pierre Affaticati, Susan Gilfillan, and Olivier Lantz. 2003. “Selection of Evolutionarily Conserved Mucosal-Associated Invariant T Cells by MR1..” *Nature* 422 (6928) (March 13): 164–169. doi:10.1038/nature01433.

Ussher, James E, Matthew Bilton, Emma Attwod, Jonathan Shadwell, Rachel Richardson, Catherine de Lara, Elisabeth Mettke, et al. 2013. “CD161(++) CD8(+) T Cells, Including the MAIT Cell Subset, Are Specifically Activated by IL-12+IL-18 in a TCR-Independent Manner..” *European Journal of Immunology* (September 10). doi:10.1002/eji.201343509.

Valitutti, S, S Müller, M Salio, and A Lanzavecchia. 1997. “Degradation of T Cell Receptor (TCR)-CD3-Zeta Complexes After Antigenic Stimulation..” *The Journal of Experimental Medicine* 185 (10) (May 19): 1859–1864.

Van Kaer, Luc. 2007. “NKT Cells: T Lymphocytes with Innate Effector Functions..” *Current Opinion in Immunology* 19 (3) (June): 354–364. doi:10.1016/j.coi.2007.03.001.

Van Kaer, Luc, Vrajesh V Parekh, and Lan Wu. 2011. “Invariant Natural Killer T

Cells: Bridging Innate and Adaptive Immunity.." *Cell and Tissue Research* 343 (1) (January): 43–55. doi:10.1007/s00441-010-1023-3.
Vilches, Carlos, and Peter Parham. 2002. "KIR: Diverse, Rapidly Evolving Receptors of Innate and Adaptive Immunity.." *Annual Review of Immunology* 20: 217–251. doi:10.1146/annurev.immunol.20.092501.134942.
Viola, A. 2001. "The Amplification of TCR Signaling by Dynamic Membrane Microdomains.." *Trends in Immunology* 22 (6) (June): 322–327.
Walker, Lucy J, Yu-Hoi Kang, Matthew O Smith, Hannah Tharmalingham, Narayan Ramamurthy, Vicki M Fleming, Natasha Sahgal, et al. 2012. "Human MAIT and CD8αα Cells Develop From a Pool of Type-17 Precommitted CD8+ T Cells.." *Blood* 119 (2) (January 12): 422–433. doi:10.1182/blood-2011-05-353789.
Wallace, Morgan E, and Mark J Smyth. 2005. "The Role of Natural Killer Cells in Tumor Control--Effectors and Regulators of Adaptive Immunity.." *Springer Seminars in Immunopathology* 27 (1) (June): 49–64. doi:10.1007/s00281-004-0195-x.
Wan, Yisong Y, and Richard A Flavell. 2009. "How Diverse--CD4 Effector T Cells and Their Functions.." *Journal of Molecular Cell Biology* 1 (1) (October): 20–36. doi:10.1093/jmcb/mjp001.
Weis, W I, M E Taylor, and K Drickamer. 1998. "The C-Type Lectin Superfamily in the Immune System.." *Immunological Reviews* 163 (June): 19–34.
Weng, Lee, Hongyue Dai, Yihui Zhan, Yudong He, Sergey B Stepaniants, and Douglas E Bassett. 2006. "Rosetta Error Model for Gene Expression Analysis.." *Bioinformatics (Oxford, England)* 22 (9) (May 1): 1111–1121. doi:10.1093/bioinformatics/btl045.
Witherden, Deborah A, and Wendy L Havran. 2012. "EPCR: a Stress Trigger for Γδ T Cells.." *Nature Immunology* 13 (9) (September): 812–814. doi:10.1038/ni.2398.
Yabe, Toshio, Cynthia McSherry, FritzH Bach, Paul Fisch, RebeccaP Schall, PaulM Sondel, and JeffreyP Houchins. 1993. "A Multigene Family on Human Chromosome 12 Encodes Natural Killer-Cell Lectins." *Immunogenetics* 37 (6) (February). doi:10.1007/BF00222470.
Yokoyama, W M, J C Ryan, and J J Hunter. 1991. "cDNA Cloning of Mouse NKR-P1 and Genetic Linkage with LY-49. Identification of a Natural Killer Cell Gene Complex on Mouse Chromosome 6.." *The Journal of …*.
Yokoyama, Wayne M, and Beatrice F M Plougastel. 2003. "Immune Functions Encoded by the Natural Killer Gene Complex.." *Nature Reviews. Immunology* 3 (4) (April): 304–316. doi:10.1038/nri1055.
Zhao, Xiang-Yu, Ling-Ling Xu, Sheng-Ye Lu, and Xiao-Jun Huang. 2011. "IL-17-Producing T Cells Contribute to Acute Graft-Versus-Host Disease in Patients Undergoing Unmanipulated Blood and Marrow Transplantation.." *European Journal of Immunology* 41 (2) (February): 514–526. doi:10.1002/eji.201040793.
Zhong, Weimin, and Ellis L Reinherz. 2005. "CD8 Alpha Alpha Homodimer Expression and Role in CD8 T Cell Memory Generation During Influenza Virus a Infection in Mice.." *European Journal of Immunology* 35 (11) (November): 3103–3110. doi:10.1002/eji.200535162.
Zinkernagel, R M, and M F Bachmann. 1996. "On Immunological Memory." *… Of Immunology*.

Appendix

Appendix 1	
PILAR	TCTTTTTCCTACAGCTCCTGGGCAACGTGCTGGTTGTTGTGCTGTCTCATCATTTTGGCAA AGAATTGCGGCCGTCTCAGGCCGAATTCAAGCTTGCCACC**ATG**GGGATCCTTCCCAGCCCT GGGATGcCTGCGCTGCTCTCCCTCGTGAGCCTTCTCTCCGTGCTGCTGATGGGTTGCGTAGC TGAAACCGGTTGGTCCAAGCATGCTAAACCTGTGGCATGTTCAGGGGACTGGCTTGGAGTG AGAGATAAGTGTTTCTATTTTTCTGATGATACCAGAAATTGGACAGCCAGTAAAATATTT TGTAGTTTGCAGAAAGCAGAACTTGCTCAGATTGATACACAAGAAGACATGGAATTTTTG AAGAGGTACGCAGGAACTGATATGCACTGGATTGGACTAAGCAGGAAACAAGGAGATTCT TGGAAATGGACAAATGGCACCACATTCAATGGTTGGTTTGAAATTATAGGGAACGGATCC TTTGCTTTCTTGAGTGCTGATGGAGTCCATAGTTCCAGAGGATTTATTGATATCAAGTGGA TTTGCAGCAAACCTAAATATTTTTTAGGTACCGGAGGTTCCGGTGGTTCCGGTCTGAATGA TATCTTTGAAGCTCAGAAGATTGAATGGCATGAAGGACGTACCAAGCACCACCATCACCAT CACTAATGATCACTCGAGACTAGTATCGCGATAATTCACTCCTCAGGTGCAGGCTGCCTAT CAGAAGGTGGTGGCTGGTGTGGCCAATGCCCTGGCTCACAAATACC
LLT1	TCTTTTTCCTACAGCTCCTGGGCAACGTGCTGGTTGTTGTGCTGTCTCATCATTTTGGCAA AGAATTGCGGCCGTCTCAGGCCGAATTCAAGCTTGCCACC**ATG**GGGATCCTTCCCAGCCCT GGGATGcCTGCGCTGCTCTCCCTCGTGAGCCTTCTCTCCGTGCTGCTGATGGGTTGCGTAGC TGAAACCGGTAGAGCTAACTGCCATCAAGAGCCATCAGTATGTCTTCAAGCTGCATGCCCA GAAAGCTGGATTGGTTTTCAAAGAAAGTGTTTCTATTTTTCTGATGACACCAAGAACTGG ACATCAAGTCAGAGGTTTTGTGACTCACAAGATGCTGATCTTGCTCAGGTTGAAAGCTTCC AGGAACTGAATTTCCTGTTGAGATATAAAGGCCCATCTGATCACTGGATTGGGCTGAGCAG AGAACAAGGCCAACCATGGAAATGGATAAATGGTACTGAATGGACAAGACAGTTTCCTAT CCTGGGAGCAGGAGAGTGTGCCTATTTGAATGACAAAGGTGCCAGTAGTGCCAGGCACTAC ACAGAGAGGAAGTGGATTTGTTCCAAATCAGATATACATGTCGGTACCGGAGGTTCCGGT GGTTCCGGTCTGAATGATATCTTTGAAGCTCAGAAGATTGAATGGCATGAAGGACGTACC AAGCACCACCATCACCATCACTAATGATCACTCGAGACTAGTATCGCGATAATTCACTCCT CAGGTGCAGGCTGCCTATCAGAAGGTGGTGGCTGGTGTGGCCAATGCCCTGGCTCACAAAT ACC
Sequence of PHL-sec-PILAR and PHL-sec-LLT1 plasmid for transfections Sequence of portion of PHLsec vector with PILAR or LLT1 extracellular region inserted. Start codon (underlined bold), secretion sequence (blue letters) AgeI restriction site (green), protein extracellular portion of protein (red), KpnI restriction site (yellow), BirA tag (grey), His tag (light blue)	

Appendix 2

GTCGACATTGATTATTGACTAGTTATTAATAGTAATCAATTACGGGGTCATTAGTTCATAGCCCATATA
TGGAGTTCCGCGTTACATAACTTACGGTAAATGGCCCGCCTGGCTGACCGCCCAACGACCCCCGCCCAT
TGACGTCAATAATGACGTATGTTCCCATAGTAACGCCAATAGGGACTTTCCATTGACGTCAATGGGTGG
ACTATTTACGGTAAACTGCCCACTTGGCAGTACATCAAGTGTATCATATGCCAAGTACGCCCCCTATTG
ACGTCAATGACGGTAAATGGCCCGCCTGGCATTATGCCCAGTACATGACCTTATGGGACTTTCCTACTT
GGCAGTACATCTACGTATTAGTCATCGCTATTACCATGGGTCGAGGTGAGCCCCACGTTCTGCTTCACT
CTCCCCATCTCCCCCCCCTCCCCACCCCCAATTTTGTATTTATTTATTTTTTAATTATTTTGTGCAGCG
ATGGGGGCGGGGGGGGGGGGGGCGCGCGCCAGGCGGGGCGGGGCGGGGCGAGGGGCGGGGCGGGGCGAG
GCGGAGAGGTGCGGCGGCAGCCAATCAGAGCGGCGCGCTCCGAAAGTTTCCTTTTATGGCGAGGCGGCG
GCGGCGGCGGCCCTATAAAAAGCGAAGCGCGCGGCGGGCGGGAGTCGCTGCGTTGCCTTCGCCCCGTGC
CCCGCTCCGCGCCGCCTCGCGCCGCCCGCCCCGGCTCTGACTGACCGCGTTACTCCCACAGGTGAGCGG
GCGGGACGGCCCTTCTCCTCCGGGCTGTAATTAGCGCTTGGTTTAATGACGGCTCGTTTCTTTTCTGTG
GCTGCGTGAAAGCCTTAAAGGGCTCCGGGAGGGCCCTTTGTGCGGGGGGGAGCGGCTCGGGGGGTGCGT
GCGTGTGTGTGTGCGTGGGGAGCGCCGCGTGCGGCCCGCGCTGCCCGGCGGCTGTGAGCGCTGCGGGCG
CGGCGCGGGGCTTTGTGCGCTCCGCGTGTGCGCGAGGGGAGCGCGGCCGGGGGCGGTGCCCCGCGGTGC
GGGGGGGCTGCGAGGGGAACAAAGGCTGCGTGCGGGGTGTGTGCGTGGGGGGGTGAGCAGGGGGTGTGG
GCGCGGCGGTCGGGCTGTAACCCCCCCCTGCACCCCCCTCCCCGAGTTGCTGAGCACGGCCCGGCTTCG
GGTGCGGGGCTCCGTGCGGGGCGTGGCGCGGGGCTCGCCGTGCCGGGCGGGGGGTGGCGGCAGGTGGGG
GTGCCGGGCGGGGCGGGGCCGCCTCGGGCCGGGGAGGGCTCGGGGGAGGGGCGCGGCGGCCCCGGAGCG
CCGGCGGCTGTCGAGGCGCGGCGAGCCGCAGCCATTGCCTTTTATGGTAATCGTGCGAGAGGGCGCAGG
GACTTCCTTTGTCCCAAATCTGGCGGAGCCGAAATCTGGGAGGCGCCGCCGCACCCCCTCTAGCGGGCG
CGGGCGAAGCGGTGCGGCGCCGGCAGGAAGGAAATGGGCGGGGAGGGCCTTCGTGCGTCGCCGCGCCGC
CGTCCCCTTCTCCATCTCCAGCCTCGGGGCTGCCGCAGGGGGACGGCTGCCTTCGGGGGGGACGGGGCA
GGGCGGGGTTCGGCTTCTGGCGTGTGACCGGCGGCTCTAGAGCCTCTGCTAACCATGTTCATGCCTTCT
TCTTTTTCCTACAGCTCCTGGGCAACGTGCTGGTTGTTGTGCTGTCTCATCATTTTGGCAAAGAATTGC
GGCCGTCTCAGGCCGAATTCAAGCTTGCCACCATGGGGATCCTTCCCAGCCCTGGGATGCCTGCGCTGC
TCTCCCTCGTGAGCCTTCTCTCCGTGCTGCTGATGGGTTGCGTAGCTGAAACCGGTGGGCGCAGCGGGG
CCCGTCTGCAGCAAGTGACCGACGGCCGGGACGGCCGCCTGCCCCCTCTGCCACCTGGGGCGGTGCGGG
CCCGGAGCCCGGAGCCCGGGTAGCGCGTAGAGCCGGCGCGATGCACGTGCGCTCACTGCGAGCTGCGGC
GCCGCACAGCTTCGTGGCGCTCTGGGCACCCCTGTTCCTGCTGCGCTCCGCCCTGGCCGACTTCAGCCT
GGACAACGAGGTGCACTCGAGCTTCATCCAGGGCGCAGCGGGGCCCGTCTGCAGCAAGTGACCGACGGC
CGGGACGGCCGCCTGCCCCCTCTGCCACCTGGGGCGGTGCGGGCCCGGAGCCCGGAGCCCGGGTAGCGC
GTAGAGCCGGCGCGATGCACGTGCGCTCACTGCGAGCTGCGGCGCCGCACAGCTTCGTGGCGCTCTGGG
CACCCCTGTTCCTGCTGCGCTCCGCCCTGGCCGACTTCAGCCTGGACAACGAGGTGCACTCGAGCTTCA
TCCAGGTACCGGAGGTTCCGGTGGTTCCGGTCTGAATGATATCTTTGAAGCTCAGAAGATTGAATGGCA
TGAAGGACGTACCAAGCACCACCATCACCATCACTAATGATCACTCGAGACTAGTATCGCGATAATTCA
CTCCTCAGGTGCAGGCTGCCTATCAGAAGGTGGTGGCTGGTGTGGCCAATGCCCTGGCTCACAAATACC
ACTGAGATCTTTTTCCCTCTGCCAAAAATTATGGGGACATCATGAAGCCCCTTGAGCATCTGACTTCTG
GCTAATAAAGGAAATTTATTTTCATTGCAATAGTGTGTTGGAATTTTTTGTGTCTCTCACTCGGAAGGA
CATATGGGAGGGCAAATCATTTAAAACATCAGAATGAGTATTTGGTTTAGAGTTTGGCAACATATGCCA
TATGCTGGCTGCCATGAACAAAGGTGGCTATAAAGAGGTCATCAGTATATGAAACAGCCCCCTGCTGTC
CATTCCTTATTCCATAGAAAAGCCTTGACTTGAGGTTAGATTTTTTTTATATTTTGTTTTGTGTTATTT
TTTTCTTTAACATCCCTAAAATTTTCCTTACATGTTTTACTAGCCAGATTTTTCCTCCTCTCCTGACTA
CTCCCAGTCATAGCTGTCCCTCTTCTCTTATGAAGATCCCTCGACCTGCAGCCCAAGCTTGGCGTAATC
ATGGTCATAGCTGTTTCCTGTGTGAAATTGTTATCCGCTCACAATTCCACACAACATACGAGCCGGAAG
CATAAAGTGTAAAGCCTGGGGTGCCTAATGAGTGAGCTAACTCACATTAATTGCGTTGCGCTCACTGCC
CGCTTTCCAGTCGGGAAACCTGTCGTGCCAGCGGATCGATCCGCTGCATTAATGAATCGGCCAACGCGC
GGGGAGAGGCGGTTTGCGTATTGGGCGCTCTTCCGCTTCCTCGCTCACTGACTCGCTGCGCTCGGTCGT

TCGGCTGCGGCGAGCGGTATCAGCTCACTCAAAGGCGGTAATACGGTTATCCACAGAATCAGGGGATAA
CGCAGGAAAGAACATGTGAGCAAAAGGCCAGCAAAAGGCCAGGAACCGTAAAAAGGCCGCGTTGCTGGC
GTTTTTCCATAGGCTCCGCCCCCCTGACGAGCATCACAAAAATCGACGCTCAAGTCAGAGGTGGCGAAA
CCCGACAGGACTATAAAGATACCAGGCGTTTCCCCCTGGAAGCTCCCTCGTGCGCTCTCCTGTTCCGAC
CCTGCCGCTTACCGGATACCTGTCCGCCTTTCTCCCTTCGGGAAGCGTGGCGCTTTCTCAATGCTCACG
CTGTAGGTATCTCAGTTCGGTGTAGGTCGTTCGCTCCAAGCTGGGCTGTGTGCACGAACCCCCCGTTCA
GCCCGACCGCTGCGCCTTATCCGGTAACTATCGTCTTGAGTCCAACCCGGTAAGACACGACTTATCGCC
ACTGGCAGCAGCCACTGGTAACAGGATTAGCAGAGCGAGGTATGTAGGCGGTGCTACAGAGTTCTTGAA
GTGGTGGCCTAACTACGGCTACACTAGAAGGACAGTATTTGGTATCTGCGCTCTGCTGAAGCCAGTTAC
CTTCGGAAAAAGAGTTGGTAGCTCTTGATCCGGCAAACAAACCACCGCTGGTAGCGGTGGTTTTTTTGT
TTGCAAGCAGCAGATTACGCGCAGAAAAAAAGGATCTCAAGAAGATCCTTTGATCTTTTCTACGGGGTC
TGACGCTCAGTGGAACGAAAACTCACGTTAAGGGATTTTGGTCATGAGATTATCAAAAAGGATCTTCAC
CTAGATCCTTTTAAATTAAAAATGAAGTTTTAAATCAATCTAAAGTATATATGAGTAAACTTGGTCTGA
CAGTTACCAATGCTTAATCAGTGAGGCACCTATCTCAGCGATCTGTCTATTTCGTTCATCCATAGTTGC
CTGACTCCCCGTCGTGTAGATAACTACGATACGGGAGGGCTTACCATCTGGCCCCAGTGCTGCAATGAT
ACCGCGAGACCCACGCTCACCGGCTCCAGATTTATCAGCAATAAACCAGCCAGCCGGAAGGGCCGAGCG
CAGAAGTGGTCCTGCAACTTTATCCGCCTCCATCCAGTCTATTAATTGTTGCCGGGAAGCTAGAGTAAG
TAGTTCGCCAGTTAATAGTTTGCGCAACGTTGTTGCCATTGCTACAGGCATCGTGGTGTCACGCTCGTC
GTTTGGTATGGCTTCATTCAGCTCCGGTTCCCAACGATCAAGGCGAGTTACATGATCCCCCATGTTGTG
CAAAAAAGCGGTTAGCTCCTTCGGTCCTCCGATCGTTGTCAGAAGTAAGTTGGCCGCAGTGTTATCACT
CATGGTTATGGCAGCACTGCATAATTCTCTTACTGTCATGCCATCCGTAAGATGCTTTTCTGTGACTGG
TGAGTACTCAACCAAGTCATTCTGAGAATAGTGTATGCGGCGACCGAGTTGCTCTTGCCCGGCGTCAAT
ACGGGATAATACCGCGCCACATAGCAGAACTTTAAAAGTGCTCATCATTGGAAAACGTTCTTCGGGGCG
AAAACTCTCAAGGATCTTACCGCTGTTGAGATCCAGTTCGATGTAACCCACTCGTGCACCCAACTGATC
TTCAGCATCTTTTACTTTCACCAGCGTTTCTGGGTGAGCAAAAACAGGAAGGCAAAATGCCGCAAAAAA
GGGAATAAGGGCGACACGGAAATGTTGAATACTCATACTCTTCCTTTTTCAATATTATTGAAGCATTTA
TCAGGGTTATTGTCTCATGAGCGGATACATATTTGAATGTATTTAGAAAAATAAACAAATAGGGGTTCC
GCGCACATTTCCCCGAAAAGTGCCACCTG

Full PHL-Sec sequence
Insert is in red. PHL-sec sequence comes from and is described by Aricescu *et al.* (Aricescu 2006)

Appendix 3

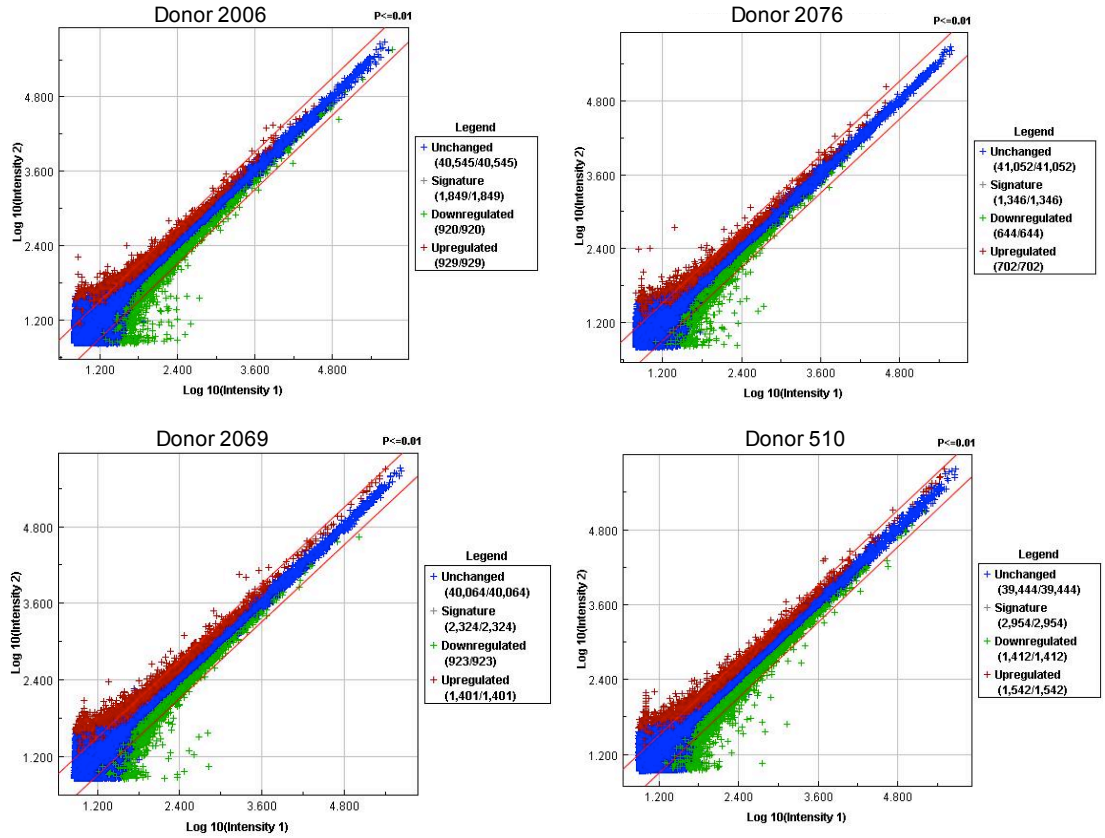

Log10 Intensity scatter plots
Representative scatterplot of the intensities of all genes tested in one donor at the 5 hour time point. Points in the space between the red lines indicates a p-value of greater than 0.01.
Figures.pzfx

Appendix 4

Donor	Primary Sequence Name	Accession #	Fold Change	P-value	Intensity1	Intensity 2
510	ADM	NM_001124	3.94447	4.33E-19	26.3548	104.509
510	CXCL16	NM_001100812	1.57606	0.00006	111.6329	176.00415
510	CXCL16	NM_022059	1.83425	8.23E-08	126.2024	231.04041
510	DNAJB1	NM_006145	2.38648	1.49E-14	1291.023	3081.6519
510	HIST1H2AB	NM_003513	3.26542	1.08E-10	174.4739	569.72992
510	HIST2H2BF	NM_001024599	4.31658	1.95E-11	55.16364	238.1181
510	HIST2H2BF	NM_001024599	6.32795	0.00053	10.06796	63.70957
510	HIST2H2BF	NM_001161334	1.31417	0.05752	1612.697	2119.363
510	HMOX1	NM_002133	-1.60102	0.00003	80.96648	50.64072
510	HSPA1B	NM_005346	4.01238	1.15E-34	4846.717	19433.754
510	HSPA8	NM_153201	-1.07958	0.49854	3288.816	3046.6436
510	HSPA8		2.2607	1.48E-06	159.4832	360.54379
510	HSPA8	AK310467	3.32905	2.01E-07	51.48103	171.3828
510	IFNG	NM_000619	2.36127	3.09E-14	80.85252	193.82057
510	RORC	NM_005060	1.63936	0.00001	1700.204	2787.5293
510	SLAMF6	NM_052931	-1.36059	0.01035	107.3202	78.54468
510	SLAMF6	NM_001184714	1.19822	0.27589	156.171	187.12711
510	HPRT1	NM_000194	-1.04166	0.71827	627.4281	602.34906
510	KLRB1	NM_002258	-1.06222	0.59367	27433.57	25833.391
2006	ADM	NM_001124	2.38187	1.71E-14	97.26	233.29
2006	CXCL16	NM_001100812	2.68785	2.34E-18	49.75	133.55
2006	CXCL16	NM_022059	-1.3448	0.00883	202.83	151.02
2006	DNAJB1	NM_006145	2.0768	1.05E-10	1286.66	2675.49
2006	HIST1H2AB	NM_003513	1.72041	0.00064	162.13	278.94
2006	HIST2H2BF	NM_001024599	5.7764	3.95E-14	41.43	239.33
2006	HIST2H2BF	NM_001024599	3.77877	0.00073	15.37	58.07
2006	HIST2H2BF	NM_001161334	1.43123	0.01368	1159.04	1658.86
2006	HMOX1	NM_002133	-2.49685	6.08E-16	64.08	24.97
2006	HSPA1B	NM_005346	3.25538	1.76E-25	5971.36	19430.59
2006	HSPA8	NM_153201	1.30354	0.01913	2763.94	3601.16
2006	HSPA8		3.0214	1.69E-09	98.77	298.43
2006	HSPA8	AK310467	1.96505	0.00056	64.48	126.71
2006	IFNG	NM_000619	1.71519	1.85E-06	114.87	197.66
2006	RORC	NM_005060	1.25246	0.04663	5424.59	6792.26
2006	SLAMF6	NM_052931	-1.30208	0.02218	82.93	63.66
2006	SLAMF6	NM_001184714	-1.53629	0.01308	158.89	103.42
2006	HPRT1	NM_000194	1.11368	0.34126	512.78	570.88
2006	KLRB1	NM_002258	-1.04867	0.67448	64698.08	61641.75
2069	ADM	NM_001124	2.19253	3.95E-12	67.71	149.80
2069	CXCL16	NM_022059	1.00132	0.99066	176.98	178.80
2069	CXCL16	NM_001100812	1.66815	6.10E-06	76.22	127.68
2069	DNAJB1	NM_006145	2.4767	1.09E-15	667.27	1656.65
2069	HIST1H2AB	NM_003513	2.15817	5.31E-06	146.40	315.96
2069	HIST2H2BF	NM_001024599	10.07224	5.37E-16	22.81	229.75
2069	HIST2H2BF	NM_001024599	7.89257	5.08E-06	10.00	78.93
2069	HIST2H2BF	NM_001161334	1.66747	0.00061	1168.52	1948.47
2069	HMOX1	NM_002133	-1.59705	0.00004	78.28	49.28
2069	HSPA1B	NM_005346	5.8187	0	1884.08	10959.07
2069	HSPA8	NM_153201	-1.07424	0.52673	2642.90	2459.83
2069	HSPA8		2.48801	1.08E-06	82.51	205.28
2069	HSPA8	AK310467	1.53002	0.14431	43.25375	66.17928
2069	IFNG	NM_000619	2.86785	1.28E-08	18.98	56.25
2069	RORC	NM_005060	1.20664	0.09686	4006.92	4832.53
2069	SLAMF6	NM_052931	-1.30391	0.09614	66.00	51.04
2069	SLAMF6	NM_001184714	-1.53763	0.01069	199.04	129.44
2069	HPRT1	NM_000194	1.0147	0.89736	554.97	562.35
2069	KLRB1	NM_002258	1.00782	0.94514	50024.28	50418.77

Donor	Primary Sequence Name	Accession #	Fold Change	P-value	Intensity1	Intensity 2
2076	ADM	NM_001124	2.673	3.61E-18	88.16	237.01
2076	CXCL16	NM_022059	1.34555	0.00871	146.47	193.23
2076	CXCL16	NM_001100812	1.86515	2.09E-06	70.16	130.58
2076	DNAJB1	NM_006145	1.6911	3.42E-06	1951.18	3301.78
2076	HIST1H2AB	NM_003513	2.70657	5.78E-09	215.18	582.41
2076	HIST2H2BF	NM_001024599	2.75244	2.76E-09	276.33	760.58
2076	HIST2H2BF	NM_001024599	3.09911	4.36E-09	72.88	225.86
2076	HIST2H2BF	NM_001161334	1.73337	0.00025	1742.96	3021.20
2076	HMOX1	NM_002133	-1.88201	5.84E-07	68.38	35.83
2076	HSPA1B	NM_005346	2.27226	4.03E-13	11126.62	25280.90
2076	HSPA8	NM_153201	1.05223	0.65274	3262.36	3433.91
2076	HSPA8		2.39466	1.54E-07	177.88	425.95
2076	HSPA8	AK310467	2.63562	1.83E-07	81.43	214.61
2076	IFNG	NM_000619	1.87758	2.57E-08	83.60	158.88
2076	RORC	NM_005060	1.6431	0.00001	3317.98	5451.80
2076	SLAMF6	NM_052931	1.1834	0.36696	43.94	51.86
2076	SLAMF6	NM_001184714	1.50569	0.03123	76.78	115.61
2076	HPRT1	NM_000194	1.09673	0.41445	478.65	524.46
2076	KLRB1	NM_002258	-1.03028	0.79205	53990.61	52402.77

qPCR genes 1.xlsx

Appendix 5 Literature Review Summary Table

Paper	Main Results
Lanier 1994	• Identified CD161 as a C-type lectin expressed as a disulfied linked homodimer with ~40 kDa subunits (digested to ~26kDa) • Defined CD161 sequence, domains and homology (NKG2A ~26%) • Cell expression patterns (NK and T cells) • NK cells and T cells have same gene product • CD161 mAb inhibited and did not induced NK cell cytotoxicity • CD161 on P815 cells (differs with different cell types)
Poggi 1996	• CD161 expressed on portion of immature thymocytes (2-20%) • CD161 not expressed on mature $CD3^+$ T cells • CD161 mAb inhibits cytolytic activity of immature thymocytes
Poggi 1997	• $CD161^+$ identifies $CD4^+$ cells displaying transendothelial migration capacity and highly positive for B1 & B2 integrins • CD161 mAb reduced transendothelial migration and inhibited adhesion • Cross-linking CD161 up-regulated LFA-1 binding site and β1 & β2 integrin expression
Poggi 1998	• IL-12 dependent up-regulation of CD161 (requires 12^+ hours) • CD161 mAb inhibited CD16 and p46 mediated cytotoxicity
Azzoni 1998	• CD161 expression increased with IL-12 and IL-15 (increased de-novo synthesis) • IL-2 downregulated CD161 expression (slight transcriptional but mostly post-translational) • CD161 mAb inhibited cytotoxicity (this is cell line dependent)
Exley 1998	• $V\alpha24^{invt}$ cells are $CD161^+$ (tiny % of total $CD161^+$ T cells) • CD161 triggered $V\alpha24^{invt}$ $CD4^+$ cells increase proliferation with CD3 but not without CD3 stimulation • CD161 mAb increased IL-4 & IFNγ from limiting CD3 (ratios remain same between IL-4 and IFNγ) • CD161 mAb not affect PMA/I stimulated cells • CD161 mAb not affect cytotoxicity on $V\alpha24^{invt}$ $CD4^+$ cells
Ishirara 1999	• $CD161^+$ cells are more frequent in hepatic lymphocytes than peripheral blood lymphocytes (no difference is seen between primary, metastatic, or healthy liver)
Eichler 2001	• Cycloheximide experiments LLT1 not regulated at mRNA level or slow turnover and CD161 likely high turnover
Iiai 2002	• $CD161^+$ cells are abundant in the liver and intestine
Rosen 2005	• LLT1 binds CD161 (using liposomes transfected cell lines and reporter chimeras) • LLT1 inhibits NK cell cytotoxicity

Aldemir 2005	• LLT1 binds CD161 (multimers and transfected cell lines) • NK cell degranulation (CD107a) inhibited by LLT1 (transfected cells) • LLT1 protects from NK specific killing (Cr release assay) - protection more significant when IL-12 activated • LLT1 decreased NK cytotoxicity with P815 redirected killing • LLT1 reduced NK cell IFNγ production • $CD3^+$ CD161 mAb plate bound increased IFNγ production • LLT1 P815 cells + CD161 mAb increased NK IFNγ production • CD161 mAb did not trigger IFNγ on its own • Mentions CD161 surface expression reduced when incubated with LLT1 expressing cells & similar with cross-linking w/ mAb (within 15 min, transwell prevented, fixation prevented -suggest internalization)
Takahashi 2006	• Phenotype of $CD161^+$ CD4 & CD8 cells (3 levels of CD161 staining) • $CD8^+$ $CD161^{++}$ mostly effector memory • CD3/28 stim CD8+ CD161++ failed to secrete IFNγ, TNFα, or IL-2 • CD3/28 stim $CD8^+$ $CD161^{++}$ failed to proliferate • $CD8^+$ $CD161^{++}$ show high levels of perforin and Granzyme A
Pozo 2006	• Primary NK cells ligation CD161 significantly increased acid sphingomyelinase (aSMase) & elevated intracellular ceramide (transient) • CD161 mAb induce 3 fold activation of PKB/Akt & Rsk1 kinases (downstream of ceramide activated proteins) • CD161 mAb increased T cell proliferation by CD3 (48-72hrs) (but not trigger proliferation on own) • CD161 mAb increased IFNy production • CD161 mAb trigger PKB/AKT activation in primary T cells • CD161 mAb promotes recruitment of aSMase and CD161 to membrane rafts
Rosen 2008	• LLT1 expression positive on several cell lines, activated B cells (several stimuli), activated pDCs and activated MoDCs • CD161 mAb + CD3/28 not effect IFNγ but decrease TNFa • CD161 surface expression reduced after stimulation of CD161 • "Hemi ITIM" AIYAEL sequence with A in -2 to Y important mutation in ITIM thought to decrease possible inhibitory capacity • Size of LLT1 significantly different than Mathew 2004. Could not repeat staining seen by Mathew 04 even when provided with L9.7 mAb

Northfield 2008	• CD161 levels on HCV specific $CD8^+$ T cells in blood same for acute, chronic, resolved, & 4 months post resolve • HBV CD161 levels in blood often below detection • HCV specific and HBC specific T cells similar level $CD161^+$ in acute disease • $CD161^+$ $CD8^+$ show effector memory phenotype • CD161 not an activation marker • Short-term IL-12 and TGFB not modulate CD161 expression • $CD161^+$ $CD8^+$ cells low in granzyme B and perforin • $CD161^+$ $CD8^+$ cells reduced proliferation compared to $CD161^-$
Germain 2010	• LLT1 has 6 splice variants (3 new described) but LLT1 isoform is the only ligand of CD161 • LLT1 is differentially glycosylated • PILAR structure supports inhibition of binding to CD161
Billerbeck 2010	• CD161 in HCV enriched in liver and associated with reductions of CD161 in blood • $CD8^+$ $CD161^{++}$ "represent prototypical response to tissue localized infection/ inflammation in major organs" • $CD8^+$ $CD161^{++}$ effector memory phenotype • $CD8^+$ $CD161^{++}$ low granzyme and perforin levels • $CD8^+$ $CD161^{++}$ association with IL-17 and IL-22
Germain 2011	• LLT1 tightly regulated and not found on resting cells • LLT1 surface expression can be up-regulated with long term stimulation (+24 hour) and found highest on activated B cells • CD3 + CD161 stimulation increases IL-17 secretion
Kamishikiryo 2011	• Structure of CD161 supports PILAR not binding • CD161 binds LLT1 with low affinity, fast kinetics, entropically and enthalpically driven thermodynamics with small heat capacity. Typical of interaction mediating cell to cell recognition
Cosgrove 2013	• HIV donors $CD161^{++}$ $CD8^+$ reduced in blood (acute and chronic) and not rebound after therapy • CD8 $CD161^{++}$ show $V\alpha7.2^+$ TCR and $CD8^+$ $CD161^+$ show diverse TCR • $CD161^{++}$ $CD8^+$ express CD69 and IFNy in MR1 dependent manner • $CD161^{++}$ $CD8^+$ increased activated caspase 3 and phosphatidyl serine when activated with *E. coli* • PMA/I and high amounts CD3/28/2 microbeads induced activated caspase 3 and phosphatidyl serine in all populations • *E. coli* activated proliferation at low levels but reduced proliferation at highest levels *E. coli* (balance between proliferation and death)

Appendix 6				
Molecule	Fluorochrome	Brand	Clone	Cat no.
a-human B7-H1 (CD274, PDL-1)	APC	E bioscience		17-5983-71
a-human ICOS (CD278)	PE	E bioscience		12-9948-71
a-mouse IgG	PE	RD		F0102B
Anti-FITC beads		MACS		120-000-293
Anti-PE beads		MACS		120-000-294
CD107a	PECy5	BD		555802
CD107a	PE Cy7	Biolegend	H4A3	328618
CD14	APC Cy7	Biolegend	HCD14	325620
CD14	Pacific Blue	Invitrogen		MHCD1428
CD161	pure	AbD Serotec	B199.2	MCA1855B
CD161	FITC	AbD Serotec	B199.2	MCA1855F
CD161	APC	BD	DX12	550968
CD161	Alexa Flour 647 (APC)	Biolegend	HP-3G10	339910
CD161	APC	MACS	191B8	130-092-678
CD161	Pure	MACS	191B8	130-092-678/ 130-092-676
CD161	FITC	MACS	191B8	130-092-907
CD161	PE	MACS	191B8	130-092-677
CD161	Biotin	Serotec	B199.2	MCA1855B
CD19	APC	BD		555415
CD19	Alexa Flour 700	E bioscience	HIB19	56-0199-42
CD19	Pacific Blue	Invitrogen		MHCD1928
CD25	PE Cy7	E bioscience		25-0259-42
CD3	PerCP	Biolegend	UCHT1	300427
CD3	efluor 450	E bioscience	UCHT1	48-0038-42
CD3	efluor 450	E bioscience	OKT3	48-0037-42
CD3	PE Cy7	E bioscience	UCHT1	25-0038-42
CD3	Pacific Orange	Invitrogen		CD0330
CD4	PE Cy7	BD	Sk 3	557852
CD4	Alexa Flour 700	BD	RPA-T4	557922
CD4	FITC	BD		555346
CD4	PercPCy 5.5	E bioscience	OKT4	45-0048-42
CD4	VioGreen	MACS		130-096-900
CD56	Brilliant Violet 421	Biolegend	HCD56	318328
CD56	APC	MACS		130-090-843
CD69	FITC	E bioscience	FN50	11-0699-42

CD8	Alexa Flour 700	BD	RPA-T8	557945
CD8	V450	BD	RPA-T8	560347
CD8	PerCP Cy5.5	BD		341050
CD8	VioGreen	MACS		130-096-092
CD8	Alexa Fluor 700			
CD8a	PercPCy 5.5	E bioscience	RPA-T8	45-0088-42
CLEC2D	PE	RD	402659	FAB3480P
ICOS (CD278)	PE		ISA-3	12-9948-71
IFNy	FITC	BD		340449
IFNy	PercPCy 5.5	E bioscience	4S.B3	45-7319-42
IgG1	pure isotype (k)	BD		557273
IgG2a	pure isotype	BD		554126
IgG2a	APC	BD		555576
IgG2a	PE	MACS		130-091-835
IgG2b pure isotype control	pure	BD		556654
IL-17a	FITC	E bioscience	ebio64dec 17	11-7179-73
IL-17a	PE	E bioscience		12-7178-42
IL-18Ra (CD218a)	PE	E bioscience	H44	12-7183-73
IL-2	FITC	BD		340448
IL-22	PE	RD		IC7821P
Live/Dead	Near IR	Invitrogen		L10119
Live/Dead	Violet (pac blue)	Invitrogen		
mouse IgG1	PE	BD		555749
Pure CD28	Pure	BD	CD28.2	555726
Pure CD3	Pure	BD	UCHT1	555330
Rat a-mouse IgG	FITC	BD		553443
Rat IgG2a iso control	PE	E bioscience		12-4321-71
Streptavidin	APC	Caltag Labs		SA1005
TNFa	PE Cy7	BD		557647
Va7.2 (TCR)	PE	Biolegend	3C10	351706
Va7.2 (TCR)	FITC	Biolegend	3C10	351704
yd	PE	BD	B1	555717
IgG2a	PE	RD		IC003P
CD8 Microbeads		MACS		120-000-244
Granzyme K	PE	Immunotools		21144054
Granzyme K	FITC	Immunotools		21144053
Granzyme B	APC	Invitrogen	MHGB05	
Granzyme A	FITC	RD		IC29051F

Perforin	Pacific Blue	Biolegend	B-D48	353305